UNIVERSITEIT VAN PRETORIA
UNIVERSITY OF PRETORIA
YUNIBESITHI YA PRETORIA

The financial benefit of using borehole radar to delineate mining blocks in underground platinum mines

by

Petro du Pisani

Submitted in partial fulfilment of the requirements for the degree MSc. (Earth Science Management and Practice) in the Faculty of Natural and Agricultural Science

University of Pretoria
Pretoria

October 2007

TABLE OF CONTENTS

SUMMARY

Title of treatise: The financial benefit of using borehole radar to delineate mining blocks in underground platinum mines

Name of author: P du Pisani

Name of supervisor: Prof. HFJ Theart

Department: Faculty of Natural and Agricultural Sciences
University of Pretoria

Degree: M.Sc. (Earth Science Management and Practice)

Borehole radar is a short-range, high-resolution geophysical technique that can be used to delineate the position of the Merensky platinum reef in underground mines situated in the Western Bushveld Complex. In this study, borehole radar is used in reflection mode from four boreholes drilled sub-parallel to the expected position of the Merensky Reef within an underground mining block bounded by two cross-cuts and a haulage. This study relates the stratigraphic column at Amandelbult Section to borehole radar reflectivity. The radar illumination line coordinates produced along the Merensky Reef surface are used to construct a three-dimensional surface of the reef within the defined mining block.

The geophysical interpretation presented here shows how a slump in the Merensky Reef, called a pothole, is imaged using borehole radar. This study analyses the increase in geological confidence related to the improved delineation of the elevation of the Merensky Reef.

The financial impact of using borehole radar to delineate this pothole is analysed at the various mining steps, namely: orebody definition, mine planning, mine development, ore extraction and ore processing. The information gained by conducting borehole radar is compared with the information acquired using only standard geological drilling.

This study concludes that the application of borehole radar significantly increases the confidence in the geological model prior to mining. Conducting borehole radar prior

to mining improves mine planning and development, ensures that less waste is mined, facilitates the effective deployment of labour crews, prevents waste being sent to the processing plant and avoids deferring income until a later date. Recommendations are made on how to plan for and include borehole radar in the mining process.

LIST OF ABBREVIATIONS

BH	Borehole
BHR	Borehole radar
CSIR	Council for Scientific and Industrial Research
GPR	Ground Penetrating Radar
PGE	Platinum Group Elements
RPM	Rustenburg Platinum Mines
SAIMM	South African Institute of Mining and Metallurgy
SAMREC	South African Mineral Resources Committee
SG	Specific Gravity

LIST OF FIGURES

LIST OF TABLES

1 INTRODUCTION

1.1 Objectives of the study

This treatise aims to quantify the cost benefit that can be achieved if borehole radar is applied as a predictive geological tool ahead of mining.
A case study was conducted at Anglo Platinum's Amandelbult Section. The treatise describes how the optimal survey design was designed in order to effectively image a mining block. A fan of boreholes was surveyed with borehole radar, which provided a detailed three-dimensional surface representing the Merensky Reef. A cost-benefit analysis was conducted to determine whether the information provided by borehole radar in this mining block provided any significant financial benefits to the mine.

The Bushveld Complex, situated north of Pretoria in South Africa, contains the world's largest known resource of platinum (Viljoen and Schürmann, 1998). The distribution of the platinum resources in relation to other mineral deposits is shown in Figure 1.

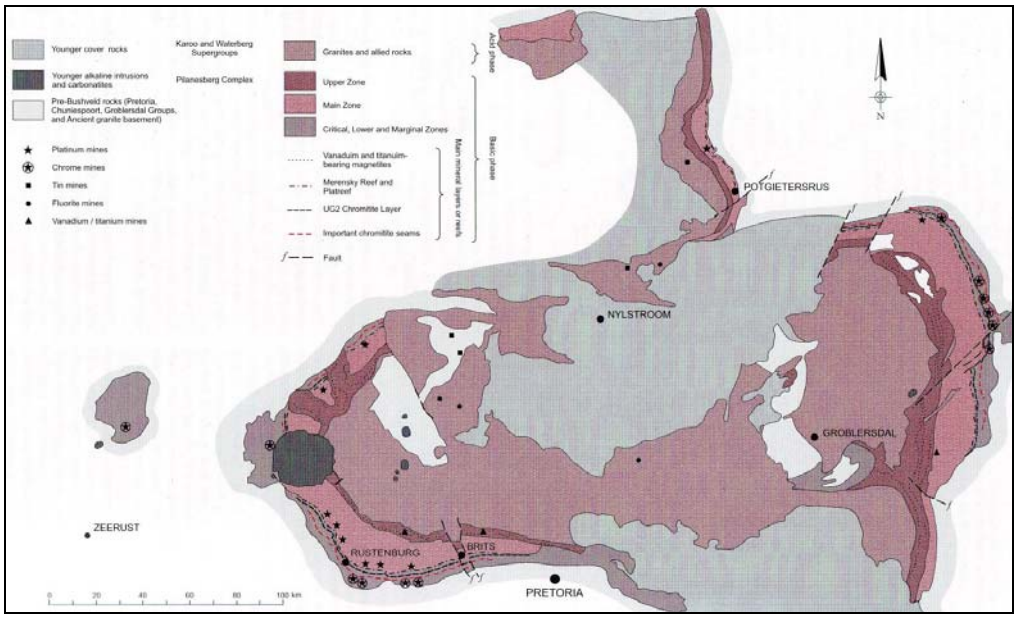

Figure 1: A geological map of the Bushveld Complex in South Africa, showing the distribution of the main economic minerals, after Viljoen and Schürmann (1998)

Economic concentrations of platinum are present in the Merensky Reef: a feldspathic pegmatoidal pyroxenite and the UG2 chromitite. These platinum-rich layers are interspersed with layers of anorthosite, norite and pyroxenite.

On a regional scale, these thin tabular ore bodies (locally called reefs) are continuous for tens to hundreds of kilometres, but on a smaller mine-block scale these reefs are often disrupted by various geological structures such as dykes, iron-rich ultramafic pegmatites (IRUPs), faults and potholes. Potholes are the most common disruption and cause most challenges to mining these reefs.

In this treatise, a geological disruption caused by a pothole is examined. In a pothole, the reef transgresses its footwall layers, resulting in slumps that have diameters that can be metres to tens of metres deep and wide (Viljoen and Schürmann, 1998). The reef is often pinched out at the edges of the pothole, resulting in degraded ore reserves. Potholes inevitably lead to significant losses and predicting their presence ahead of mining is advantageous for a number of reasons:

- Less waste rock is mined, resulting in a significant cost benefit to the mine.
- Improved knowledge of the ore body means that less money is spent on unnecessary development towards severely disrupted or degraded reef.
- Mining can be planned smarter so that, for example, support pillars are left where less ore is present due to potholing.
- If it is known that mining is approaching a pothole, mining can be relocated timeously and work crews can be moved to a different location, i.e. the work force is used more efficiently.
- Pothole edges are often related to unstable hanging wall conditions, which could lead to falls of ground. If the pothole edge is delineated before mining starts, additional precautionary measures can be taken to ensure the safety of mine workers.

1.2 The Platmine Research Collaborative

The work presented here was conducted under the Platmine collaborative research programme. This research programme, initiated in 2003, involves the Council for Scientific and Industrial Research (CSIR), Anglo Platinum, Impala Platinum, Lonmin Platinum and Northam Platinum. Its main focus is the long-term sustainability of the platinum industry in South Africa. Among its primary goals listed at www.platmine.co.za are:

- To increase productivity.
- To develop technologies and competencies to improve overall safety and health.
- To facilitate mechanisation by solving common technological problems.
- To improve the underground working environment.

This treatise ties in with the first objective listed above, i.e. increasing productivity in the platinum industry, but borehole radar is also increasingly being used in conjunction with other geophysical methods to characterise the rock mass prior to mining in order to pre-empt hazardous conditions.

1.3 Delimitations

It is important to note that this treatise will only deal with determining the elevation of the Merensky Reef within the defined mining block. In particular, the position of the bottom contact of the Merensky Reef is delineated.

This treatise assumes that the grade information pertaining to the Merensky Reef is predictable and that grade variation is acceptable within the mining block. A constant grade is used for financial calculations. This value is defined in Section 6.2.1.

2 BOREHOLE RADAR

Borehole radar is ground penetrating radar (GPR) applied from within a borehole. GPR is a geophysical technique whereby radio waves are transmitted into the ground to locate buried objects or hidden interfaces (Daniel *et al.*, 2004). GPR measures differences in the dielectric property permittivity, and the distance that radar waves travel in a medium is determined by its conductivity (Du Pisani and Vogt, 2003).

A typical bi-static borehole radar instrument consists of separate transmitter and receiver probes that are deployed inside a borehole. In this study, the CSIR's Aardwolf BR40 was used to acquire the borehole radar data. This instrument has a centre frequency of 40 MHz and a vertical resolution of approximately 1 m (Vogt *et al.*, 2005). A schematic of the Aardwolf BR40 is shown in Figure 2.

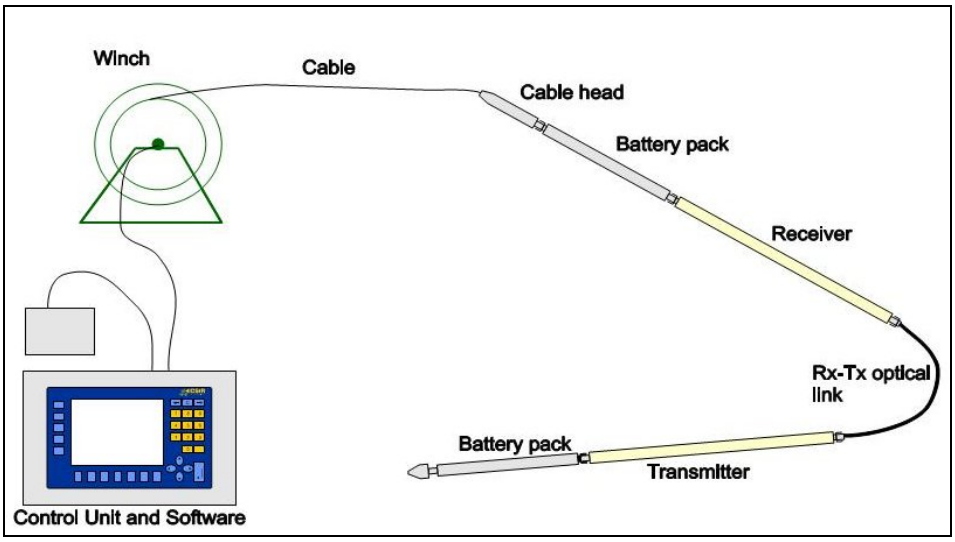

Figure 2: Schematic for the Aardwolf BR40 instrument, showing the radar transmitter, receiver, optical-fibre links, winch and control unit (Vogt 2002)

Borehole radar can be applied in reflection mode from within a single borehole (Vogt, 2006) or in transmission mode, whereby the transmitter is located in one borehole and the receiver in an adjacent borehole. In transmission mode, borehole radar can determine whether conductive material is present between two boreholes (Turner *et al.*, 2000).

For the study presented in this treatise, borehole radar is used in single-borehole reflection mode to image the boundary of the Merensky Reef within a section of Anglo Platinum's Amandelbult Section.

In borehole radar reflection mode, radar waves are transmitted into the rock mass and the time taken for these waves to travel to a reflective interface is measured in nanoseconds (Vogt *et al.*, 2005). If the velocity of the radar waves in the rock mass is known, the distance to the interface can be calculated.

In order for a reflection borehole radar survey to be successful, the following factors are of importance (Vogt, 2006):

- The borehole from which borehole radar is applied should be oriented parallel or sub-parallel to the target to be imaged, as shown in Figure 3.
- There should be a significant permittivity contrast between the target and its host rocks.
- The technique works best if the borehole is situated in a host rock that is resistive and delineates a target that is conductive.
- The reflective contact should be sharp as opposed to gradationally changing into a different rock type.

More technical information about borehole radar will be discussed throughout this treatise as it becomes necessary.

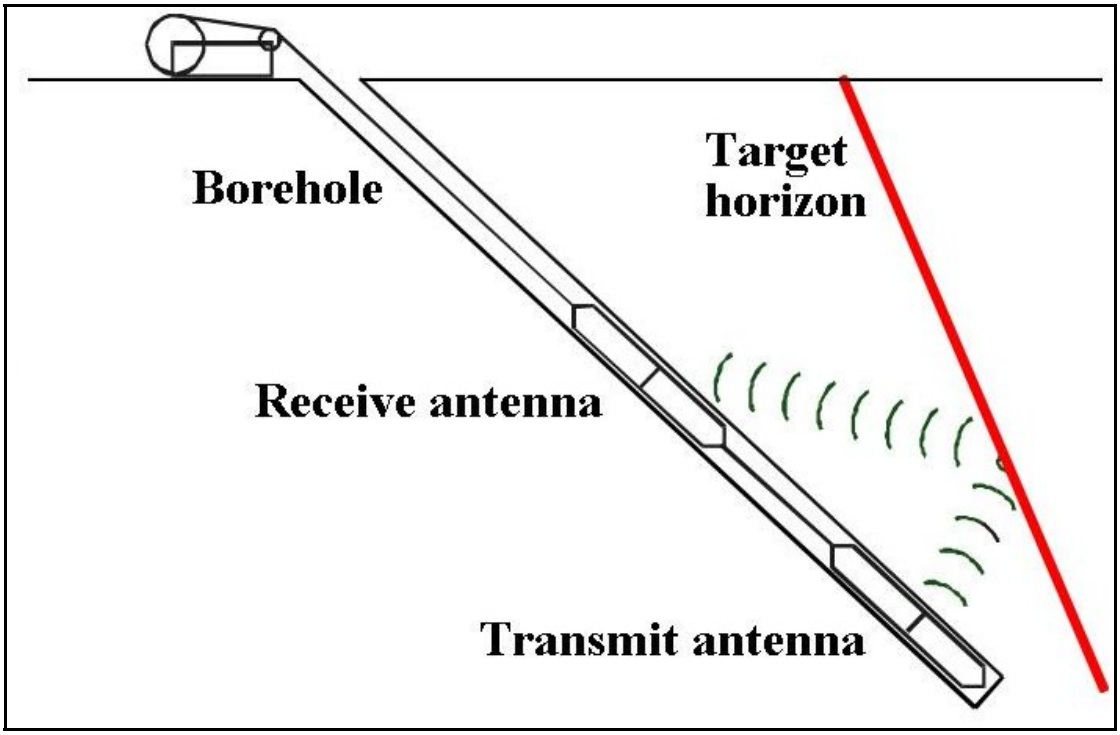

Figure 3: The optimal survey geometry for a borehole radar reflection survey orients the borehole parallel to sub-parallel to the intended radar target (Image courtesy CSIR)

3 THE MERENSKY REEF AT RPM AMANDELBULT SECTION

3.1 Regional setting of RPM Amandelbult Section

Anglo Platinum's Amandelbult Section is located in South Africa's Limpopo province (Figure 4). The mine is approximately 100 km north of Rustenburg and 40 km south of Thabazimbi. As seen in Figure 5, Amandelbult Section's lease area is in the shape of a rectangle with the long axis oriented NE-SW, and approximately 4 km wide on the short side and 20 km wide on the long side (Viljoen *et al.*, 1986b).

The topography surrounding the mine is relatively flat and the surface is covered by a thin layer of black turf soil. The only noticeable topography is a group of small hills to the south of the main entrance of the mine, which are locally termed *pyramid gabbros*. According to Viljoen *et al.* (1986b), these small hills form part of the Bushveld Complex's Main Zone, and they consist of gabbro-norite, which is the prevalent rock type in the Main Zone of the Bushveld Complex.

To the west and north of Amandelbult Section, the quartzites of the Transvaal Supergroup form the Witfontein Mountains. In the north-eastern part of the lease area, the Crocodile River runs from south to north.

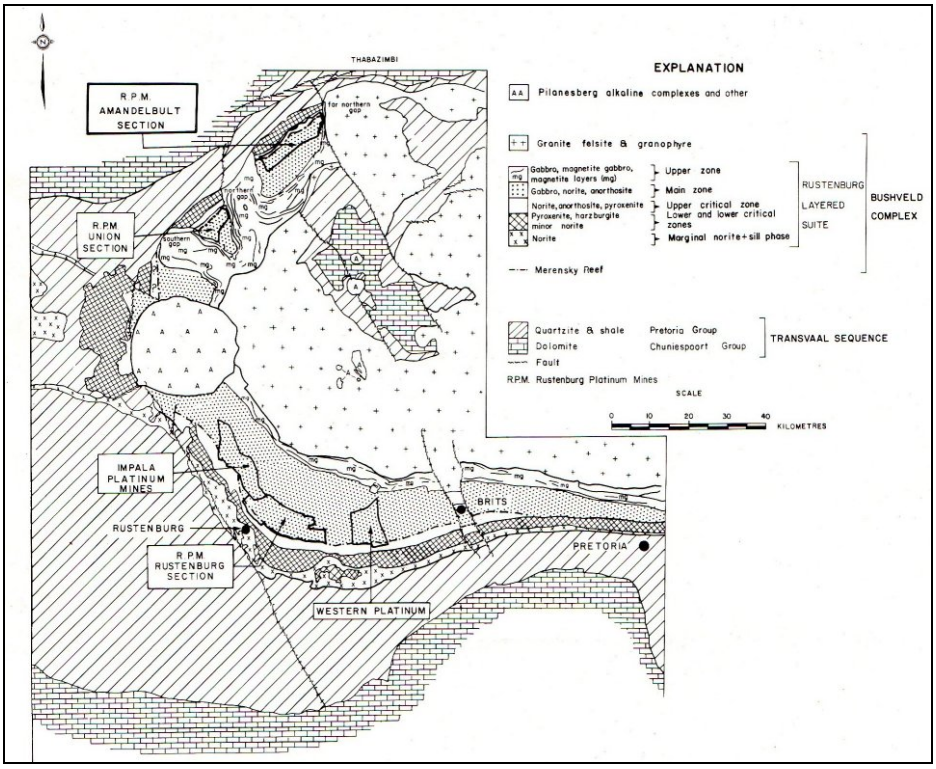

Figure 4: Locality plan showing Amandelbult Section in relation to the major geological rock types of the Bushveld Complex, after Viljoen *et al.*, 1986b

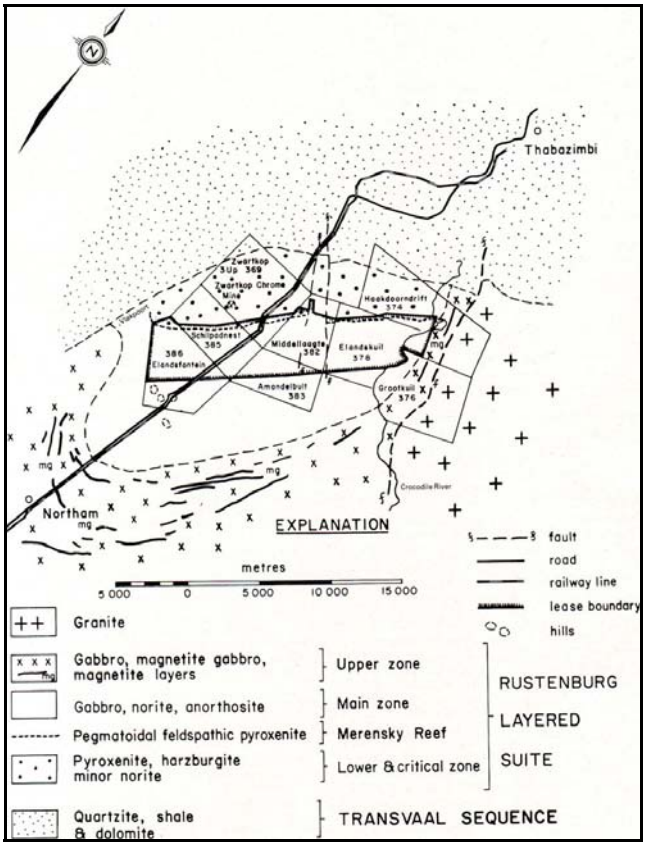

Figure 5: Map of Amandelbult Section's lease area, showing the main geological features and farm boundaries (Viljoen *et al.*, 1986b)

3.2 History of the Amandelbult Mine

The Merensky Reef was discovered by A.F. Lombaard in 1924 (Viljoen *et al.*, 1986b). Although the Merensky Reef was discovered in the Eastern Bushveld, almost all of the platinum mining that occurred up until the mid-Seventies in South Africa was due to the extraction of the Merensky Reef in the Western Bushveld (Cawthorn, 1999).

The Merensky Reef was discovered in the Western Bushveld near Rustenburg in 1925 (Viljoen *et al.*, 1986b), leading to more widespread exploration. Amandelbult Section was prospected in 1926 by the Steelpoort Platinum Syndicate. Shortly thereafter, ownership of Amandelbult transferred to Potgietersrust Platinum Limited, but interest in the area decreased during the 1930s' Depression, during which all platinum mining was suspended.

Rustenburg Platinum Mines (RPM), which eventually became part of Anglo Platinum, acquired the mineral rights for Amandelbult Section in 1964 and mining eventually commenced on the farm Schilpadsnest in 1974 (Viljoen *et al.*, 1986b). Platinum production at Amandelbult ceased in 1975 due to a slump in the platinum market, but after it restarted in 1976, production increased on a yearly basis (www.platinummetalsreview.co.za).

Currently both the Merensky and UG2 reefs are mined at Amandelbult Section. Amandelbult is expecting to increase the rate of equivalent refined platinum production to approximately 625,000 ounces in 2007 (Anglo Platinum Annual Report 2006).

3.3 Regional Geology of the Merensky Reef

The Merensky Reef occurs in the Upper Critical Zone of the Bushveld Complex. According to Viljoen (1999), the reef has been delineated for approximately 145 km in the Western Lobe of the Bushveld Complex. Underground and opencast extraction of the reef is taking place over a strike distance of approximately 90 km (Viljoen *et*

al., 1986b). The Merensky Reef's dip changes from approximately 9° to 12° as it is traced inwards towards the centre of the Bushveld Complex, with steeply dipping exceptions in parts of the complex.

The thickness of the Merensky Reef can vary between 2 cm and 14 m (Viljoen *et al.*, 1986b). Its down-dip extension has been traced with the help of seismic surveys for up to 50 km, and to depths of 6 km (Du Plessis and Kleinwegt, 1987). Since mining on the Merensky Reef commenced in 1929, a large amount of data has been gathered about this particular reef (Viljoen, 1999), and it is evident that the Merensky Reef varies dramatically regionally with regard to geology, mineralogy and PGE-grade distribution (Kinloch and Peyerl, 1990; Eales *et al*., 1993; Viljoen *et al.*, 1986a; 1986b; Viljoen, 1994; Eales and Cawthorn, 1996; Viljoen and Schürmann, 1998).

Viljoen (1999) says the Merensky Reef is typically a heterogeneous pegmatoidal feldspathic pyroxenite bounded by two thin chromitite layers, generally referred to as Bottom Chromitite and Top Chromitite. Viljoen (1999) continues to say that PGE-grades generally increase as the pegmatoidal nature of the reef increases.

This treatise does not examine grade distribution within the Merensky Reef, but concentrates on delineating the position of the reef in three dimensions for mining purposes.

3.4 Regional Geology of the Merensky Reef at Amandelbult Section

As seen in Figure 4, Amandelbult Section is located in the north-western lobe of the Bushveld Complex (Viljoen *et al.*, 1986b). The platiniferous layers, i.e. the Merensky and UG2 reefs, occur within a portion of the Lower, Critical and Main zones of the Bushveld Complex, with Upper Zone rocks above (Viljoen *et al.*, 1986b). The Upper Zone layers cut off the bottom three layers to the north and south of Amandelbult Section, resulting in an area known as the "northern gap" located to the south of the mine.

According to *A guide to the geology at Amandelbult*, which is an updated version of the geology of Amandelbult as described by Viljoen *et al.* (1986b), it has been established by underground workings that the Merensky Reef continues to the north-east of the mine.

3.5 Stratigraphy at Amandelbult Section

3.5.1 Stratigraphy related to borehole radar penetration and reflection

3.5.1.1 Radar penetration

For borehole radar to be successful, the radar waves need to travel from the borehole to the target surface, i.e. the rocks between the borehole and target surface need to be translucent to radar waves. As described by Du Pisani and Vogt (2003), the attenuation, or rate of decay, of radar waves is controlled by the conductivity of the rocks through which they are travelling. If the rocks between the borehole and target are too conductive, the radar waves will attenuate rapidly and not reach their intended target.

Radar attenuation is usually described through the loss tangent:

$$\tan\delta = \frac{\sigma}{\omega\varepsilon_r\varepsilon_0} \qquad (1)$$

As described by Vogt *et al.* (2005), the conductivity, σ, and permittivity, ε, are measured at a specific frequency, *f*. This frequency can be converted to the angular frequency ω, which is defined by $\omega = 2\pi f$. In equation (1), ε_r is the relative permittivity and $\varepsilon_0 = 8.854\times10^{-12}$ is the permittivity of free space.

Turner and Siggins (1994) explained that for most rocks suitable for GPR, the loss tangent is constant over the frequency range of the GPR instrument. Vogt (2000) showed that this constant loss-tangent estimation is an acceptable approximation to measured properties, when he analysed a database of 15,057 electrical property measurements. If a constant loss tangent is used, a nomogram from Noon *et al.* (1998)

for a smooth planar reflector (Figure 6) can be used to predict with how many wavelengths radar waves will penetrate into a rock with a given loss tangent.

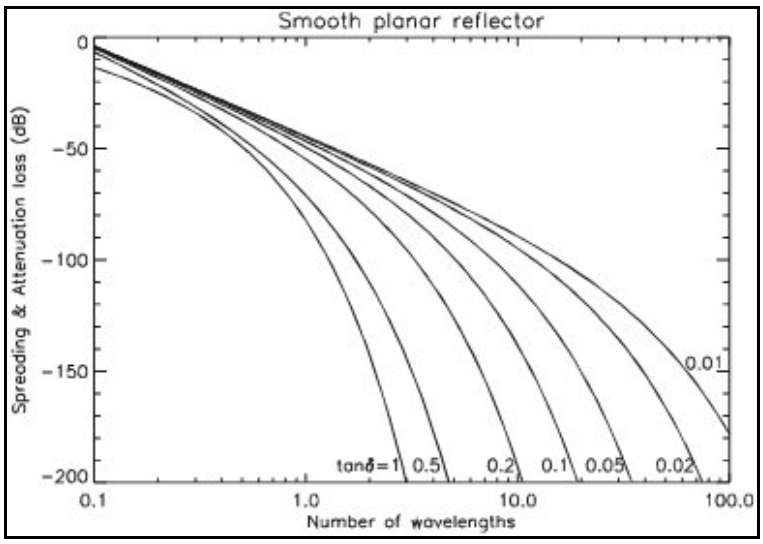

Figure 6: Radar performance prediction for a smooth planar target after Noon *et al.* (1998)

Between 1980 and 2003, Vogt measured the electrical properties of approximately 4,500 rock samples, at a range of frequencies from 1 MHz to 64 MHz, using the rock sample as a dielectric in a capacitor (Du Pisani and Vogt, 2003). Du Pisani and Vogt (2003) used this database to calculate loss-tangent values for some of the Bushveld Complex rocks related to the economic platinum horizons, i.e. anorthosite, norite and pyroxenite. The loss-tangent values at a frequency of 64 MHz were used, as this was closest to the centre frequency of the CSIR's Aardwolf BR40 used for the case study described in this treatise.

The distribution of the loss-tangent values for the three rock types are shown in Figure 7.

A (Anorthosite)

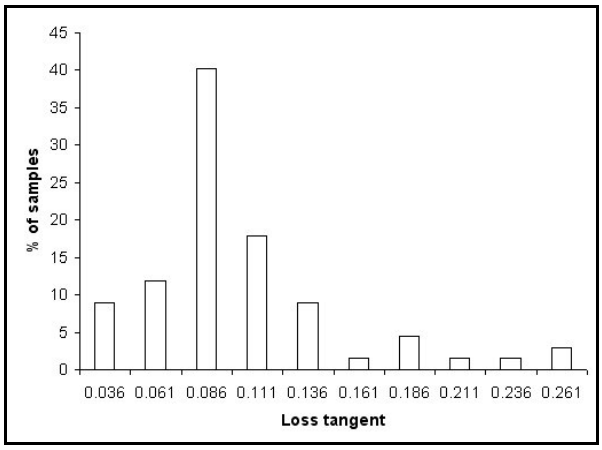

B (Norite)

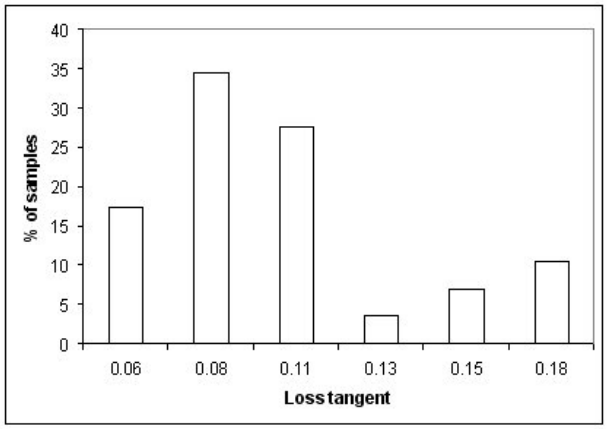

C (Pyroxenite)

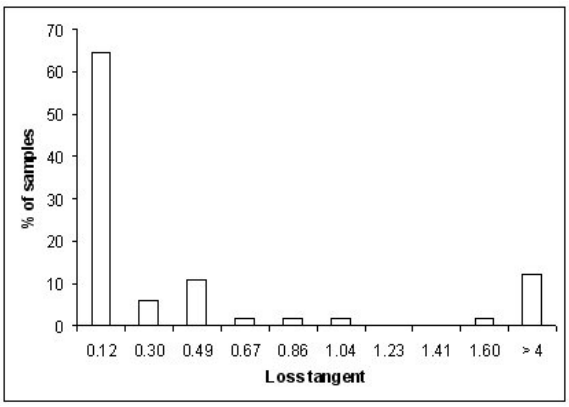

Figure 7: Distribution of loss-tangent values for (A) anorthosite, (B) norite and (C) pyroxenite after Du Pisani and Vogt (2003)

The system performance of the CSIR's Aardwolf BR40 is approximately 120 dB (Vogt, *pers comm*). As described by Du Pisani and Vogt (2003), the wavelength in metres can be estimated as 100/*f*, where *f* is the frequency in MHz. For a 40 MHz system, such as the Aardwolf BR40, the wavelength is then 2.5 m.

In Table 1, the typical loss-tangent values for anorthosite, norite and pyroxenite and their radar penetrations in these rocks, as determined from the nomogram in Figure 6, are summarised.

Table 1: The loss tangent and radar penetrations for anorthosite, norite and pyroxenite

Rock type	Loss tangent	Radar penetration (wavelengths)	Radar penetration (m)
Anorthosite	0.09	9	22.5
Norite	0.08	10	25
Pyroxenite	0.12	7	17.5

The radar penetrations shown in Table 1 are consistent with penetration achieved during experimental and commercial surveys conducted from 2001 to 2007 with the CSIR's Aardwolf BR40 system (Vogt, *et al.*, 2005; De Vries and Du Pisani, 2005).

3.5.1.2 Radar reflection

Radar reflection is controlled by a difference in permittivity between two adjacent materials though which the radar waves are travelling. According to Vogt *et al.* (2005), this difference in permittivity influences how much of the radar signal is reflected where two media border:

$$\Gamma = \frac{\varepsilon_2 - \varepsilon_1}{\varepsilon_2 + \varepsilon_1} \quad (2)$$

where ε_1 and ε_2 are the permittivities of medium 1 and medium 2 respectively. If medium 2 is very conductive, ε_2 approaches infinity and the entire radar signal will be reflected.

Du Pisani and Vogt (2003) compared the measured permittivity values of a number of samples from across the Bushveld Complex for anorthosite, norite and pyroxenite. The distribution of permittivity values for theses three rock types is shown in Figure 8.

A (Anorthosite)

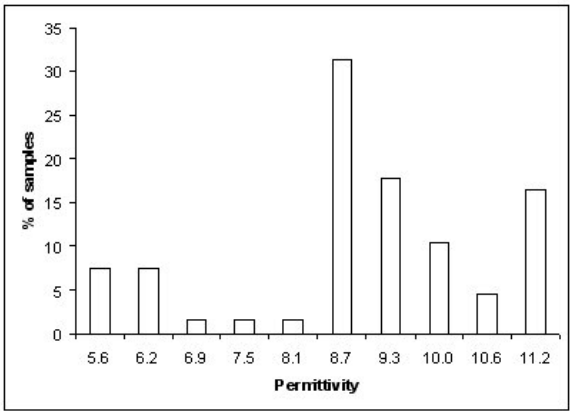

B (Norite)

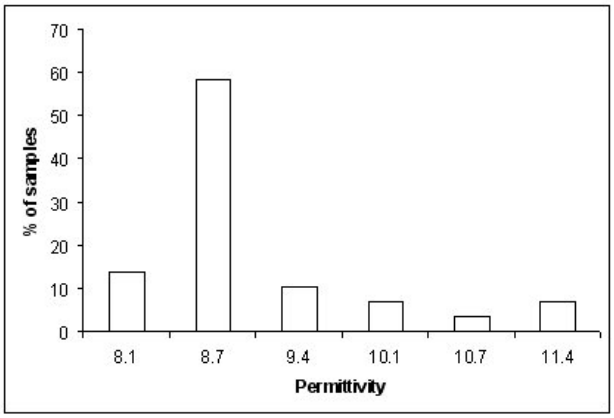

C (Pyroxenite)

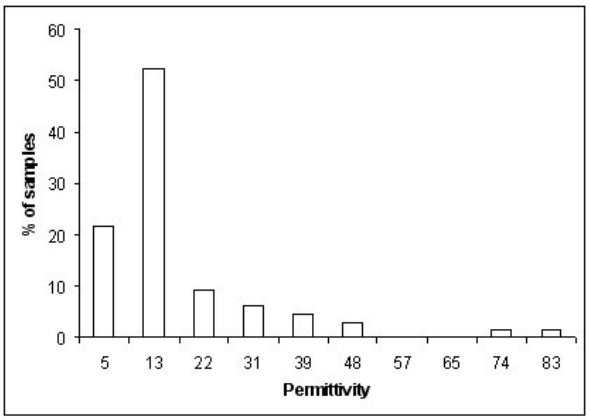

Figure 8: The distribution of permittivity values for (A) anorthosite (B) norite and (C) pyroxenite at a radar frequency of 64 MHz after Du Pisani and Vogt (2003)

As seen in Figure 8, the permittivity values for anorthosite and norite are very similar, hence the boundary between these two rock types is not expected to produce a significant radar reflector. The permittivity contrast between pyroxenite and either anorthosite or norite is much larger, and this boundary should produce a good radar reflector.

3.5.1.3 Radar stratigraphy at Amandelbult Section

The general stratigraphic column for the economic horizons at Amandelbult Section is given in Figure 9. The borehole radar holes used in the case study described in Section 5 were situated in the norite between the Merensky and Bastard reefs.

The distance that radar waves are expected to travel is indicated by the radar range shown in Figure 9. During initial test surveys carried out at Amandelbult Section at

the start of the Platmine borehole radar project in 2002, it was found that the P2 marker was a highly conductive unit that limited the penetration of radar waves. Hence radar waves are not expected to penetrate through the P2 marker.

In accordance with the findings presented by Du Pisani and Vogt (2003), the following boundaries (Figure 9), within the radar range, are expected to reflect radar waves:

- Reflector 1: Boundary between P2 marker (feldspathic harzburgite) and the norite above it.
- Reflector 2: Boundary between footwall mottled anorthosite and Merensky Reef.
- Reflector 3: Boundary between anorthosite and Bastard Reef (poikilitic pyroxenite).

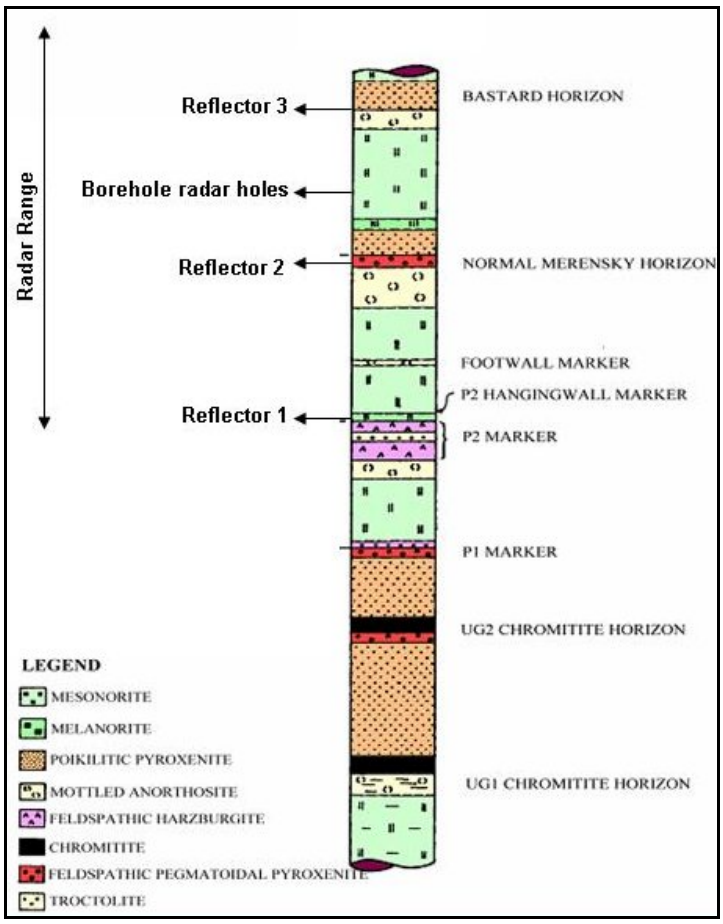

Figure 9: General stratigraphic column for Amandelbult Section, showing the position of the borehole radar holes, the expected radar reflectors and the range of the borehole radar instrument (stratigraphic column from *A guide to the geology of Amandelbult*)

Only the rocks that are within the borehole radar's range are discussed within the context of radar penetration and reflectivity in the next sections.
The units that are examined include:

- Upper pseudoreef (P2 marker)
- P2 hanging wall marker
- Footwall marker
- Merensky Reef unit
- Bastard Reef unit

3.5.2 Upper pseudoreef (P2 marker)

The P2 marker comprises feldspathic harzburgite (Viljoen *et al.*, 1986b). As seen in Figure 9, the immediate footwall of the P2 marker is anorthosite.

The P2 marker is split into two layers in the south-western part of Amandelbult mine (Viljoen *et al.*, 1986b). The lower P2 layer is approximately 3 m thick, and is separated from the top P2 layer by what is termed the *middling anorthosite* (0 m to 1.2 m). The top P2 layer can be up to 1 m in thickness. Both P2 layers usually have thin chromitite stringers at their base. To the north-east of the mine, the two P2 layers merge into one composite feldspathic harzburgite (Viljoen *et al.*, 1986b).

The overlying cycle of the P2 starts with a 10 mm-thick chromitite stringer (Viljoen *et al.*, 1986b), which provides a sharp reflective contact for radar waves. Above this thin chromitite there is approximately 10 cm to 15 cm of coarse pegmatoidal feldspathic harzburgite, which changes gradually into a 2 m-wide melanorite (Viljoen *et al.*, 1986b).

The dielectric properties of harzburgite have not been examined in detail, but it is the author's experience that the P2 is usually very conductive and that most of the radar signal is reflected back when this unit is encountered. Both the sharp chromitite boundary and coarse, conductive harzburgite contribute to the author's observation that radar waves generally do not penetrate through this unit.

According to Du Pisani and Vogt (2003), the boundary between pyroxenite and norite provides a good radar reflection, and even though the boundary between the harzburgite and norite is gradational, their difference in permittivity should contribute towards imaging the P2 with borehole radar.

3.5.3 P2 hanging wall marker

The P2 hanging wall marker is a remarkably consistent marker horizon consisting of an anorthosite layer on top of a pyroxenite layer (Viljoen *et al.*, 1986b) inside the melanorite above the P2 marker. This thin band is 10 cm to 15 cm thick, and occurs approximately 70 cm above the P2 marker. Even though the boundary between anorthosite and pyroxenite provides a good reflective target for radar (Du Pisani and Vogt, 2003), the vertical resolution of the Aardwolf BR40 instrument is in the order of 1 m (Vogt *et al.*, 2005), hence this thin marker horizon will not be detected with this instrument.

Upwards from the P2 hanging wall marker, the melanorite in which it occurs gradationally changes into norite and then into anorthositic norite until it reaches a very distinctive anorthosite band called the Footwall marker (Viljoen *et al.*, 1986b).

3.5.4 Footwall marker

The thin (40 cm to 50 cm) anorthosite Footwall marker occurs approximately 8 m above the P2 marker and approximately 10 m below the Merensky Reef (Viljoen *et al.*, 1986b). Above the Footwall marker there is 3 m to 5 m of norite, followed by 5 m to 6 m of poikilitic anorthosite, after which the bottom chromitite stringer, signifying the start of the Merensky Reef cycle, is reached (Viljoen *et al.*, 1986b).

According to Du Pisani and Vogt (2003), the contact between anorthosite and norite will not provide a significant radar contrast, hence it is not expected that any of the anorthosite-norite boundaries between the P2 pseudoreef and Merensky Reef will be imaged with borehole radar.

3.5.5 Merensky Reef unit

The Merensky Reef can vary significantly regionally (Viljoen, 1999), but it is broadly defined as "a mineralised zone within the ultramafic cumulate at the base of the Merensky cyclic unit" (Viljoen and Schürmann, 1998). The Merensky Reef is typically a heterogeneous pegmatoidal feldspathic pyroxenite (Viljoen and Schürmann, 1998), which may contain various sulphides such as pyrrhotite, pendlandite and chalcopyrite (Viljoen *et al.*, 1986b). The boundaries of the Merensky Reef are generally characterised by narrow (approximately 1 cm thick) chromitite stringers (Viljoen and Schürmann 1998).

At Amandelbult Section, the bottom chromitite stringer below the Merensky Reef is typically 5 mm to 15 mm thick (Viljoen *et al.*, 1986b). The contact with the underlying mottled anorthosite is usually very sharp, providing an excellent reflective surface for borehole radar.

The lower chromitite stringer then grades upwards into the pegmatoidal feldspathic pyroxenite and harzburgite of the Merensky Reef (Viljoen *et al.*, 1986b). According to Du Pisani and Vogt (2003), the boundary between anorthosite and pyroxenite has a significant permittivity contrast and it is expected that the chromitite stringer on this boundary will also contribute towards strengthening the dielectric contrast. Hence the bottom of contact of the Merensky Reef is expected to provide a strong radar reflector.

At Amandelbult Section, the Merensky Reef package can vary in thickness between 0 m and 5 m. Since the vertical resolution of the borehole radar instrument used in this study is approximately 1 m, it is expected that the Merensky Reef will only be imaged where it is thicker than 1 m. In the author's experience, however, layers thinner than 1 m have been imaged using 40 MHz to 50 MHz borehole radars, especially where a significant contrast in the permittivity was present between two layers (Chalke *et al.*, 2006). Since there is a significant contrast between the Merensky Reef and its underlying layers, together with the sharp chromitite boundary, it is expected that the Merensky Reef will be imaged even where it is thinner than 1 m.

The top contact of the Merensky Reef is also characterised by a thin chromitite layer, which is normally not thicker than 20 mm (Viljoen *et al.*, 1986b). Above this chromitite stringer there is a thin layer of poikilitic feldspathic pyroxenite which gradationally changes into norite (Viljoen *et al.*, 1986b).

Since the contact between the Merensky Reef pyroxenite and its overlying pyroxenite is essentially a contact between two similar rock types, the top Merensky Reef contact is not expected to be a good radar reflector. Furthermore, the hanging wall pyroxenite above the top Merensky chromitite stringer grades into norite and although the boundary between pyroxenite and norite provides a good radar reflector (Du Pisani and Vogt, 2003) due to the gradational transition, a radar reflection is not expected.

The norite layer above the Merensky Reef is topped by a prominent mottled anorthosite, which is 2 m to 3 m thick (Viljoen *et al.*, 1986b). According to Du Pisani and Vogt (2003), the boundary between norite and anorthosite does not have enough of a dielectric contrast to produce a radar reflection.

The entire Merensky Reef cyclic unit from the pegmatoidal pyroxenite to the mottled anorthosite is typically approximately 16 m thick (Viljoen *et al.*, 1986b).

3.5.6 Bastard Reef unit

The Bastard Reef cyclic unit is very similar to the Merensky Reef cyclic unit, except that this cycle is spread over a thickness of 32 m, where the Merensky unit is 16 m thick (Viljoen *et al.*, 1986b). The lower portion of the Bastard Reef cycle does not contain pegmatoidal pyroxenite and it is also not characterised by a thin chromitite base (Viljoen *et al.*, 1986b). Instead, the Bastard Reef usually consists of a fine-grained pyroxenite that changes gradationally into norite.

Since the poikilitic pyroxenite at the base of the Bastard Reef unit has a sharp contact with the underlying mottled anorthosite, this contact should produce a good radar

reflection. According to Du Pisani and Vogt (2003), the contact between anorthosite and pyroxenite will produce a good radar reflection.

3.5.7 Notes on the UG2 chromitite

As seen in Figure 10 when normal Merensky Reef is present, the UG2 chromitite is expected 38.3 m beneath the Merensky Reef. The radar waves are not expected to travel all the way from the borehole (drilled in Merensky Reef footwall norite) to the UG2 due to two reasons:

1. The UG2 is too far from the borehole.
2. The feldspathic harzburgite P2 marker is expected to attenuate the radar signal.

In order to evaluate the topography of the UG2 Reef with borehole radar, new radar boreholes would have to be drilled below the P2 marker.

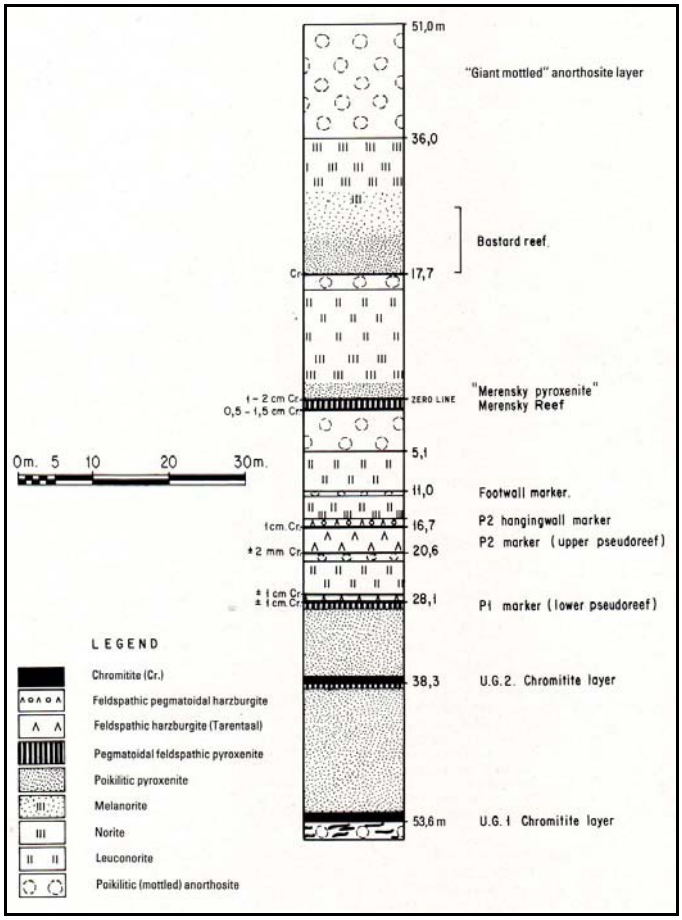

Figure 10: Stratigraphic column for the economic reefs at Amandelbult Section after Viljoen *et al.*, 1986b

4 POTHOLES

4.1 Potholes in the Western Bushveld Complex

Irvine (1982) and Kruger (1990) described the Merensky Reef as paraconformable with the underlying cumulates. According to Viljoen and Schürmann (1998), the Merensky Reef forms a regional discontinuity in the western lobe of the Bushveld Complex. Viljoen (1999) describes how the Merensky Reef can slump into its footwall layers to form structures broadly termed *potholes*. According to Carr *et al.* (1994), Merensky Reef potholes are significant disruptions to the normal magmatic layering in the Upper Critical Zone of the Bushveld Complex.

According to Viljoen *et al.* (1986b), potholes are circular or elliptical in plan view, and Viljoen (1999) states that a pothole can slump downwards for 1 m to tens of

metres. It is also possible for the Merensky Reef to transgress downwards in a step-like fashion (Viljoen and Schürmann, 1998), with steps associated with steep portions of thin contact reef. As the reef cascades downwards, it is also possible for mineralised reef to form on various footwall units (Viljoen and Schürmann, 1998).

Various types of pothole structures and pothole reefs have been classified and identified (Farquar, 1986; Leeb du Toit, 1986; Viljoen and Hieber, 1986; Kinloch and Peyerl, 1990; Viljoen *et al.*, 1986a; 1986b; Schürmann, 1991).

Wagner (1929) divided the Western Bushveld Complex rocks into the Rustenburg facies to the south of Pilanesberg and the Swartklip facies to the north. These two facies were then sub-divided into subfacies, which can, among other things, be distinguished by the abundance, size and type of potholes present (Figure 11).

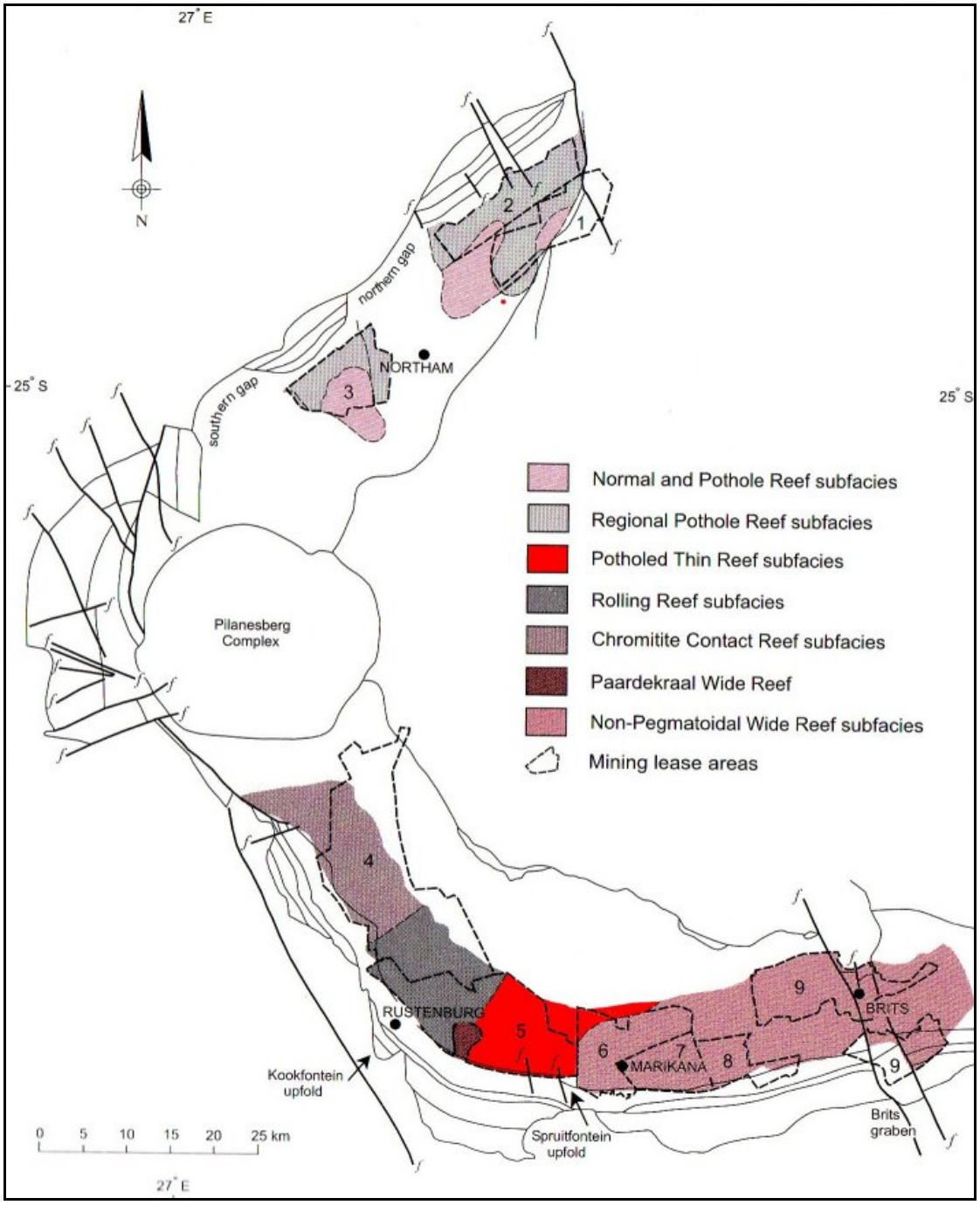

Figure 11: Merensky Reef facies map for the Western Bushveld Complex, after Viljoen and Schürmann (1998)

4.2 Potholes at Amandelbult Section

According to Viljoen *et al.* (1986b), potholes at Amandelbult Section are similar to potholes elsewhere in the Bushveld Complex in that the Merensky Reef and its hanging wall plunge abruptly and transgress their footwall layers.

Viljoen *et al.* (1986b), documented the potholes they were aware of at Amandelbult Section, according to their size, shape and distribution, as shown in Figure 12.

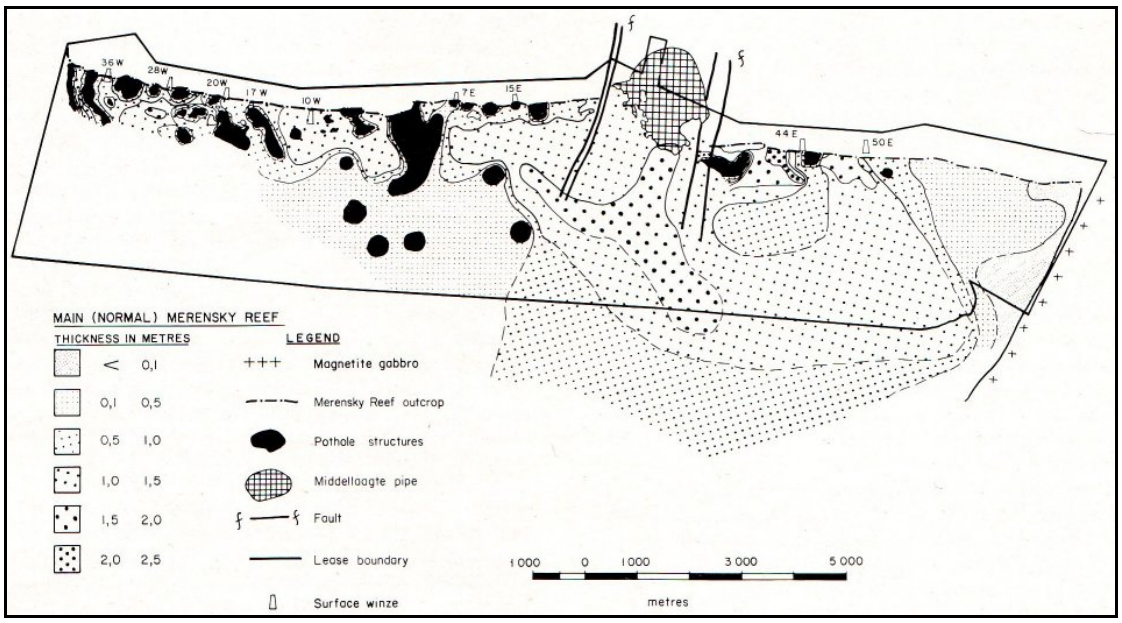

Figure 12: Distribution of pothole structures and isopach map for normal Merensky Reef at Amandelbult Section after Viljoen *et al.*, 1986b

According to Viljoen (1994), a local, rapid thinning of the Merensky Reef is evident towards the edges of individual potholes, especially at Amandelbult Section (Figure 13). Viljoen *et al.* (1986b), state that contact-type reef is usually developed around and on the edges of potholes. They further describe how the top and bottom chromitite stringers associated with the top and bottom contacts of the normal Merensky Reef converge and can even merge into a single chromitite layer with hanging wall poikilitic pyroxenite above and footwall mottled anorthosite below. This thin chromitite contact is called *contact reef* (Viljoen, 1994) and according to Viljoen *et al.* (1986b), it can transgress downwards and cut across the footwall succession. This contact reef may be mineralised, but due to its unpredictable behaviour and thinness, it is often not viable to mine it (Viljoen *et al.*, 1986b).

At the base of the pothole structure, the contact-type reef approaches the upper pseudoreef or P2 (Viljoen *et al.*, 1986b). Here, pegmatoidal feldspathic pyroxenite, which is very similar to normal Merensky Reef, occurs directly above the P2. This reef is called *pothole reef* and it is typically about 16 m below the normal Merensky Reef elevation (Viljoen, 1994). The generalised pothole model as given in *A guide to*

the geology of Amandelbult is shown in Figure 14, where it is also evident that the footwall of the pothole reef is the feldspathic harzburgite of the P2 as opposed to the mottled anorthosite of the normal Merensky Reef.

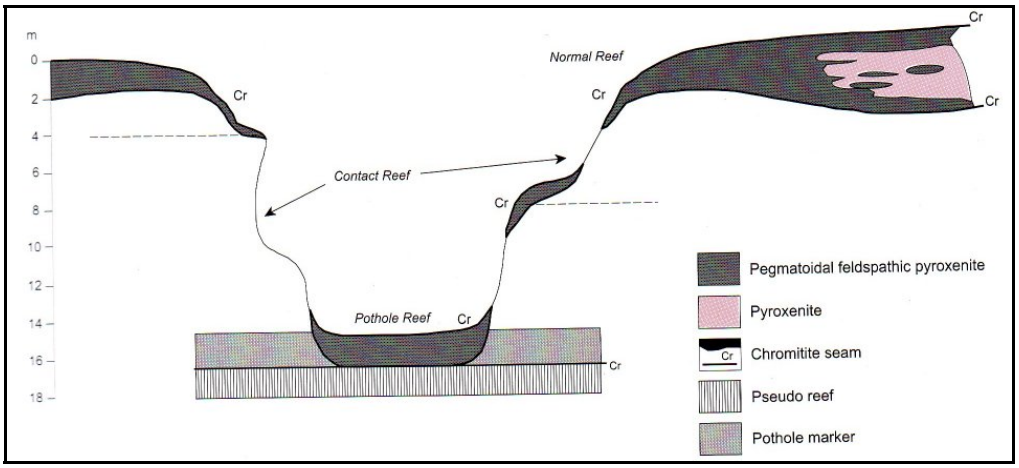

Figure 13: Generalised pothole model for the potholes within the Swartklip facies as developed by Viljoen (1994)

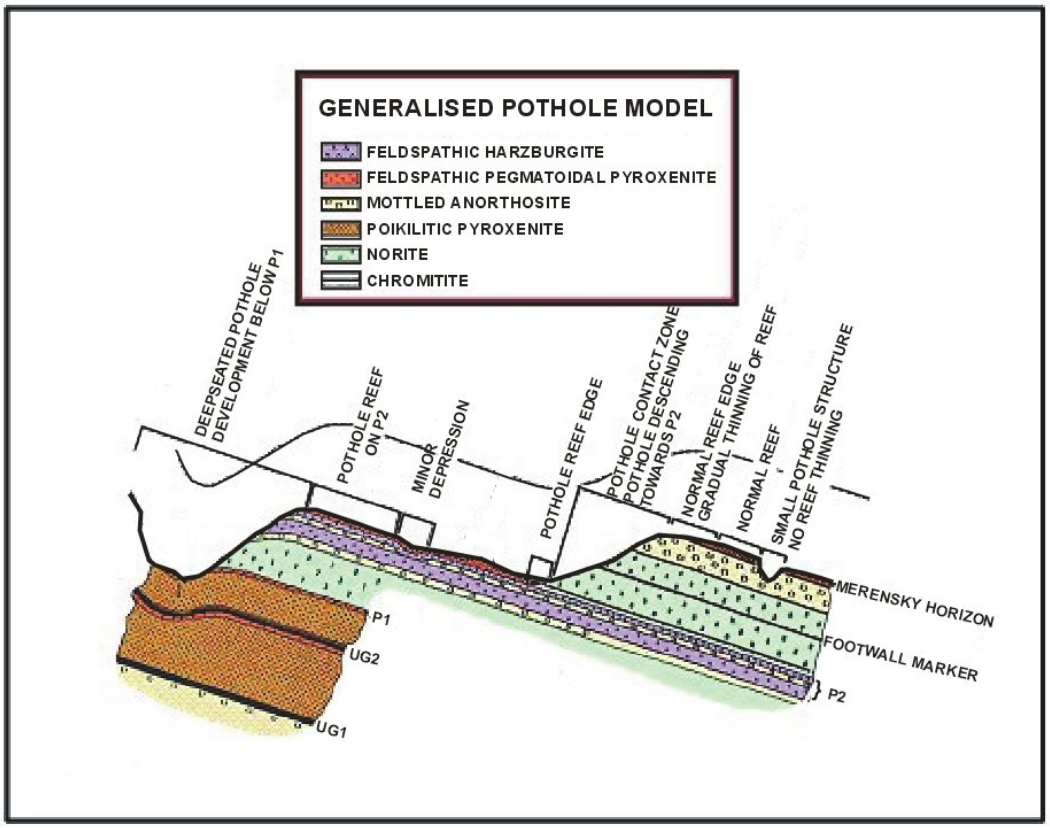

Figure 14: Generalised pothole model for pothole formation at Amandelbult Section from *A guide to the geology of Amandelbult*

4.3 The influence of potholes on mining

4.3.1 Mining of the Merensky Reef at Amandelbult Section

The Merensky Reef topography is initially estimated by extrapolating reef intersections from deep exploration boreholes. From these boreholes, the general dip and strike of the ore body is approximated. 3D-Seismic surveys from the surface provide a more continuous picture of the Merensky Reef and valuable information on large potholes and structures that could negatively affect the positioning of expensive capital expenditure such as main and ventilation shafts.

Thin Merensky Reef types are generally mined by narrow (80cm to 100cm) conventional breast stoping methods (Viljoen, 1994). From deep vertical shafts sunk through the ore body, haulages are developed parallel to the strike of the reef, approximately 30 m below it (Figure 15). Horizontal cross-cuts are then developed towards the dipping reef plane (Figure 16A). Raise lines are excavated in the dip direction on the reef elevation (Figure 16B). Mining then commences in panels, with face widths of typically 35 m, from opposite raises (Figure 16C). At the end of the mining process, a natural dip pillar is left in the middle of the mining block to provide support.

In the case study presented in this treatise, borehole radar was used to delineate a mining block bounded by two cross-cuts and a haulage, i.e. a block of approximately 200 m by 200 m.

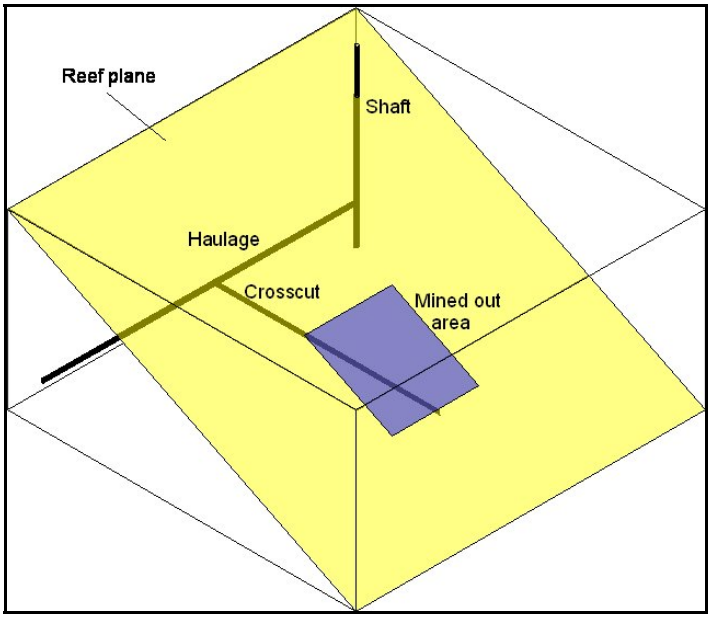

Figure 15: Diagram showing the simplified methodology for conventional breast stoping

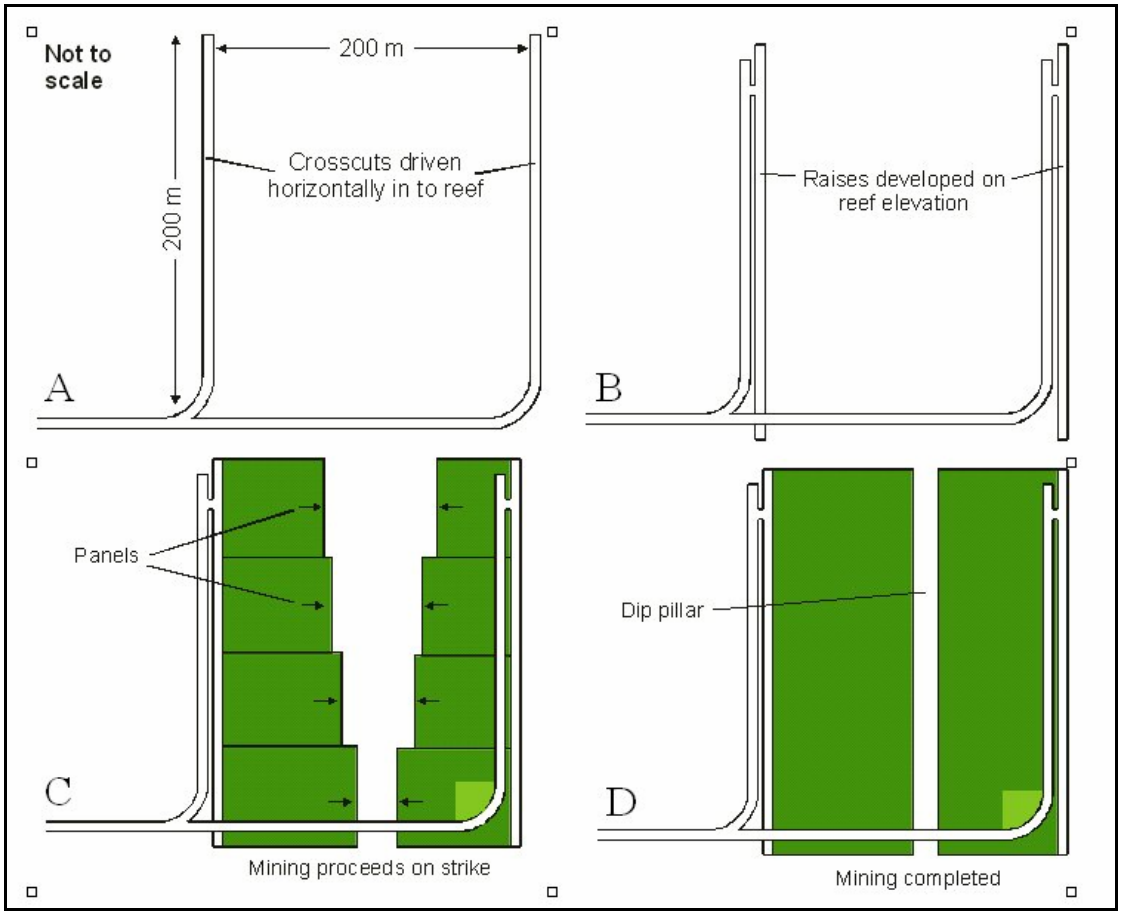

Figure 16: The process of mining thin reefs using conventional breast stoping: (A) Cross-cuts are developed from the haulage to the reef. (B) Raises are developed along the reef elevation. (C) Panels are mined out from opposite raise lines. (D) A dip pillar is left in the middle of the mining block to provide support. (After Du Pisani and Vogt, 2004)

4.3.2 Influence of potholes in mining the Merensky Reef at Amandelbult Section

According to Viljoen (1994), for normal Merensky Reef within the Swartklip facies, which is up to 150 cm thick, the entire reef package is mined together with its bounding chromitite stringers.

If the reef is thicker than 150 cm, the position of the mining cut is based upon the vertical grade distribution of the Merensky Reef as described by Viljoen (1994). Viljoen (1994) states that for the Merensky Reef within the Swartklip facies (thicker than 150 cm), it is usually the top portion of the reef package that is mined, and that the bottom pegmatoidal portion and lower chromitite band are left behind.

Potholes in the Swartklip facies are usually identified from local thinning and, according to Viljoen (1994), the proximity to a pothole can potentially be inferred by monitoring reef thickness and gradient. As pothole reef typically occurs approximately 16 m below the normal Merensky Reef elevation (Viljoen, 1994), mine excavations need to be redeveloped at a lower elevation to access portions of pothole reef.

Viljoen (1994) advises that an assessment be made of the pothole reef, and the intermediary contact reef between the normal and pothole reef, before mining decisions are concluded. He states that due to the irregularity and unpredictable nature of the contact reef, it is regularly unmineable, and that if a long section of irregular contact reef is present between the normal and pothole reef, it will lead to a section of total reef loss.

According to the on-shaft geologist (Marais, *pers comm*) at the time of the borehole radar surveys, current practice for predicting potholes is:

- Outlines of potholes are based on information gathered from the surface as well as underground drilling and mapping in stope panels.
- When a pothole is intersected in an underground borehole, a fan of boreholes is drilled in order to determine the extent of the pothole.

- In ideal situations the miners notify the geologist as soon as they encounter a pothole in the stope. If a pothole is detected in the stope, the geologist goes to that working area and tries to map it, and then plots it on to the 1:1000 working plans for that area.
- The interpretation of geological structures on the working plans is always a combination of information from boreholes and underground mapping.

At Amandelbult Section, a pothole is considered significant when it fills up one-third of a mining panel, i.e. it has a diameter of roughly 10 m to 12 m. According to Marais (*pers comm*), miners are supposed to notify the geologist as soon as they intersect a pothole while stoping. Once the miners have notified the geologist of a pothole intersection, he will then visit the panel and make a recommendation either to stop the panel, if the pothole is large enough, or to advance until such a time that the panel comprises one-third of the total panel length. The geologist's recommendations are put in writing and sent to the production manager, section manager, mine overseer and shift supervisor, as well as the shaft surveyor and shaft rock engineer. Transgression of the geologist's recommendations could be liable to disciplinary procedures. Marais (*pers comm*) stresses that the above scenario is the ideal situation. He further states that miners are compensated per square metre advanced and not for ounces of PGE-minerals delivered to the processing plant, and that in some cases miners will not disclose that they have encountered a pothole. In such a case, waste material will then be sent to the plant. Daily reports from the plant will immediately alert managers when the head grade drops significantly. When this happens, "grade raids" are done by the surveyors and geologists, during which all stope panels will be visited within the space of two days to check for off-reef mining.

Marais (*pers comm*) does, however, say that generally there is good cooperation between most miners and their line management and that tools such as photogrammetry (a photographic report of sample sections) could alert the geologist to the existence of a pothole on a panel. The geologist will then investigate and report on his findings.

The geological losses due to potholes at Amandelbult Section are estimated to be between 20% and 22% (Marais, *pers comm*). The term *geological losses* refers to areas of the ore body that are unmineable due to geological features such as dykes, iron-rich ultramafic pegmatites, faults and in this case potholes.

Through cover drilling the geologist can get an idea that mining may be approaching a pothole, but cover drilling only gives point-information that can make it difficult to extrapolate pothole boundaries from one borehole to the next. Borehole radar can provide a continuous illumination line of coordinates highlighting the pothole contact; that is, if the physical properties of the rocks and survey geometry are optimal.
Through the application of borehole radar it is endeavoured to:

- Predict the position of potholes before they are mined into.
- Track the thinning of the normal Merensky Reef as it approaches a pothole.
- Locate portions of mineable pothole reef.

It must, however, be stressed that borehole radar cannot provide an indication of the reef grade. It can only delineate the position of the reef more accurately.

5 CASE STUDY

5.1 Introduction

In the Platmine collaborative research programme, the CSIR relies on the participating mining companies to supply case-study sites for their research. A case-study site was identified at Anglo Platinum's Amandelbult Section. The mine geologist selected an area of the mine where mining had ceased due to a number of potholes being encountered while mining. The aim of the borehole radar surveys conducted in four boreholes was to see whether borehole radar could be used to delineate pothole boundaries. The borehole radar surveys were conducted in November 2005.

5.2 Borehole radar survey design

The survey design was based on delineating a mining block defined by the area between two cross-cuts (or raise lines) and the haulage from which these cross-cuts were developed.

A number of survey layouts were considered. The survey layout needed to:

- Cover as much of the mining block as possible.
- Eliminate the necessity for developing too many cubbies from which to drill the boreholes required for borehole radar.

Some of the survey designs that were considered are shown in Figure 17.

Designs A to D were all deemed impractical due to the fact that the drill rig would have to be moved a number of times in order to drill all the boreholes required to cover the mining block. Using more than one drill rig to drill holes simultaneously was also considered impractical for a test study, since drill rigs were being used for other drilling purposes (such as cover drilling) in other sections of the mine.

It was decided that drilling a fan of boreholes from a single cubby as seen in Figure 17E, some distance along a cross-cut, would provide sufficient cover of the mining block and eliminate having to move the drill rig unnecessarily. The two boreholes numbered 1 and 8 were eliminated from the plan, because they would be too close to the cross-cut, and the reflection produced by the cross-cut would mask reflections produced by the reef.

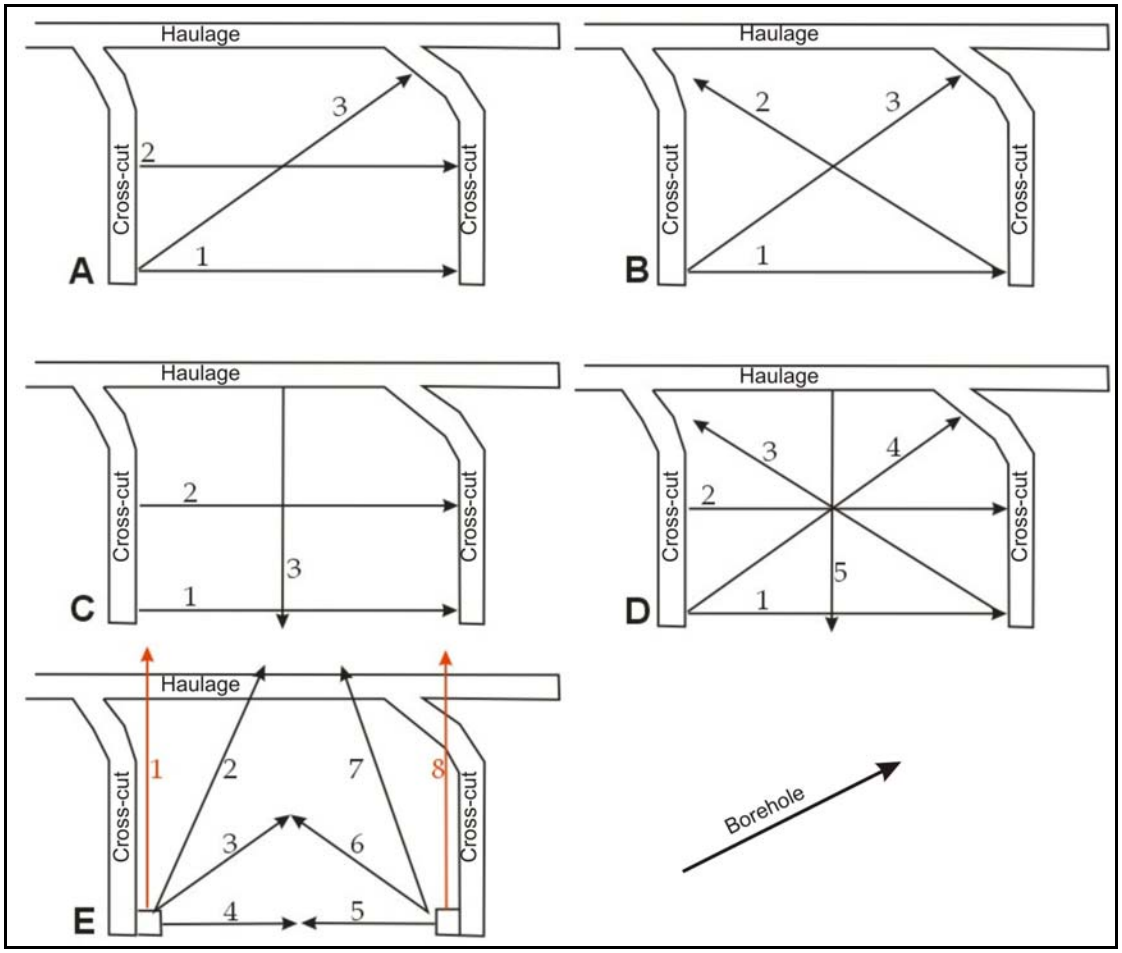

Figure 17: Borehole layouts considered for the borehole radar case study at Amandelbult Section. The arrowed lines indicate possible borehole positions.

The radar boreholes were drilled at Amandelbult 10-Level, from 9W cross-cut. Access was only available from one cross-cut, hence only one fan of boreholes was drilled, aiming to cover the entire block bounded by 9W and 8W cross-cuts by using longer boreholes as planned in Figure 17E. The survey layout is shown in plan in Figure 18, where the red lines represent the borehole radar holes and the purple dots represent some of the geological boreholes drilled for reef intersection within the area.

The radar boreholes were planned to cover the entire mining block bounded by 9W and 8W cross-cuts on 10-Level. The boreholes were drilled up to 250 m each, in order to provide the required coverage, but due to operational problems and borehole blockages, not one of the holes were surveyed with borehole radar up to 250 m. The coverage provided by the actual radar survey lengths is represented in Figure 18.

In Figure 19, a map is presented that shows the location of the boreholes drilled for borehole radar in relation to all the geological boreholes drilled for reef intersection in the vicinity of the borehole radar survey area.

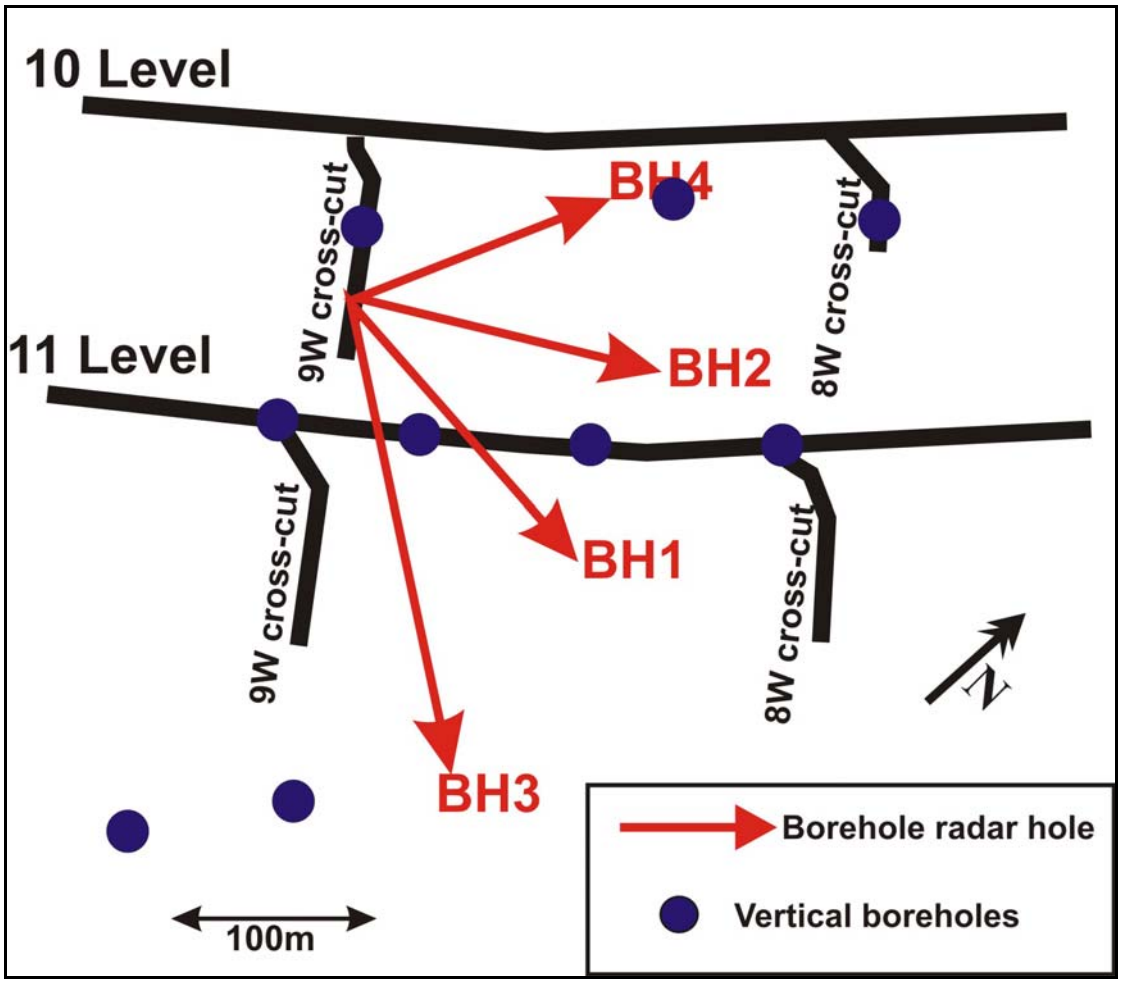

Figure 18: Simplified mine plan showing the positions of the four boreholes drilled for borehole radar as red lines and the location of geological reef intersect boreholes

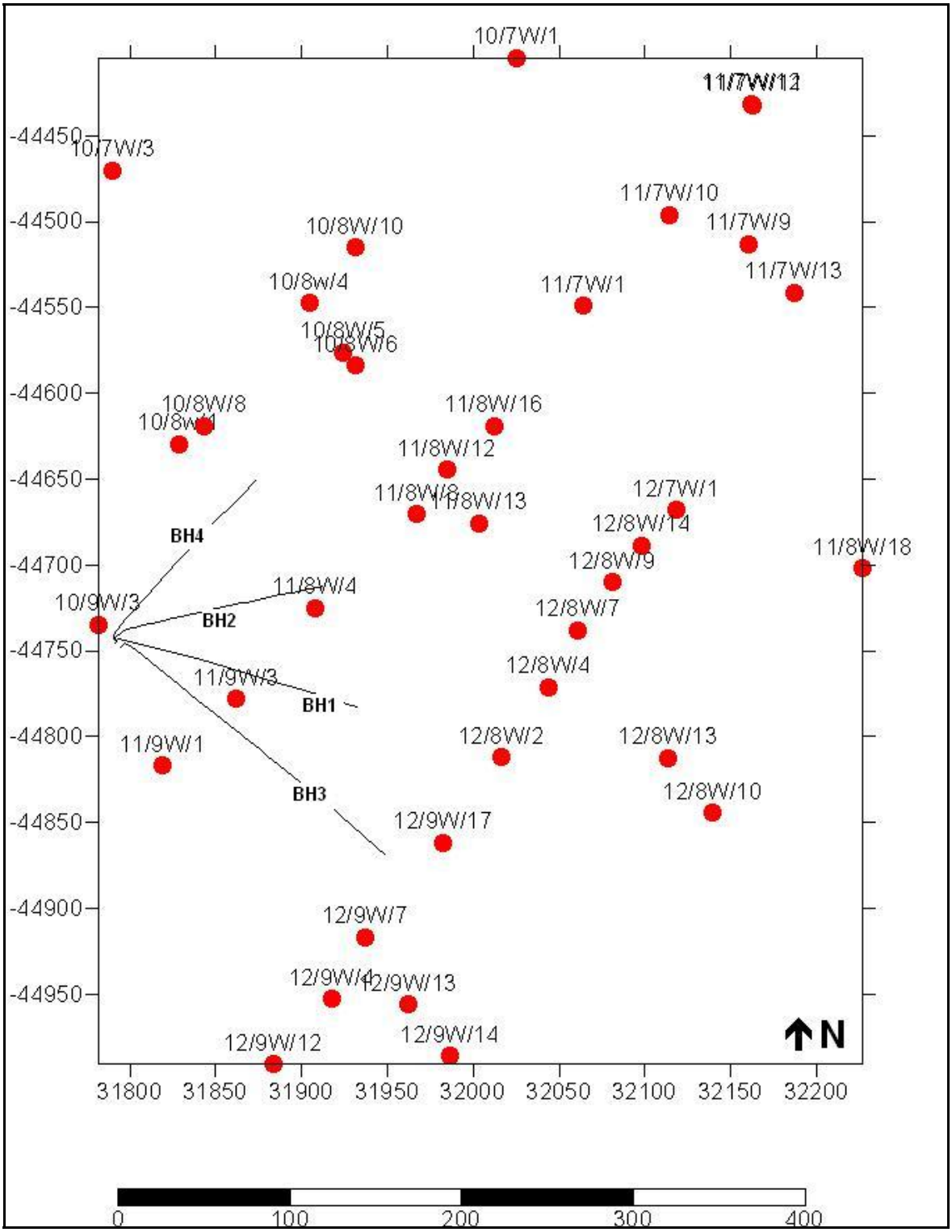

Figure 19: The location of the borehole radar holes in relation to some of the geological drilling in the vicinity

The boreholes were drilled in the norite between the Merensky and Bastard reefs (see the stratigraphic column in Figure 9). As described in Section 3, the bottom contacts of both the Merensky and Bastard reefs are expected to produce radar reflections.

The boreholes were angled away from the Merensky Reef and towards the Bastard Reef so that these two reflectors could be distinguishable on the radargrams. A radargram acquired for borehole 1 is shown in Figure 20A to demonstrate how the two radar reflectors produced by the Merensky and Bastard reefs could be distinguished from one another. At the collar of borehole 1, it is close to the Merensky Reef and far from the Bastard Reef. As we progress along the borehole, the borehole moves further away from the Merensky Reef and closer to the Bastard Reef. Hence, the Merensky Reef reflector on the radargram starts close to the borehole position at 0m along the x-axis, and moves further away from the borehole position as we progress along the borehole. The Bastard Reef reflector starts far from the borehole position at its collar and moves closer to the borehole. Both reflectors manifest within the two-dimensional space of the radargram as a function of their distance away from the borehole.

Figure 20B provides a schematic showing the positions of the Bastard and Merensky reefs above and below the borehole respectively.

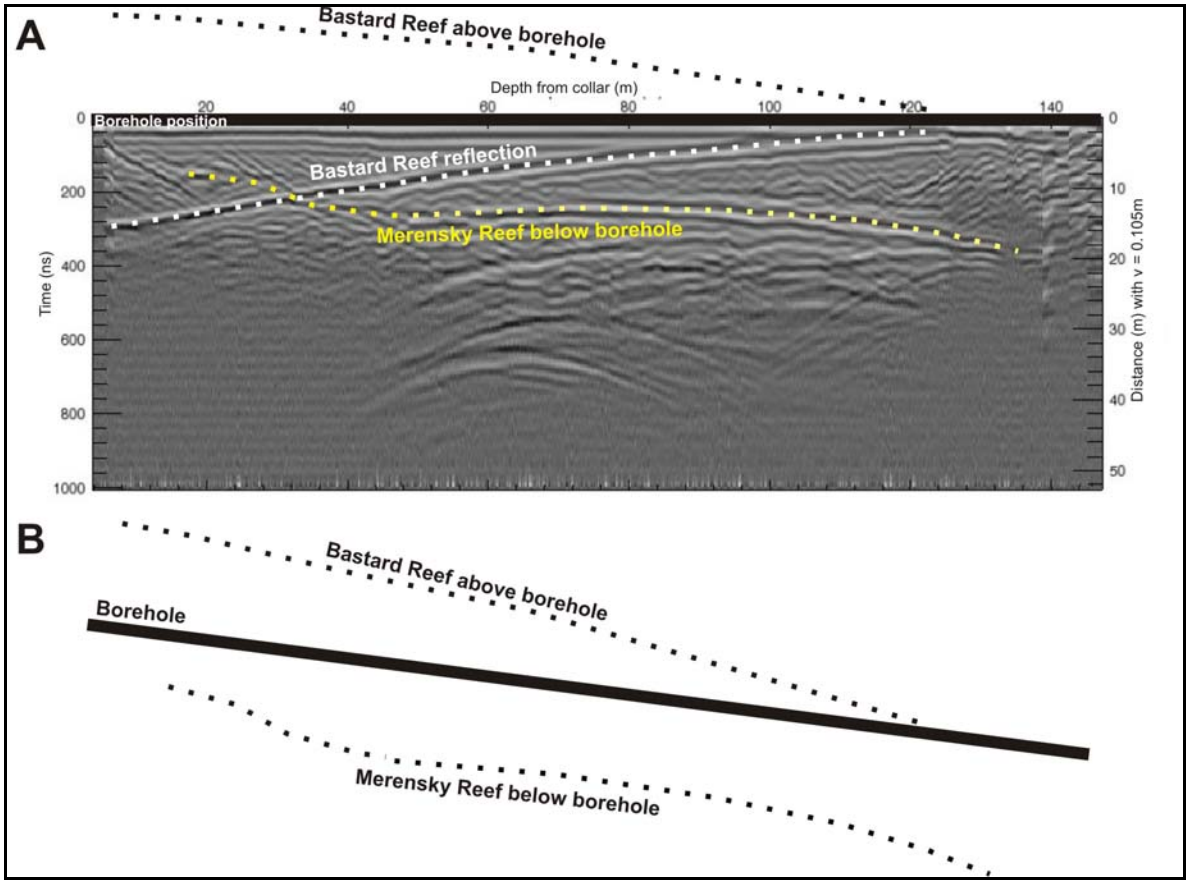

Figure 20: A) Radargram for borehole 1 showing how the Merensky and Bastard Reef reflectors plot at similar distances away from the borehole position; and

B) Schematic showing the Bastard Reef position above the borehole and the Merensky Reef below the borehole.

The basic planned case-study layout is shown in section in Figure 21. The boreholes are indicated by slanted red lines. In Figure 22, the positions of the radar boreholes are shown in section in the software package that was used to conduct the borehole radar modelling. Both Figure 21 and Figure 22 show the planned borehole positions prior to conducting the surveys and radar modelling. In reality, some boreholes started much closer to the Merensky Reef and in some cases the boreholes even started inside the Merensky Reef unit.

The boreholes could not be drilled below the Merensky Reef due to access problems and due to the presence of the very conductive harzburgite layer, the P2, through which radar waves are generally not able to penetrate, as discussed in Section 3. The boreholes were numbered by the drilling contractor from north to south in the

following order: BH4, BH2, BH1 and BH3 (where BH is an abbreviation for "borehole").

The drilling inclination and radar survey length for each borehole is summarised in Table 2.

Table 2: Borehole information for the radar boreholes

Borehole	Inclination	Radar survey length (m)
BH4	+ 16 °	132
BH2	+ 6 °	132
BH1	- 7 °	147
BH3	- 12 °	200

These boreholes were drilled specifically for the application of borehole radar surveys and according to recommendations from the CSIR, namely:

- The boreholes were drilled sub-parallel to the expected Merensky Reef plane.
- The boreholes were close enough to the Merensky Reef so that radar waves could reach it, i.e. within 30 m.
- The boreholes were not drilled to provide Merensky Reef intersection for grade information.

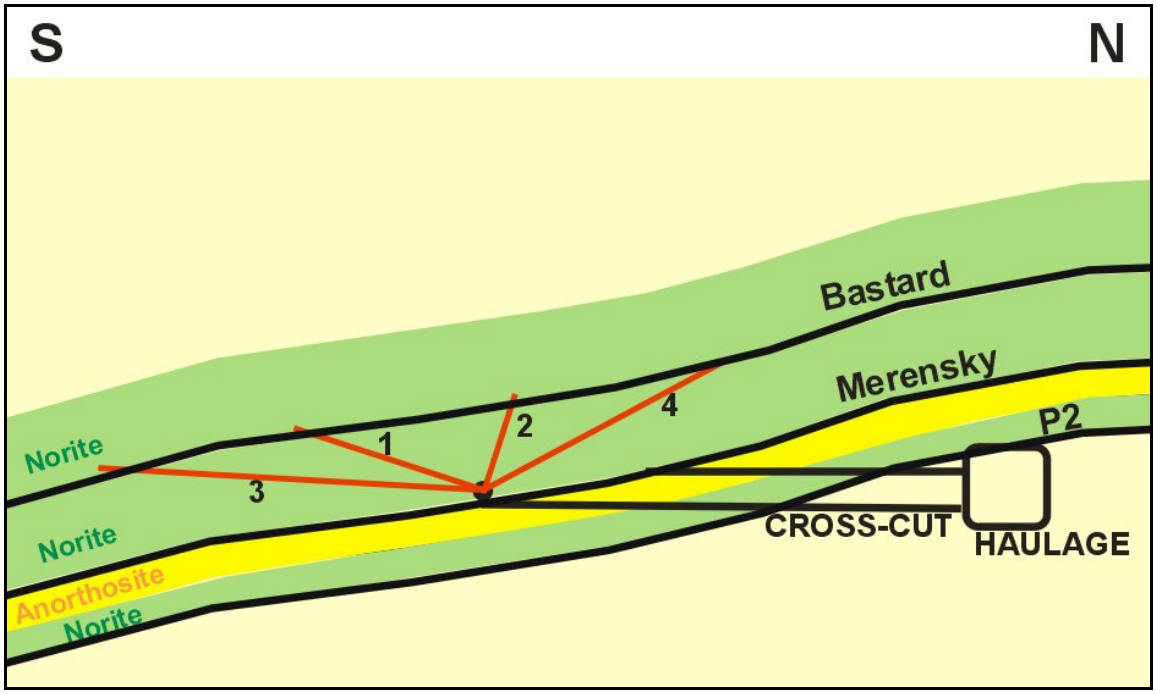

Not according to scale

Figure 21: Schematic showing the case-study layout in section (looking from the east), with the boreholes (red lines) drilled between the Bastard and Merensky reefs, with boreholes angled towards the Bastard Reef

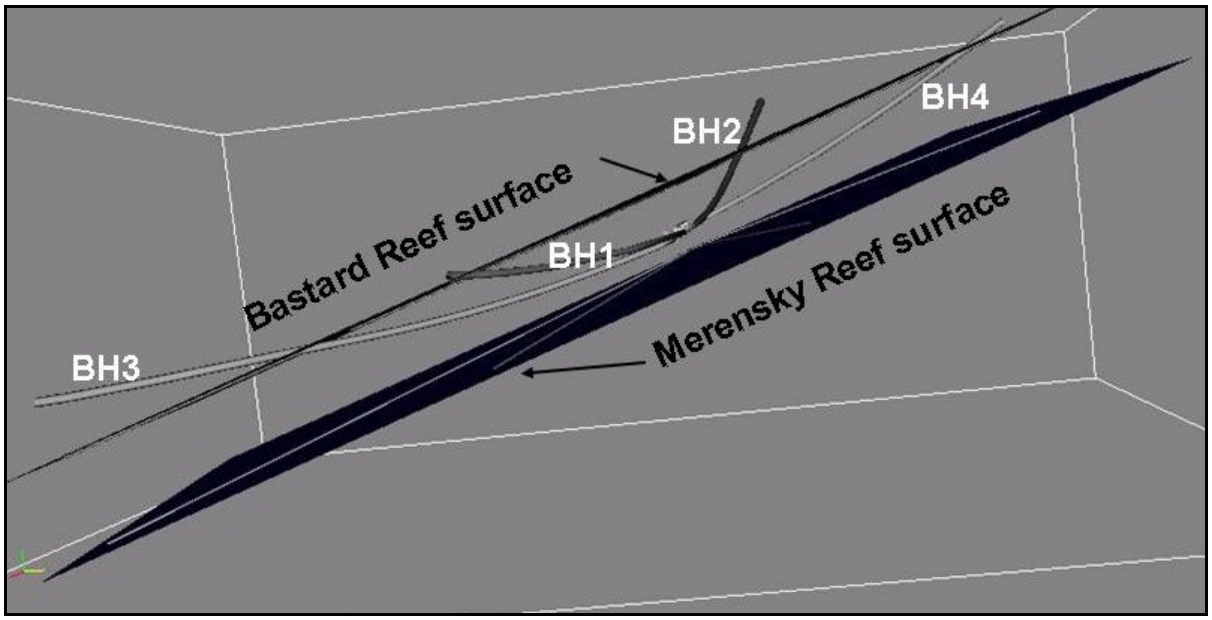

Figure 22: Case-study layout in section, showing radar boreholes as observed from the west. This is the hypothetical base model with flat surfaces for the Merensky and Bastard reefs.

5.3 Borehole radar results

5.3.1 Methodology

The borehole radar results are given and discussed from north to south. After data acquisition, the radar data were processed using band-pass and automatic gain control filters. The band-pass filter eliminated all frequencies not within the range of the Aardwolf borehole radar. Two-dimensional radargrams are presented for all four holes, without interpretation and with the interpreted reflectors indicated.

After the initial processing, all the radar data, together with the individual directional surveys, were imported into Fresco, an open-source 3D visualisation program developed under the Platmine collaborative research programme. Fresco uses forward modelling to aide the interpreter to visualise reflective planes in relation to the borehole radar holes. Radar illumination lines were produced along these reflective surfaces, which were then exported as XYZ coordinates and used together with other borehole information to construct a surface for the Merensky Reef below the borehole radar boreholes.

This methodology is explained in more detail during the discussion for borehole 4, and the same technique was used to interpret the results for the other three boreholes.

5.3.2 Borehole 4

Borehole radar data were collected for 132 m along borehole 4. The directional survey and geological log for borehole 4 are given in Appendix 1. The radargram for borehole 4 is shown in Figure 23, with and without interpretation. Good radar data were acquired up to approximately 96 m along the borehole. The loss of signal between 96 m and 110 m is visible on both the in- and out-surveys. This loss of signal is typical for what is expected when conductive water pools in the borehole, because radar waves generally do not penetrate through very conductive water. This borehole is, however, drilled at an upward angle, i.e. no water is expected inside the borehole.

The geological log for borehole 4 (Appendix 1) shows that iron-replacement was logged in the borehole between 97.4 m and 97.87 m and then again between 103.34 m and 106.56 m. Iron-replacement is very conductive, and it would explain the signal loss seen on the radargram.

In Figure 23, two radargrams are presented for the borehole radar survey conducted in borehole 4. The top radargram is the radar data after initial filtering. The bottom radargram is the same, but the two prominent radar reflectors, namely those produced from the Merensky and Bastard reefs, are annotated. The Bastard Reef reflection is shown as a white dotted line on the bottom radargram in Figure 23 and is interpreted to be in this position due to the fact that it intersects the borehole at approximately 100 m along the borehole, which is consistent with Bastard Reef logged in the drill core at this position. The Merensky Reef reflection is shown as a yellow dotted line in Figure 23. It is not as clear as the Bastard Reef reflection, and its position was interpreted as a result of Merensky Reef pyroxenite logged at the start of the borehole as well as a discussion with the mine geologist, where the most likely position of the Merensky Reef was ascertained. The very straight reflector seen between approximately 50 m and 90 m, starting at a distance of 40 m away from the borehole and moving towards it, is typical of the signature that a near-vertical structure intersecting the borehole would produce. A number of fractures are logged in the borehole between 108 m and 118 m (geological log in (Appendix 1). One of these fractures may be producing this radar reflection.

After the initial 2D interpretation presented in Figure 23, the radargram for borehole 4 was imported into the 3D visualisation software package Fresco to have a look at borehole radar data in 3D space.

Slim-line borehole radars are cylindrically omni-directional (Simmat *et al.*, 2002). This directional ambiguity leads to uncertainty in the interpretation of the reef elevation from borehole radar data. According to Du Pisani and Vogt (2004), the borehole radar receiver only receives reflections from sections of the target surface that are oriented perpendicular to the antennas. When borehole radar is applied from a

borehole drilled parallel to the reef horizon, it maps a single illumination line along the reef surface (Du Pisani and Vogt, 2004). One way to resolve the directional ambiguity is through the use of *a priori* information. The regional dip and strike of the ore body are known, and can be used as a first approximation of the position of the reflector. The drill core of the radar borehole is used to orient the borehole within the local stratigraphy; hence it can be determined whether reflections originate above or below the borehole. Furthermore, any other *a priori* geological information is used to improve the interpretation and resolve directional ambiguity. Geological intersections from other boreholes within the borehole radar survey area, as well as reef pegs from mining in the immediate vicinity, are used to get a better picture of the reef surface.

The radargram for borehole 4 was imported into Fresco together with the borehole's trajectory survey. In this way the curvature of the borehole is taken into consideration, and the interpreter is forced to consider the geometry of the borehole in relation to possible reflectors. In Fresco a candidate ore body can be manipulated, and its radar response can be modelled in real time. The model can then be manipulated until its response agrees with the measured response. The forward modelling approach has three advantages:

- It avoids the need for migration of the radar data. When borehole radar data is migrated, it must take into account the curvature of the borehole, which requires an assumption about the direction to various targets.
- Borehole data remains inherently ambiguous in azimuth. The 3D forward modelling environment forces the interpreter to constantly confront the ambiguity, ensuring that the output is a product of the interpreter's understanding of the problem and not simply automatically generated.
- The position of the illumination line on the target is produced directly in 3D space. This is the required product from a borehole radar survey, and is difficult to produce using other techniques.

As seen in Figure 24, candidate surfaces were constructed for the Bastard and Merensky reefs above and below borehole 4. In the three-dimensional modelling for all four boreholes, the Bastard Reef surface is red and the Merensky Reef surface is

blue. Both candidate surfaces were manipulated until forward modelled responses matched the radar reflectors seen on the radargrams. As topography was added to the Merensky Reef surface, an illumination line was produced on this surface, which simulated the radar ray paths emanating from the borehole radar instrument. In Fresco, topography can only be added in either the dip or strike direction of the candidate surface.

Figure 24 shows how topography was added in the strike direction of the Merensky Reef. Another model was constructed, adding topography in the dip direction. The illumination line coordinates from both strike and dip models were exported in XYZ-format and used in the next phase of modelling (presented in section 5.3.6) to construct a three-dimensional surface using the radar results from all four boreholes.

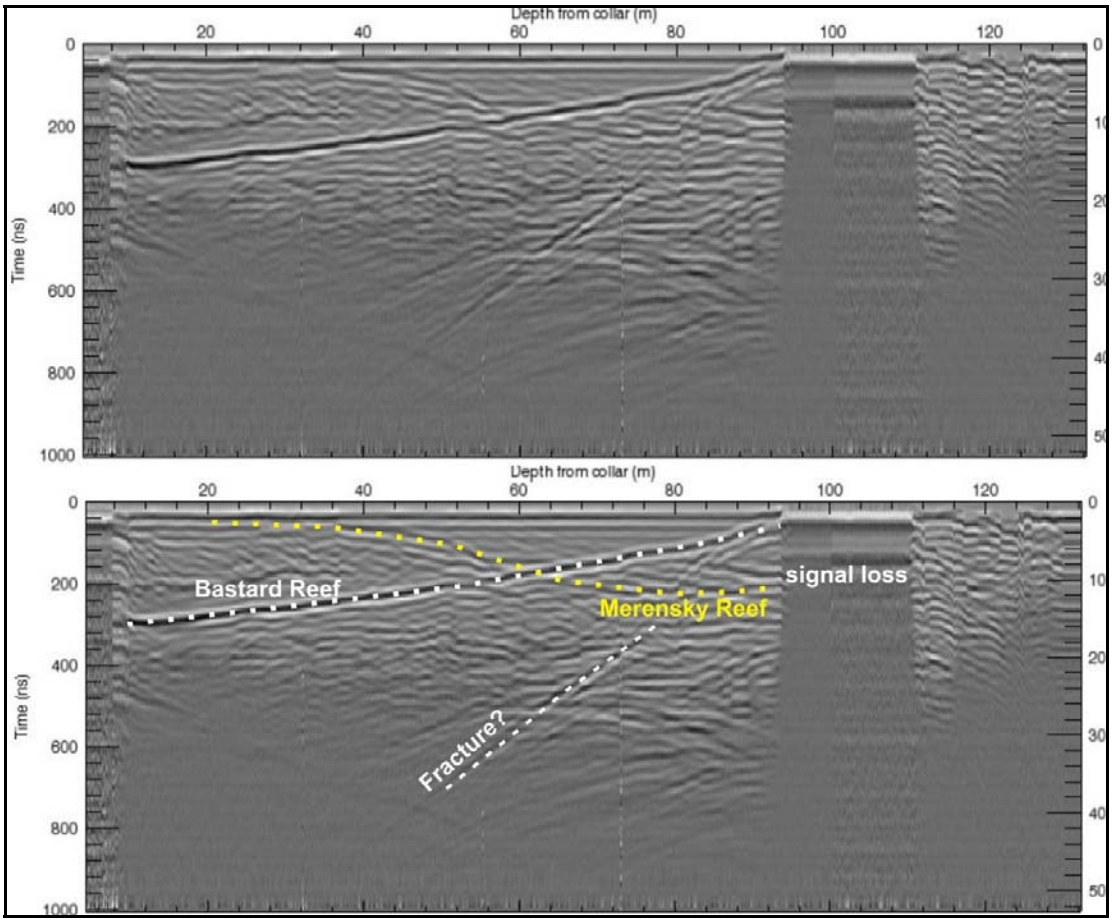

Figure 23: The radargram for borehole 4 without (top) and with interpretation (bottom). The Merensky Reef reflector is indicated by a yellow dotted line and the Bastard Reef reflector is indicated by a white dotted line.

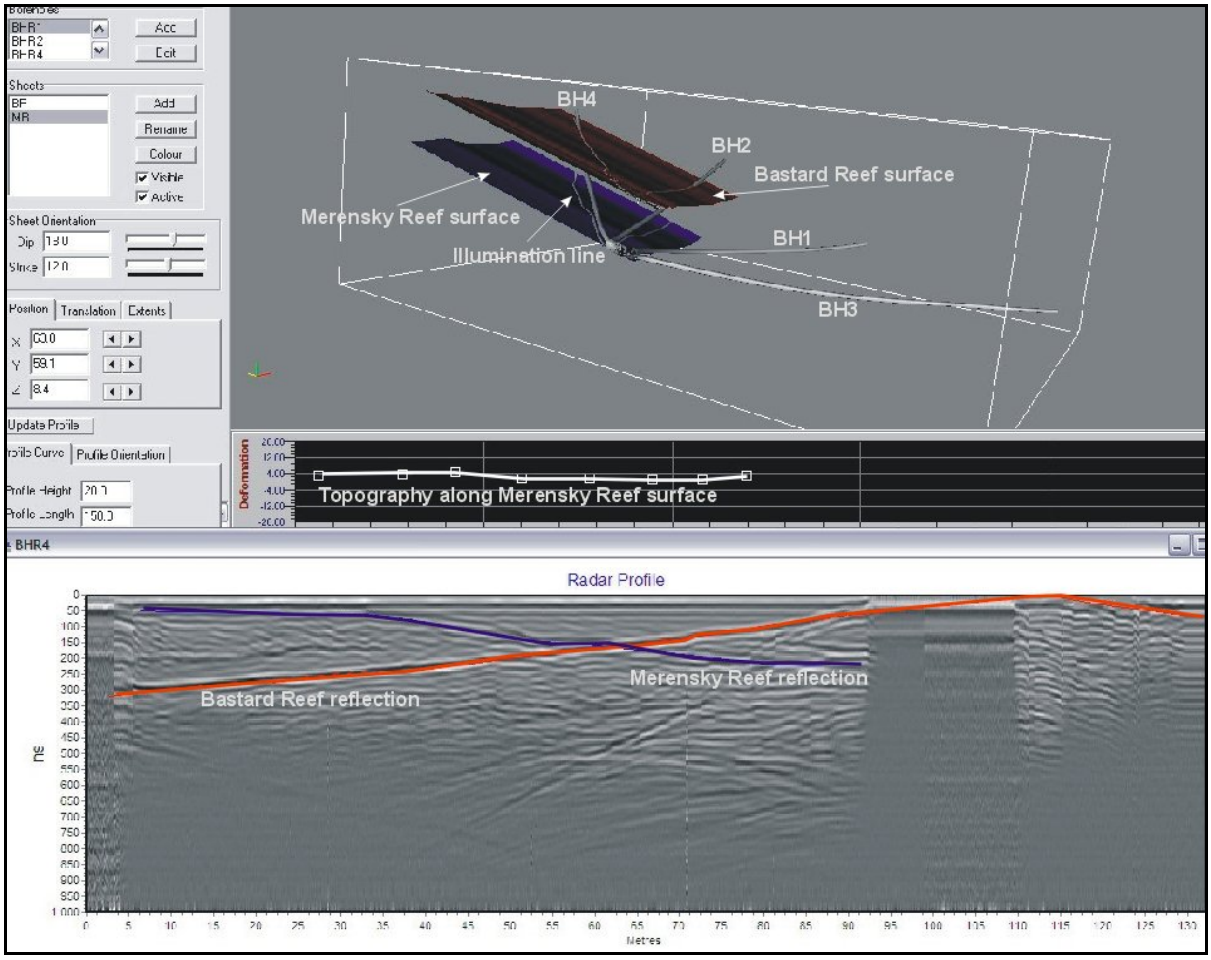

Figure 24: Three-dimensional visualisation for the borehole radar data acquired in borehole 4. The Merensky Reef surface is indicated in blue, while the Bastard Reef surface is shown in red. The radar illumination line is tracked along the Merensky Reef surface.

5.3.3 Borehole 2

The directional survey and geological log for borehole 2 are provided in Appendix 1. The radargram for borehole 2 is shown in Figure 25 with and without interpretation. Borehole radar data were collected for 132 m along borehole 2. The position of the Bastard Reef reflector (indicated in white) could be fixed due to an intersection point in the borehole at approximately 72 m. The interpreted Merensky Reef reflector (indicated by the yellow dotted line) could be imaged clearly for the first 62 m along the borehole, after which its position became unclear. Using three-dimensional visualisation (Figure 26) and adding topography to the Merensky Reef surface in the strike direction, it could be seen that subtle changes in the reef topography led to no reflection line being present between 65 m and approximately 94 m. The Merensky Reef is imaged again between 94 m and 105 m.

Since borehole 2 was oriented along the strike of the ore body, only one three-dimensional visualisation was conducted, i.e. the Merensky Reef surface was only manipulated along the strike direction. Manipulating the topography in the dip direction would not have made a significant difference to the reflection line. The illumination line coordinates for the model constructed in the strike orientation were exported in XYZ-format.

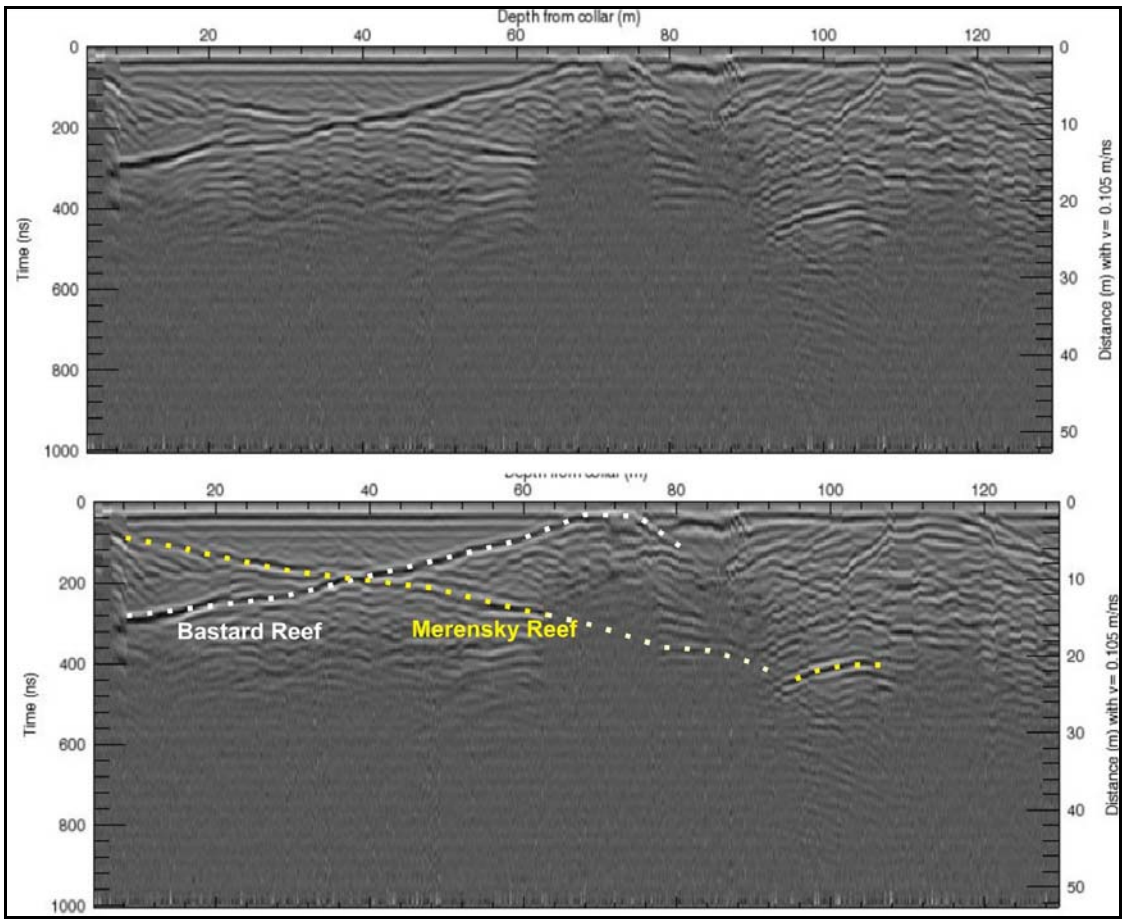

Figure 25: Radargram for borehole 2 without (top) and with interpretation (bottom). The Merensky Reef reflector is indicated by the yellow dotted line, while the Bastard Reef reflector is shown by a white dotted line.

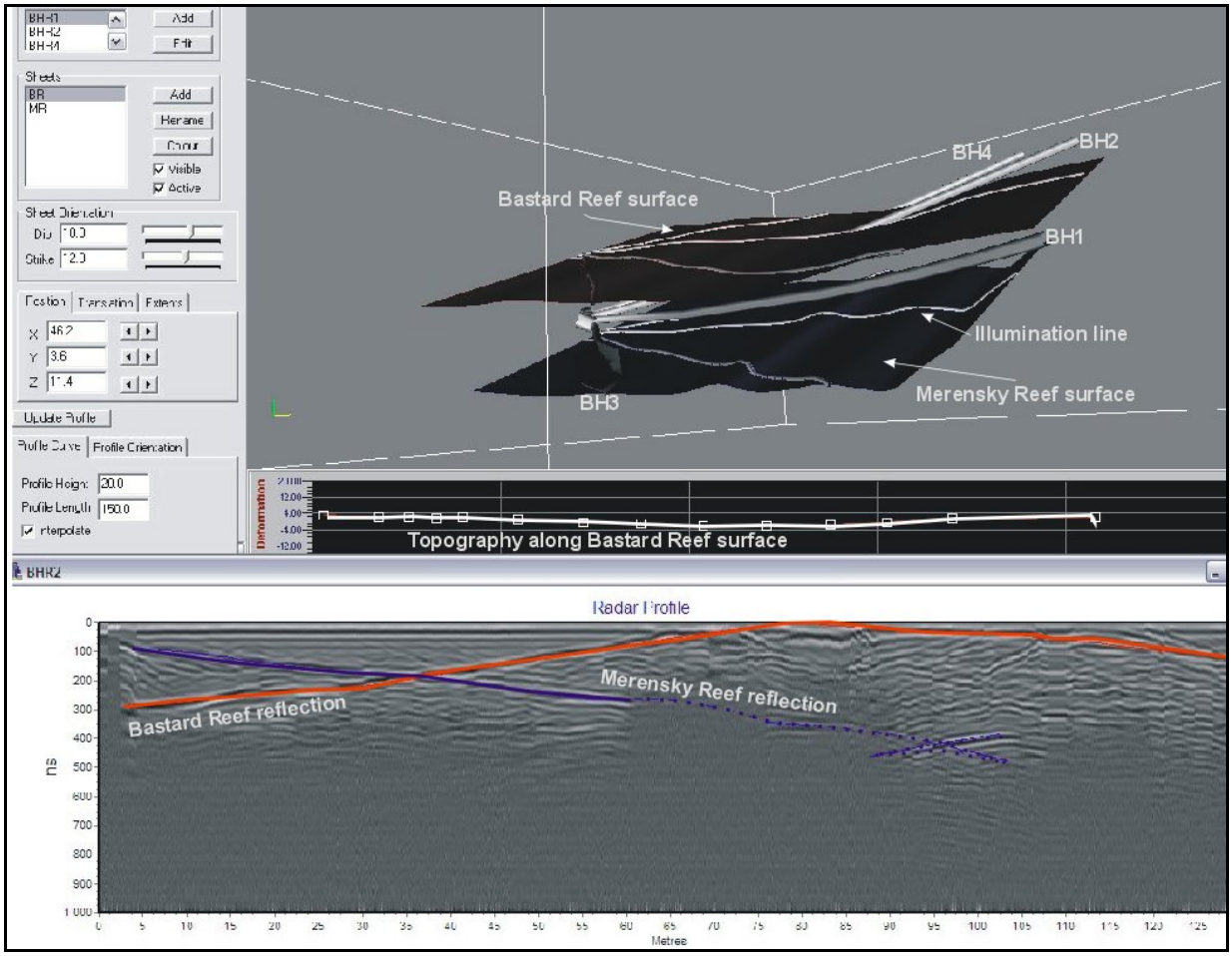

Figure 26:Three-dimensional visualisation in Fresco for the borehole radar data acquired in borehole 2. The Merensky Reef surface is shown in blue and the Bastard Reef surface is shown in red.

5.3.4 Borehole 1

Borehole radar data were collected for 147 m along borehole 1. The directional survey and geological log for borehole 2 are provided in Appendix 1. Both the Bastard and Merensky reefs were imaged clearly for virtually the entire length of the borehole. The Bastard Reef reflector is shown as a white dotted line on Figure 27, while the Merensky Reef reflector is shown as a yellow dotted line. Prominent hyperbolic reflectors seen further away from the borehole may be due to the side-swipe off sharp contacts, possibly due to a pothole structure in the vicinity of borehole 3. These hyperbolic reflectors are not expected to represent reflectors such as the UG2 Reef below the P2 marker, due to the P2's ability to absorb radar waves.

In Figure 28, the surfaces constructed in Fresco for the Bastard and Merensky reefs are shown. Figure 28 shows the three-dimensional visualisation in which topography was added in the strike direction along the Merensky Reef surface. Another model was constructed adding topography in the dip direction. The illumination line coordinates produced along the Merensky Reef surface were exported in XYZ-format for both models.

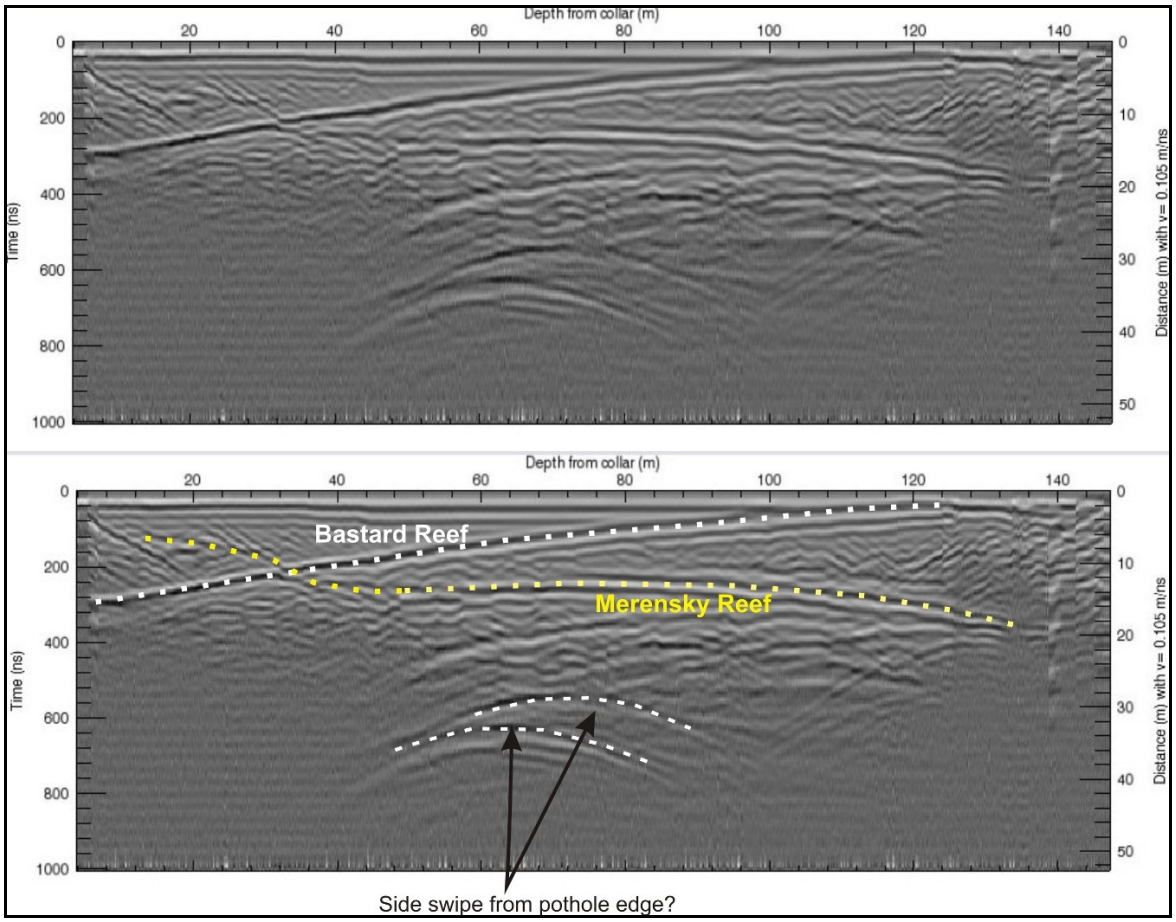

Figure 27: Radargram for borehole 1 without (top) and with interpretation (bottom). The Merensky Reef reflector is shown as a yellow dotted line and the Bastard Reef reflector is shown as a white dotted line.

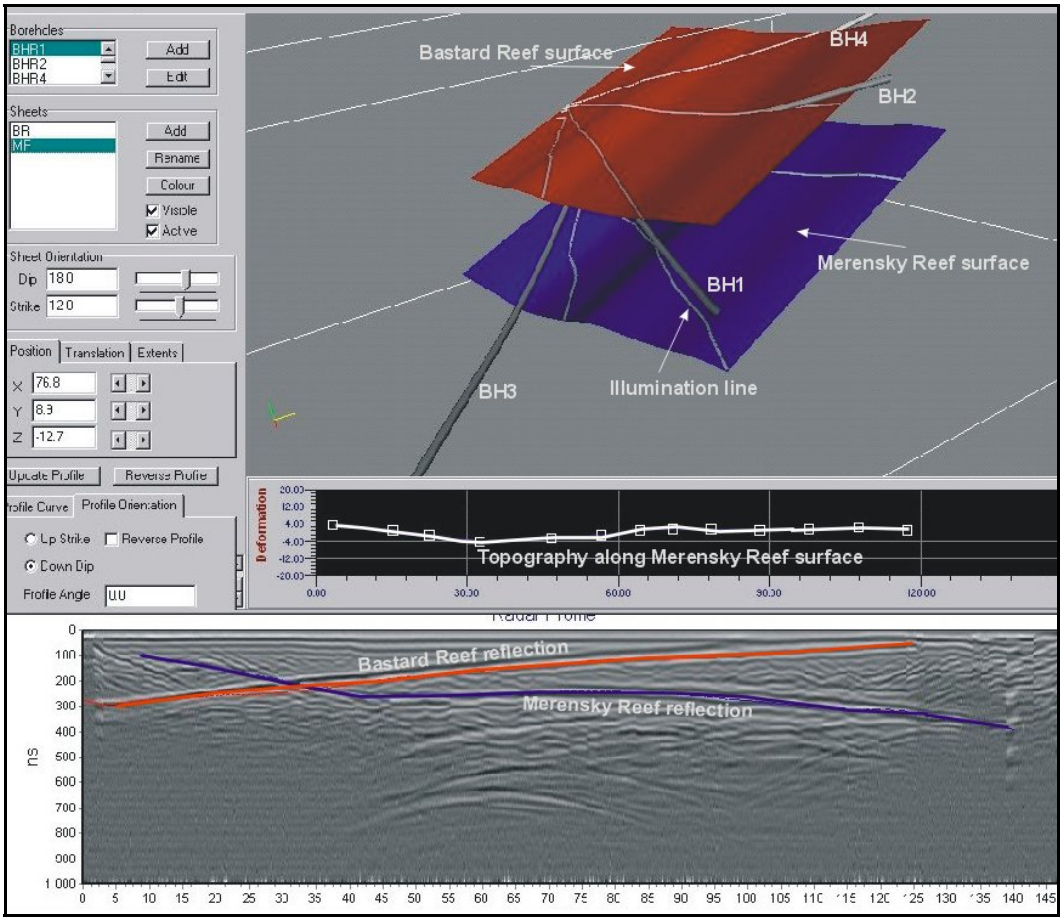

Figure 28: Three-dimensional visualisation for borehole radar data acquired in borehole 1. The Merensky Reef surface is shown in red and the Bastard Reef surface is shown in blue.

5.3.5 Borehole 3

Borehole radar data were collected for 200 m along borehole 3 (Figure 29). The directional survey and geological log for borehole 3 are provided in Appendix 1.

The Bastard Reef reflector (shown in white) can clearly be seen between 0 m and 116 m, after which it intersects the borehole. The Merensky Reef reflector is not very clear on the radargram for borehole 3, but there are sections of a reflector between 0 m and 136 m that correspond to where the Merensky Reef reflector is expected as a result of the three-dimensional visualisation done in the previous three boreholes. The inferred position of the Merensky Reef reflector is shown as a yellow dotted line in Figure 29. Another steeply dipping reflector (represented by the dashed white line in Figure 29), can be seen between 0 m and 80 m on the radargram. This reflector may be due to a dyke in the vicinity of the boreholes.

The Merensky Reef surface produced in Fresco is shown in blue in Figure 30. The visualisation where topography was manipulated in the dip direction is shown here. The illumination line coordinates produced by visualisation in the dip and strike directions were exported in XYZ-format and used for further modelling.

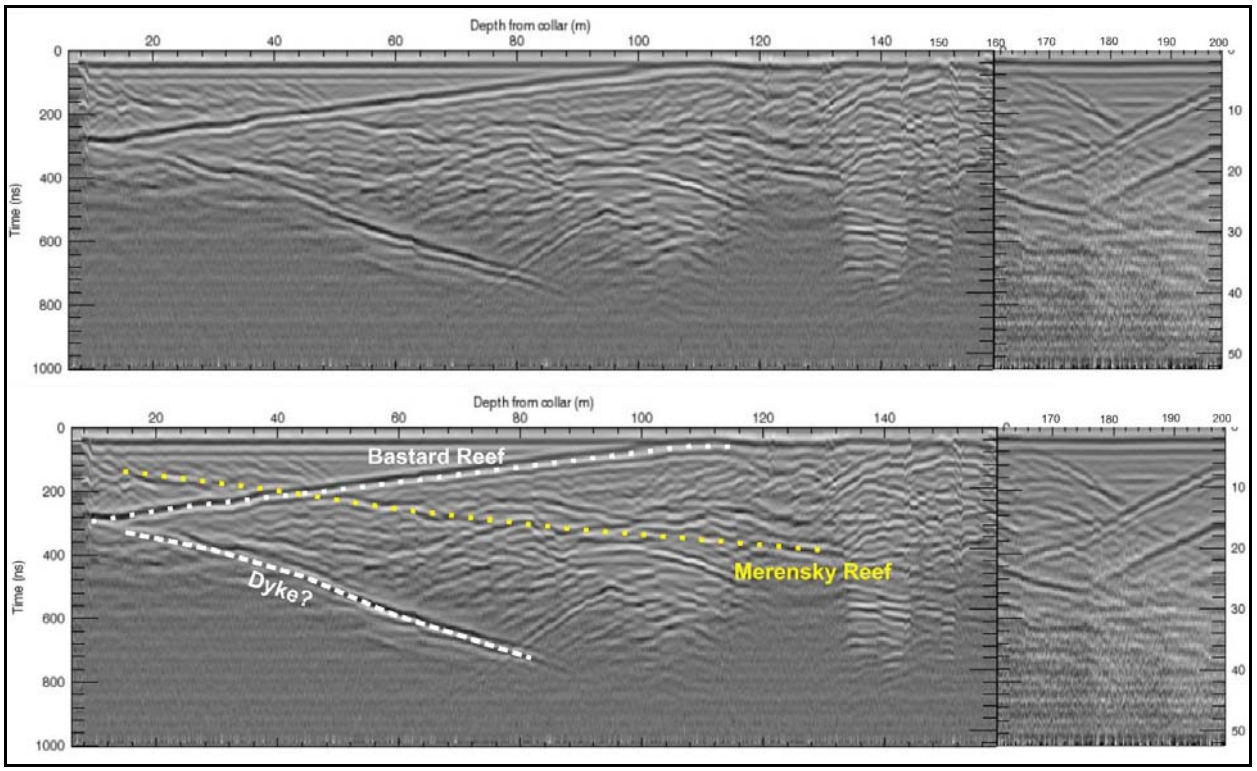

Figure 29: Radargram for borehole 3 without (top) and with interpretation (bottom). The interpreted Merensky Reef reflector is shown as a yellow dotted line and the Bastard Reef reflector is shown as a white dotted line.

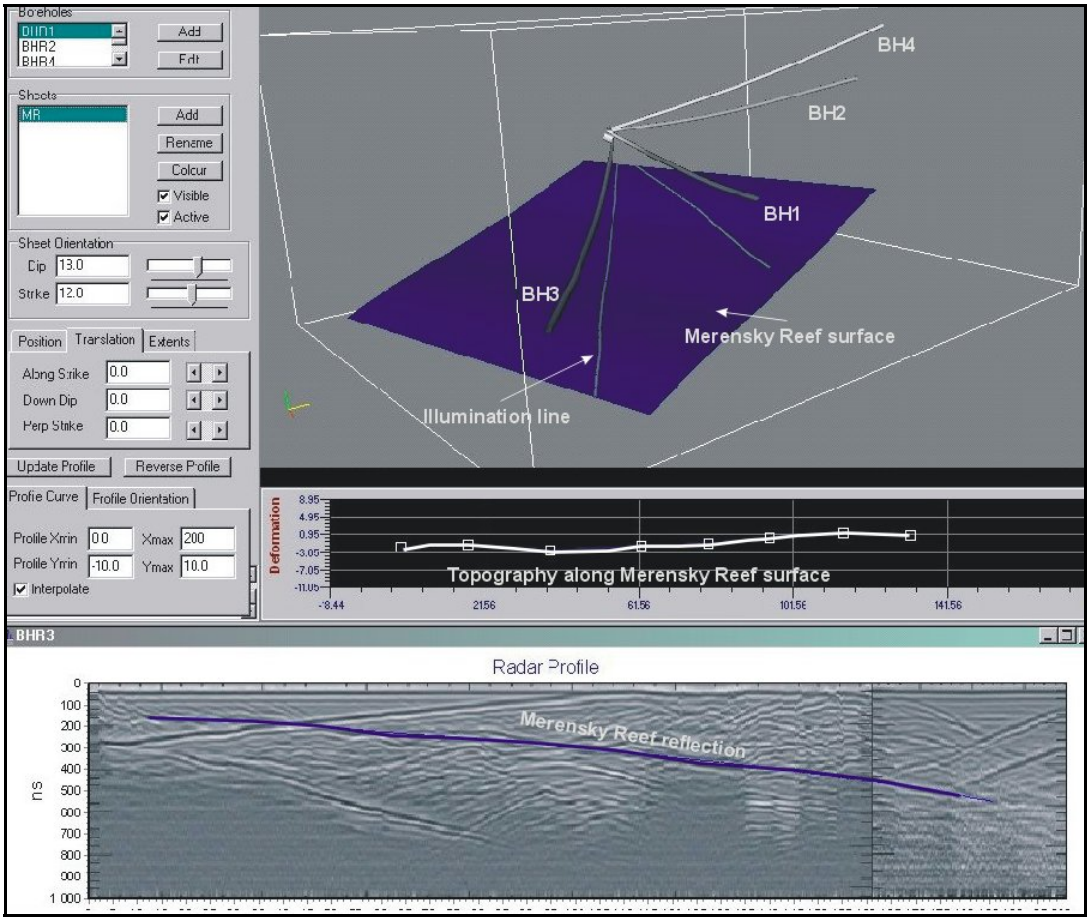

Figure 30: Three-dimensional visualisation for borehole radar data acquired in borehole 3. The Merensky Reef reflector is shown as a blue surface.

5.3.6 Contouring of geological and borehole radar illumination line coordinates

Two contour maps were produced to show the increase in data density if borehole radar is applied. In Figure 31, the contours that were produced by gridding the Merensky Reef intersection coordinates in the geological boreholes in the vicinity of the borehole radar boreholes is presented. Figure 32 shows the contours produced by gridding the illumination line coordinates produced for the Merensky Reef by conducting borehole radar in the four boreholes. It can be observed that more information is available for interrogation after borehole radar was applied. There is much more geological detail to be seen for the Merensky Reef in the area where borehole radar was conducted.

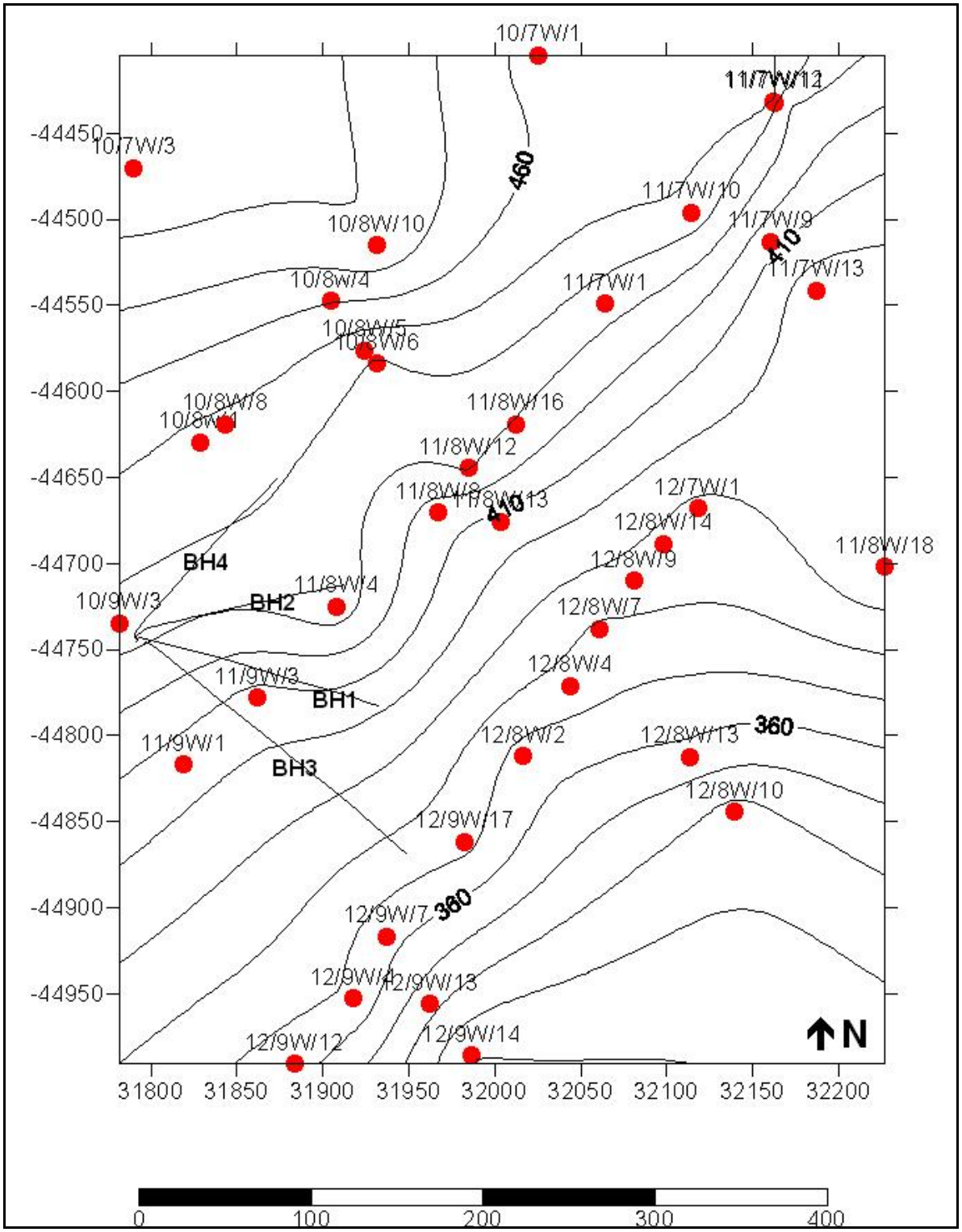

Figure 31: Contour map produced by gridding the Merensky Reef elevation as logged from geological boreholes in the vicinity of the borehole radar survey

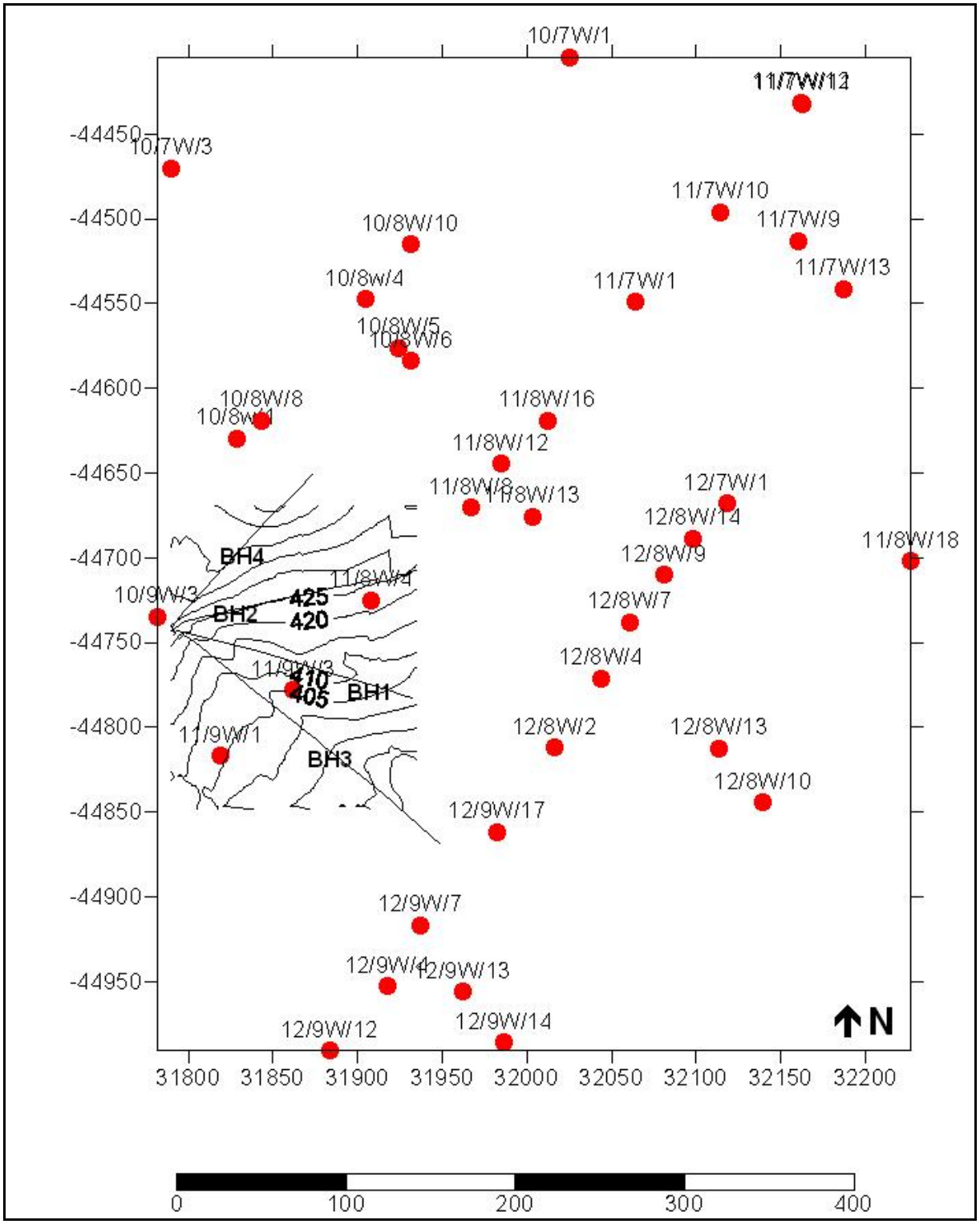

Figure 32: Contour map produced by gridding the illumination line coordinates produced by conducting borehole radar in boreholes 1 to 4

5.3.7 Three-dimensional surface (all boreholes)

The illumination lines produced by all the three-dimensional visualisations done for boreholes 1 to 4 were used, together with some Merensky Reef intersections from geological boreholes in the borehole radar block, to produce a three-dimensional surface. All the illumination line coordinates used for this study are presented in Appendix B.

In Figure 33A, the surface constructed by using only the Merensky Reef intersection from geological boreholes is shown in grey (Surface A). The positions of the geological boreholes are indicated as red dots.

The surface produced by gridding the XYZ-coordinates of all the illumination lines is shown in blue (Surface B). In Figure 33A, it can be observed that Surface B slumps below Surface A, indicating that the borehole radar results show that there is a pothole structure in the west of the mining block that would not have been detected if only the reef intersections from the geological boreholes had been used. Only the portion of the slumped Surface B that differs significantly (more that 1 m) is defined as the pothole in Figure 34.

This pothole (annotated in Figure 34) has an elliptical shape that is approximately 50 m across and slumps approximately 5 m, which would have significant implications for the mining of this block. The financial implication of mining into this pothole is discussed in the cost-benefit analysis conducted in Section 6.

Furthermore, the upward slope of the illumination line for borehole 4 indicates that the reef may be rolling upwards in the north of the block defined by borehole radar. This information may also be useful when this block is eventually mined, both financially and from a safety point of view.

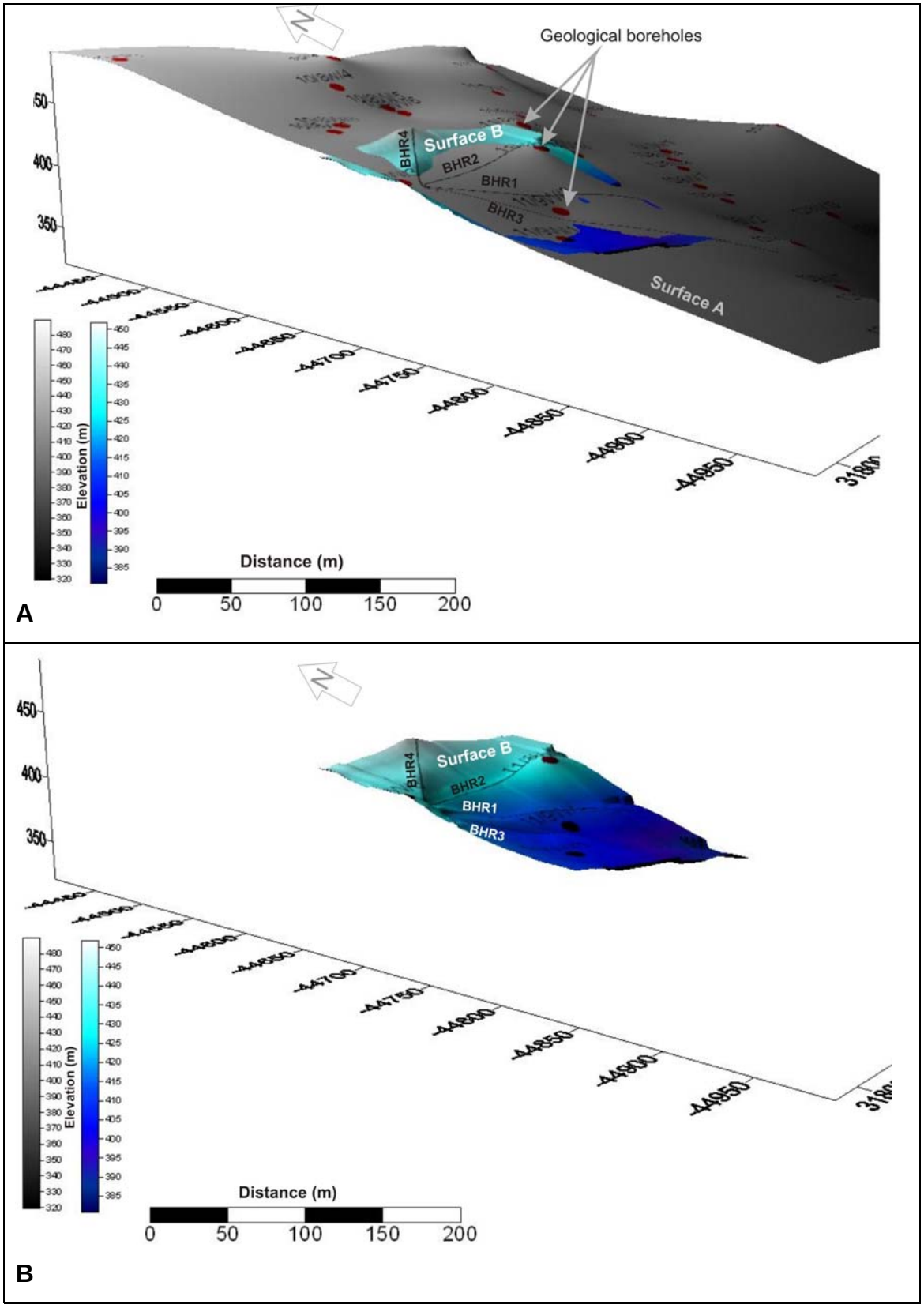

Figure 33: Three-dimensional surfaces constructed for the reef block imaged by borehole radar: A) the grey surface constructed from geological borehole information only, and B) the blue surface constructed by using the borehole radar illumination lines

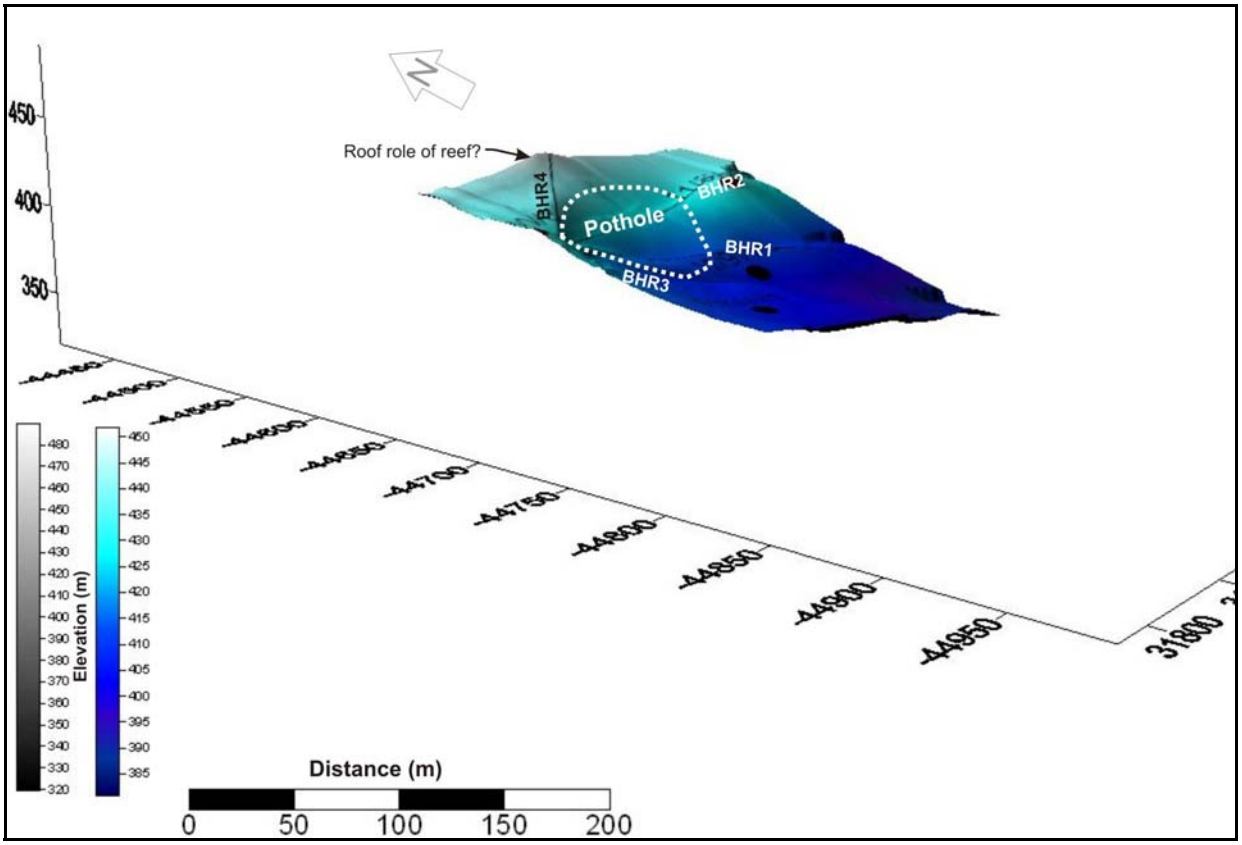

Figure 34: The surface produced by gridding the XYZ-coordinates from the borehole radar modelling, with the positions of the imaged pothole indicated

6 COST-BENEFIT ANALYSIS

6.1 Introduction

Advance knowledge of the reef topography ahead of mining should lead to increased profitability to the mine as a result of reducing the geological risk associated with features such as potholes, faulting, dykes and reef replacement due to iron-rich ultramafic pegmatites (IRUPs). Safety issues associated with the aforementioned geological features can also be negated if the features are known before they are encountered.

Currently, information about the reef is obtained through surface and cover drilling and mapping the reef surface while developing raises and stopes. Both drilling and excavating tunnels are expensive practices. Any way to reduce unnecessary drilling and/or development would imply a cost saving to the mine. The cost-benefit analysis described in this section aims to prove that the use of borehole radar can minimise wasted development and improve efficiencies throughout the mining cycle.

While exploiting an ore body there are various phases through which the mining cycle progresses, namely:

- Ore body definition.
- Mine design.
- Development.
- Extraction.
- Processing.

The effect of applying borehole radar is described in the following sub-sections as it relates to each of the abovementioned mining stages. Where possible, an attempt is made to quantify the cost benefit that borehole radar provides.

6.2 Assumptions

6.2.1 Definition of borehole radar coverage and delineation

The aerial coverage provided by the borehole radar surveys, through the extrapolation of the illumination lines produced by the borehole radar surveys, is shown in Figure 35A. The area covered by borehole radar is calculated to be: 15,231 m².

In Figure 35B, the area covered by the pothole delineated by the borehole radar surveys is schematically illustrated. The area of the pothole was defined in the software package Surfer and measured to be 3,927 m².

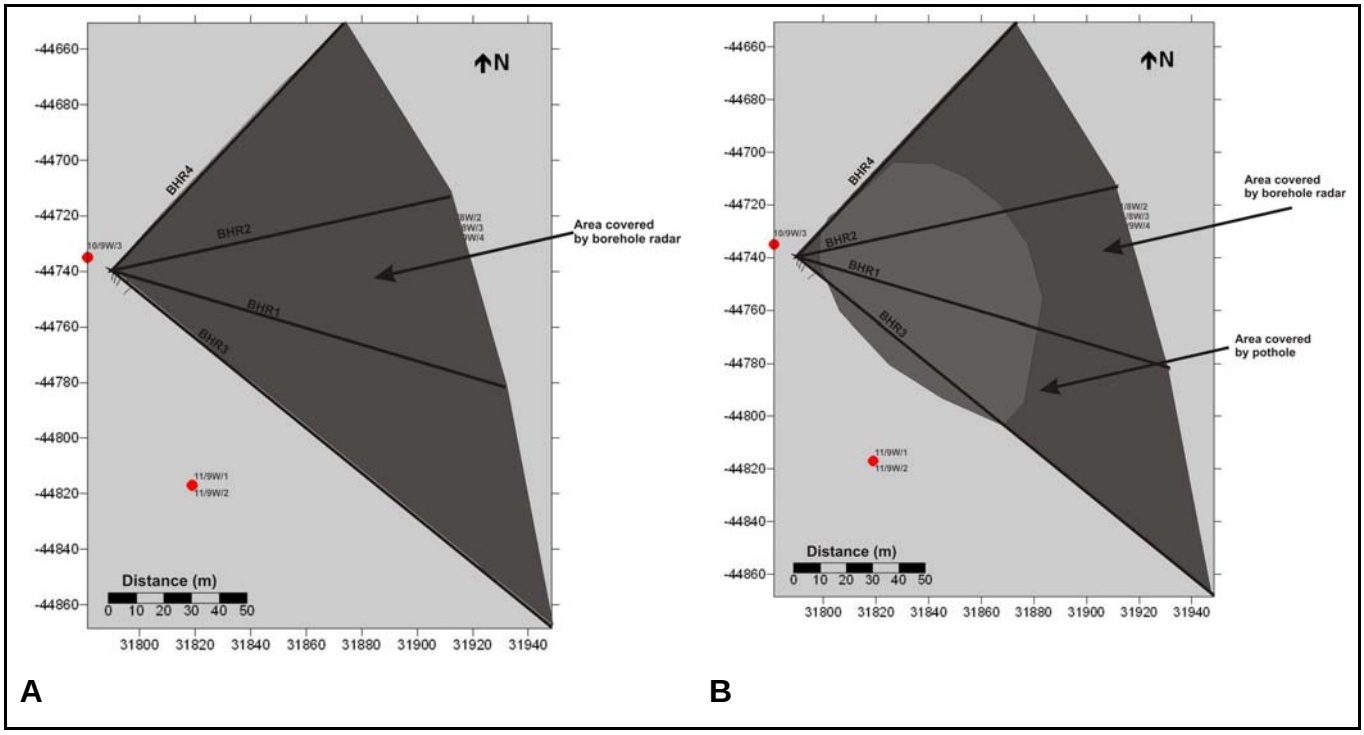

Figure 35: Schematic representation of A) the area covered by borehole radar, and B) the area covered by the pothole defined by borehole radar

6.2.2 Values used in cost-benefit analysis

6.2.2.1 Platinum Price

The daily London platinum prices for 2006 are shown in Figure 36.

The average platinum price for 2006, as defined in Platinum 2007, is used: US$1,141.84

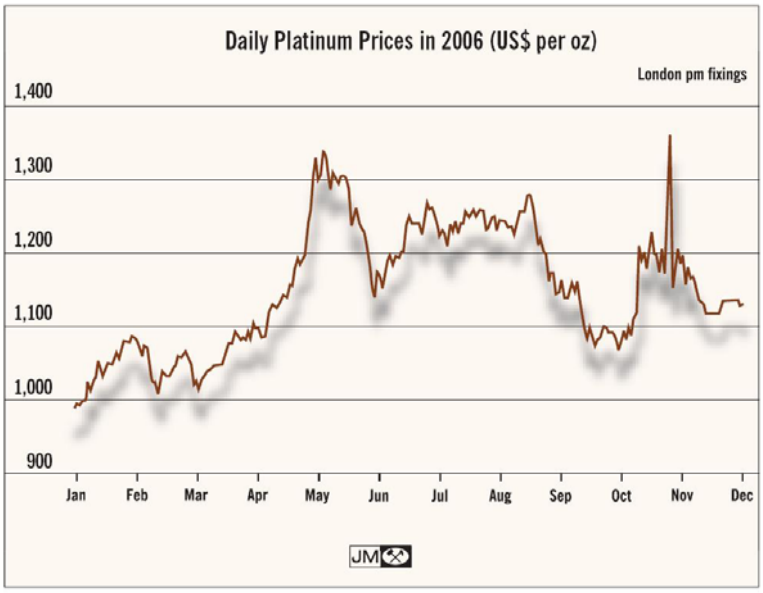

Figure 36: Daily platinum prices in 2006, given in US$, after Platinum 2007

6.2.2.2 Platinum grade

As stated earlier in this treatise, a fixed platinum grade is used for all the financial calculations in this treatise. The platinum grade used for the Merensky Reef at Amandelbult is 6.26 g/t. (Anglo Platinum Annual Report 2006).

For this treatise only the platinum values are used for calculation. The other PGE-metals are not considered.

6.2.2.3 Rand/dollar exchange rate

The average monthly rand/US dollar currency rates for 2006 as provided by www.gocurrency.com are shown in Figure 37.

The exchange rate used in this treatise is the annual average: 6.73.

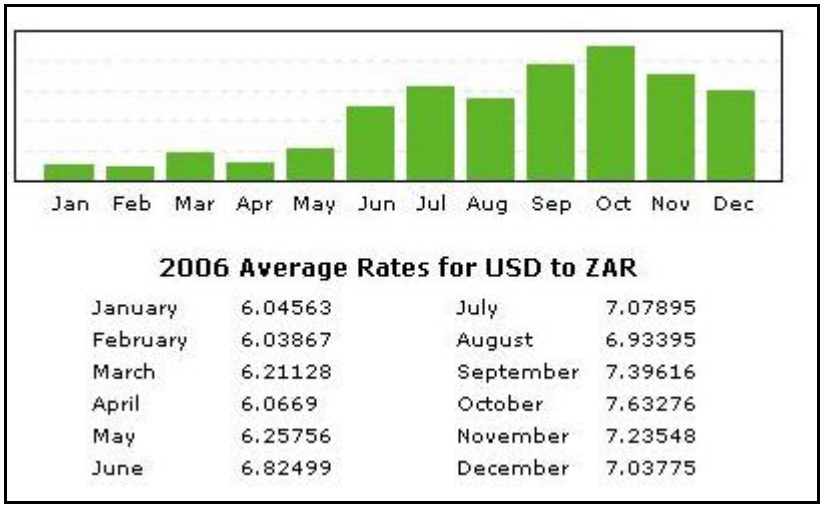

Figure 37: Average 2006 rand/US dollar exchange rate (www.gocurrency.com)

6.2.2.4 Reef thickness

A constant reef thickness of 1 m is used for all the financial calculations in this treatise.

6.2.2.5 Density

A density value of 3.4 t/m³ is used in this treatise.

6.3 Ore body definition

The relationship between mineral resources and mineral reserves as outlined in the SAMREC code (2000) is shown in Figure 38. As confidence in the geoscientific knowledge increases, mineral resources are upgraded from "inferred" to "indicated" and finally to "measured". When further modifying factors relating to the mining, metallurgical processing, economic characteristics, marketing potential, legal implications, environmental impact and governmental factors concerning the ore body are taken into consideration, mineral resources become mineral reserves, which can either be "probable" or "proved".

Borehole radar is a geoscientific method that can be used to increase the level of geoscientific knowledge and therefore improve the confidence in the geological

model. Borehole radar can be used in the process of converting resources to reserves or it can upgrade the status of either of these two classifications.

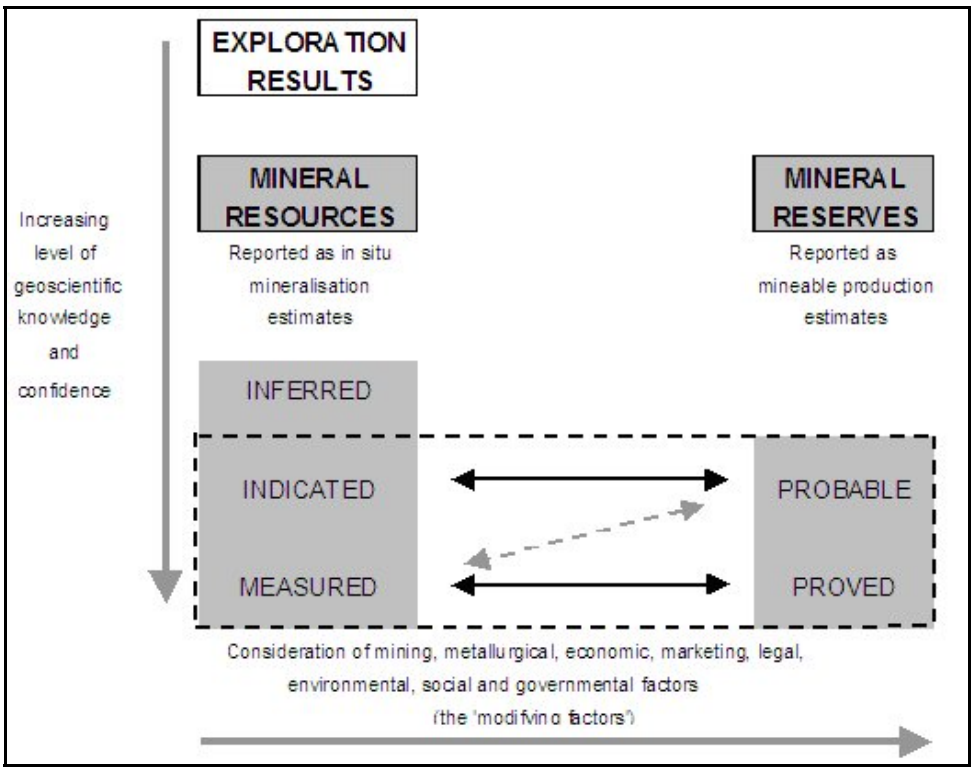

Figure 38: Mineral reserves and resources according to the SAMREC code (2000)

6.3.1 Geological drilling

The case study in Section 5 of this treatise describes how borehole radar was used to image the Merensky Reef within a mining block at Amandelbult Section. Prior to conducting borehole radar, 10 vertical geological boreholes were drilled within the block covered by the borehole radar survey. The positions of these boreholes are given in Figure 39. Due to the complexity of the reef topography in this part of the mine, a number of holes were drilled from similar positions in order to get clarity on how the reef topography was changing. In Figure 39, it can be observed how geological boreholes 11/8W1, 11/8W2, 11/8W3, 11/8W4 and 11/8W5 were drilled within 5 m of each other in order to determine the position of the Merensky Reef. The boreholes located along the straight line running from south-west to north-east were drilled upwards from development on the next lower level (11-Level).

As seen in Table 3, the total amount of geological drilling, prior to borehole radar, up to the bottom Merensky Reef contact adds up to 457 m. At an average cost of R300/m, the total cost of drilling geological boreholes to determine the position of the bottom Merensky Reef contact was R137,000.

In this study, the cost to assay the geological borehole core is not considered. This study focuses on defining the position of the Merensky Reef with the defined block, and not the grade.

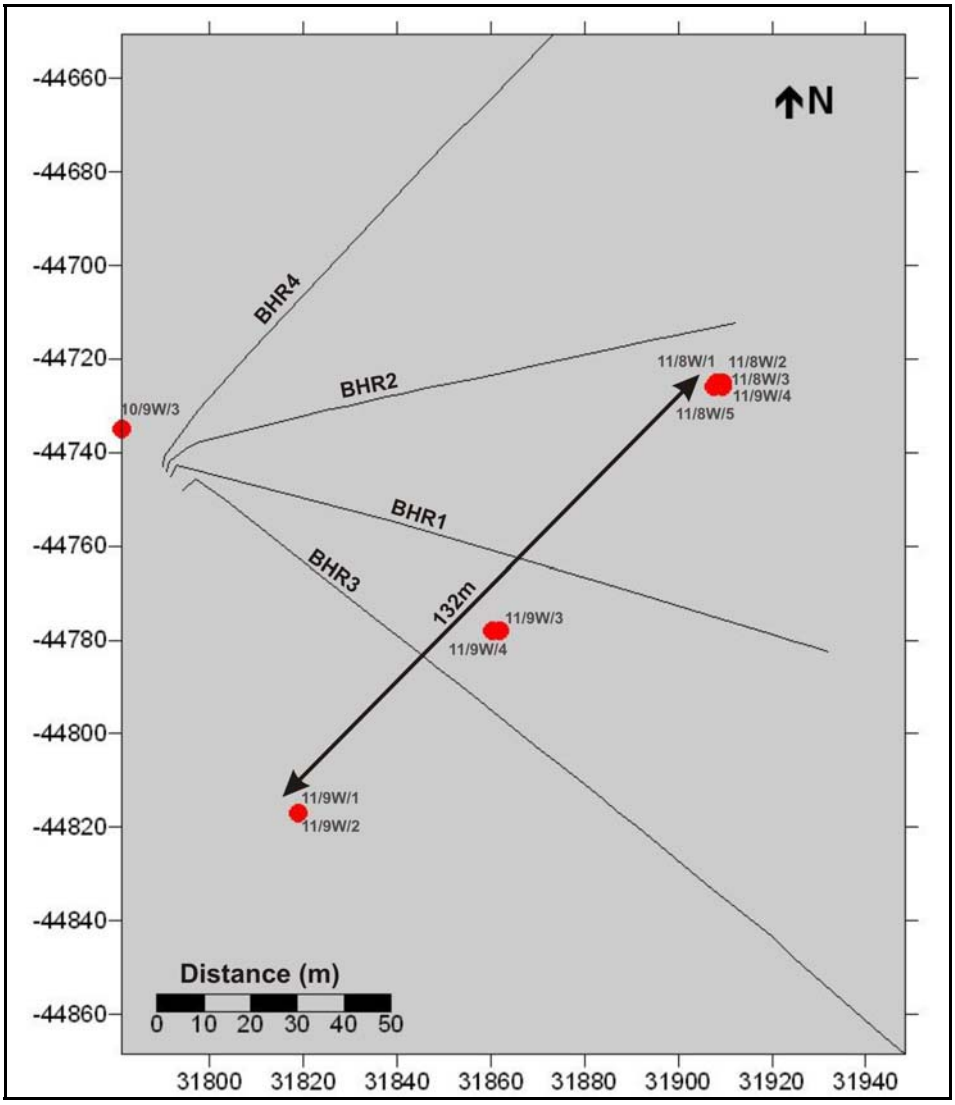

Figure 39: A map showing the area covered by the four borehole radar boreholes, indicating the positions of geological boreholes drilled prior to the borehole radar survey

Table 3: Geological boreholes in the area covered by the borehole radar surveys. The distance from the borehole collar to the bottom Merensky Reef contact is shown in the last column.

Borehole No:	X Collar	Y Collar	Z (Mer)	Merensky Bottom
10/9W/3	-44735.0000	31781.4000	436.0700	2.32
11/8W/1	-44725.5000	31908.0000	413.4400	36.44
11/8W/2	-44726.0000	31909.5000	473.0700	96.07
11/8W/3	-44726.0000	31907.5000	462.0700	85.07
11/8W/4	-44725.0000	31908.0000	436.3100	59.31
11/8W/5	-44725.0000	31909.5000	420.6400	43.64
11/9W/1	-44817.0000	31819.0000	405.1000	29.10
11/9W/2	-44816.5000	31818.5000	412.1200	36.12
11/9W/3	-44778.0000	31862.0000	405.9700	29.47
11/9W/4	-44778.0000	31860.4000	415.7900	39.29
			Total	456.83

Effectively, due to boreholes being drilled from similar positions, only three geological borehole positions along a straight line (approximately 132 m in length) were drilled to intersect the bottom contact of the Merensky Reef. From these boreholes an estimate of the Merensky Reef position could be made at three points along this line.

6.3.2 Borehole radar along a single line

If one borehole was drilled parallel to the Merensky Reef contact along this 132 m-long line, the cost of a borehole radar survey in that hole would be:

Drilling of hole (R300/m): R39,600

Directional survey: R3,000

Borehole radar survey: R44,000

Total: R86,600.

The borehole radar survey will give a continuous line of Merensky Reef coordinates below this theoretical borehole.

6.3.3 Geological intersect drilling vs. borehole radar

Cost of drilling geological boreholes: R137,000

Cost of one borehole radar survey in hypothetical borehole: R86,600

For 1.6 times less the cost of drilling clusters of geological boreholes at three points along an imaginary line, a borehole radar survey conducted from a borehole along this theoretical line will yield continuous reef elevation positions all along the line as opposed to reef intersections at three points. It is clear that the level of geological confidence acquired from reef elevation coordinates along a continuous line is much higher than only having the reef intersection at three points. Conducting borehole radar in a 132 m borehole will yield at the very least 44 illumination line coordinates, if the sampling interval of the trajectory survey is 3 m. In Table 4, the cost per reef elevation point is compared when geological drilling is conducted vs. applying borehole radar. It can be seen that the cost per point is 23 times smaller when using borehole radar to determine the reef elevation.

Table 4: Cost per reef elevation point for geological drilling, compared with conducting a borehole radar survey

	Points defined	Cost	Cost/point
Geological drilling	3	R137,000	R45,667
Borehole radar	44	R86,600	R1,968

This comparison did not take into account that the up-holes drilled from the lower level could not pinpoint the position of the reef.

As the geological confidence is increased, the mineral resource can be converted from “inferred” to “indicated”, which is associated with a reduction in risk when mining the ore body.

6.3.4 Borehole radar over the entire block

Four borehole radar surveys were conducted to define the mining block. The total lengths of borehole radar data collected are given in Table 5.

Table 5: Survey lengths for all four radar boreholes

Borehole	Length (m)
BHR1	147
BHR2	132
BHR3	200
BHR4	132
Total	**611**

The total cost of drilling 611 m for the borehole radar holes at a cost of R300/m is R183,300.

The total cost of applying borehole radar at commercial rates (November 2005) when all four surveys are completed during one week, i.e. mobilisation to Amandelbult, approximately 430 km from Johannesburg takes place only once: R185,000 (including VAT).

Furthermore, directional surveys at an estimated cost of R3,000 per survey are required in order to interpret the borehole radar data.

The total cost of borehole radar:

Drilling:	R183,300
Borehole radar:	R185,000
Directional surveys:	R12,000
Total cost:	**R380,300**

From Section 6.1.1, the cost of drilling geological boreholes within the survey area: R137,000.

Although applying borehole radar in the area was approximately 2.8 times more expensive than all the geological drilling done in the same area, the coverage gained by the borehole radar survey is approximately 15,231 m², as opposed to only three points/intersections spaced approximately 60 m apart along a 132 m straight line.

If the area imaged from the four borehole radar holes represents the area of Merensky Reef for that block, the value of that reef section can be calculated as follows:

Area of Merensky Reef	15,231	m^2	Defined in Section 6.2.1
Average thickness of reef	1	m	
Volume of reef	15,231	m^3	
SG	3.4	t/m^3	
Tonnes of reef	51,785.4	t	
Average grade/tonne (Pt)	6.26	g/t	Anglo Platinum Annual Report (2006)
Grams of Pt in situ	324,176.604	g	
Grams in a troy ounce	31.1		
Ounces of Pt in situ	10,423.68502	$	
Average Pt price (2006)	1,141.84	$	Platinum 2007
Value of Pt in situ	11,902,180.5	$	
Average R/$ exchange (2006)	6.73		www.gocurrency.com
Rand value of Pt in situ	80,101,674.76	R	

If we take the rand value of the platinum in the Merensky Reef (R80,101,674.76) and compare it with the price of applying borehole radar for that mining block (R380,300), we can see that for 0.47% of the value of the in situ reef, the geological confidence in the mining block can be significantly increased.

Expressed differently: if the cost of borehole radar is calculated per tonne of Merensky Reef, it can be shown that to delineate 51,785 t of reef with borehole radar will cost R380,300, i.e. R7.34 per tonne. Compared with an average production cost of R380/t (De Jager, *pers comm*) for producing one tonne of platinum at Amandelbult Section, borehole radar makes out 1.9% of the total production cost.

The cost of applying borehole radar in relation to the in situ value of the platinum as well as in relation to the total production cost for the defined area is represented with pie charts in Figure 40.

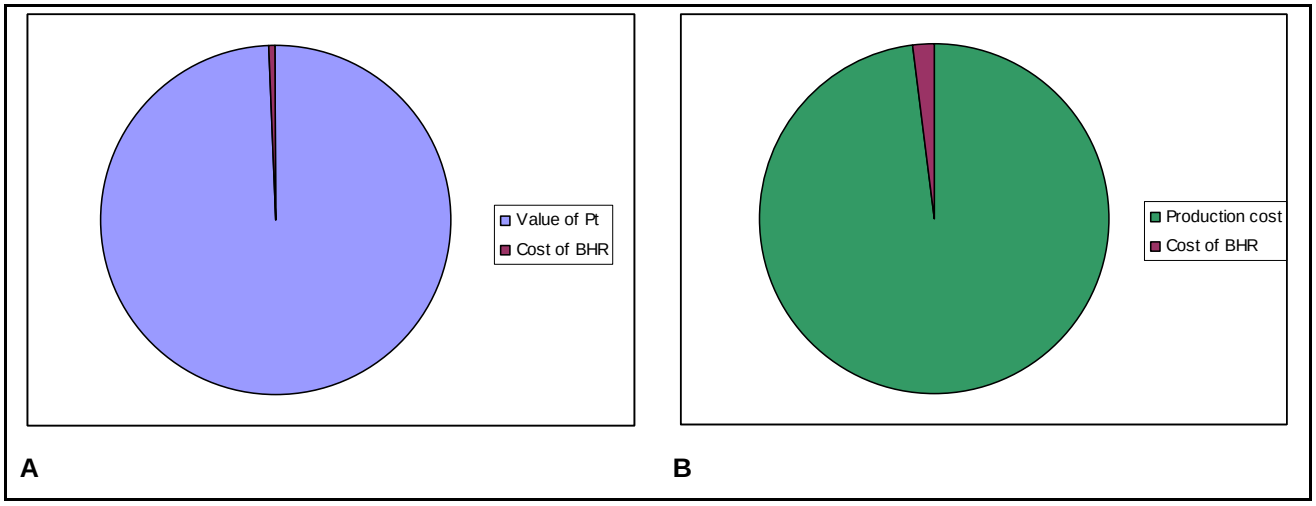

Figure 40: Cost of borehole radar compared with A) the value of the in situ platinum in block delineated by borehole radar and B) the production cost per tonne of platinum

6.3.5 Geostatistical increase in confidence

It was attempted to define the increase in confidence levels for the elevation of the Merensky Reef in the mining block by conducting geostatistical calculations for two scenarios within the Amandelbult mining block.

These scenarios were:

- Using only the available geological drill holes within the block.
- Using the illumination line coordinates from the borehole radar surveys conducted within the block.

6.3.5.1 Scenario 1

Confidence in the reef elevation within the mining block using only the initial geological boreholes

In Scenario 1, 10 geological drill holes were available for geostatistical analysis. The parameter analysed was the elevation (z) of the Merensky Reef measured in metres.

The position of these geological drill holes are shown in Figure 17.

Using the software program Geoeas, standard statistical parameters were calculated:

n:	10 (number of points)
Mean ($\bar{g}$):	428 m
Median:	418.5 m

Standard deviation (s): 23.56 m

Since the mean and median were similar, a normal distribution was assumed for further calculations. Since there were fewer than 10 data points, the following equation was used to calculate confidence levels:

$$\mu - 1.833\frac{s}{\sqrt{n}} < \bar{g} < \mu + 1.833\frac{s}{\sqrt{n}} \quad (2)\ \text{(Clarke, 2000)}$$

In this treatise, the 90% confidence level is used for consistency.

Using equation (2), it can be deducted that the analyst can be 90% sure that the mean of this dataset is between 414 m and 442 m. The confidence range is 28 m.

This means that the elevation of the Merensky Reef within the area defined by the borehole radar boreholes can be estimated with an error of up to 28 m, if only the elevation information from the 10 geological boreholes is used.

6.3.5.2 Scenario 2

Confidence in the reef elevation using the borehole radar illumination line coordinates

In Scenario 2, all the illumination line coordinates produced for radar boreholes 1 to 4 were used for geostatistical analysis. The modelling both in the dip and strike direction was considered. A total of 716 elevation points were generated in the mining block using illumination line forward modelling.

Using the software program Geoeas, various statistical parameters were calculated:

n: 716 (number of points)

Mean ($\bar{g}$): 416 m

Median: 415 m

Standard deviation (σ): 16.33 m

It stands to reason that the increase in data points will improve the level of confidence at which the mean can be calculated.

Since there were more than 25 data points, the following equation was used to determine the confidence levels:

$$\mu - 1.645\frac{\sigma}{\sqrt{n}} < \bar{g} < \mu + 1.645\frac{\sigma}{\sqrt{n}} \quad (3)\ \text{(Clarke, 2000)}$$

Using equation (3), it follows that the analyst can be 90% sure that the mean of this dataset is between 415 m and 417 m, i.e. the confidence range is 2 m.

This means that the elevation of the Merensky Reef can be estimated at a much higher accuracy than using only the geological drilling within the mining block. The confidence range has improved from 28 m to 2 m, a 14-fold improvement.

Therefore, if borehole radar is used to delineate a mining block, the reef elevation can be determined with much more confidence than relying on geological borehole intersections alone.

6.3.5.3 Discussion

Using basic geostatistical equations, it can be concluded that the application of borehole radar in the mining block has significantly improved the level of confidence in the position of the Merensky Reef.

Stated differently, to achieve the same level of confidence as provided by borehole radar, 716 vertical geological boreholes would have been required.

The average length of the geological boreholes used in the mining block to intersect the Merensky Reef was 46 m (using values in Table 3). If 716 of these boreholes were drilled at a drilling cost of R300/m, the total cost would be 716 x 46 x 300m = R9,880,800.

The same level of confidence was achieved with four borehole radar surveys at a cost of R380,300, i.e. 3.84% of the cost of drilling 716 geological boreholes.

6.4 Mine design

Mine design and mine development are very closely related. In this section it is shown that the area that is to be developed is sampled better if borehole radar is applied prior to development as opposed to only using geological boreholes to fix the position of

the reef. If the position of the ore body ahead of mining can be determined accurately, the mine design can be fixed and mining can continue unhindered, without any surprises.

6.4.1 Area of Merensky Reef sampled with standard geological drilling

At Amandelbult Section, it is currently normal practice to drill three vertical boreholes per planned cross-cut spacing, i.e. approximately three boreholes per 200 m of haulage development (Figure 41).

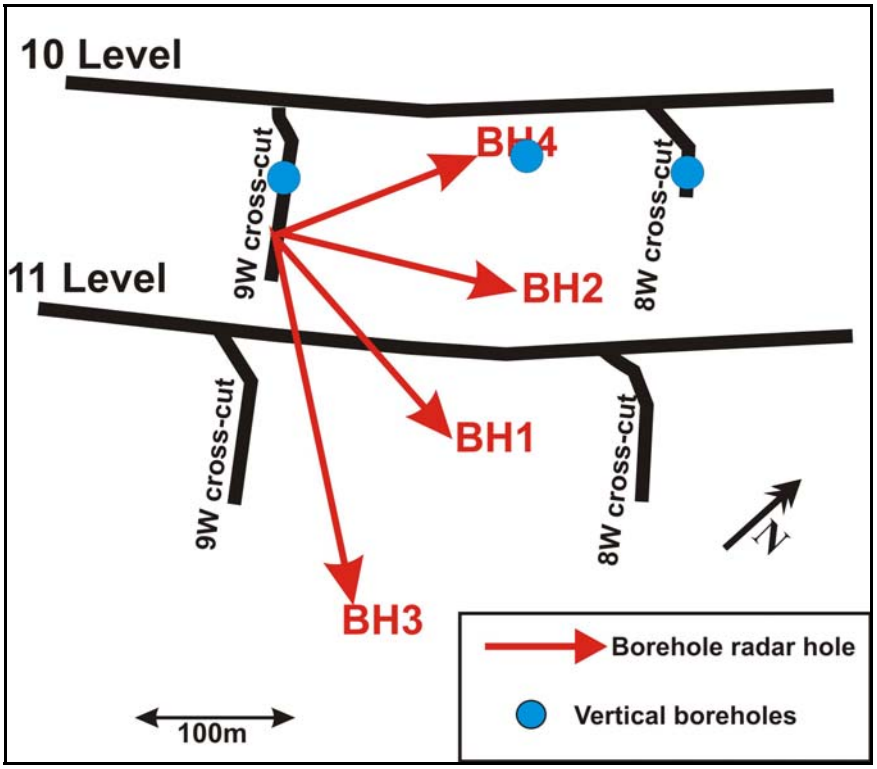

Figure 41: Borehole radar survey layout indicating vertical boreholes meant to "cover" mining block between 9W and 8W crosscut on 10-Level

Approximately 100 m of reef intersection (vertical) drilling is completed in one month to cover the position of cross-cuts and raises. If a drilling cost of R300/m is used, this equates to R30,000 of drilling per month to ensure that development is placed optimally to extract the ore body, and this is assuming that the geology is not complex, i.e. no additional drilling is required to pinpoint the position of the reef.

For R30,000 three pierce points through the Merensky Reef are obtained along a 200 m line defined by the haulage position.

The mine planner can now be confident that the position of the Merensky Reef is fixed where the boreholes pierce the reef. Exploratory underground geological boreholes are drilled with AXT drill bits. These drill bits have a diameter of 48 mm (Heinz, 1994). Since these are vertical up-holes, they intersect the reef plane with a circular shape, i.e. the positions of three circular pieces of reef within the reef plane are known. The area of each piece is:

$A = \pi r^2 = \pi (0.024)^2 = 0.0018 \text{ m}^2$

Area of Merensky Reef sampled: 0.0054 m² (3 x AXT size boreholes)

6.4.2 Area of Merensky Reef sampled using borehole radar

The horizontal resolution of a radar instrument is defined by the size of its first Fresnel zone (Vogt, 2003). The radius of the first Fresnel zone is defined by the distance of the radar antenna from the target horizon as seen in Figure 42.

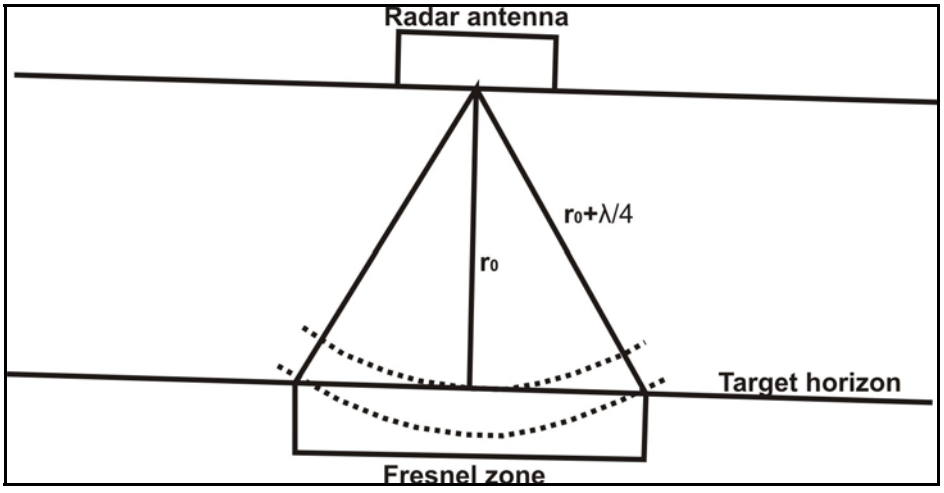

Figure 42: The first Fresnel zone (Vogt 2003)

Radar information about the reflective surface is gathered from an area below the boreholes of the Amandelbult case study as defined by the following equation:

$$R_F = \sqrt{\lambda r_0 + \tfrac{1}{4}\lambda^2} \qquad (4) \qquad \text{(Vogt, 2003)}$$

Equation (4) defines the radius of the first Fresnel zone.

The areas from which radar data are gathered for each of the Amandelbult radar boreholes are shown in Figure 43. This figure shows that borehole radar effectively samples 474 m² + 528 m² + 528 m² + 800 m² = 2,330 m² of the mining block.

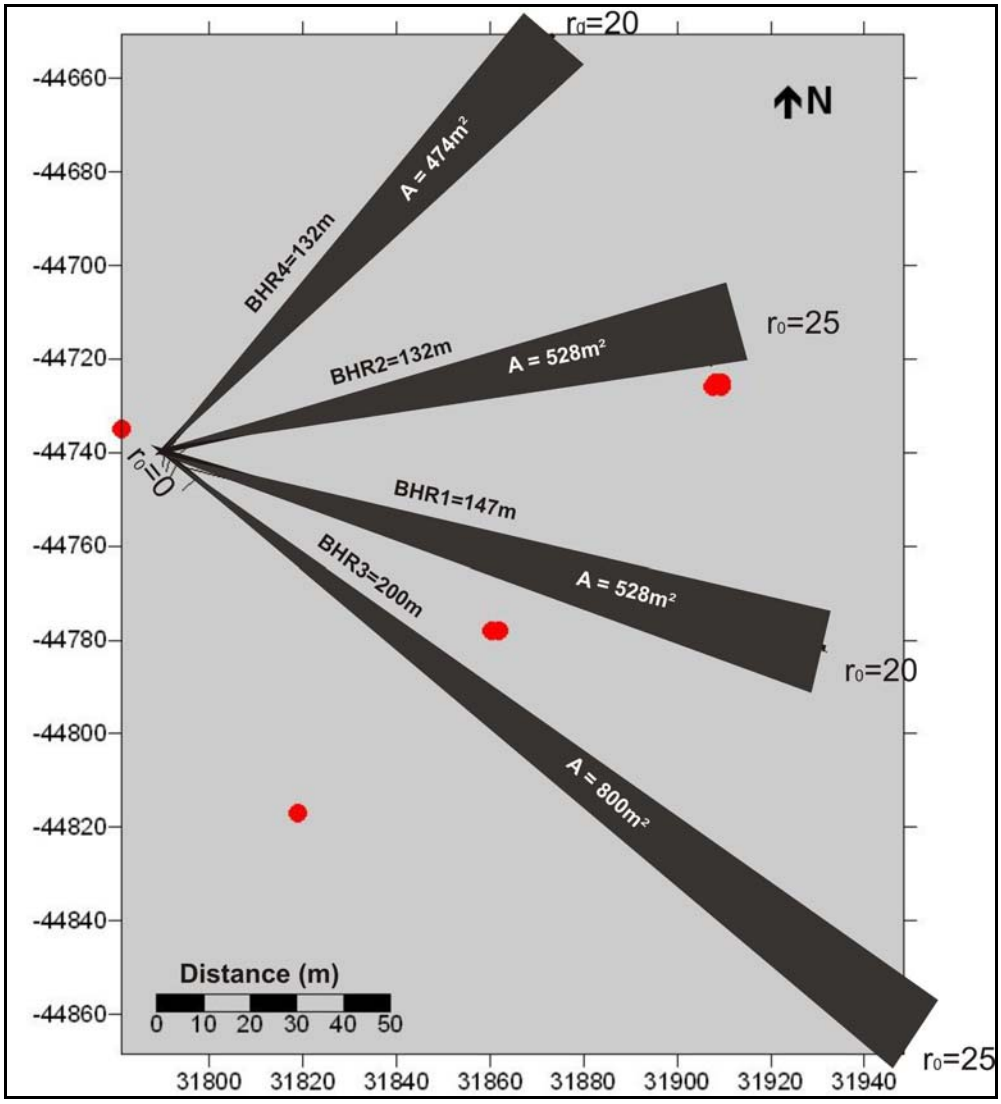

Figure 43: The areas from which borehole radar data is gathered for boreholes 1 to 4

6.4.3 Discussion

When standard geological drilling is done at regular intervals down the haulage to get an idea of the block that is to be mined into, the position of the Merensky Reef is known over an area of 0.0054 m² at a cost of R30,000, i.e. R5,600,000 per m².
Using standard geological drilling, 0.00035% of the 15,231 m² mining block is sampled.

When borehole radar is applied from four boreholes drilled sub-parallel to the target surface, an area of 2,330 m² is sampled at a cost of R380,300, i.e. R163 per m².
Using borehole radar, 15.3% of the 15,231 m² mining block is sampled.

Borehole radar increases the sampling area 431,481 times over standard geological drilling at a significantly reduced cost (Figure 44). It is clear that the application of borehole radar prior to mining significantly increases the knowledge about the ore body prior to mining. A much larger area of the area to be mined is sampled and if the cost of this sampling is compared with standard geological drilling conducted to "cover" the position of the Merensky Reef within the mining block, it can be seen that borehole radar is also significantly cheaper.

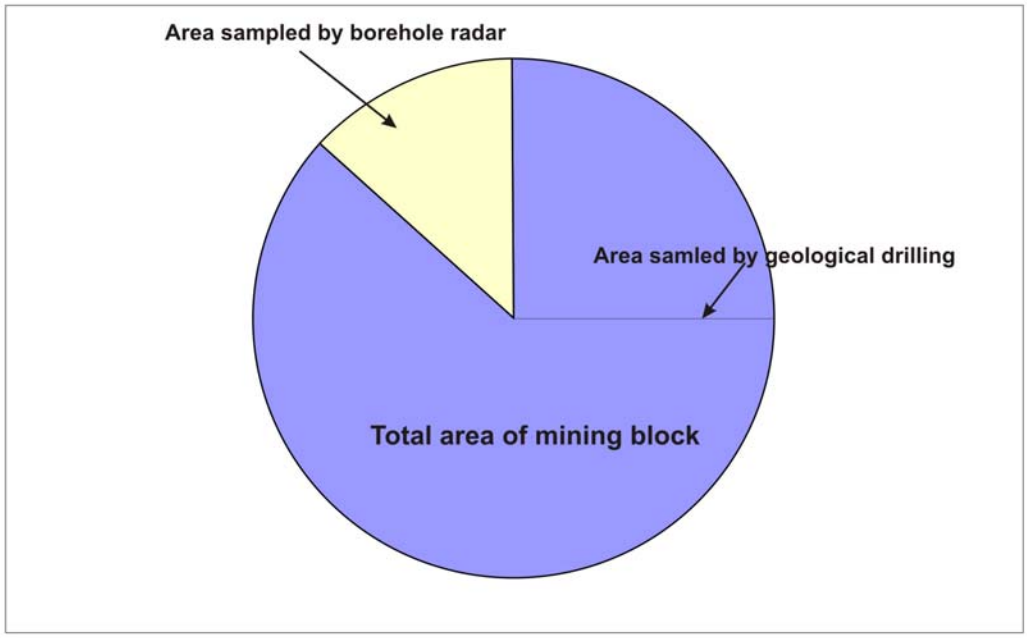

Figure 44: Increase in sampling area if borehole radar is conducted

6.5 Development

The conventional mining layout is used at Amandelbult Section (shown in Figure 15). Development takes place in three ways:

1. Secondary development

   Footwall haulages, developed on strike at a constant distance below the reef plane.

   Cross-cuts, developed horizontally to intersect the reef plane.

2. Primary development

   Raises developed in the reef plane.

3. Ancillary development

   Other development such as travelling ways, ore passes, timber pays, drilling cubbies et cetera.

In Section 4.3.2 (Figure 16), the conventional mining progression within a mining block is described. From opposite raise lines, mining proceeds in panels until a natural dip pillar is left for support in the centre of the block.

Once the raises have been developed, the reef between two neighbouring raises is extracted or stoped. Mine development is expressed as a ratio called the m^2/m ratio, where:

The m^2 refers to the area of reef that is available for mining after the necessary development is done, and the m refers to the development required to provide access to the reef.

The m^2/m ratio is affected by various factors, such as the geometry of the reef, the dip and structural complexity of the reef as well as the mining efficiencies achieved when extracting the reef. According to De Jager (*pers comm*), the m^2/m ratio should theoretically be in the vicinity of 50 m²/m, but due to the factors listed above, typical values range between of 20 m²/m and 25 m²/m.

The m^2/m ratio for the mining block imaged by borehole radar is calculated below.

Let's assume the area of reef available for mining is 15,231 m², i.e. we take the same amount of reef available for mining as imaged by borehole radar described in Section 6.2.1 (Figure 35).

If the *m²/m* ratio is taken as 25, then 609 m of development was required to make this reef available.

This case study described in Section 3 shows that borehole radar imaged a pothole in the Merensky Reef. This pothole is an elliptical feature with a long axis of approximately 100 m, a short axis of approximately 50 m and a slump of approximately 5 m. Due to the size of the slump, this elliptical area defined by the pothole is not available for mining. The area of the pothole was calculated in the mapping software as 3,927 m².

The total area available for mining is now 15,231 m² – 3,927 m² = 11,304 m².
If the presence of the pothole was unknown (i.e. borehole radar had not been applied), then the same amount of development would have taken place, i.e. 609 m.
The *m²/m* ratio would then have been 11,304/609 = 18.56 m²/m, i.e. with the same amount of development, 6.4 m² less would have been available for mining.
Converted to monetary values:

If the development cost is taken at R3,500/m (De Jager, *pers comm*):

	A	B
Development cost	609 x R3,500 =R2,131,500	609 x R3500 =R2,131,500
Reef available	15,231 m²	11,304 m²
Reef thickness	1 m²	1 m²
Reef volume	15,231 m³	11,304 m³
SG	3.4 t/m³	3.4 t/m³
Tonnes of reef	51,784.4 t	38,433.6 t
Average grade	6.26 g/t	6.26 g/t
Grams of Pt in situ	324,177 g	240,594 g
Ounces of Pt in situ	10,423 oz	7,736 oz
Average platinum price	$1141.84/oz	$1141.84/oz
$ value of Pt in situ	$11,902,181	$8,833,448
R/$ exchange (Apr 2006)	6.73	6.73
R value of Pt in situ	R80,101,675	R59,449,106

In Case A, R2,688,000 was spent on development for in situ ore worth R80,101,675, while in Case B the same amount was spent on development for in situ ore worth R20,652,569 less.

As described above, 609 m of development is required to make a potential 15,231 m² of reef available for mining. The percentage of reef affected by pothole A is 25.78%.

Development cost per metre: R3,500

Development metres at risk due to 25.78% geological loss: 157.02 m

Cost of development at risk: **R549,563**

This result relates back to the scenario described in Section 6.4, which relates to mine planning. If the position of the pothole had been known the design of the mine could have been adapted in order to minimise the amount of ore lost due to the pothole. According to Van Wyk (*pers comm*), the position of development can be adapted if the positions of disruptions to the reef plane are known. According to Van Wyk (*pers comm*), cross-cuts can be positioned up to 1 km apart if necessary.

6.6 Extraction

6.6.1 Deferred income

As described in Section 4.3.2, a pothole is considered a problem to mining if it fills up more than one-third of a mining panel. The pothole delineated by borehole radar on 10-Level 9W cross-cut, as described in Section 5.3.7, would have posed a problem to mining, since its side view at this section is approximately 100 m long. If it was mined until one-third of a panel was exposed (i.e. 12 m of the face), the following calculations can be done:

For 1 m advance at a face length of 12 m (i.e. per blast):

Area of Merensky Reef displaced	12	m²	
Average thickness of reef	1	m	
Volume of reef	12	m³	
SG	3.4	t/m³	
Tonnes of reef	40.8	t	
Average grade/tonne (Pt)	6.26	g/t	Anglo Platinum Annual Report (2006)
Grams of Pt in situ	255.408	g	
Grams in a troy ounce	31.1		
Ounces of Pt in situ	8.21	$	
Average Pt price (2006)	1,141.84	$	Platinum 2007
Value of Pt in situ	9377	$	
Average R/$ exchange (2006)	6.73		www.gocurrency.com
Rand value of Pt in situ	63,109	R	

This means that for each blast that is mined into the pothole, R63,109 of income is deferred until a later date.

6.6.2 Labour efficiency

The ore body is extracted by stoping. Stoping is carried out by mining crews. For this exercise it is assumed that there are 14 people in a mining crew.
Average cost to company per month per mining-crew employee: R8,000
Total monthly cost to company for 14-person mining crew: R112,000

Let's assume this mining crew is advancing along a panel that is 35 m wide as shown in Figure 45.

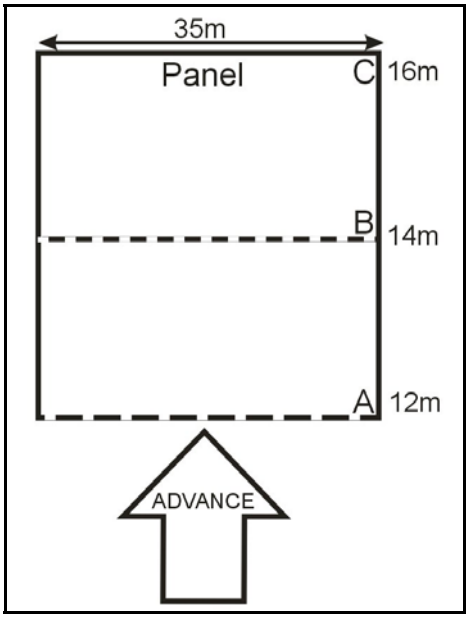

Figure 45: Hypothetical monthly advance of a mining crew along a 35 m long panel

For three cases A, B and C, the situation is as follows:

Per month:	A	B	C
Advance	12 m	14 m	16 m
Area	420 m²	490 m²	560 m²
Employee cost	R112,000	R112,000	R112,000
Employee cost/m²	R267/m²	R229/m²	R200/m²

The calculation above shows that the saving in labour due to efficiency for advancing 14 m instead of 12 m is: R267 – R229 = R38/m².
If this cost is applied to the mining block covered by borehole radar that has a surface area of 15,231 m², the saving is 15,231 m² x R38 = R578,778.

Predicted in situ value of ore in mining block: R80,101,674.76

Although the example given here is hypothetical, it serves to demonstrate that if disruptions in the ore body can be predicted using borehole radar and stope advance can be increased by as little as 2 m the mine can save 0.7% of the value of the in situ ore.

The result is that mining crews can be used more efficiently, and unnecessary development into waste rock can be prevented.

6.7 Processing

The processing of the ore extracted is directly affected by the presence of waste material. The ore is effectively diluted and waste material that displaces ore in the mill will lead to inefficiencies and a loss of revenue.

In this example it is assumed that the pothole material is mined through and reports to ore in the plant, i.e. it is not detected as waste material. According to Marais (*pers comm*), this scenario will most likely be prevented by daily monitoring of the plant head-grade, but another reason why this calculation is of importance is that if the pothole is mined through in the hope that reef will be encountered, the result is "deferred income", i.e. waste is being mined as ore and income that would have been derived from ore is being postponed until a later date.

Tonnes covered by mining block described in Section 6.5:	51,784 t
Tonnes of waste due to pothole A:	13,350 t
Cost per tonne (shaft head + overheads + concentrator):	R380
Mining cost of waste tonnes mined as ore:	**R5,073,000**

The loss of revenue due to mining through the pothole can be calculated as follows:

Tonnes milled from mining block described in Section 6.5:	51,784 t
Planned contained Pt at 6.26g/t:	10,423 ounces
Actual contained Pt (diluted 25.78%):	7,736 ounces
Lost Pt:	2,687 ounces
Lost revenue at $1,141.84/oz and exchange rate of 6.73:	**R20,648,475**

If the loss of revenue for one mining block is R20,648,475, the impact on the entire mine where waste is mined instead of ore due to unpredicted geological losses will be significant.

7 CONCLUSIONS AND RECOMMENDATIONS

7.1 Conclusions

This project aimed to provide clear evidence that incorporating borehole radar in the mining cycle will provide significant cost benefit in the long term.
This study has shown that the application of borehole radar prior to mining:

- Provides more geological information about the reef prior to mining than relying only on geological intersection of the reef.
- Can provide continuous reef coordinates along the illumination line, as opposed to the point intersections provided by geological cover drilling.
- Significantly improves the confidence in the elevation of the Merensky Reef within the mining block.
- Samples a much larger portion of the reef to be extracted than standard geological drilling at a significantly reduced cost.
- Improves mine planning and ensures that mine development is put in the correct place.
- Avoids unnecessary mine development.
- Can ensure that mining teams are deployed more effectively in areas where reef has been defined by borehole radar.
- Can prevent sending waste to the plant instead of ore.
- Can avoid deferring income until a later date.

The findings that were calculated in the previous sections are summarised in Table 6. Results are given for the scenario where only geological drilling would have been used to make mining decisions about the defined mining block, as opposed to the situation after borehole radar was applied. The broad impact of borehole radar at the various mining cycles is shown in Table 7.

Table 6: Conclusions summarised for applying only geological drilling, compared with conducting borehole radar

	Geological drilling (before borehole radar was applied)	**Borehole radar**
Number of reef elevation coordinates	4	716
Cost per reef elevation point	R45,667	R1,968
Extrapolated area covered	4 intersection points within block	15,231 m²
Confidence range (of geostatistical mean)	28 m	2 m
Actual area of reef sampled	0.0054 m²	2,330 m²
% of mining block sampled	0.00035%	15.3%
Cost per m² sampled	R5,600,000	R163
m²/m ratio	18.56	25
Expected value of in situ platinum	R80,101,675	R59,449,106
Cost of development at risk	R549,563	R0
Income deferred	R63,109 per 12 x 1 m advance	R0
Reduction in labour cost per block	R0	R578,778
Cost of processing waste as ore (or deferred income)	R20,648,475	R0

Table 7: The impact of borehole radar at the five stages of mining an ore body

	Mining stage	Impact of borehole radar
1.	Ore body definition	Increased knowledge leads to improved reserve definition and improved confidence
2.	Mine design	Improved mine planning
3.	Development	Improvement in m^2/m ratio
4.	Extraction	Improved planning and improvement of efficiencies
5.	Processing	Dilution lowered and better recoveries

7.2 Recommendations

It is recommended that:

- The borehole radar interpretation made in this treatise be reconciled with the actual situation once the area discussed is mined.
- Further work is done in order to determine how the mine layout can be optimised in order to accommodate operational borehole radar surveys.
- The impact of borehole radar on mine design is investigated further.

Borehole radar should become a routine tool with which to predict disruptions in the reef prior to mining. It is recommended that borehole radar be conducted from regularly spaced boreholes drilled from haulages, prior to developing cross-cuts. The proposed borehole layout is shown in section (Figure 46) and plan (Figure 47).

When disruptions in the reef are detected using borehole radar, the position of development can then be optimised (Figure 48).

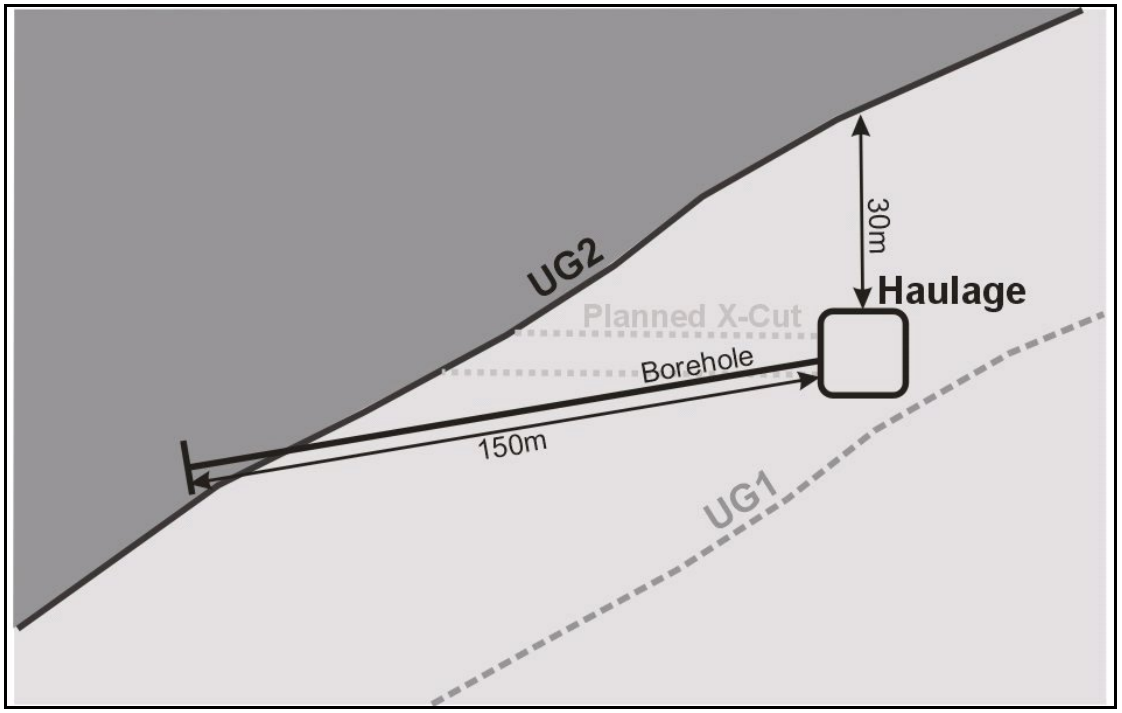

Figure 46: Proposed borehole layout in section for applying borehole radar to detect geological deviations prior to mining

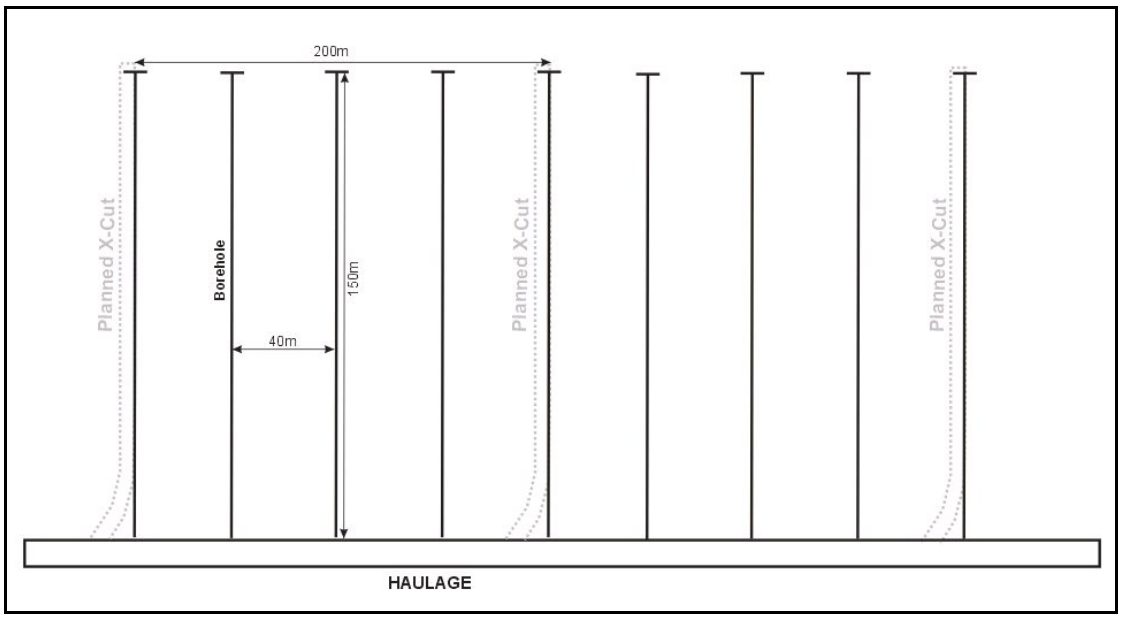

Figure 47: Proposed borehole radar layout in plan for the prediction of geological disruptions prior to mine development

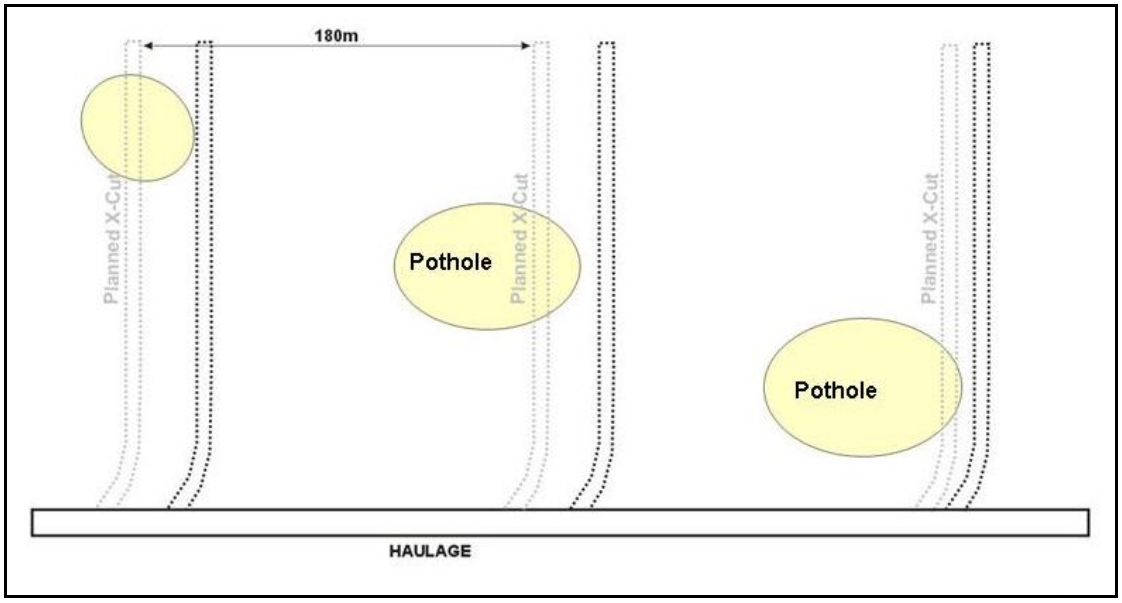

Figure 48: Optimisation of mine development after the application of borehole radar

8 ACKNOWLEDGEMENTS

The Platmine Research Collaborative is thanked for allowing this work to be published.

Declan Vogt at the CSIR, is thanked for many useful discussions and being my borehole radar guru.

Bruce Walters, Quartus Snyman and Wian Marais at Anglo Platinum are thanked for their efforts in securing the case-study site at Amandelbult Section as well as for their inputs in useful discussion relating to the results produced here.

Alan King from Anglo Technical Division is thanked for his valuable input to financial discussions and for motivating me to go the extra mile.

Andy Rompel Stompel is thanked for checking that a geophysicist is getting the geology right.

Carel de Jager from Anglo Platinum is thanked for providing the basis of the financial analysis.

Ferdi Camisani-Calzolari is thanked for teaching me the basics of geostatistics.

Prof. Hennie Theart is thanked for his inputs and suggestions, and for throwing my first draft across the room.

My family is thanked for giving me nonsense whenever I procrastinated.

My friend, “Eagle-eye” Riaan Wolmarans, is thanked for wading through a very technical piece of editing.

My friends are thanked for partying on my behalf while I was chained to my computer.

Last but by no means least, my husband, Albert Swart, is thanked for supporting me in every crazy project that I tackle.

9 REFERENCES

Anglo Platinum. (2006) Annual Report.

Carr, H.W., Groves, D.I. and Cawthorn, R.G. (1994). The importance of synmagmatic deformation of Merensky Reef potholes in the Bushveld Complex, *Economic Geology*, **89**, 1398 – 1410.

Cawthorn, R.G. (1999). The platinum and palladium resources of the Bushveld Complex, *South African Journal of Science,* **95**, 481 – 489.

Chalke, B.L., Chalke, T. and Rompel, A.K.K. (2006) Paardekraal #2 Mine Expansion Project, PDL 159 Geotechnical Interpretation Report. Internal Anglo Technical Division Report Number 15/173/141/2006/158, 51pp.

Clarke, I. and Harper, W.V. (2000) Practical Geostatistics 2000, Ecosse North America Llc, Columbus, Ohio, USA. 342pp.

Daniels, J.D. (2004) Ground Penetrating Radar, 2nd Edition. The Institution of Electrical Engineers, London.

De Jager, C. (2006) Principal Mining Economist, Mining Economics, Anglo Technical Division, *Personal Communication*.

De Vries, P. and Du Pisani, P. (2005) Borehole radar delineation of the UG2 Reef at Modikwa Mine. *9th SAGA Biennial Technical Meeting and Exhibition*. September 2005. Cape Town.

Du Pisani, P. and Vogt, D. (2003) Radar frequency electrical properties of rocks associated with the VCR, UG2 and Merensky ore bodies. *8th SAGA Biennial Technical Meeting and Exhibition*. September 2003. Pilanesberg.

Du Pisani, P. and Vogt, D. (2004) Borehole radar delineation of the Ventersdorp Contact Reef in Three Dimensions. *Exploration Geophysics*. **35**, 319 – 323.

Du Plessis, A. and Kleywegt, R.J. (1987) A dipping sheet model for the mafic lobes of the Bushveld Complex. *South African Journal of Geology*. **90**, 1 – 6.

Eales, H.V., Botha, W.J., Hattingh, P.J., De Klerk, W.J., Maier, W.D. and Odgers, A.T.R. (1993) The mafic rocks of the Bushveld Complex: a review of emplacement and crystallization history, and mineralization, in light of recent data. *Journal of African Earth Science.* **16**, 121 – 142.

Eales, H.V. and Cawthorn, R.G. (1996) The Bushveld Complex. In: Cawthorn, R.G. (Ed.), Layered Intrusions. Elsevier, Amsterdam, 181 – 230.

Farquar, J. (1986) The Western Platinum Mine. In: Anhaeusser, C.R. and Maske, S. (Eds.), Mineral Deposits of Southern Africa. Geological Society of South Africa. Johannesburg, South Africa, **II**, 1135 – 1142.

Heinz, W.F. (1994) Diamond Drilling Handbook 3rd Edition. W.F. Heinz, Halfway House.

Irvine, T.N. (1982) Terminology for layered intrusions. *Journal of Petrology*. **23**, 127 – 162.

Kinloch, E.D. and Peyerl, W. (1990) Platinum-group minerals in various rock types of the Merensky Reef: genetic implications. *Economic Geology*. **85**, 537 – 555.

Kruger, F.J. (1990) The stratigraphy of the Bushveld Complex: a reappraisal and the relocation of the Main Zone boundaries. *South African Journal of Geology*. **94**, 376 – 381.

Leeb Du Toit, A. (1986). The Impala Platinum Mines. In: Anhaeusser, C. R. and Maske, S (Eds.), Mineral Deposits of Southern Africa. Geological Society of South Africa. Johannesburg, South Africa, **II**, 1091 – 1106.

Marais, W. (2007) Senior Geologist, Central Functions, Anglo Platinum Rustenburg Section. *Personal communication.*

Noon, D.A., Stickley, G.F., and Longstaff, D. (1998). A frequency independent characterisation of GPR penetration and resolution performance. *Journal of Applied Geophysics*. **40**, 127 – 137.

Platinum 2007 (2007). Johnson Matthey, Hertfordshyre, England. 56pp.

SAMREC Code. (2000) South African code for reporting of mineral resources and mineral reserves (the SAMREC code) – Prepared by the South African mineral resource committee (SAMREC) under the auspices of the SAIMM. Effective March 2000, SAIMM, Johannesburg, South Africa, 39pp.

Schürmann, L.W. (1991) The geochemistry and petrology of the upper critical zone of the Boshoek section of the western Bushveld Complex. *Bulletin of the Geological Survey of South Africa*. **113**, 88pp.

Simmat, C. M., Osman, N., Hargreaves., Mason, I. M., (2002) Borehole radar imaging from deviating boreholes: *Ninth International Conference on Ground Penetrating Radar*, S.K. Koppenjan, H. Lee, (Eds.), Proceedings of SPIE. **4758**, 404 – 409.

Turner, G., Mason, I., Hargreaves J., and Wellington, A. (2000) Borehole radar surveying for orebody delineation: *Eighth International Conference on Ground Penetrating Radar*, D.A. Noon., G.F. Stickley, D. Longstaff, (Eds.), Proceedings of SPIE. **4084**, 282 – 287.

Turner, G. and Siggins, A.F. (1994) Constant Q attenuation of subsurface radar pulses. *Geophysics*. **59**. 1192 – 1200.

Unknown. (1986) A Guide to the Geology of Amandelbult, based on Anhaeusser and Maske, 1986.

Van Wyk, A. (2006) Production Manager, Amandelbult 1-Shaft. *Personal communication*.

Viljoen, M.J. (1994) A review of regional variations in facies and grade distribution of the Merensky Reef, Western Bushveld Complex, with some mining implications. *Proceedings of the 15th CMMI Congress*. South African Institute of Mining and Metallurgy, 183 – 194.

Viljoen, M.J. (1999) The nature and origin of the Merensky Reef of the Western Bushveld Complex based on geological facies and geophysical data. *South African Journal of Geology*. **102**. 221 – 239.

Viljoen, M.J. and Hieber, R.W. (1986) The Rustenburg Section of Rustenburg Platinum Mines Limited, with reference to the Merensky Reef. In: Anhaeusser, C.R. and Maske, S. (Eds), Mineral Deposits of Southern Africa. Geological Society of South Africa Johannesburg, South Africa, **II**. 1107 – 1134.

Viljoen, M.J. and Schürmann, L.W. (1998) Platinum Group Metals. In: Wilson, M.G.C. and Annhaeusser, C.R. (Eds.), The Mineral Resources of South Africa. Council for Geoscience, South Africa, Pretoria, 532 – 568.

Viljoen, M.J., De Klerk, W.J., Coetzer., Hatch, N.P., Kinloch, E.D. and Peyerl, W. (1986a) The Union Section of Rustenburg Platinum Mines Limited, with reference to the Merensky Reef. In: Anhaeusser, C.R. and Maske, S. (Eds.), Mineral Deposits of Southern Africa. Geological Society of South Africa, Johannesburg, South Africa, **II**. 1061 – 1190.

Viljoen, M.J., Theron, J., Underwood, B., Walters, B.M., Weaver, J. and Peyerl, W. (1986b) The Amandelbult Section of Rustenburg Platinum Mines Limited, with reference to the Merensky Reef. In. Anhaeusser, C.R. and Maske, S. (Eds), Mineral Deposits of Southern Africa. Geological Society of South Africa Johannesburg, South Africa, **II**. 1041 – 1060.

Vogt, D. (2000) The modelling and design of Radio Tomography antennas: D.Phil. Thesis, University of York.

Vogt, D. (2002) A Slimline Borehole Radar for In-Mine Use. *9th International Conference on Ground Penetrating Radar*, Proceedings of SPIE, **5758**, 31 – 36.

Vogt, D. (2003) An introduction to Ground Penetrating Radar. Course notes for geophysicists. Wits University. CSIR Miningtek. Johannesburg.

Vogt, D., Van Schoor, M. and Du Pisani, P. (2005) The application of radar techniques for in-mine feature mapping in the Bushveld Complex of South Africa. *The Journal of the South African Institute of Mining and Metallurgy*. **105**. 391 – 399.

Vogt, D. (2006) A borehole radar system for South African gold and platinum mines. *South African Journal of Geology*. **109**. 521 – 528.

Vogt, D. (2007) Competency Area Manager, Mining, Department of Natural Resources and the Environment, CSIR, *Personal communication*.

Wagner, P.A. (1929) The Platinum Deposits and Mines of South Africa. Oliver and Boyd, Edinburgh, Scotland, 326pp.

www.gocurrency.com, [Web page]: accessed 17 September 2007.

www.platmine.co.za, [Web page]: accessed 9 July 2006.

www.platinummetalsreview.com, [Web page]: accessed 12 July 2007.

APPENDIX A BOREHOLE INFORMATION

Rock and stratigraphy codes

Code	Explanation
BR	Bastard Reef
COL	Collar
DYK	Dyke
EOH	End of hole
FERPL	Iron replacement
FRAC	Fracture
FRZONE	Fracture zone
FWM	Footwall marker
LN	Leuco-norite
MESN	Meso-norite
MN	Mela-norite
POIKFPYX	Poikilitic Feldspathic Pyroxenite
POIKPYX	Poikilitic Pyroxenite
SHR	Shear

Borehole information for borehole 1

BHID	FROM	TO	X	Y	Z	ROCK
10/9W/BHR1 D0	0	0	31791.8	-44745.2	432.665	COL
10/9W/BHR1 D0	0	1.43	31792.02	-44744.4	432.543	POIKFPYX
10/9W/BHR1 D0	1.43	1.44	31792.3	-44743.8	432.4282	SF
10/9W/BHR1 D0	1.44	1.68	31792.35	-44743.6	432.4091	POIKFPYX
10/9W/BHR1 D0	1.68	2.06	31792.5	-44743.4	432.3627	MN
10/9W/BHR1 D0	2.06	2.07	31792.59	-44743.3	432.3341	SF
10/9W/BHR1 D0	2.07	3.91	31793.12	-44742.7	432.2047	MN
10/9W/BHR1 D0	3.91	98.7	31839.2	-44754.7	428.3869	MESN
10/9W/BHR1 D0	98.7	98.91	31884.71	-44768.2	426.4627	LN
10/9W/BHR1 D0	98.91	102.79	31886.67	-44768.7	426.4267	POIKAN
10/9W/BHR1 D0	102.79	103.3	31888.78	-44769.4	426.3924	LN
10/9W/BHR1 D0	103.3	104.92	31889.8	-44769.7	426.3781	POIKAN
10/9W/BHR1 D0	104.92	105.6	31890.9	-44770	426.3646	LN
10/9W/BHR1 D0	105.6	114.8	31895.64	-44771.4	426.3275	POIKAN
10/9W/BHR1 D0	114.8	115.2	31900.23	-44772.8	426.3198	LN
10/9W/BHR1 D0	115.2	117.2	31901.38	-44773.1	426.3226	POIKAN
10/9W/BHR1 D0	117.2	118.08	31902.76	-44773.6	426.3287	LN
10/9W/BHR1 D0	118.08	123.08	31905.57	-44774.4	426.3506	MESN
10/9W/BHR1 D0	123.08	126.04	31909.38	-44775.6	426.4032	POIKAN
10/9W/BHR1 D0	126.04	126.1	31910.82	-44776	426.4304	SHR
10/9W/BHR1 D0	126.1	126.83	31911.2	-44776.1	426.4381	POIKAN
10/9W/BHR1 D0	126.83	135.89	31915.88	-44777.6	426.5486	POIKFPYX
10/9W/BHR1 D0	135.89	135.9	31920.21	-44778.9	426.6759	SF
10/9W/BHR1 D0	135.9	135.93	31920.23	-44778.9	426.6766	POIKFPYX
10/9W/BHR1 D0	135.93	135.95	31920.26	-44778.9	426.6773	SF
10/9W/BHR1 D0	135.95	136.01	31920.29	-44778.9	426.6786	DYK
10/9W/BHR1 D0	136.01	136.12	31920.38	-44778.9	426.6812	POIKFPYX
10/9W/BHR1 D0	136.12	136.55	31920.63	-44779	426.6896	DYK
10/9W/BHR1 D0	136.55	137.49	31921.29	-44779.2	426.7112	POIKFPYX
10/9W/BHR1 D0	137.49	137.54	31921.76	-44779.4	426.7272	DYK
10/9W/BHR1 D0	137.54	138.1	31922.05	-44779.5	426.7372	POIKFPYX
10/9W/BHR1 D0	138.1	138.4	31922.46	-44779.6	426.7515	SF
10/9W/BHR1 D0	138.4	138.84	31922.82	-44779.7	426.7641	POIKFPYX
10/9W/BHR1 D0	138.84	138.85	31923.03	-44779.8	426.7718	SF
10/9W/BHR1 D0	138.85	141.16	31924.14	-44780.1	426.8131	POIKFPYX
10/9W/BHR1 D0	141.16	141.17	31925.25	-44780.4	426.8568	SF
10/9W/BHR1 D0	141.17	143.01	31926.13	-44780.7	426.8933	POIKFPYX
10/9W/BHR1 D0	143.01	145.06	31927.99	-44781.3	426.975	POIKAN
10/9W/BHR1 D0	145.06	145.09	31928.99	-44781.6	427.0214	DYK
10/9W/BHR1 D0	145.09	145.51	31929.2	-44781.6	427.0316	POIKAN
10/9W/BHR1 D0	145.51	149.09	31931.12	-44782.2	427.1269	MN

Borehole information for borehole 2

BHID	FROM	TO	X	Y	Z	ROCK
10/9W/BHR2 D0	0	0	31791	-44744	433.14	COL
10/9W/BHR2 D0	0	0.44	31791.02	-44743.8	433.1676	MN
10/9W/BHR2 D0	0.44	1.06	31791.1	-44743.2	433.2339	FRAC
10/9W/BHR2 D0	1.06	3.03	31791.45	-44742	433.3961	MN
10/9W/BHR2 D0	3.03	3.21	31791.92	-44741.1	433.5328	MESN
10/9W/BHR2 D0	3.21	3.22	31791.97	-44741	433.5452	FRAC
10/9W/BHR2 D0	3.22	4.44	31792.32	-44740.6	433.6259	MESN
10/9W/BHR2 D0	4.44	4.7	31792.82	-44740.1	433.7263	FRAC
10/9W/BHR2 D0	4.7	6.71	31793.77	-44739.4	433.889	MESN
10/9W/BHR2 D0	6.71	7.14	31794.9	-44738.9	434.0543	FRAC
10/9W/BHR2 D0	7.14	8.17	31795.57	-44738.6	434.1497	LN
10/9W/BHR2 D0	8.17	8.26	31796.09	-44738.4	434.223	FRAC
10/9W/BHR2 D0	8.26	9.79	31796.84	-44738.2	434.3289	LN
10/9W/BHR2 D0	9.79	9.84	31797.58	-44737.9	434.4321	FRAC
10/9W/BHR2 D0	9.84	9.94	31797.65	-44737.9	434.4419	LN
10/9W/BHR2 D0	9.94	9.98	31797.71	-44737.9	434.4511	FRAC
10/9W/BHR2 D0	9.98	10.59	31798.02	-44737.8	434.4936	LN
10/9W/BHR2 D0	10.59	11.63	31798.8	-44737.5	434.6015	MESN
10/9W/BHR2 D0	11.63	11.93	31799.44	-44737.3	434.6891	OLVN
10/9W/BHR2 D0	11.93	14.51	31800.82	-44737	434.8776	MESN
10/9W/BHR2 D0	14.51	14.57	31802.09	-44736.6	435.0514	FRAC
10/9W/BHR2 D0	14.57	14.92	31802.28	-44736.6	435.0784	MESN
10/9W/BHR2 D0	14.92	15.01	31802.49	-44736.5	435.1075	FRAC
10/9W/BHR2 D0	15.01	15.46	31802.75	-44736.5	435.1432	MESN
10/9W/BHR2 D0	15.46	16.8	31803.61	-44736.2	435.262	MN
10/9W/BHR2 D0	16.8	17.59	31804.63	-44736	435.4038	MESN
10/9W/BHR2 D0	17.59	17.76	31805.09	-44735.9	435.468	FRAC
10/9W/BHR2 D0	17.76	23.29	31807.83	-44735.2	435.8526	MESN
10/9W/BHR2 D0	23.29	23.35	31810.51	-44734.5	436.2365	FRAC
10/9W/BHR2 D0	23.35	24.8	31811.24	-44734.3	436.3414	MESN
10/9W/BHR2 D0	24.8	25	31812.03	-44734.1	436.4567	LN
10/9W/BHR2 D0	25	25.05	31812.15	-44734.1	436.4742	FRAC
10/9W/BHR2 D0	25.05	27.71	31813.46	-44733.8	436.6655	LN
10/9W/BHR2 D0	27.71	37.84	31819.6	-44732.3	437.5977	MESN
10/9W/BHR2 D0	37.84	37.93	31824.52	-44731.1	438.3833	FRAC
10/9W/BHR2 D0	37.93	49.89	31830.31	-44729.8	439.3584	MESN
10/9W/BHR2 D0	49.89	49.98	31836.1	-44728.5	440.3924	FRAC
10/9W/BHR2 D0	49.98	50.81	31836.55	-44728.4	440.4734	MESN
10/9W/BHR2 D0	50.81	50.83	31836.96	-44728.3	440.5484	FRAC
10/9W/BHR2 D0	50.83	50.89	31836.99	-44728.3	440.5555	LN
10/9W/BHR2 D0	50.89	53.08	31838.07	-44728	440.7553	MESN
10/9W/BHR2 D0	53.08	53.13	31839.15	-44727.8	440.9556	FRAC
10/9W/BHR2 D0	53.13	53.26	31839.24	-44727.8	440.9717	MESN
10/9W/BHR2 D0	53.26	54.07	31839.69	-44727.7	441.0563	LN
10/9W/BHR2 D0	54.07	55.56	31840.79	-44727.5	441.2643	MESN
10/9W/BHR2 D0	55.56	60.67	31843.96	-44726.8	441.8716	LN
10/9W/BHR2 D0	60.67	60.7	31846.43	-44726.2	442.3554	FRAC
10/9W/BHR2 D0	60.7	60.93	31846.56	-44726.2	442.3802	MESN
10/9W/BHR2 D0	60.93	60.98	31846.69	-44726.2	442.4068	FRAC
10/9W/BHR2 D0	60.98	61.64	31847.03	-44726.1	442.4745	MESN
10/9W/BHR2 D0	61.64	61.67	31847.37	-44726	442.5405	FRAC
10/9W/BHR2 D0	61.67	61.77	31847.43	-44726	442.5529	MESN
10/9W/BHR2 D0	61.77	61.82	31847.5	-44726	442.5673	FRAC
10/9W/BHR2 D0	61.82	61.89	31847.56	-44726	442.5788	MESN
10/9W/BHR2 D0	61.89	61.91	31847.6	-44726	442.5874	FRAC
10/9W/BHR2 D0	61.91	64.83	31849.01	-44725.7	442.8709	MESN
10/9W/BHR2 D0	64.83	64.86	31850.43	-44725.4	443.1585	FRAC
10/9W/BHR2 D0	64.86	65.18	31850.6	-44725.4	443.1928	MESN
10/9W/BHR2 D0	65.18	65.21	31850.77	-44725.3	443.2272	FRAC
10/9W/BHR2 D0	65.21	66.22	31851.27	-44725.2	443.3296	MESN
10/9W/BHR2 D0	66.22	71.88	31854.47	-44724.6	443.9966	POIKAN
10/9W/BHR2 D0	71.88	72.71	31857.59	-44724	444.6639	MESN
10/9W/BHR2 D0	72.71	76.41	31859.76	-44723.6	445.1404	POIKAN
10/9W/BHR2 D0	76.41	76.76	31861.7	-44723.2	445.5738	POIKPYX
10/9W/BHR2 D0	76.76	83.53	31865.08	-44722.4	446.352	POIKPYX
10/9W/BHR2 D0	83.53	83.66	31868.37	-44721.7	447.1235	FRAC
10/9W/BHR2 D0	83.66	104.18	31878.17	-44719.5	449.5288	POIKPYX
10/9W/BHR2 D0	104.18	104.28	31887.95	-44717.4	451.9963	FRAC
10/9W/BHR2 D0	104.28	104.62	31888.16	-44717.3	452.049	POIKAN
10/9W/BHR2 D0	104.62	104.7	31888.36	-44717.3	452.0995	FRAC
10/9W/BHR2 D0	104.7	106.17	31889.09	-44717.1	452.2856	POIKAN
10/9W/BHR2 D0	106.17	110.27	31891.74	-44716.6	452.9576	FRAC
10/9W/BHR2 D0	110.27	110.64	31893.86	-44716.1	453.4983	POIKPYX

Borehole information for borehole 3

BHID	FROM	TO	X	Y	Z	ROCK
10/9W/BHR3 D0	0	0	31794.4	-44748	432.013	COL
10/9W/BHR3 D0	0	1.5	31794.69	-44747.2	431.7234	MN
10/9W/BHR3 D0	1.5	7.95	31797.11	-44745.7	430.3627	MESN
10/9W/BHR3 D0	7.95	16.69	31803.24	-44749.9	428.6192	LN
10/9W/BHR3 D0	16.69	41.75	31816.25	-44760.2	425.3955	MESN
10/9W/BHR3 D0	41.75	49.1	31828.74	-44770.1	422.5459	LN
10/9W/BHR3 D0	49.1	58.43	31835.19	-44775.2	421.1751	MESN
10/9W/BHR3 D0	58.43	70.48	31843.49	-44781.8	419.5261	LN
10/9W/BHR3 D0	70.48	73.56	31849.36	-44786.4	418.4584	MESN
10/9W/BHR3 D0	73.56	76.33	31851.63	-44788.2	418.0689	LN
10/9W/BHR3 D0	76.33	78.53	31853.56	-44789.8	417.7497	MESN
10/9W/BHR3 D0	78.53	86.51	31857.52	-44792.9	417.1351	LN
10/9W/BHR3 D0	86.51	97.48	31864.89	-44798.8	416.1231	LN
10/9W/BHR3 D0	97.48	101.65	31870.77	-44803.5	415.4192	POIKAN
10/9W/BHR3 D0	101.65	102.14	31872.58	-44804.9	415.2199	MESN
10/9W/BHR3 D0	102.14	102.41	31872.88	-44805.2	415.1882	LN
10/9W/BHR3 D0	102.41	111.18	31876.39	-44808	414.8332	POIKAN
10/9W/BHR3 D0	111.18	111.57	31879.96	-44810.8	414.5125	MESN
10/9W/BHR3 D0	111.57	114.55	31881.27	-44811.9	414.4024	POIKAN
10/9W/BHR3 D0	114.55	116.08	31883.02	-44813.3	414.2617	LN
10/9W/BHR3 D0	116.08	116.51	31883.78	-44813.9	414.2032	POIKAN
10/9W/BHR3 D0	116.51	116.67	31884.01	-44814.1	414.1859	MESN
10/9W/BHR3 D0	116.67	119.15	31885.04	-44814.9	414.1105	LN
10/9W/BHR3 D0	119.15	119.39	31886.09	-44815.8	414.036	FRAC
10/9W/BHR3 D0	119.39	119.65	31886.29	-44815.9	414.0226	LN
10/9W/BHR3 D0	119.65	119.85	31886.46	-44816.1	414.0105	DYK
10/9W/BHR3 D0	119.85	121.36	31887.13	-44816.6	413.9659	LN
10/9W/BHR3 D0	121.36	125.48	31889.31	-44818.4	413.8268	POIKAN
10/9W/BHR3 D0	125.48	125.6	31890.95	-44819.7	413.7297	FRAC
10/9W/BHR3 D0	125.6	127.03	31891.55	-44820.2	413.6957	POIKPYX
10/9W/BHR3 D0	127.03	127.1	31892.13	-44820.7	413.6627	DYK
10/9W/BHR3 D0	127.1	127.25	31892.21	-44820.8	413.6578	POIKPYX
10/9W/BHR3 D0	127.25	127.37	31892.31	-44820.9	413.6518	DYK
10/9W/BHR3 D0	127.37	162.8	31906.04	-44832.1	412.859	POIKPYX
10/9W/BHR3 D0	162.8	163.44	31920.01	-44843.5	411.9177	POIKPYX
10/9W/BHR3 D0	163.44	174.71	31924.35	-44847.6	411.5753	POIKPYX
10/9W/BHR3 D0	174.71	175.93	31928.95	-44851.8	411.2388	MN
10/9W/BHR3 D0	175.93	176.39	31929.58	-44852.3	411.1966	MESN
10/9W/BHR3 D0	176.39	176.46	31929.78	-44852.5	411.1834	LN
10/9W/BHR3 D0	176.46	213.26	31943.73	-44864.5	410.5221	POIKAN

Borehole information for borehole 4

BHID	FROM	TO	X	Y	Z	ROCK
10/9W/BHR4 D0	0	0	31790.2	-44743	433.554	COL
10/9W/BHR4 D0	0	4.4	31790.45	-44740.9	434.1758	POIKPYX
10/9W/BHR4 D0	4.4	25.56	31797.6	-44731	437.4726	MESN
10/9W/BHR4 D0	25.56	39.28	31808.91	-44718.6	442.0609	MN
10/9W/BHR4 D0	39.28	83.52	31827.71	-44698.1	450.3586	MESN
10/9W/BHR4 D0	83.52	85.33	31842.6	-44682.2	457.7849	LN
10/9W/BHR4 D0	85.33	96.46	31846.75	-44677.8	460.0024	MESN
10/9W/BHR4 D0	96.46	97.17	31850.56	-44673.7	462.0715	POIKPYX
10/9W/BHR4 D0	97.17	97.4	31850.86	-44673.4	462.2373	MESN
10/9W/BHR4 D0	97.17	97.4	31850.86	-44673.4	462.2373	MESN
10/9W/BHR4 D0	97.4	97.87	31851.09	-44673.2	462.3609	FERPL
10/9W/BHR4 D0	97.87	103.34	31853.06	-44671.2	463.4136	POIKPYX
10/9W/BHR4 D0	103.34	106.56	31856	-44668.4	464.9654	FERPL
10/9W/BHR4 D0	106.56	108.14	31857.6	-44666.9	465.8271	POIKPYX
10/9W/BHR4 D0	108.14	108.34	31858.19	-44666.3	466.1474	FRAC
10/9W/BHR4 D0	108.34	109.7	31858.7	-44665.8	466.4285	POIKPYX
10/9W/BHR4 D0	109.7	109.83	31859.19	-44665.3	466.6972	FRAC
10/9W/BHR4 D0	109.83	109.87	31859.25	-44665.2	466.7279	POIKPYX
10/9W/BHR4 D0	109.87	110.01	31859.31	-44665.2	466.7604	FRAC
10/9W/BHR4 D0	110.01	129.71	31865.74	-44658.5	470.3781	POIKPYX
10/9W/BHR4 D0	129.71	129.82	31872.19	-44652	474.0662	DYK
10/9W/BHR4 D0	129.82	139.75	31875.43	-44648.6	475.9535	POIKPYX

APPENDIX B BOREHOLE RADAR ILLUMINATION LINE COORDINATES

Borehole 1: Borehole radar illumination line coordinates – dip direction

X	Y	Z	X	Y	Z
31791	-44739.5	426.972	31843.2	-44756.3	413.384
31839.1	-44754	413.39	31842.1	-44755.7	413.354
31839	-44753.6	413.412	31841.1	-44755	413.348
31838.2	-44753	413.471	31840.1	-44754.3	413.365
31837.2	-44752.3	413.559	31839.1	-44753.6	413.406
31836.3	-44751.7	413.671	31894.5	-44766.3	410.894
31835.5	-44751	413.807	31892.9	-44766.1	411.08
31834.6	-44750.4	413.966	31889.8	-44765.4	411.489
31833.8	-44749.7	414.149	31886.7	-44764.9	411.854
31833	-44749.1	414.356	31908	-44769	408.922
31832.2	-44748.5	414.586	31907.2	-44768.9	409.005
31831.4	-44747.9	414.84	31903.4	-44768.2	409.59
31830.6	-44747.3	415.118	31899.7	-44767.4	410.131
31830.1	-44746.6	415.42	31896.3	-44766.7	410.628
31829.7	-44745.9	415.763	31918.6	-44771.2	407.194
31828.9	-44745.3	416.168	31915.4	-44770.6	407.702
31827.8	-44744.7	416.633	31911.2	-44769.8	408.376
31826.5	-44744.1	417.16	31919.8	-44771.5	406.985
31824.9	-44743.5	417.747			
31823	-44742.9	418.395			
31820.9	-44742.4	419.105			
31818.5	-44741.9	419.875			
31815.8	-44741.4	420.706			
31812.9	-44740.9	421.598			
31809.8	-44740.4	422.551			
31806.4	-44740	423.565			
31802.7	-44739.5	424.639			
31798.9	-44739.1	425.775			
31885.8	-44764.6	411.976			
31883.8	-44764.4	412.174			
31881	-44763.9	412.45			
31878.3	-44763.5	412.682			
31875.6	-44763.2	412.871			
31872.9	-44762.9	413.014			
31870.7	-44762.7	413.114			
31868.9	-44762.3	413.188			
31867.2	-44762	413.254			
31865.4	-44761.6	413.312			
31863.6	-44761.2	413.362			
31861.8	-44760.8	413.404			
31860	-44760.4	413.437			
31858.2	-44760	413.463			
31856.3	-44759.6	413.481			
31854.4	-44759.2	413.491			
31852.5	-44758.7	413.493			
31850.6	-44758.3	413.488			
31848.7	-44757.8	413.474			
31846.7	-44757.4	413.452			
31844.7	-44756.9	413.422			

Borehole 1: Borehole radar illumination line coordinates – strike direction

X	Y	Z	X	Y	Z	X	Y	Z
31799.2	-44743.2	425.805	31856.9	-44754.4	414.819	31900.8	-44767.3	409.863
31801.4	-44743.7	425.008	31857.7	-44754.6	414.915	31901.9	-44767.6	409.807
31803.5	-44744.1	424.265	31858.6	-44754.9	414.969	31902.9	-44767.8	409.757
31805.4	-44744.5	423.576	31859.4	-44755.2	414.982	31904	-44768.1	409.708
31807.1	-44744.9	422.941	31860.2	-44755.6	414.983	31905.2	-44768.6	409.54
31808.7	-44745.2	422.359	31861	-44756	414.97	31906.5	-44769.3	409.292
31810.1	-44745.6	421.831	31861.8	-44756.4	414.945	31907.8	-44769.9	409.008
31811.3	-44745.8	421.354	31862.6	-44756.7	414.905	31909.3	-44770.5	408.688
31812.4	-44746.1	420.928	31863.4	-44757.1	414.852	31910.8	-44771.1	408.327
31813.2	-44746.4	420.55	31864.2	-44757.4	414.786	31912.5	-44771.7	407.922
31814	-44746.6	420.203	31864.9	-44757.8	414.705	31914.2	-44772.3	407.473
31814.8	-44746.8	419.86	31865.6	-44758.1	414.61	31916	-44772.9	406.978
31815.7	-44746.9	419.504	31866.4	-44758.4	414.515	31916.4	-44773.1	406.831
31816.5	-44747.1	419.133	31867.1	-44758.7	414.43	31917.9	-44773.5	406.438
31817.4	-44747.3	418.747	31867.8	-44758.9	414.34	31919.8	-44774.1	405.875
31818.3	-44747.5	418.347	31868.6	-44759.2	414.244			
31819.3	-44747.7	417.932	31869.3	-44759.5	414.142			
31820.2	-44747.9	417.503	31870.1	-44759.7	414.034			
31821.3	-44748.2	417.059	31870.9	-44760	413.92			
31822.3	-44748.4	416.6	31871.7	-44760.2	413.8			
31823.3	-44748.6	416.164	31872.5	-44760.5	413.674			
31824.4	-44748.4	415.856	31873.3	-44760.7	413.541			
31825.5	-44748.3	415.592	31874.1	-44761	413.402			
31826.6	-44748.3	415.362	31874.9	-44761.3	413.255			
31827.8	-44748.2	415.165	31875.8	-44761.5	413.101			
31829	-44748.2	415.002	31876.7	-44761.8	412.939			
31830.3	-44748.3	414.872	31877.6	-44762.1	412.77			
31831.6	-44748.4	414.775	31878.5	-44762.3	412.593			
31832.9	-44748.5	414.71	31879.4	-44762.6	412.407			
31834.3	-44748.6	414.677	31880.4	-44762.9	412.215			
31835.8	-44748.9	414.668	31881.4	-44763.2	412.014			
31837.2	-44749.2	414.621	31882.4	-44763.5	411.805			
31838.7	-44749.6	414.572	31883.4	-44763.7	411.597			
31840	-44749.9	414.53	31884.4	-44763.9	411.426			
31841.4	-44750.3	414.485	31885.1	-44764	411.319			
31842.7	-44750.7	414.447	31885.4	-44764.1	411.269			
31843.9	-44751	414.417	31886.4	-44764.3	411.123			
31845.1	-44751.3	414.395	31887.4	-44764.5	410.987			
31846.3	-44751.6	414.379	31888.5	-44764.6	410.861			
31847.4	-44751.9	414.371	31889.5	-44764.8	410.744			
31848.5	-44752.2	414.371	31890.5	-44765	410.638			
31849.5	-44752.5	414.383	31891.5	-44765.2	410.54			
31850.5	-44752.8	414.406	31892.5	-44765.4	410.453			
31851.5	-44753	414.437	31893.6	-44765.6	410.373			
31852.5	-44753.2	414.478	31894.6	-44765.8	410.289			
31853.4	-44753.5	414.528	31895.6	-44766.1	410.209			
31854.3	-44753.7	414.587	31896.7	-44766.3	410.129			
31855.2	-44753.9	414.655	31897.7	-44766.6	410.055			
31856.1	-44754.1	414.732	31898.8	-44766.8	409.986			

Borehole 2: Borehole radar illumination line coordinates – strike direction

X	Y	Z	X	Y	Z	X	Y	Z
31793.1	-44738.4	429.094	31825.6	-44727.2	427.845	31865.9	-44715.5	426.811
31794.2	-44737.4	429.105	31826.4	-44727	427.838	31866.8	-44715.2	426.823
31794.4	-44737.2	429.106	31827.3	-44726.7	427.822	31867.3	-44715.1	426.822
31795.3	-44736.8	429.01	31828.2	-44726.4	427.796	31867.2	-44715.1	426.829
31796.4	-44736.3	428.896	31828.8	-44726.3	427.774	31868.5	-44714.8	426.871
31796.7	-44736.2	428.857	31829.1	-44726.2	427.76	31870	-44714.4	426.949
31797.4	-44735.9	428.777	31830	-44725.9	427.715	31871.6	-44714	427.06
31798.4	-44735.6	428.659	31831	-44725.6	427.659	31873.3	-44713.5	427.207
31799.4	-44735.2	428.553	31832	-44725.2	427.593	31875.2	-44713.1	427.387
31800.3	-44734.9	428.457	31833	-44724.9	427.524	31877.2	-44712.6	427.602
31801.1	-44734.6	428.373	31834	-44724.6	427.457	31878.9	-44712.1	427.804
31801.4	-44734.5	428.342	31834.5	-44724.5	427.425	31879.3	-44712	427.851
31801.9	-44734.3	428.296	31835	-44724.3	427.393	31881.5	-44711.5	428.133
31802.6	-44734.1	428.23	31836	-44724	427.333	31883.8	-44710.9	428.449
31803.3	-44733.8	428.174	31837	-44723.7	427.277	31886.3	-44710.3	428.798
31804	-44733.6	428.129	31837.9	-44723.5	427.225	31888.9	-44709.6	429.181
31804.6	-44733.4	428.089	31838.8	-44723.2	427.178	31889.5	-44709.5	429.278
31805.3	-44733.2	428.05	31839.7	-44722.9	427.133	31891.6	-44709	429.594
31805.9	-44733	428.011	31840.6	-44722.7	427.094			
31806.6	-44732.8	427.972	31841.5	-44722.4	427.058			
31807.2	-44732.6	427.932	31842.4	-44722.2	427.026			
31807.9	-44732.4	427.892	31843.2	-44721.9	426.999			
31808.6	-44732.2	427.852	31844.1	-44721.7	426.975			
31809.3	-44731.9	427.813	31844.7	-44721.5	426.959			
31810	-44731.7	427.774	31844.9	-44721.4	426.954			
31810.7	-44731.5	427.735	31845.7	-44721.2	426.933			
31810.8	-44731.4	427.727	31846.5	-44721	426.913			
31811.4	-44731.3	427.695	31847.3	-44720.8	426.895			
31812.1	-44731	427.656	31848.1	-44720.5	426.878			
31812.9	-44730.8	427.617	31848.9	-44720.3	426.863			
31813.6	-44730.6	427.583	31849.7	-44720.1	426.847			
31814.3	-44730.4	427.557	31850.5	-44719.9	426.833			
31815	-44730.2	427.537	31851.2	-44719.7	426.82			
31815.7	-44730	427.524	31852	-44719.5	426.808			
31816.4	-44729.8	427.519	31852.7	-44719.3	426.798			
31817.1	-44729.6	427.52	31853.5	-44719.1	426.789			
31817.8	-44729.4	427.529	31854.2	-44718.9	426.781			
31818.5	-44729.2	427.545	31855	-44718.7	426.774			
31819.1	-44729	427.564	31855.8	-44718.4	426.768			
31819.2	-44729	427.568	31856	-44718.4	426.767			
31819.9	-44728.8	427.597	31856.7	-44718.2	426.767			
31820.5	-44728.7	427.634	31857.5	-44717.9	426.767			
31821.2	-44728.5	427.678	31858.5	-44717.7	426.769			
31821.9	-44728.3	427.726	31859.4	-44717.4	426.771			
31822.5	-44728.1	427.77	31860.4	-44717.1	426.774			
31823.3	-44727.9	427.804	31861.4	-44716.8	426.778			
31823.9	-44727.7	427.824	31862.5	-44716.5	426.783			
31824	-44727.7	427.828	31863.4	-44716.3	426.787			
31824.8	-44727.5	427.841	31863.6	-44716.2	426.789			

Borehole 3: Borehole radar illumination line coordinates – dip direction

X	Y	Z	X	Y	Z	X	Y	Z
31802.7	-44747.4	419.844	31858.2	-44790.1	402.535	31916.9	-44834.7	387.42
31815.6	-44757.3	416.084	31857.1	-44789.4	402.811	31915.7	-44833.9	387.765
31814.4	-44756.4	416.469	31869.8	-44798.9	399.401	31914.4	-44833	388.095
31813	-44755.3	416.883	31869.6	-44798.8	399.445	31913.2	-44832.2	388.411
31811.6	-44754.2	417.301	31868.8	-44798.2	399.687	31912.1	-44831.4	388.713
31810.1	-44753.1	417.723	31867.9	-44797.5	399.931	31910.9	-44830.7	389
31808.7	-44752	418.149	31866.9	-44796.8	400.179	31909.8	-44830	389.273
31807.2	-44750.9	418.579	31866	-44796.1	400.429	31908.8	-44829.2	389.531
31805.6	-44749.7	419.012	31865.1	-44795.4	400.682	31907.7	-44828.6	389.775
31804.1	-44748.5	419.449	31864.1	-44794.7	400.939	31906.8	-44827.9	390.005
31827.9	-44766.3	412.164	31871.6	-44800.3	398.914	31905.9	-44827.2	390.23
31826.8	-44765.6	412.536	31871.4	-44800.1	398.97	31905	-44826.5	390.451
31825.7	-44764.7	412.912	31870.5	-44799.5	399.206	31922.6	-44839.1	385.65
31824.5	-44763.9	413.292	31875.4	-44803.2	397.851	31921.8	-44838.5	385.895
31823.3	-44763	413.676	31874.7	-44802.7	398.054	31920.6	-44837.5	386.298
31822.1	-44762.2	414.063	31873.9	-44802	398.279	31919.4	-44836.6	386.686
31820.9	-44761.2	414.455	31873.1	-44801.4	398.506	31927	-44842.7	384.15
31819.6	-44760.3	414.85	31872.2	-44800.8	398.737	31925.7	-44841.6	384.6
31818.4	-44759.4	415.249	31879	-44806.1	396.854	31924.4	-44840.6	385.046
31817.1	-44758.4	415.652	31878.5	-44805.8	396.973	31923.1	-44839.5	385.478
31815.7	-44757.4	416.058	31877.8	-44805.1	397.183	31934.7	-44848.4	381.62
31834.3	-44771.1	409.857	31877	-44804.5	397.397	31933.1	-44847.2	382.153
31833.9	-44770.8	410.007	31876.2	-44803.9	397.613	31931.5	-44846	382.671
31833	-44770.1	410.358	31883	-44809.4	395.768	31930	-44844.9	383.175
31832.1	-44769.3	410.712	31882.3	-44808.8	395.962	31928.5	-44843.8	383.665
31831.1	-44768.6	411.07	31881.5	-44808.2	396.158			
31830.1	-44767.9	411.431	31880.8	-44807.6	396.358			
31829	-44767.1	411.795	31880	-44807	396.56			
31842.6	-44777.8	407	31879.3	-44806.4	396.765			
31841.7	-44777	407.313	31886.1	-44812	394.951			
31840.7	-44776.2	407.639	31885.9	-44811.8	395.021			
31839.7	-44775.4	407.967	31885.2	-44811.2	395.204			
31838.7	-44774.6	408.299	31884.5	-44810.6	395.389			
31837.8	-44773.9	408.634	31883.7	-44810	395.577			
31836.8	-44773.1	408.973	31890	-44815.2	394.018			
31835.8	-44772.3	409.314	31889.4	-44814.7	394.151			
31834.9	-44771.6	409.659	31888.7	-44814.1	394.32			
31848.5	-44782.6	405.174	31888	-44813.6	394.491			
31847.7	-44781.9	405.427	31887.3	-44813	394.665			
31846.7	-44781.1	405.734	31886.6	-44812.4	394.842			
31845.7	-44780.2	406.043	31904.8	-44826.4	390.49			
31844.7	-44779.4	406.356	31904.1	-44825.9	390.671			
31843.7	-44778.6	406.672	31903.2	-44825.2	390.887			
31852.8	-44786	403.971	31902.3	-44824.5	391.101			
31851.8	-44785.3	404.234	31901.5	-44823.9	391.312			
31850.8	-44784.4	404.528	31900.6	-44823.2	391.52			
31849.7	-44783.6	404.824	31899.8	-44822.6	391.726			
31848.7	-44782.7	405.124	31898.9	-44822	391.929			
31856.7	-44789	402.929	31898.1	-44821.3	392.129			
31856.1	-44788.6	403.09	31897.3	-44820.7	392.326			
31855	-44787.8	403.372	31896.5	-44820.1	392.521			
31854	-44786.9	403.656	31895.6	-44819.5	392.713			
31852.9	-44786.1	403.944	31894.8	-44818.9	392.902			
31864	-44794.6	400.975	31894	-44818.2	393.089			
31863.2	-44793.9	401.197	31893.2	-44817.6	393.273			
31862.2	-44793.2	401.459	31892.5	-44817.1	393.454			
31861.2	-44792.5	401.724	31891.7	-44816.5	393.632			
31860.2	-44791.7	401.991	31890.9	-44815.9	393.808			
31859.2	-44790.9	402.262	31890.1	-44815.3	393.981			

Borehole 3: Borehole radar illumination line coordinates – strike direction

X	Y	Z	X	Y	Z	X	Y	Z
31800.1	-44746.3	421.041	31853	-44785.3	403.385	31891.2	-44813.9	393.73
31801.7	-44747.3	420.477	31853.9	-44786	403.13	31892.2	-44814.7	393.442
31802	-44747.5	420.393	31854.9	-44786.6	402.88	31893.2	-44815.5	393.15
31803.3	-44748.5	419.869	31855.8	-44787.3	402.634	31894.2	-44816.3	392.852
31804.9	-44749.7	419.264	31856.7	-44787.9	402.392	31895.3	-44817.2	392.534
31806.5	-44750.9	418.67	31857	-44788.1	402.322	31896.5	-44818.1	392.195
31808.1	-44752.1	418.087	31857.6	-44788.5	402.153	31897.8	-44819.1	391.835
31809.6	-44753.2	417.516	31858.6	-44789.2	401.918	31899.1	-44820.1	391.453
31811.2	-44754.4	416.956	31859.5	-44789.8	401.686	31900.5	-44821.2	391.048
31812.7	-44755.5	416.409	31860.4	-44790.5	401.457	31902	-44822.3	390.622
31814.1	-44756.6	415.872	31861.3	-44791.1	401.231	31903.5	-44823.5	390.174
31815	-44757.2	415.581	31862.2	-44791.7	401.009	31905.1	-44824.7	389.731
31815.6	-44757.7	415.348	31863.1	-44792.4	400.79	31905.2	-44824.7	389.704
31817	-44758.8	414.835	31864.1	-44793	400.575	31906.9	-44826	389.215
31818.5	-44759.9	414.334	31864.9	-44793.6	400.391	31908.7	-44827.4	388.703
31819.9	-44760.9	413.844	31865	-44793.6	400.362	31910.6	-44828.8	388.17
31821.2	-44761.9	413.366	31865.9	-44794.3	400.154	31912.5	-44830.2	387.614
31822.6	-44762.9	412.899	31866.8	-44794.9	399.949	31914.5	-44831.8	387.037
31823.9	-44763.9	412.445	31867.7	-44795.5	399.747	31916.6	-44833.3	386.437
31825.2	-44764.9	412.002	31868.6	-44796.2	399.548	31918.8	-44835	385.815
31826.5	-44765.9	411.57	31869.5	-44796.8	399.353	31918.9	-44835.1	385.785
31827.6	-44766.6	411.225	31870.4	-44797.4	399.16	31921.1	-44837	385.071
31827.8	-44766.8	411.151	31871.2	-44797.9	399.006	31923.2	-44838.8	384.398
31829.1	-44767.7	410.746	31871.3	-44798.1	398.971	31923.5	-44839.1	384.299
31830.3	-44768.6	410.349	31872.3	-44798.7	398.787	31925.9	-44841.1	383.519
31831.5	-44769.5	409.951	31873.1	-44799.3	398.604	31927.7	-44842.6	382.957
31832.8	-44770.4	409.557	31874.1	-44800.1	398.36	31928.5	-44843.2	382.73
31834	-44771.3	409.171	31875	-44800.9	398.127	31931.1	-44845.3	381.955
31834.2	-44771.5	409.114	31876	-44801.6	397.891			
31835.1	-44772.2	408.793	31876.7	-44802.2	397.703			
31836.3	-44773.1	408.422	31876.9	-44802.4	397.653			
31837.5	-44773.9	408.058	31877.9	-44803.1	397.413			
31838.6	-44774.8	407.701	31878.8	-44803.9	397.17			
31839.7	-44775.6	407.349	31879.8	-44804.7	396.924			
31840.8	-44776.4	407.004	31880.1	-44804.9	396.833			
31841.9	-44777.2	406.666	31880.7	-44805.4	396.675			
31842.5	-44777.7	406.488	31881.7	-44806.2	396.424			
31843	-44778	406.335	31882.6	-44807	396.169			
31844.1	-44778.8	406.01	31883.6	-44807.7	395.912			
31845.1	-44779.6	405.691	31883.9	-44808	395.81			
31846.2	-44780.3	405.379	31884.5	-44808.5	395.651			
31847.2	-44781.1	405.074	31885.5	-44809.3	395.386			
31848.2	-44781.8	404.776	31886.4	-44810	395.118			
31848.5	-44782	404.69	31886.8	-44810.4	394.995			
31849.2	-44782.5	404.484	31887.4	-44810.8	394.846			
31850.2	-44783.3	404.199	31888.3	-44811.6	394.572			
31851.1	-44784	403.921	31889.3	-44812.4	394.295			
31852.1	-44784.6	403.649	31890.3	-44813.2	394.015			
31852.8	-44785.2	403.443	31890.4	-44813.3	393.966			

Borehole 4: Borehole radar illumination line coordinates – dip direction

X	Y	Z	X	Y	Z
31790.1	-44741.9	430.542	31832.6	-44690.7	440.797
31790.3	-44740.5	430.825	31833.2	-44689.4	441.008
31790.3	-44740.2	430.898	31833.7	-44688.2	441.257
31791	-44739.1	431.088	31834.1	-44687.1	441.542
31792	-44737.8	431.331	31834.4	-44686.1	441.864
31792.9	-44736.5	431.555	31834.5	-44685.1	442.223
31793.8	-44735.3	431.76	31834.6	-44684.2	442.619
31794.5	-44734.2	431.944	31834.6	-44683.4	443.051
31795.3	-44733.1	432.109	31834.6	-44682.6	443.521
31795.9	-44732.2	432.278	31834.9	-44681.8	444.065
31796.3	-44731.3	432.489	31835.6	-44680.7	444.704
31796.7	-44730.4	432.744	31836.6	-44679.5	445.438
31797.2	-44729.5	433.042	31837.8	-44678.1	446.268
31797.2	-44729.2	433.149	31839.1	-44676.7	447.194
31797.8	-44728.5	433.383	31840.6	-44675.1	448.214
31798.5	-44727.6	433.768	31841	-44674.6	448.516
31799.2	-44726.6	434.196	31842.3	-44673.4	449.33
31800	-44725.6	434.668	31844.1	-44671.5	450.541
31800.8	-44724.6	435.183	31845.2	-44670.4	451.277
31801.7	-44723.6	435.722	31846.1	-44669.5	451.848
31802.8	-44722.5	436.232			
31803.9	-44721.5	436.712			
31805	-44720.5	437.16			
31806.1	-44719.4	437.577			
31807.1	-44718.4	437.962			
31808.2	-44717.4	438.316			
31808.6	-44717.1	438.417			
31809.2	-44716.4	438.638			
31810.2	-44715.4	438.929			
31811.2	-44714.4	439.189			
31812.3	-44713.4	439.416			
31813.4	-44712.3	439.61			
31814.6	-44711.2	439.772			
31815.8	-44710.1	439.901			
31817.1	-44708.9	439.998			
31818.4	-44707.7	440.062			
31819.7	-44706.5	440.094			
31821.2	-44705.3	440.092			
31822.6	-44704	440.063			
31823.6	-44702.7	440.046			
31824.6	-44701.5	440.048			
31825.5	-44700.2	440.07			
31826.5	-44699	440.112			
31827.5	-44697.6	440.174			
31827.6	-44697.4	440.19			
31828.6	-44696.3	440.256			
31829.6	-44694.9	440.358			
31830.7	-44693.5	440.48			
31831.8	-44692	440.622			

Borehole 4: Borehole radar illumination line coordinates – strike direction

X	Y	Z	X	Y	Z
31789.5	-44740.1	431.174	31818.2	-44704.1	440.146
31790	-44739.3	431.236	31819.3	-44702.6	440.2
31790.9	-44737.9	431.35	31820.4	-44701.1	440.226
31791.8	-44736.6	431.472	31821.5	-44699.8	440.239
31792.6	-44735.4	431.604	31822.6	-44698.5	440.27
31793.5	-44734.3	431.745	31823.7	-44697.3	440.32
31794.2	-44733.3	431.894	31824.8	-44696.1	440.389
31795	-44732.4	432.052	31825.6	-44695.3	440.444
31795.6	-44731.6	432.219	31825.8	-44695	440.48
31796.3	-44731	432.393	31826.9	-44693.9	440.593
31796.9	-44730.4	432.575	31827.9	-44692.9	440.725
31797.5	-44730	432.763	31829	-44691.9	440.878
31798.1	-44729.6	432.958	31830	-44691	441.053
31798.5	-44729.4	433.15	31831	-44690.1	441.248
31799	-44728.9	433.454	31832	-44689.3	441.466
31799.5	-44728.3	433.744	31833	-44688.5	441.709
31799.9	-44727.8	434.025	31834.1	-44687.7	442.006
31800.4	-44727.2	434.298	31835.3	-44686.7	442.397
31800.8	-44726.7	434.561	31836.6	-44685.6	442.884
31801.3	-44726.1	434.817	31838	-44684.4	443.463
31801.7	-44725.6	435.063	31839.4	-44683.1	444.133
31802.2	-44725.1	435.302	31841	-44681.6	444.893
31802.6	-44724.5	435.532	31842.6	-44680	445.741
31803.1	-44724	435.753	31844.4	-44678.4	446.677
31803.5	-44723.4	435.967	31844.7	-44678.1	446.826
31804	-44722.8	436.173	31846.2	-44676.5	447.7
31804.4	-44722.3	436.367	31848.1	-44674.6	448.81
31804.9	-44721.8	436.554	31849	-44673.8	449.344
31805.4	-44721.3	436.741	31850.1	-44672.6	450.004
31805.8	-44720.8	436.928	31852.2	-44670.5	451.282
31806.3	-44720.3	437.115			
31806.8	-44719.8	437.302			
31807.2	-44719.2	437.489			
31807.7	-44718.7	437.675			
31808.2	-44718.2	437.862			
31808.6	-44717.7	438.049			
31809	-44717.3	438.21			
31809.5	-44716.7	438.422			
31810	-44716.1	438.615			
31810.5	-44715.4	438.84			
31811	-44714.6	439.048			
31811.6	-44713.7	439.234			
31812.3	-44712.8	439.402			
31813	-44711.8	439.552			
31813.7	-44710.7	439.686			
31814.5	-44709.5	439.805			
31815.4	-44708.3	439.91			
31816.3	-44707	440.001			
31817.2	-44705.6	440.08			

TABLE OF CONTENTS

SUMMARY

Title of treatise: The financial benefit of using borehole radar to delineate mining blocks in underground platinum mines

Name of author: P du Pisani

Name of supervisor: Prof. HFJ Theart

Department: Faculty of Natural and Agricultural Sciences
University of Pretoria

Degree: M.Sc. (Earth Science Management and Practice)

Borehole radar is a short-range, high-resolution geophysical technique that can be used to delineate the position of the Merensky platinum reef in underground mines situated in the Western Bushveld Complex. In this study, borehole radar is used in reflection mode from four boreholes drilled sub-parallel to the expected position of the Merensky Reef within an underground mining block bounded by two cross-cuts and a haulage. This study relates the stratigraphic column at Amandelbult Section to borehole radar reflectivity. The radar illumination line coordinates produced along the Merensky Reef surface are used to construct a three-dimensional surface of the reef within the defined mining block.

The geophysical interpretation presented here shows how a slump in the Merensky Reef, called a pothole, is imaged using borehole radar. This study analyses the increase in geological confidence related to the improved delineation of the elevation of the Merensky Reef.

The financial impact of using borehole radar to delineate this pothole is analysed at the various mining steps, namely: orebody definition, mine planning, mine development, ore extraction and ore processing. The information gained by conducting borehole radar is compared with the information acquired using only standard geological drilling.

This study concludes that the application of borehole radar significantly increases the confidence in the geological model prior to mining. Conducting borehole radar prior

to mining improves mine planning and development, ensures that less waste is mined, facilitates the effective deployment of labour crews, prevents waste being sent to the processing plant and avoids deferring income until a later date. Recommendations are made on how to plan for and include borehole radar in the mining process.

LIST OF ABBREVIATIONS

BH	Borehole
BHR	Borehole radar
CSIR	Council for Scientific and Industrial Research
GPR	Ground Penetrating Radar
PGE	Platinum Group Elements
RPM	Rustenburg Platinum Mines
SAIMM	South African Institute of Mining and Metallurgy
SAMREC	South African Mineral Resources Committee
SG	Specific Gravity

LIST OF FIGURES

LIST OF TABLES

1 INTRODUCTION

1.1 Objectives of the study

This treatise aims to quantify the cost benefit that can be achieved if borehole radar is applied as a predictive geological tool ahead of mining.
A case study was conducted at Anglo Platinum's Amandelbult Section. The treatise describes how the optimal survey design was designed in order to effectively image a mining block. A fan of boreholes was surveyed with borehole radar, which provided a detailed three-dimensional surface representing the Merensky Reef. A cost-benefit analysis was conducted to determine whether the information provided by borehole radar in this mining block provided any significant financial benefits to the mine.

The Bushveld Complex, situated north of Pretoria in South Africa, contains the world's largest known resource of platinum (Viljoen and Schürmann, 1998). The distribution of the platinum resources in relation to other mineral deposits is shown in Figure 1.

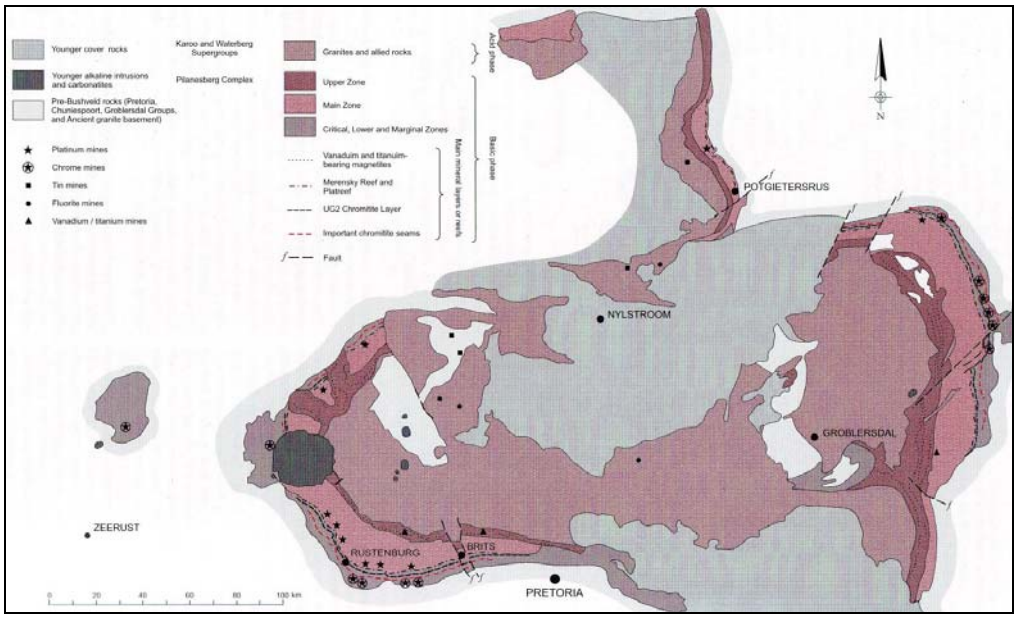

Figure 1: A geological map of the Bushveld Complex in South Africa, showing the distribution of the main economic minerals, after Viljoen and Schürmann (1998)

Economic concentrations of platinum are present in the Merensky Reef: a feldspathic pegmatoidal pyroxenite and the UG2 chromitite. These platinum-rich layers are interspersed with layers of anorthosite, norite and pyroxenite.

On a regional scale, these thin tabular ore bodies (locally called reefs) are continuous for tens to hundreds of kilometres, but on a smaller mine-block scale these reefs are often disrupted by various geological structures such as dykes, iron-rich ultramafic pegmatites (IRUPs), faults and potholes. Potholes are the most common disruption and cause most challenges to mining these reefs.

In this treatise, a geological disruption caused by a pothole is examined. In a pothole, the reef transgresses its footwall layers, resulting in slumps that have diameters that can be metres to tens of metres deep and wide (Viljoen and Schürmann, 1998). The reef is often pinched out at the edges of the pothole, resulting in degraded ore reserves. Potholes inevitably lead to significant losses and predicting their presence ahead of mining is advantageous for a number of reasons:

- Less waste rock is mined, resulting in a significant cost benefit to the mine.
- Improved knowledge of the ore body means that less money is spent on unnecessary development towards severely disrupted or degraded reef.
- Mining can be planned smarter so that, for example, support pillars are left where less ore is present due to potholing.
- If it is known that mining is approaching a pothole, mining can be relocated timeously and work crews can be moved to a different location, i.e. the work force is used more efficiently.
- Pothole edges are often related to unstable hanging wall conditions, which could lead to falls of ground. If the pothole edge is delineated before mining starts, additional precautionary measures can be taken to ensure the safety of mine workers.

1.2 The Platmine Research Collaborative

The work presented here was conducted under the Platmine collaborative research programme. This research programme, initiated in 2003, involves the Council for Scientific and Industrial Research (CSIR), Anglo Platinum, Impala Platinum, Lonmin Platinum and Northam Platinum. Its main focus is the long-term sustainability of the platinum industry in South Africa. Among its primary goals listed at www.platmine.co.za are:

- To increase productivity.
- To develop technologies and competencies to improve overall safety and health.
- To facilitate mechanisation by solving common technological problems.
- To improve the underground working environment.

This treatise ties in with the first objective listed above, i.e. increasing productivity in the platinum industry, but borehole radar is also increasingly being used in conjunction with other geophysical methods to characterise the rock mass prior to mining in order to pre-empt hazardous conditions.

1.3 Delimitations

It is important to note that this treatise will only deal with determining the elevation of the Merensky Reef within the defined mining block. In particular, the position of the bottom contact of the Merensky Reef is delineated.

This treatise assumes that the grade information pertaining to the Merensky Reef is predictable and that grade variation is acceptable within the mining block. A constant grade is used for financial calculations. This value is defined in Section 6.2.1.

2 BOREHOLE RADAR

Borehole radar is ground penetrating radar (GPR) applied from within a borehole. GPR is a geophysical technique whereby radio waves are transmitted into the ground to locate buried objects or hidden interfaces (Daniel *et al.*, 2004). GPR measures differences in the dielectric property permittivity, and the distance that radar waves travel in a medium is determined by its conductivity (Du Pisani and Vogt, 2003).

A typical bi-static borehole radar instrument consists of separate transmitter and receiver probes that are deployed inside a borehole. In this study, the CSIR's Aardwolf BR40 was used to acquire the borehole radar data. This instrument has a centre frequency of 40 MHz and a vertical resolution of approximately 1 m (Vogt *et al.*, 2005). A schematic of the Aardwolf BR40 is shown in Figure 2.

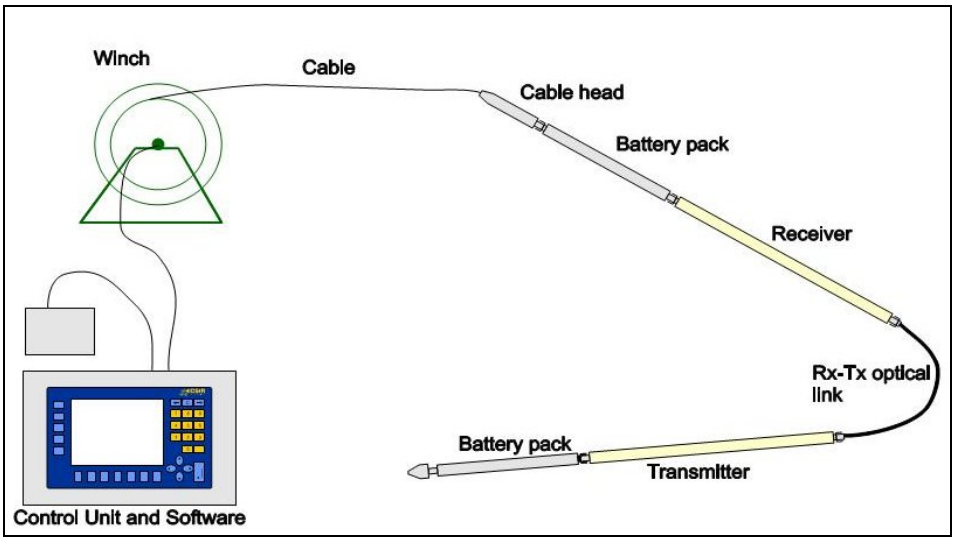

Figure 2: Schematic for the Aardwolf BR40 instrument, showing the radar transmitter, receiver, optical-fibre links, winch and control unit (Vogt 2002)

Borehole radar can be applied in reflection mode from within a single borehole (Vogt, 2006) or in transmission mode, whereby the transmitter is located in one borehole and the receiver in an adjacent borehole. In transmission mode, borehole radar can determine whether conductive material is present between two boreholes (Turner *et al.*, 2000).

For the study presented in this treatise, borehole radar is used in single-borehole reflection mode to image the boundary of the Merensky Reef within a section of Anglo Platinum's Amandelbult Section.

In borehole radar reflection mode, radar waves are transmitted into the rock mass and the time taken for these waves to travel to a reflective interface is measured in nanoseconds (Vogt *et al.*, 2005). If the velocity of the radar waves in the rock mass is known, the distance to the interface can be calculated.

In order for a reflection borehole radar survey to be successful, the following factors are of importance (Vogt, 2006):

- The borehole from which borehole radar is applied should be oriented parallel or sub-parallel to the target to be imaged, as shown in Figure 3.
- There should be a significant permittivity contrast between the target and its host rocks.
- The technique works best if the borehole is situated in a host rock that is resistive and delineates a target that is conductive.
- The reflective contact should be sharp as opposed to gradationally changing into a different rock type.

More technical information about borehole radar will be discussed throughout this treatise as it becomes necessary.

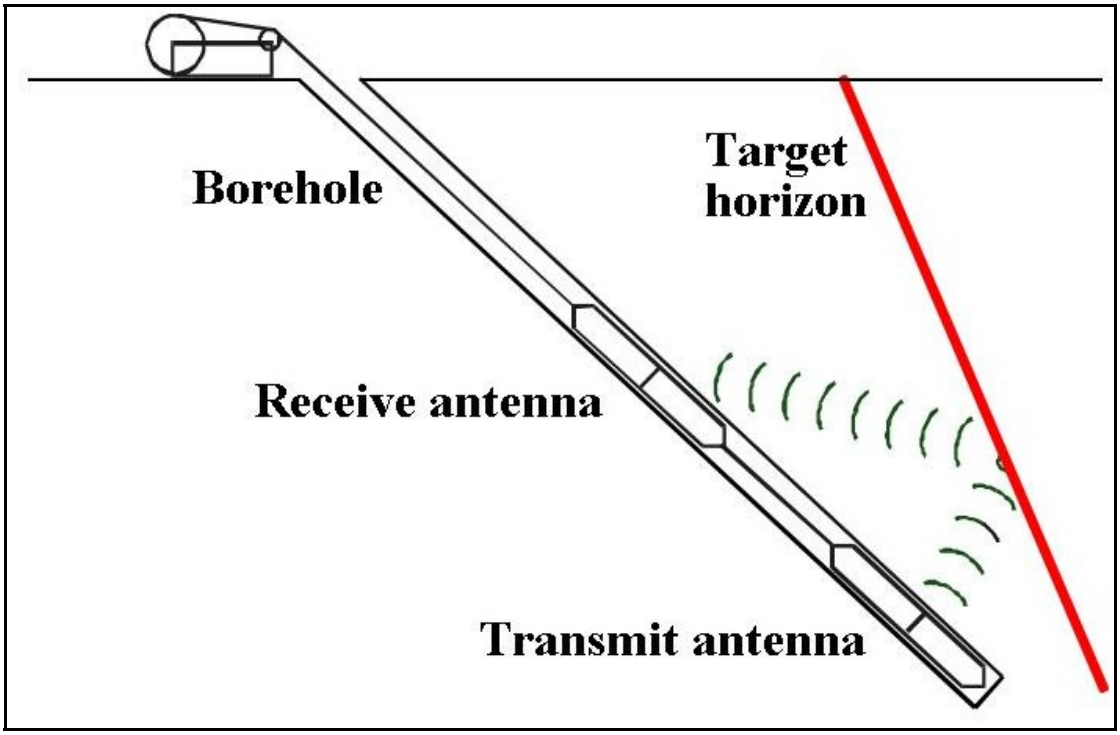

Figure 3: The optimal survey geometry for a borehole radar reflection survey orients the borehole parallel to sub-parallel to the intended radar target (Image courtesy CSIR)

3 THE MERENSKY REEF AT RPM AMANDELBULT SECTION

3.1 Regional setting of RPM Amandelbult Section

Anglo Platinum's Amandelbult Section is located in South Africa's Limpopo province (Figure 4). The mine is approximately 100 km north of Rustenburg and 40 km south of Thabazimbi. As seen in Figure 5, Amandelbult Section's lease area is in the shape of a rectangle with the long axis oriented NE-SW, and approximately 4 km wide on the short side and 20 km wide on the long side (Viljoen *et al.*, 1986b).

The topography surrounding the mine is relatively flat and the surface is covered by a thin layer of black turf soil. The only noticeable topography is a group of small hills to the south of the main entrance of the mine, which are locally termed *pyramid gabbros*. According to Viljoen *et al.* (1986b), these small hills form part of the Bushveld Complex's Main Zone, and they consist of gabbro-norite, which is the prevalent rock type in the Main Zone of the Bushveld Complex.

To the west and north of Amandelbult Section, the quartzites of the Transvaal Supergroup form the Witfontein Mountains. In the north-eastern part of the lease area, the Crocodile River runs from south to north.

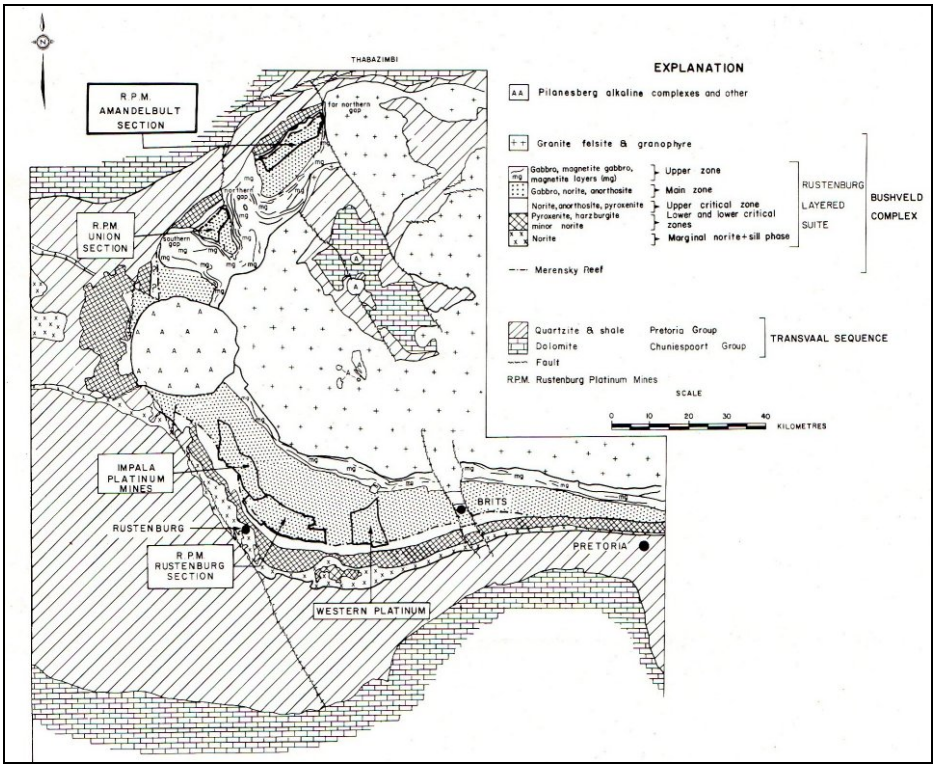

Figure 4: Locality plan showing Amandelbult Section in relation to the major geological rock types of the Bushveld Complex, after Viljoen *et al.*, 1986b

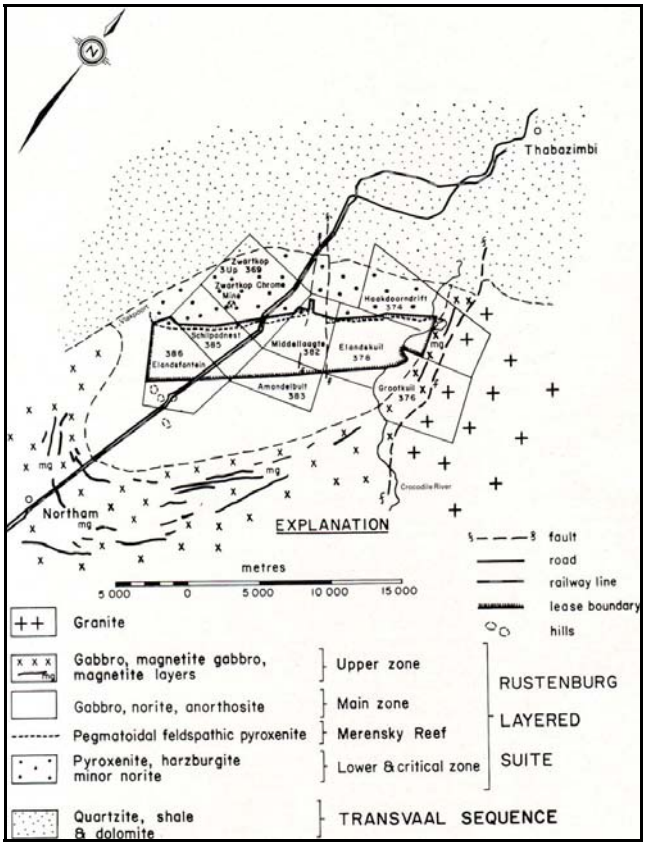

Figure 5: Map of Amandelbult Section's lease area, showing the main geological features and farm boundaries (Viljoen *et al.*, 1986b)

3.2 History of the Amandelbult Mine

The Merensky Reef was discovered by A.F. Lombaard in 1924 (Viljoen *et al.*, 1986b). Although the Merensky Reef was discovered in the Eastern Bushveld, almost all of the platinum mining that occurred up until the mid-Seventies in South Africa was due to the extraction of the Merensky Reef in the Western Bushveld (Cawthorn, 1999).

The Merensky Reef was discovered in the Western Bushveld near Rustenburg in 1925 (Viljoen *et al.*, 1986b), leading to more widespread exploration. Amandelbult Section was prospected in 1926 by the Steelpoort Platinum Syndicate. Shortly thereafter, ownership of Amandelbult transferred to Potgietersrust Platinum Limited, but interest in the area decreased during the 1930s' Depression, during which all platinum mining was suspended.

Rustenburg Platinum Mines (RPM), which eventually became part of Anglo Platinum, acquired the mineral rights for Amandelbult Section in 1964 and mining eventually commenced on the farm Schilpadsnest in 1974 (Viljoen *et al.*, 1986b). Platinum production at Amandelbult ceased in 1975 due to a slump in the platinum market, but after it restarted in 1976, production increased on a yearly basis (www.platinummetalsreview.co.za).

Currently both the Merensky and UG2 reefs are mined at Amandelbult Section. Amandelbult is expecting to increase the rate of equivalent refined platinum production to approximately 625,000 ounces in 2007 (Anglo Platinum Annual Report 2006).

3.3 Regional Geology of the Merensky Reef

The Merensky Reef occurs in the Upper Critical Zone of the Bushveld Complex. According to Viljoen (1999), the reef has been delineated for approximately 145 km in the Western Lobe of the Bushveld Complex. Underground and opencast extraction of the reef is taking place over a strike distance of approximately 90 km (Viljoen *et*

al., 1986b). The Merensky Reef's dip changes from approximately 9° to 12° as it is traced inwards towards the centre of the Bushveld Complex, with steeply dipping exceptions in parts of the complex.

The thickness of the Merensky Reef can vary between 2 cm and 14 m (Viljoen *et al.*, 1986b). Its down-dip extension has been traced with the help of seismic surveys for up to 50 km, and to depths of 6 km (Du Plessis and Kleinwegt, 1987). Since mining on the Merensky Reef commenced in 1929, a large amount of data has been gathered about this particular reef (Viljoen, 1999), and it is evident that the Merensky Reef varies dramatically regionally with regard to geology, mineralogy and PGE-grade distribution (Kinloch and Peyerl, 1990; Eales *et al*., 1993; Viljoen *et al.*, 1986a; 1986b; Viljoen, 1994; Eales and Cawthorn, 1996; Viljoen and Schürmann, 1998).

Viljoen (1999) says the Merensky Reef is typically a heterogeneous pegmatoidal feldspathic pyroxenite bounded by two thin chromitite layers, generally referred to as Bottom Chromitite and Top Chromitite. Viljoen (1999) continues to say that PGE-grades generally increase as the pegmatoidal nature of the reef increases.

This treatise does not examine grade distribution within the Merensky Reef, but concentrates on delineating the position of the reef in three dimensions for mining purposes.

3.4 Regional Geology of the Merensky Reef at Amandelbult Section

As seen in Figure 4, Amandelbult Section is located in the north-western lobe of the Bushveld Complex (Viljoen *et al.*, 1986b). The platiniferous layers, i.e. the Merensky and UG2 reefs, occur within a portion of the Lower, Critical and Main zones of the Bushveld Complex, with Upper Zone rocks above (Viljoen *et al.*, 1986b). The Upper Zone layers cut off the bottom three layers to the north and south of Amandelbult Section, resulting in an area known as the "northern gap" located to the south of the mine.

According to *A guide to the geology at Amandelbult*, which is an updated version of the geology of Amandelbult as described by Viljoen *et al.* (1986b), it has been established by underground workings that the Merensky Reef continues to the north-east of the mine.

3.5 Stratigraphy at Amandelbult Section

3.5.1 Stratigraphy related to borehole radar penetration and reflection

3.5.1.1 Radar penetration

For borehole radar to be successful, the radar waves need to travel from the borehole to the target surface, i.e. the rocks between the borehole and target surface need to be translucent to radar waves. As described by Du Pisani and Vogt (2003), the attenuation, or rate of decay, of radar waves is controlled by the conductivity of the rocks through which they are travelling. If the rocks between the borehole and target are too conductive, the radar waves will attenuate rapidly and not reach their intended target.

Radar attenuation is usually described through the loss tangent:

$$\tan\delta = \frac{\sigma}{\omega\varepsilon_r\varepsilon_0} \qquad (1)$$

As described by Vogt *et al.* (2005), the conductivity, σ, and permittivity, ε, are measured at a specific frequency, *f*. This frequency can be converted to the angular frequency ω, which is defined by $\omega = 2\pi f$. In equation (1), ε_r is the relative permittivity and $\varepsilon_0 = 8.854\times10^{-12}$ is the permittivity of free space.

Turner and Siggins (1994) explained that for most rocks suitable for GPR, the loss tangent is constant over the frequency range of the GPR instrument. Vogt (2000) showed that this constant loss-tangent estimation is an acceptable approximation to measured properties, when he analysed a database of 15,057 electrical property measurements. If a constant loss tangent is used, a nomogram from Noon *et al.* (1998)

for a smooth planar reflector (Figure 6) can be used to predict with how many wavelengths radar waves will penetrate into a rock with a given loss tangent.

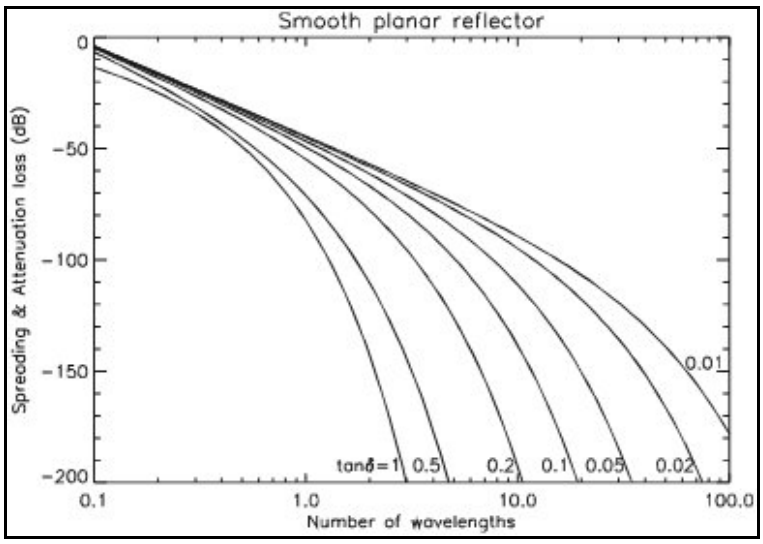

Figure 6: Radar performance prediction for a smooth planar target after Noon *et al.* (1998)

Between 1980 and 2003, Vogt measured the electrical properties of approximately 4,500 rock samples, at a range of frequencies from 1 MHz to 64 MHz, using the rock sample as a dielectric in a capacitor (Du Pisani and Vogt, 2003). Du Pisani and Vogt (2003) used this database to calculate loss-tangent values for some of the Bushveld Complex rocks related to the economic platinum horizons, i.e. anorthosite, norite and pyroxenite. The loss-tangent values at a frequency of 64 MHz were used, as this was closest to the centre frequency of the CSIR's Aardwolf BR40 used for the case study described in this treatise.

The distribution of the loss-tangent values for the three rock types are shown in Figure 7.

A (Anorthosite)

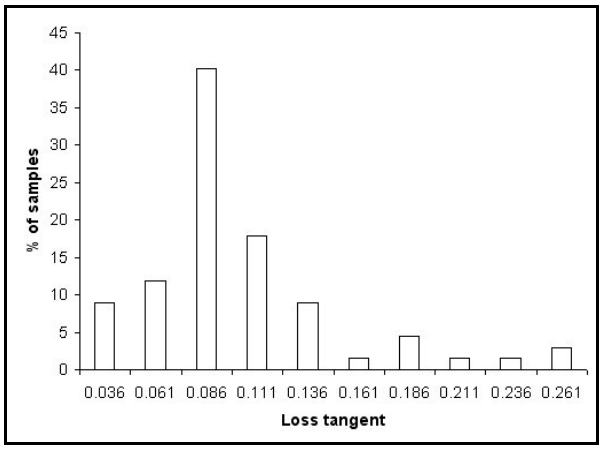

B (Norite)

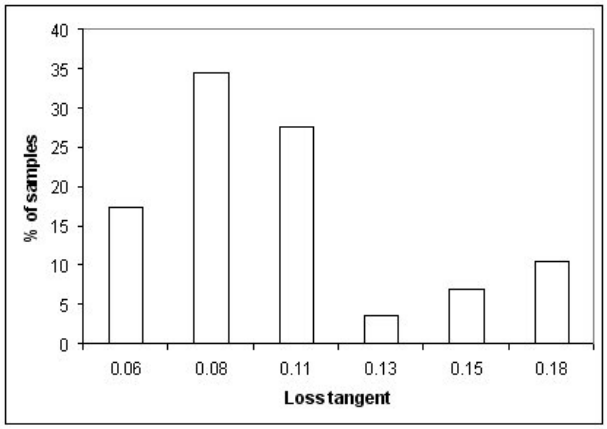

C (Pyroxenite)

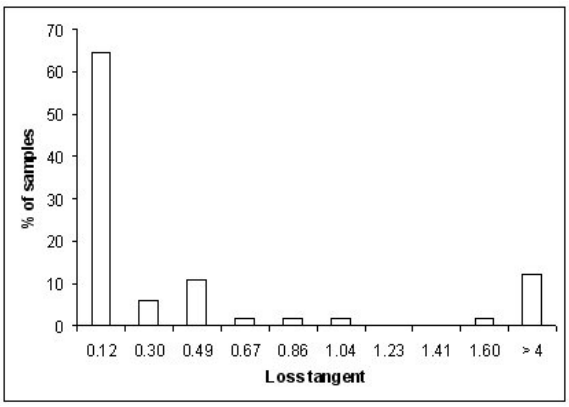

Figure 7: Distribution of loss-tangent values for (A) anorthosite, (B) norite and (C) pyroxenite after Du Pisani and Vogt (2003)

The system performance of the CSIR's Aardwolf BR40 is approximately 120 dB (Vogt, *pers comm*). As described by Du Pisani and Vogt (2003), the wavelength in metres can be estimated as 100/*f*, where *f* is the frequency in MHz. For a 40 MHz system, such as the Aardwolf BR40, the wavelength is then 2.5 m.

In Table 1, the typical loss-tangent values for anorthosite, norite and pyroxenite and their radar penetrations in these rocks, as determined from the nomogram in Figure 6, are summarised.

Table 1: The loss tangent and radar penetrations for anorthosite, norite and pyroxenite

Rock type	Loss tangent	Radar penetration (wavelengths)	Radar penetration (m)
Anorthosite	0.09	9	22.5
Norite	0.08	10	25
Pyroxenite	0.12	7	17.5

The radar penetrations shown in Table 1 are consistent with penetration achieved during experimental and commercial surveys conducted from 2001 to 2007 with the CSIR's Aardwolf BR40 system (Vogt, *et al.*, 2005; De Vries and Du Pisani, 2005).

3.5.1.2 Radar reflection

Radar reflection is controlled by a difference in permittivity between two adjacent materials though which the radar waves are travelling. According to Vogt *et al.* (2005), this difference in permittivity influences how much of the radar signal is reflected where two media border:

$$\Gamma = \frac{\varepsilon_2 - \varepsilon_1}{\varepsilon_2 + \varepsilon_1} \quad (2)$$

where ε_1 and ε_2 are the permittivities of medium 1 and medium 2 respectively. If medium 2 is very conductive, ε_2 approaches infinity and the entire radar signal will be reflected.

Du Pisani and Vogt (2003) compared the measured permittivity values of a number of samples from across the Bushveld Complex for anorthosite, norite and pyroxenite. The distribution of permittivity values for theses three rock types is shown in Figure 8.

A (Anorthosite)

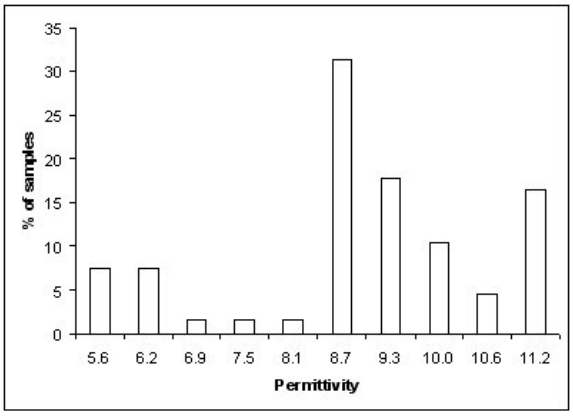

B (Norite)

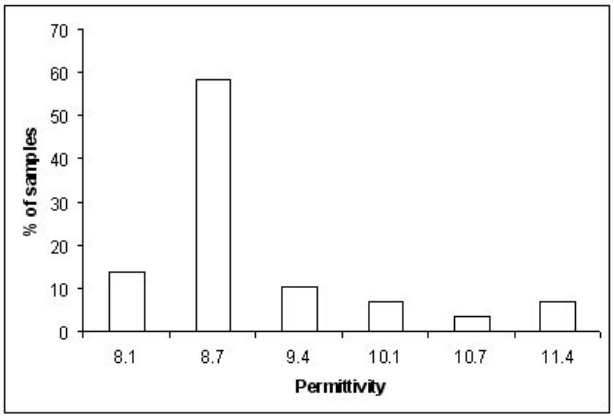

C (Pyroxenite)

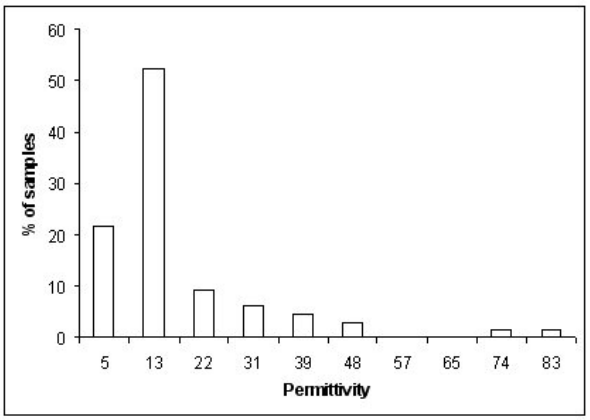

Figure 8: The distribution of permittivity values for (A) anorthosite (B) norite and (C) pyroxenite at a radar frequency of 64 MHz after Du Pisani and Vogt (2003)

As seen in Figure 8, the permittivity values for anorthosite and norite are very similar, hence the boundary between these two rock types is not expected to produce a significant radar reflector. The permittivity contrast between pyroxenite and either anorthosite or norite is much larger, and this boundary should produce a good radar reflector.

3.5.1.3 Radar stratigraphy at Amandelbult Section

The general stratigraphic column for the economic horizons at Amandelbult Section is given in Figure 9. The borehole radar holes used in the case study described in Section 5 were situated in the norite between the Merensky and Bastard reefs.

The distance that radar waves are expected to travel is indicated by the radar range shown in Figure 9. During initial test surveys carried out at Amandelbult Section at

the start of the Platmine borehole radar project in 2002, it was found that the P2 marker was a highly conductive unit that limited the penetration of radar waves. Hence radar waves are not expected to penetrate through the P2 marker.

In accordance with the findings presented by Du Pisani and Vogt (2003), the following boundaries (Figure 9), within the radar range, are expected to reflect radar waves:

- Reflector 1: Boundary between P2 marker (feldspathic harzburgite) and the norite above it.
- Reflector 2: Boundary between footwall mottled anorthosite and Merensky Reef.
- Reflector 3: Boundary between anorthosite and Bastard Reef (poikilitic pyroxenite).

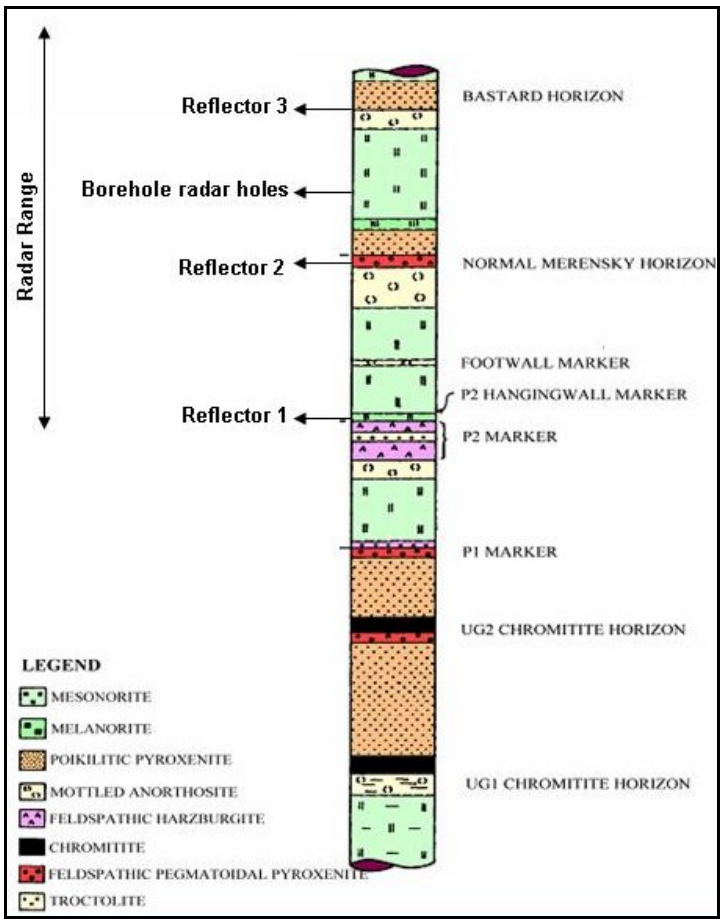

Figure 9: General stratigraphic column for Amandelbult Section, showing the position of the borehole radar holes, the expected radar reflectors and the range of the borehole radar instrument (stratigraphic column from *A guide to the geology of Amandelbult*)

Only the rocks that are within the borehole radar's range are discussed within the context of radar penetration and reflectivity in the next sections.
The units that are examined include:

- Upper pseudoreef (P2 marker)
- P2 hanging wall marker
- Footwall marker
- Merensky Reef unit
- Bastard Reef unit

3.5.2 Upper pseudoreef (P2 marker)

The P2 marker comprises feldspathic harzburgite (Viljoen *et al.*, 1986b). As seen in Figure 9, the immediate footwall of the P2 marker is anorthosite.

The P2 marker is split into two layers in the south-western part of Amandelbult mine (Viljoen *et al.*, 1986b). The lower P2 layer is approximately 3 m thick, and is separated from the top P2 layer by what is termed the *middling anorthosite* (0 m to 1.2 m). The top P2 layer can be up to 1 m in thickness. Both P2 layers usually have thin chromitite stringers at their base. To the north-east of the mine, the two P2 layers merge into one composite feldspathic harzburgite (Viljoen *et al.*, 1986b).

The overlying cycle of the P2 starts with a 10 mm-thick chromitite stringer (Viljoen *et al.*, 1986b), which provides a sharp reflective contact for radar waves. Above this thin chromitite there is approximately 10 cm to 15 cm of coarse pegmatoidal feldspathic harzburgite, which changes gradually into a 2 m-wide melanorite (Viljoen *et al.*, 1986b).

The dielectric properties of harzburgite have not been examined in detail, but it is the author's experience that the P2 is usually very conductive and that most of the radar signal is reflected back when this unit is encountered. Both the sharp chromitite boundary and coarse, conductive harzburgite contribute to the author's observation that radar waves generally do not penetrate through this unit.

According to Du Pisani and Vogt (2003), the boundary between pyroxenite and norite provides a good radar reflection, and even though the boundary between the harzburgite and norite is gradational, their difference in permittivity should contribute towards imaging the P2 with borehole radar.

3.5.3 P2 hanging wall marker

The P2 hanging wall marker is a remarkably consistent marker horizon consisting of an anorthosite layer on top of a pyroxenite layer (Viljoen *et al.*, 1986b) inside the melanorite above the P2 marker. This thin band is 10 cm to 15 cm thick, and occurs approximately 70 cm above the P2 marker. Even though the boundary between anorthosite and pyroxenite provides a good reflective target for radar (Du Pisani and Vogt, 2003), the vertical resolution of the Aardwolf BR40 instrument is in the order of 1 m (Vogt *et al.*, 2005), hence this thin marker horizon will not be detected with this instrument.

Upwards from the P2 hanging wall marker, the melanorite in which it occurs gradationally changes into norite and then into anorthositic norite until it reaches a very distinctive anorthosite band called the Footwall marker (Viljoen *et al.*, 1986b).

3.5.4 Footwall marker

The thin (40 cm to 50 cm) anorthosite Footwall marker occurs approximately 8 m above the P2 marker and approximately 10 m below the Merensky Reef (Viljoen *et al.*, 1986b). Above the Footwall marker there is 3 m to 5 m of norite, followed by 5 m to 6 m of poikilitic anorthosite, after which the bottom chromitite stringer, signifying the start of the Merensky Reef cycle, is reached (Viljoen *et al.*, 1986b).

According to Du Pisani and Vogt (2003), the contact between anorthosite and norite will not provide a significant radar contrast, hence it is not expected that any of the anorthosite-norite boundaries between the P2 pseudoreef and Merensky Reef will be imaged with borehole radar.

3.5.5 Merensky Reef unit

The Merensky Reef can vary significantly regionally (Viljoen, 1999), but it is broadly defined as "a mineralised zone within the ultramafic cumulate at the base of the Merensky cyclic unit" (Viljoen and Schürmann, 1998). The Merensky Reef is typically a heterogeneous pegmatoidal feldspathic pyroxenite (Viljoen and Schürmann, 1998), which may contain various sulphides such as pyrrhotite, pendlandite and chalcopyrite (Viljoen *et al.*, 1986b). The boundaries of the Merensky Reef are generally characterised by narrow (approximately 1 cm thick) chromitite stringers (Viljoen and Schürmann 1998).

At Amandelbult Section, the bottom chromitite stringer below the Merensky Reef is typically 5 mm to 15 mm thick (Viljoen *et al.*, 1986b). The contact with the underlying mottled anorthosite is usually very sharp, providing an excellent reflective surface for borehole radar.

The lower chromitite stringer then grades upwards into the pegmatoidal feldspathic pyroxenite and harzburgite of the Merensky Reef (Viljoen *et al.*, 1986b). According to Du Pisani and Vogt (2003), the boundary between anorthosite and pyroxenite has a significant permittivity contrast and it is expected that the chromitite stringer on this boundary will also contribute towards strengthening the dielectric contrast. Hence the bottom of contact of the Merensky Reef is expected to provide a strong radar reflector.

At Amandelbult Section, the Merensky Reef package can vary in thickness between 0 m and 5 m. Since the vertical resolution of the borehole radar instrument used in this study is approximately 1 m, it is expected that the Merensky Reef will only be imaged where it is thicker than 1 m. In the author's experience, however, layers thinner than 1 m have been imaged using 40 MHz to 50 MHz borehole radars, especially where a significant contrast in the permittivity was present between two layers (Chalke *et al.*, 2006). Since there is a significant contrast between the Merensky Reef and its underlying layers, together with the sharp chromitite boundary, it is expected that the Merensky Reef will be imaged even where it is thinner than 1 m.

The top contact of the Merensky Reef is also characterised by a thin chromitite layer, which is normally not thicker than 20 mm (Viljoen *et al.*, 1986b). Above this chromitite stringer there is a thin layer of poikilitic feldspathic pyroxenite which gradationally changes into norite (Viljoen *et al.*, 1986b).

Since the contact between the Merensky Reef pyroxenite and its overlying pyroxenite is essentially a contact between two similar rock types, the top Merensky Reef contact is not expected to be a good radar reflector. Furthermore, the hanging wall pyroxenite above the top Merensky chromitite stringer grades into norite and although the boundary between pyroxenite and norite provides a good radar reflector (Du Pisani and Vogt, 2003) due to the gradational transition, a radar reflection is not expected.

The norite layer above the Merensky Reef is topped by a prominent mottled anorthosite, which is 2 m to 3 m thick (Viljoen *et al.*, 1986b). According to Du Pisani and Vogt (2003), the boundary between norite and anorthosite does not have enough of a dielectric contrast to produce a radar reflection.

The entire Merensky Reef cyclic unit from the pegmatoidal pyroxenite to the mottled anorthosite is typically approximately 16 m thick (Viljoen *et al.*, 1986b).

3.5.6 Bastard Reef unit

The Bastard Reef cyclic unit is very similar to the Merensky Reef cyclic unit, except that this cycle is spread over a thickness of 32 m, where the Merensky unit is 16 m thick (Viljoen *et al.*, 1986b). The lower portion of the Bastard Reef cycle does not contain pegmatoidal pyroxenite and it is also not characterised by a thin chromitite base (Viljoen *et al.*, 1986b). Instead, the Bastard Reef usually consists of a fine-grained pyroxenite that changes gradationally into norite.

Since the poikilitic pyroxenite at the base of the Bastard Reef unit has a sharp contact with the underlying mottled anorthosite, this contact should produce a good radar

reflection. According to Du Pisani and Vogt (2003), the contact between anorthosite and pyroxenite will produce a good radar reflection.

3.5.7 Notes on the UG2 chromitite

As seen in Figure 10 when normal Merensky Reef is present, the UG2 chromitite is expected 38.3 m beneath the Merensky Reef. The radar waves are not expected to travel all the way from the borehole (drilled in Merensky Reef footwall norite) to the UG2 due to two reasons:

1. The UG2 is too far from the borehole.
2. The feldspathic harzburgite P2 marker is expected to attenuate the radar signal.

In order to evaluate the topography of the UG2 Reef with borehole radar, new radar boreholes would have to be drilled below the P2 marker.

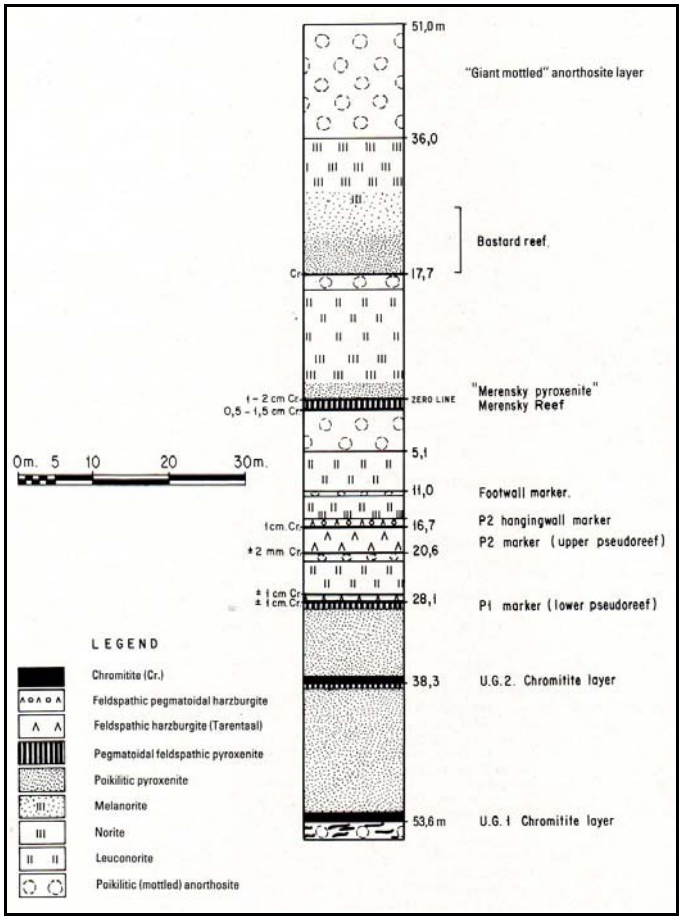

Figure 10: Stratigraphic column for the economic reefs at Amandelbult Section after Viljoen *et al.*, 1986b

4 POTHOLES

4.1 Potholes in the Western Bushveld Complex

Irvine (1982) and Kruger (1990) described the Merensky Reef as paraconformable with the underlying cumulates. According to Viljoen and Schürmann (1998), the Merensky Reef forms a regional discontinuity in the western lobe of the Bushveld Complex. Viljoen (1999) describes how the Merensky Reef can slump into its footwall layers to form structures broadly termed *potholes*. According to Carr *et al.* (1994), Merensky Reef potholes are significant disruptions to the normal magmatic layering in the Upper Critical Zone of the Bushveld Complex.

According to Viljoen *et al.* (1986b), potholes are circular or elliptical in plan view, and Viljoen (1999) states that a pothole can slump downwards for 1 m to tens of

metres. It is also possible for the Merensky Reef to transgress downwards in a step-like fashion (Viljoen and Schürmann, 1998), with steps associated with steep portions of thin contact reef. As the reef cascades downwards, it is also possible for mineralised reef to form on various footwall units (Viljoen and Schürmann, 1998).

Various types of pothole structures and pothole reefs have been classified and identified (Farquar, 1986; Leeb du Toit, 1986; Viljoen and Hieber, 1986; Kinloch and Peyerl, 1990; Viljoen *et al.*, 1986a; 1986b; Schürmann, 1991).

Wagner (1929) divided the Western Bushveld Complex rocks into the Rustenburg facies to the south of Pilanesberg and the Swartklip facies to the north. These two facies were then sub-divided into subfacies, which can, among other things, be distinguished by the abundance, size and type of potholes present (Figure 11).

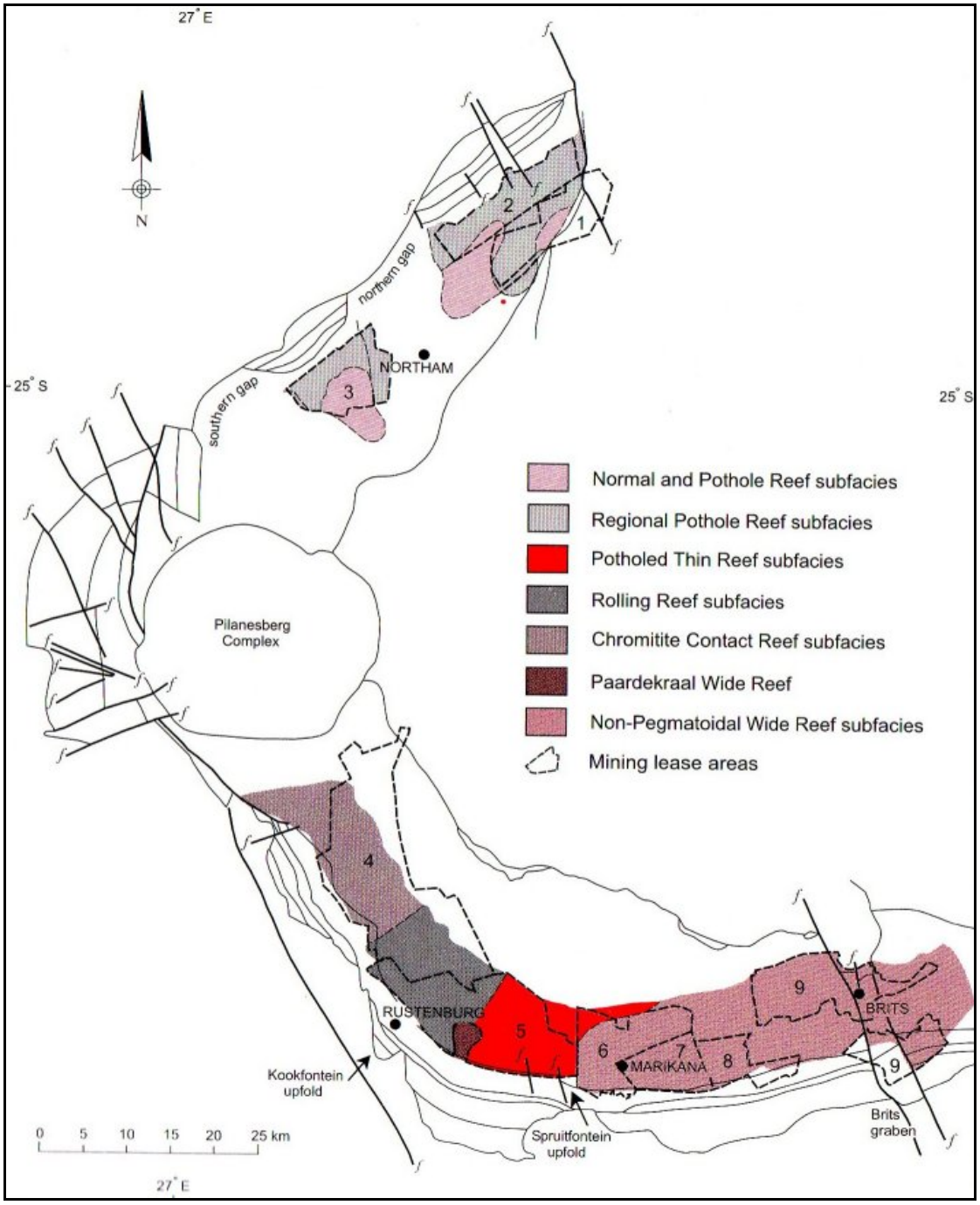

Figure 11: Merensky Reef facies map for the Western Bushveld Complex, after Viljoen and Schürmann (1998)

4.2 Potholes at Amandelbult Section

According to Viljoen *et al.* (1986b), potholes at Amandelbult Section are similar to potholes elsewhere in the Bushveld Complex in that the Merensky Reef and its hanging wall plunge abruptly and transgress their footwall layers.

Viljoen *et al.* (1986b), documented the potholes they were aware of at Amandelbult Section, according to their size, shape and distribution, as shown in Figure 12.

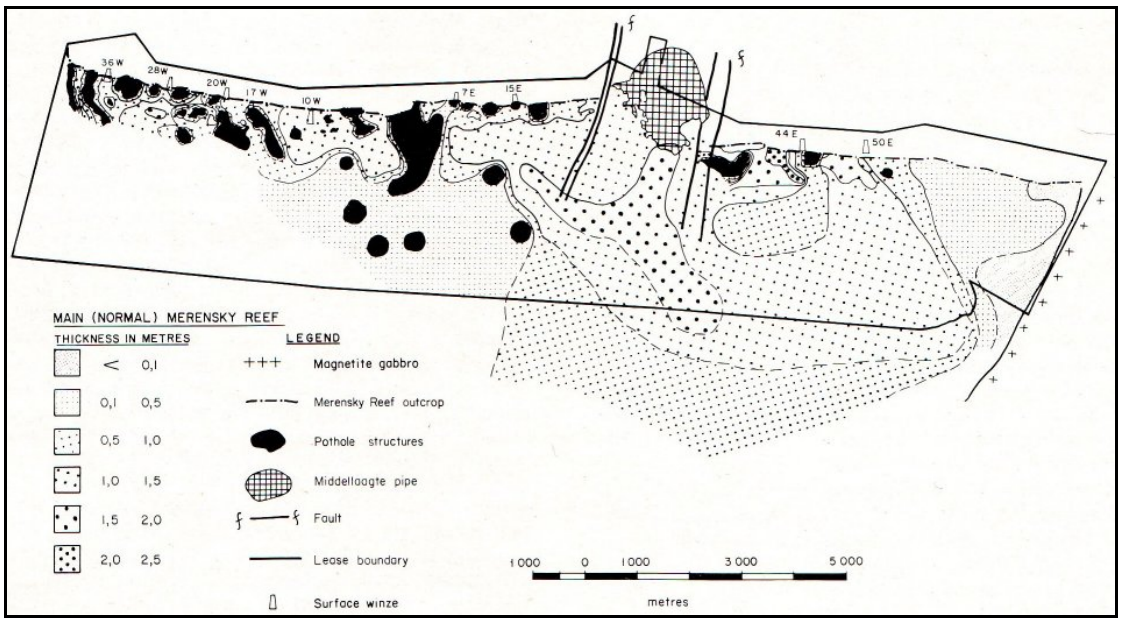

Figure 12: Distribution of pothole structures and isopach map for normal Merensky Reef at Amandelbult Section after Viljoen *et al.*, 1986b

According to Viljoen (1994), a local, rapid thinning of the Merensky Reef is evident towards the edges of individual potholes, especially at Amandelbult Section (Figure 13). Viljoen *et al.* (1986b), state that contact-type reef is usually developed around and on the edges of potholes. They further describe how the top and bottom chromitite stringers associated with the top and bottom contacts of the normal Merensky Reef converge and can even merge into a single chromitite layer with hanging wall poikilitic pyroxenite above and footwall mottled anorthosite below. This thin chromitite contact is called *contact reef* (Viljoen, 1994) and according to Viljoen *et al.* (1986b), it can transgress downwards and cut across the footwall succession. This contact reef may be mineralised, but due to its unpredictable behaviour and thinness, it is often not viable to mine it (Viljoen *et al.*, 1986b).

At the base of the pothole structure, the contact-type reef approaches the upper pseudoreef or P2 (Viljoen *et al.*, 1986b). Here, pegmatoidal feldspathic pyroxenite, which is very similar to normal Merensky Reef, occurs directly above the P2. This reef is called *pothole reef* and it is typically about 16 m below the normal Merensky Reef elevation (Viljoen, 1994). The generalised pothole model as given in *A guide to*

the geology of Amandelbult is shown in Figure 14, where it is also evident that the footwall of the pothole reef is the feldspathic harzburgite of the P2 as opposed to the mottled anorthosite of the normal Merensky Reef.

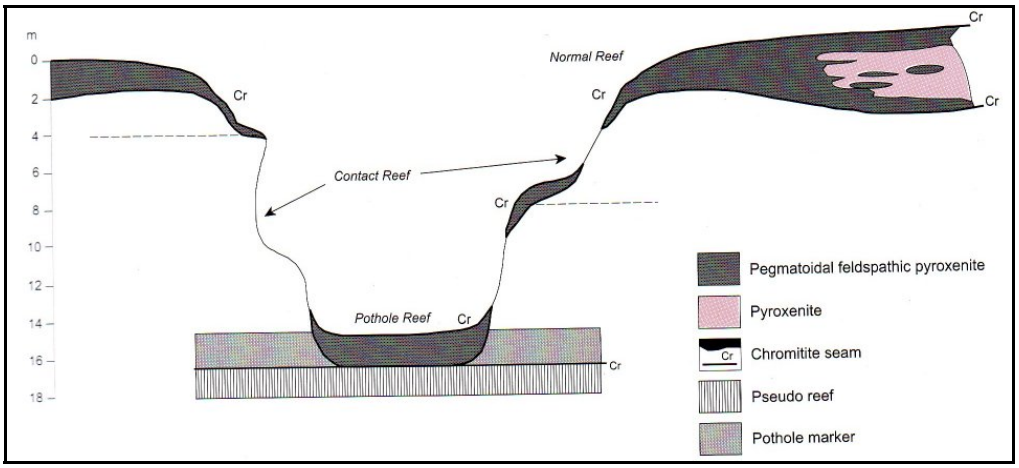

Figure 13: Generalised pothole model for the potholes within the Swartklip facies as developed by Viljoen (1994)

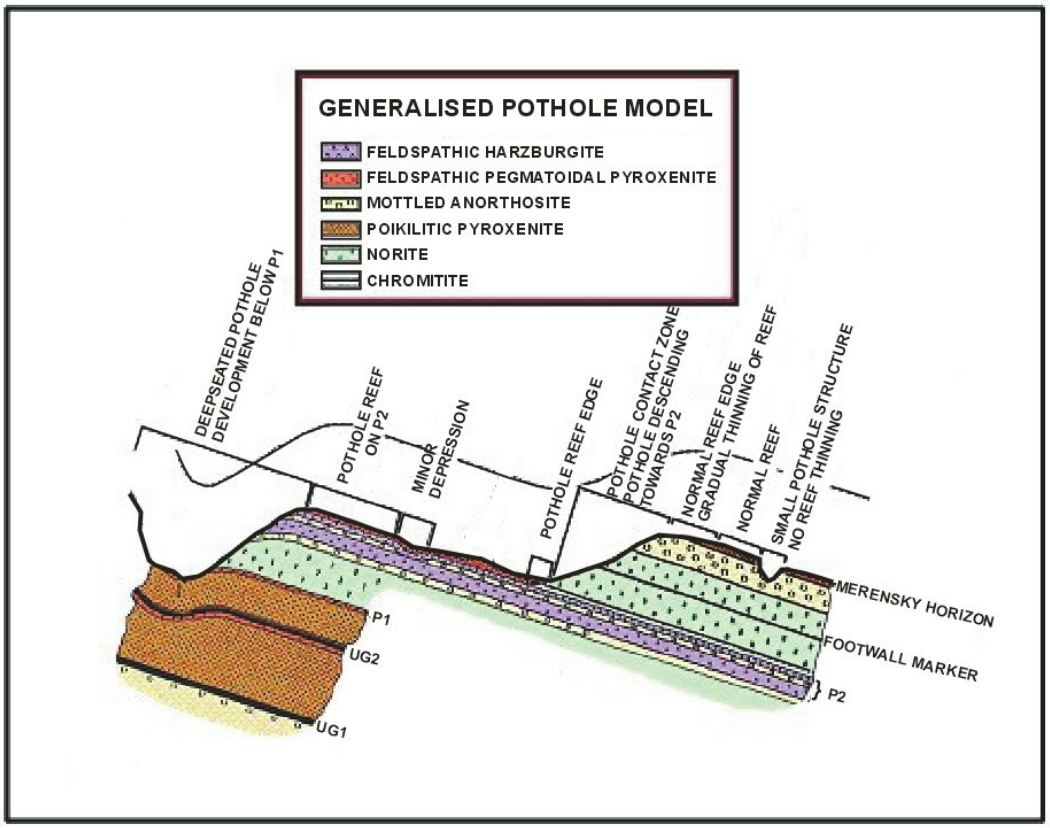

Figure 14: Generalised pothole model for pothole formation at Amandelbult Section from *A guide to the geology of Amandelbult*

4.3 The influence of potholes on mining

4.3.1 Mining of the Merensky Reef at Amandelbult Section

The Merensky Reef topography is initially estimated by extrapolating reef intersections from deep exploration boreholes. From these boreholes, the general dip and strike of the ore body is approximated. 3D-Seismic surveys from the surface provide a more continuous picture of the Merensky Reef and valuable information on large potholes and structures that could negatively affect the positioning of expensive capital expenditure such as main and ventilation shafts.

Thin Merensky Reef types are generally mined by narrow (80cm to 100cm) conventional breast stoping methods (Viljoen, 1994). From deep vertical shafts sunk through the ore body, haulages are developed parallel to the strike of the reef, approximately 30 m below it (Figure 15). Horizontal cross-cuts are then developed towards the dipping reef plane (Figure 16A). Raise lines are excavated in the dip direction on the reef elevation (Figure 16B). Mining then commences in panels, with face widths of typically 35 m, from opposite raises (Figure 16C). At the end of the mining process, a natural dip pillar is left in the middle of the mining block to provide support.

In the case study presented in this treatise, borehole radar was used to delineate a mining block bounded by two cross-cuts and a haulage, i.e. a block of approximately 200 m by 200 m.

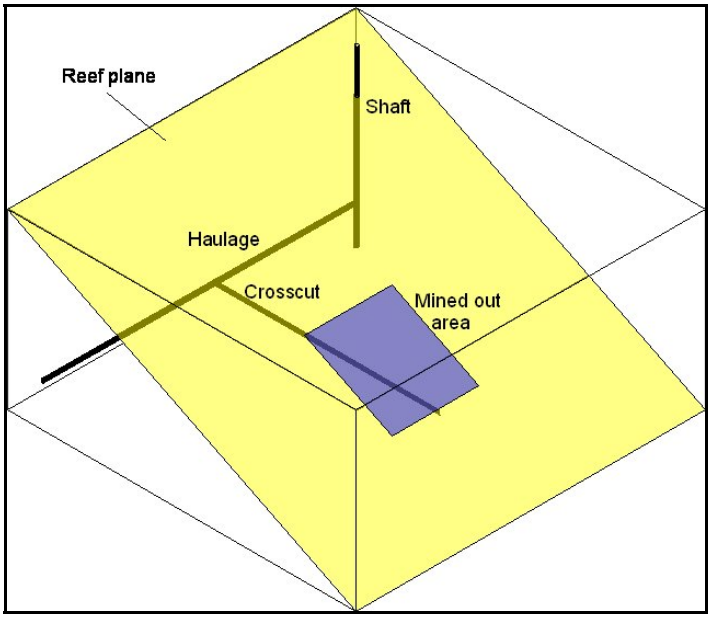

Figure 15: Diagram showing the simplified methodology for conventional breast stoping

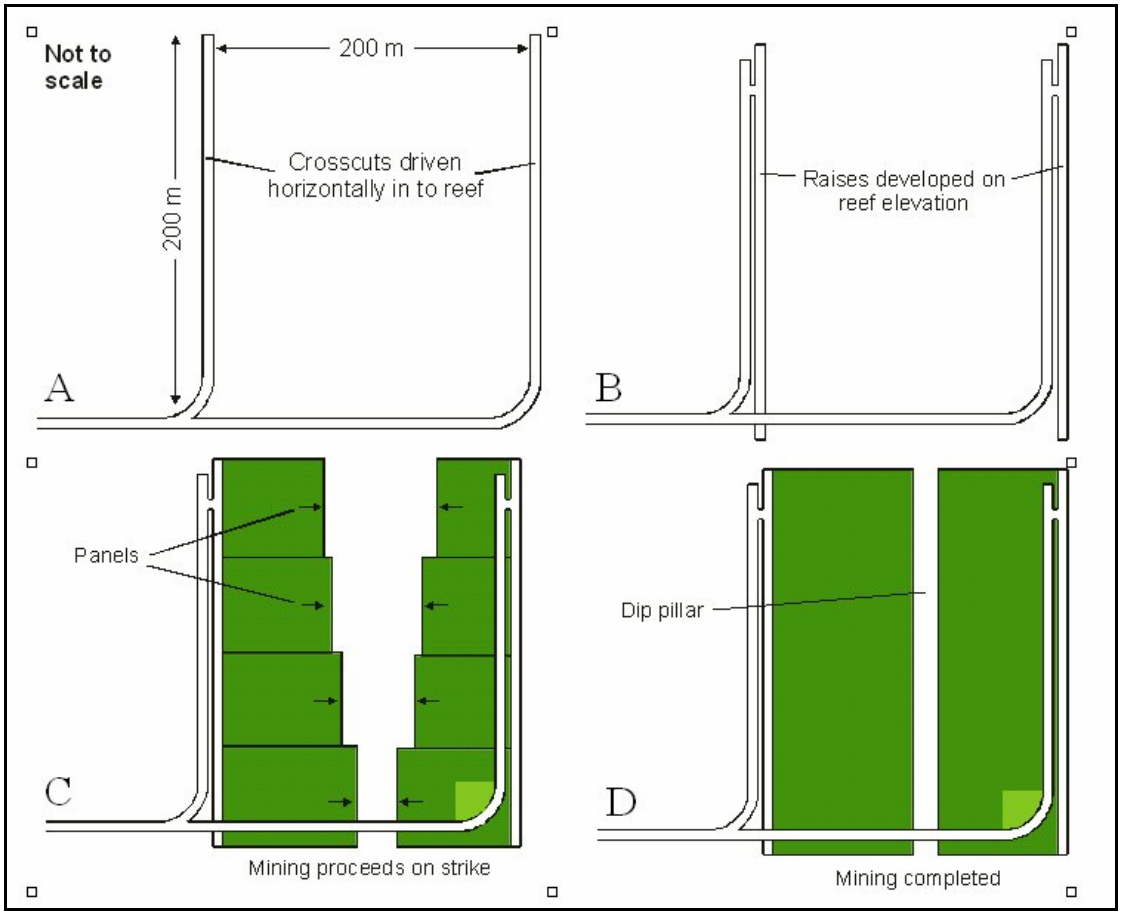

Figure 16: The process of mining thin reefs using conventional breast stoping: (A) Cross-cuts are developed from the haulage to the reef. (B) Raises are developed along the reef elevation. (C) Panels are mined out from opposite raise lines. (D) A dip pillar is left in the middle of the mining block to provide support. (After Du Pisani and Vogt, 2004)

4.3.2 Influence of potholes in mining the Merensky Reef at Amandelbult Section

According to Viljoen (1994), for normal Merensky Reef within the Swartklip facies, which is up to 150 cm thick, the entire reef package is mined together with its bounding chromitite stringers.

If the reef is thicker than 150 cm, the position of the mining cut is based upon the vertical grade distribution of the Merensky Reef as described by Viljoen (1994). Viljoen (1994) states that for the Merensky Reef within the Swartklip facies (thicker than 150 cm), it is usually the top portion of the reef package that is mined, and that the bottom pegmatoidal portion and lower chromitite band are left behind.

Potholes in the Swartklip facies are usually identified from local thinning and, according to Viljoen (1994), the proximity to a pothole can potentially be inferred by monitoring reef thickness and gradient. As pothole reef typically occurs approximately 16 m below the normal Merensky Reef elevation (Viljoen, 1994), mine excavations need to be redeveloped at a lower elevation to access portions of pothole reef.

Viljoen (1994) advises that an assessment be made of the pothole reef, and the intermediary contact reef between the normal and pothole reef, before mining decisions are concluded. He states that due to the irregularity and unpredictable nature of the contact reef, it is regularly unmineable, and that if a long section of irregular contact reef is present between the normal and pothole reef, it will lead to a section of total reef loss.

According to the on-shaft geologist (Marais, *pers comm*) at the time of the borehole radar surveys, current practice for predicting potholes is:

- Outlines of potholes are based on information gathered from the surface as well as underground drilling and mapping in stope panels.
- When a pothole is intersected in an underground borehole, a fan of boreholes is drilled in order to determine the extent of the pothole.

- In ideal situations the miners notify the geologist as soon as they encounter a pothole in the stope. If a pothole is detected in the stope, the geologist goes to that working area and tries to map it, and then plots it on to the 1:1000 working plans for that area.
- The interpretation of geological structures on the working plans is always a combination of information from boreholes and underground mapping.

At Amandelbult Section, a pothole is considered significant when it fills up one-third of a mining panel, i.e. it has a diameter of roughly 10 m to 12 m. According to Marais (*pers comm*), miners are supposed to notify the geologist as soon as they intersect a pothole while stoping. Once the miners have notified the geologist of a pothole intersection, he will then visit the panel and make a recommendation either to stop the panel, if the pothole is large enough, or to advance until such a time that the panel comprises one-third of the total panel length. The geologist's recommendations are put in writing and sent to the production manager, section manager, mine overseer and shift supervisor, as well as the shaft surveyor and shaft rock engineer. Transgression of the geologist's recommendations could be liable to disciplinary procedures. Marais (*pers comm*) stresses that the above scenario is the ideal situation. He further states that miners are compensated per square metre advanced and not for ounces of PGE-minerals delivered to the processing plant, and that in some cases miners will not disclose that they have encountered a pothole. In such a case, waste material will then be sent to the plant. Daily reports from the plant will immediately alert managers when the head grade drops significantly. When this happens, "grade raids" are done by the surveyors and geologists, during which all stope panels will be visited within the space of two days to check for off-reef mining.

Marais (*pers comm*) does, however, say that generally there is good cooperation between most miners and their line management and that tools such as photogrammetry (a photographic report of sample sections) could alert the geologist to the existence of a pothole on a panel. The geologist will then investigate and report on his findings.

The geological losses due to potholes at Amandelbult Section are estimated to be between 20% and 22% (Marais, *pers comm*). The term *geological losses* refers to areas of the ore body that are unmineable due to geological features such as dykes, iron-rich ultramafic pegmatites, faults and in this case potholes.

Through cover drilling the geologist can get an idea that mining may be approaching a pothole, but cover drilling only gives point-information that can make it difficult to extrapolate pothole boundaries from one borehole to the next. Borehole radar can provide a continuous illumination line of coordinates highlighting the pothole contact; that is, if the physical properties of the rocks and survey geometry are optimal.
Through the application of borehole radar it is endeavoured to:

- Predict the position of potholes before they are mined into.
- Track the thinning of the normal Merensky Reef as it approaches a pothole.
- Locate portions of mineable pothole reef.

It must, however, be stressed that borehole radar cannot provide an indication of the reef grade. It can only delineate the position of the reef more accurately.

5 CASE STUDY

5.1 Introduction

In the Platmine collaborative research programme, the CSIR relies on the participating mining companies to supply case-study sites for their research. A case-study site was identified at Anglo Platinum's Amandelbult Section. The mine geologist selected an area of the mine where mining had ceased due to a number of potholes being encountered while mining. The aim of the borehole radar surveys conducted in four boreholes was to see whether borehole radar could be used to delineate pothole boundaries. The borehole radar surveys were conducted in November 2005.

5.2 Borehole radar survey design

The survey design was based on delineating a mining block defined by the area between two cross-cuts (or raise lines) and the haulage from which these cross-cuts were developed.

A number of survey layouts were considered. The survey layout needed to:

- Cover as much of the mining block as possible.
- Eliminate the necessity for developing too many cubbies from which to drill the boreholes required for borehole radar.

Some of the survey designs that were considered are shown in Figure 17.

Designs A to D were all deemed impractical due to the fact that the drill rig would have to be moved a number of times in order to drill all the boreholes required to cover the mining block. Using more than one drill rig to drill holes simultaneously was also considered impractical for a test study, since drill rigs were being used for other drilling purposes (such as cover drilling) in other sections of the mine.

It was decided that drilling a fan of boreholes from a single cubby as seen in Figure 17E, some distance along a cross-cut, would provide sufficient cover of the mining block and eliminate having to move the drill rig unnecessarily. The two boreholes numbered 1 and 8 were eliminated from the plan, because they would be too close to the cross-cut, and the reflection produced by the cross-cut would mask reflections produced by the reef.

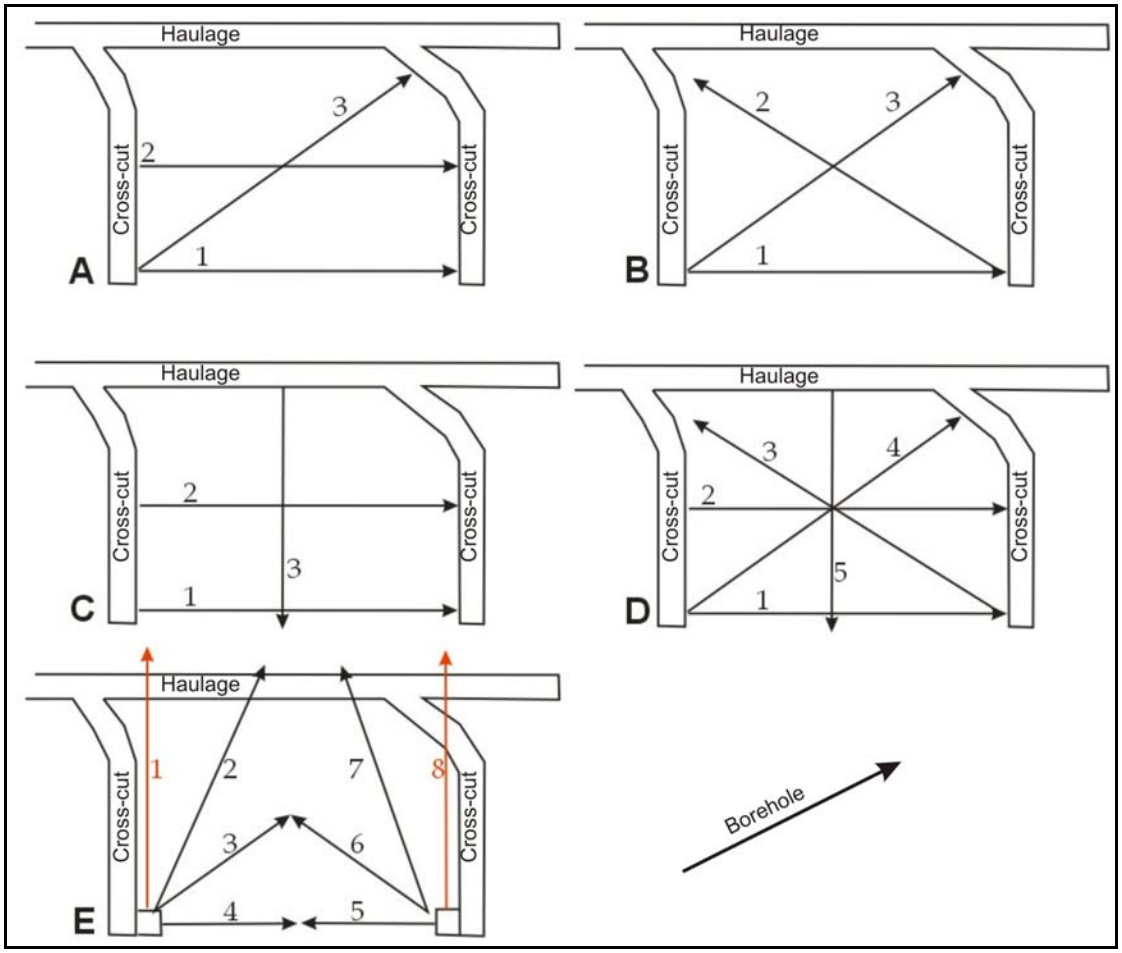

Figure 17: Borehole layouts considered for the borehole radar case study at Amandelbult Section. The arrowed lines indicate possible borehole positions.

The radar boreholes were drilled at Amandelbult 10-Level, from 9W cross-cut. Access was only available from one cross-cut, hence only one fan of boreholes was drilled, aiming to cover the entire block bounded by 9W and 8W cross-cuts by using longer boreholes as planned in Figure 17E. The survey layout is shown in plan in Figure 18, where the red lines represent the borehole radar holes and the purple dots represent some of the geological boreholes drilled for reef intersection within the area.

The radar boreholes were planned to cover the entire mining block bounded by 9W and 8W cross-cuts on 10-Level. The boreholes were drilled up to 250 m each, in order to provide the required coverage, but due to operational problems and borehole blockages, not one of the holes were surveyed with borehole radar up to 250 m. The coverage provided by the actual radar survey lengths is represented in Figure 18.

In Figure 19, a map is presented that shows the location of the boreholes drilled for borehole radar in relation to all the geological boreholes drilled for reef intersection in the vicinity of the borehole radar survey area.

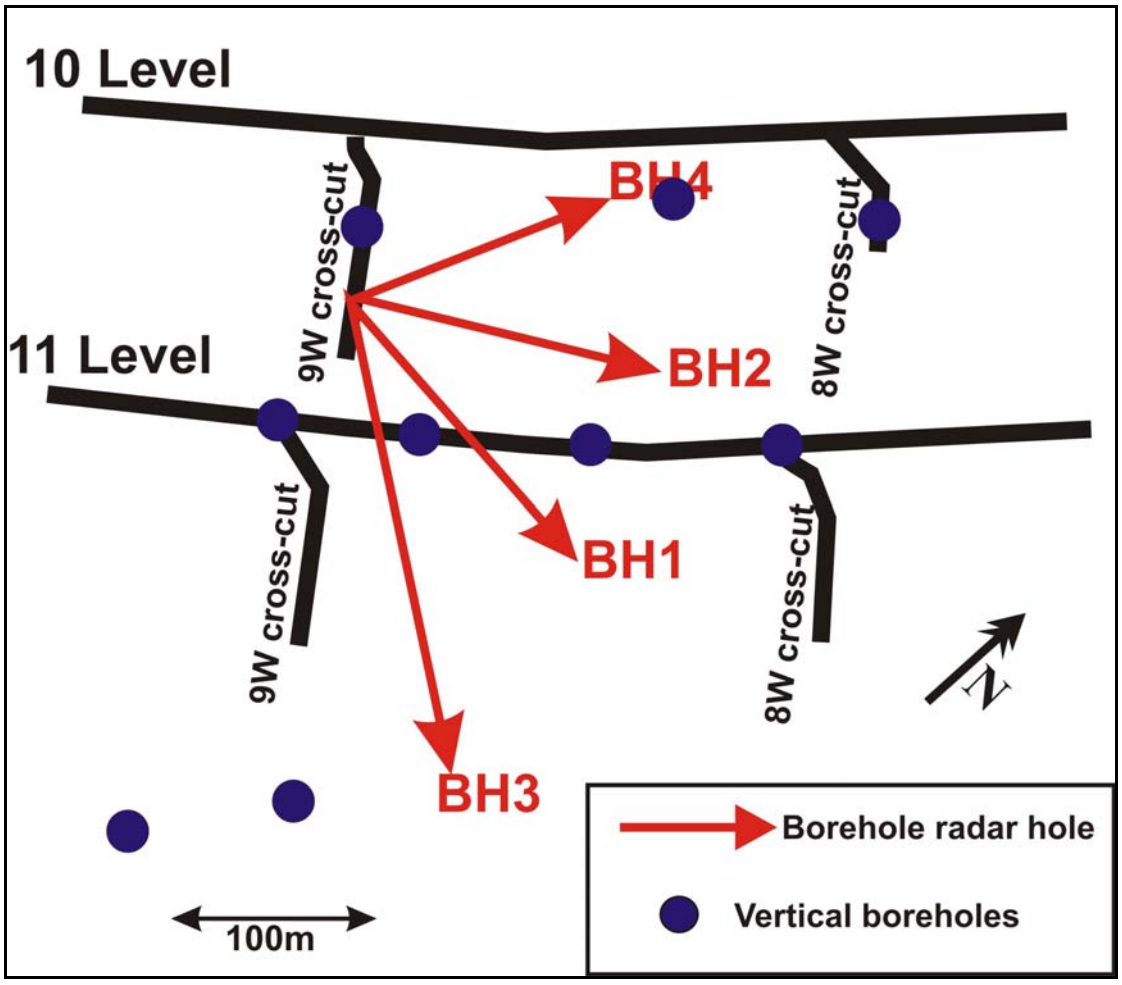

Figure 18: Simplified mine plan showing the positions of the four boreholes drilled for borehole radar as red lines and the location of geological reef intersect boreholes

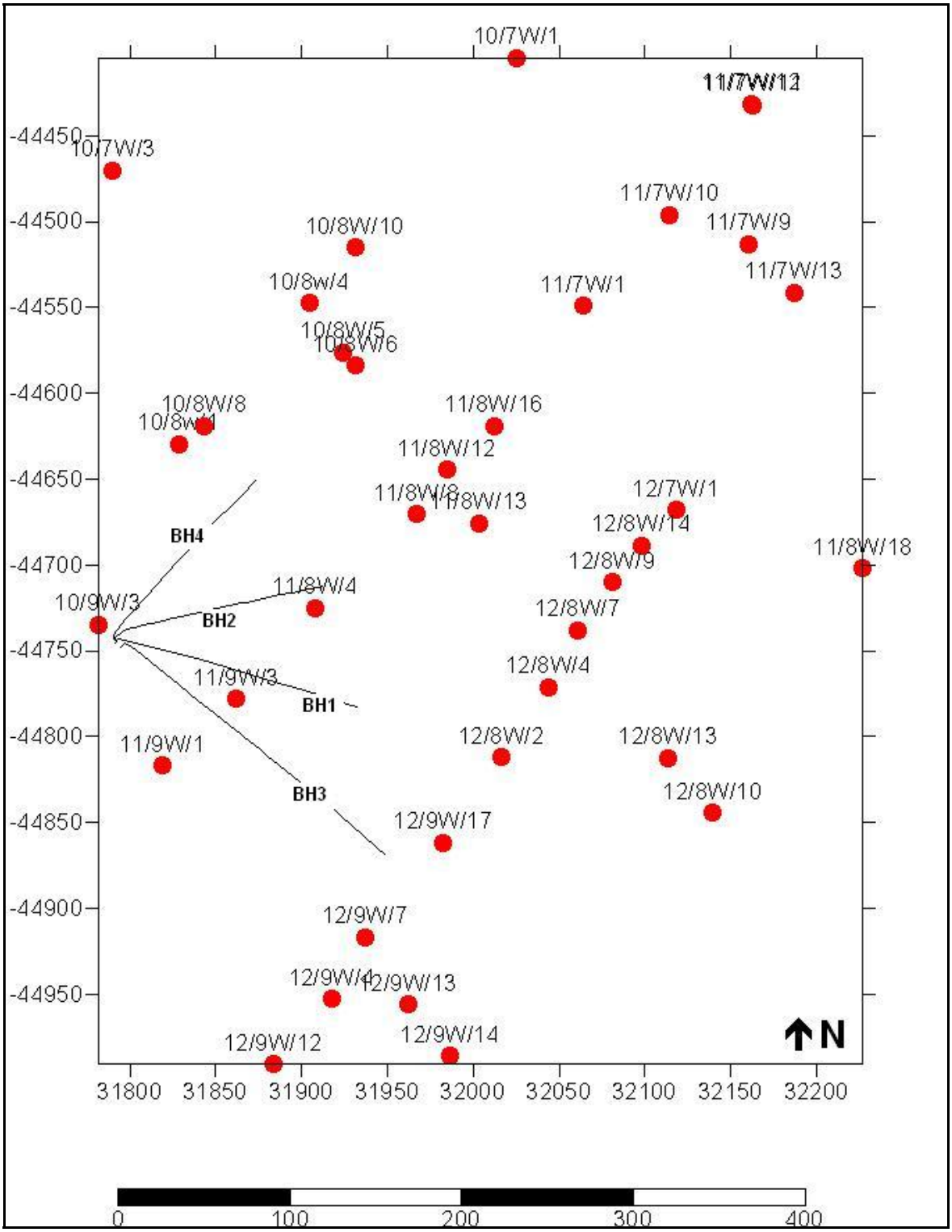

Figure 19: The location of the borehole radar holes in relation to some of the geological drilling in the vicinity

The boreholes were drilled in the norite between the Merensky and Bastard reefs (see the stratigraphic column in Figure 9). As described in Section 3, the bottom contacts of both the Merensky and Bastard reefs are expected to produce radar reflections.

The boreholes were angled away from the Merensky Reef and towards the Bastard Reef so that these two reflectors could be distinguishable on the radargrams. A radargram acquired for borehole 1 is shown in Figure 20A to demonstrate how the two radar reflectors produced by the Merensky and Bastard reefs could be distinguished from one another. At the collar of borehole 1, it is close to the Merensky Reef and far from the Bastard Reef. As we progress along the borehole, the borehole moves further away from the Merensky Reef and closer to the Bastard Reef. Hence, the Merensky Reef reflector on the radargram starts close to the borehole position at 0m along the x-axis, and moves further away from the borehole position as we progress along the borehole. The Bastard Reef reflector starts far from the borehole position at its collar and moves closer to the borehole. Both reflectors manifest within the two-dimensional space of the radargram as a function of their distance away from the borehole.

Figure 20B provides a schematic showing the positions of the Bastard and Merensky reefs above and below the borehole respectively.

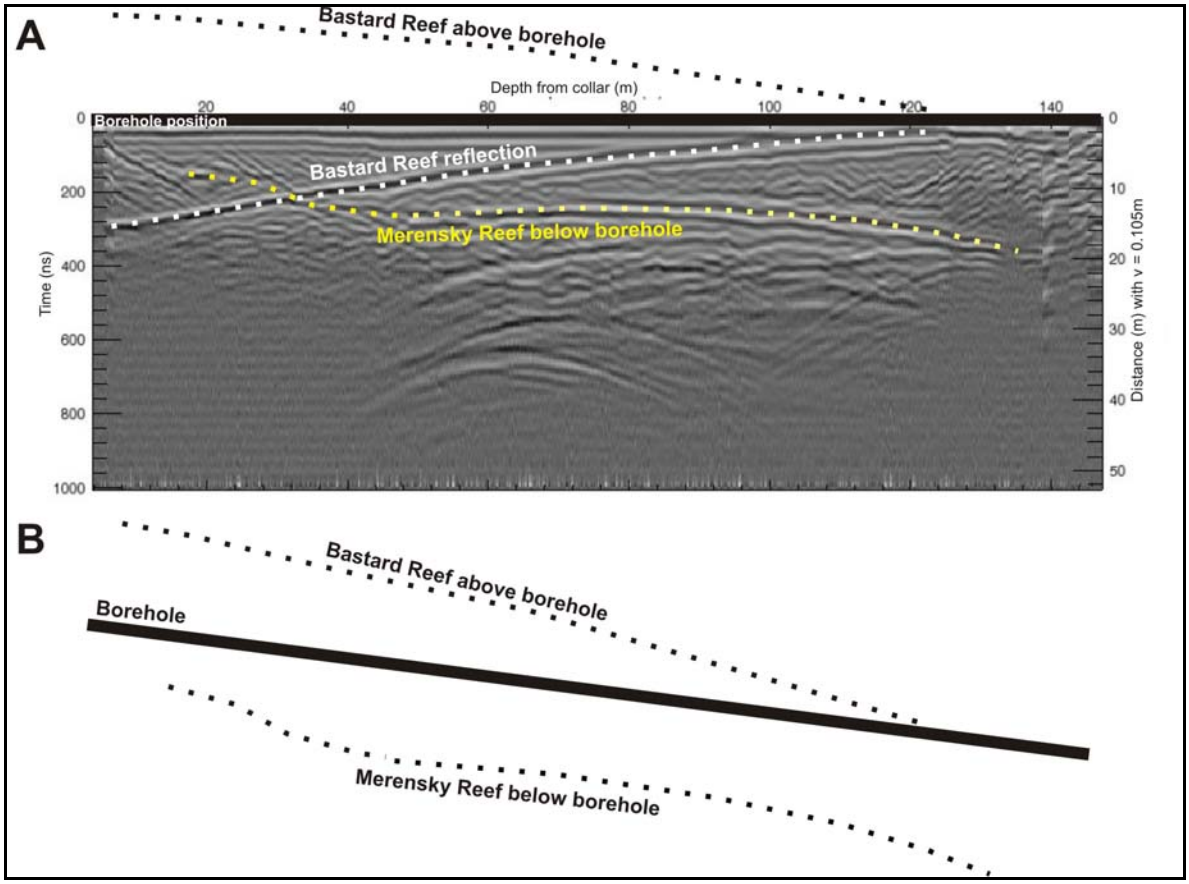

Figure 20: A) Radargram for borehole 1 showing how the Merensky and Bastard Reef reflectors plot at similar distances away from the borehole position; and

B) Schematic showing the Bastard Reef position above the borehole and the Merensky Reef below the borehole.

The basic planned case-study layout is shown in section in Figure 21. The boreholes are indicated by slanted red lines. In Figure 22, the positions of the radar boreholes are shown in section in the software package that was used to conduct the borehole radar modelling. Both Figure 21 and Figure 22 show the planned borehole positions prior to conducting the surveys and radar modelling. In reality, some boreholes started much closer to the Merensky Reef and in some cases the boreholes even started inside the Merensky Reef unit.

The boreholes could not be drilled below the Merensky Reef due to access problems and due to the presence of the very conductive harzburgite layer, the P2, through which radar waves are generally not able to penetrate, as discussed in Section 3. The boreholes were numbered by the drilling contractor from north to south in the

following order: BH4, BH2, BH1 and BH3 (where BH is an abbreviation for "borehole").

The drilling inclination and radar survey length for each borehole is summarised in Table 2.

Table 2: Borehole information for the radar boreholes

Borehole	Inclination	Radar survey length (m)
BH4	+ 16 °	132
BH2	+ 6 °	132
BH1	- 7 °	147
BH3	- 12 °	200

These boreholes were drilled specifically for the application of borehole radar surveys and according to recommendations from the CSIR, namely:

- The boreholes were drilled sub-parallel to the expected Merensky Reef plane.
- The boreholes were close enough to the Merensky Reef so that radar waves could reach it, i.e. within 30 m.
- The boreholes were not drilled to provide Merensky Reef intersection for grade information.

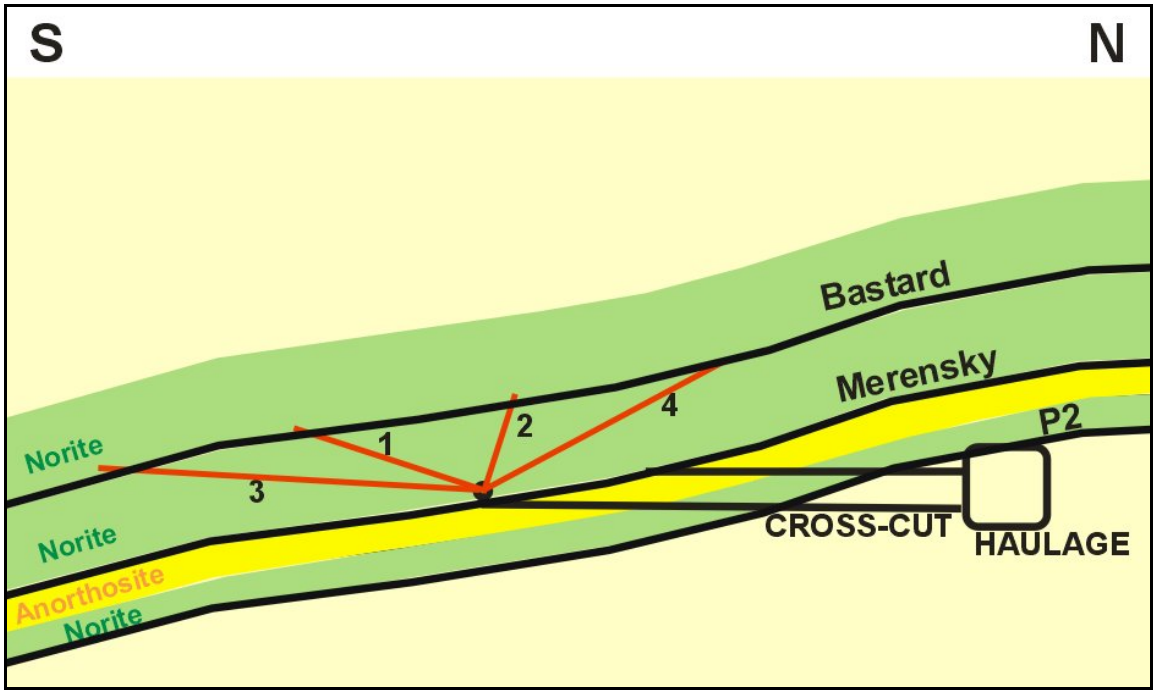

Not according to scale

Figure 21: Schematic showing the case-study layout in section (looking from the east), with the boreholes (red lines) drilled between the Bastard and Merensky reefs, with boreholes angled towards the Bastard Reef

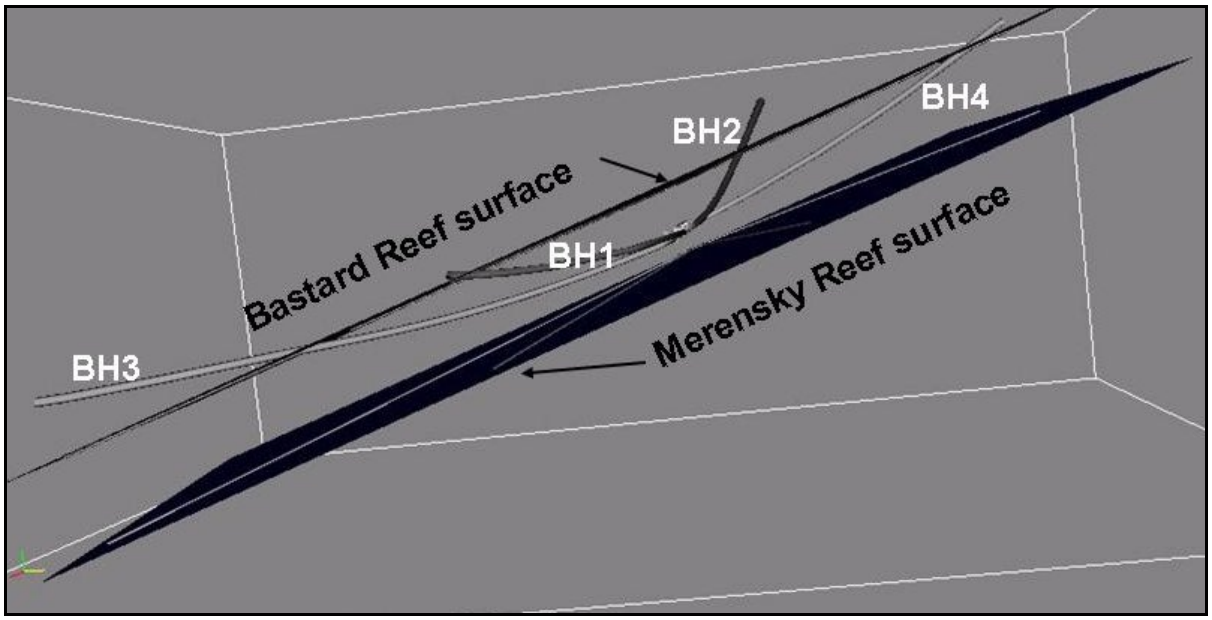

Figure 22: Case-study layout in section, showing radar boreholes as observed from the west. This is the hypothetical base model with flat surfaces for the Merensky and Bastard reefs.

5.3 Borehole radar results

5.3.1 Methodology

The borehole radar results are given and discussed from north to south. After data acquisition, the radar data were processed using band-pass and automatic gain control filters. The band-pass filter eliminated all frequencies not within the range of the Aardwolf borehole radar. Two-dimensional radargrams are presented for all four holes, without interpretation and with the interpreted reflectors indicated.

After the initial processing, all the radar data, together with the individual directional surveys, were imported into Fresco, an open-source 3D visualisation program developed under the Platmine collaborative research programme. Fresco uses forward modelling to aide the interpreter to visualise reflective planes in relation to the borehole radar holes. Radar illumination lines were produced along these reflective surfaces, which were then exported as XYZ coordinates and used together with other borehole information to construct a surface for the Merensky Reef below the borehole radar boreholes.

This methodology is explained in more detail during the discussion for borehole 4, and the same technique was used to interpret the results for the other three boreholes.

5.3.2 Borehole 4

Borehole radar data were collected for 132 m along borehole 4. The directional survey and geological log for borehole 4 are given in Appendix 1. The radargram for borehole 4 is shown in Figure 23, with and without interpretation. Good radar data were acquired up to approximately 96 m along the borehole. The loss of signal between 96 m and 110 m is visible on both the in- and out-surveys. This loss of signal is typical for what is expected when conductive water pools in the borehole, because radar waves generally do not penetrate through very conductive water. This borehole is, however, drilled at an upward angle, i.e. no water is expected inside the borehole.

The geological log for borehole 4 (Appendix 1) shows that iron-replacement was logged in the borehole between 97.4 m and 97.87 m and then again between 103.34 m and 106.56 m. Iron-replacement is very conductive, and it would explain the signal loss seen on the radargram.

In Figure 23, two radargrams are presented for the borehole radar survey conducted in borehole 4. The top radargram is the radar data after initial filtering. The bottom radargram is the same, but the two prominent radar reflectors, namely those produced from the Merensky and Bastard reefs, are annotated. The Bastard Reef reflection is shown as a white dotted line on the bottom radargram in Figure 23 and is interpreted to be in this position due to the fact that it intersects the borehole at approximately 100 m along the borehole, which is consistent with Bastard Reef logged in the drill core at this position. The Merensky Reef reflection is shown as a yellow dotted line in Figure 23. It is not as clear as the Bastard Reef reflection, and its position was interpreted as a result of Merensky Reef pyroxenite logged at the start of the borehole as well as a discussion with the mine geologist, where the most likely position of the Merensky Reef was ascertained. The very straight reflector seen between approximately 50 m and 90 m, starting at a distance of 40 m away from the borehole and moving towards it, is typical of the signature that a near-vertical structure intersecting the borehole would produce. A number of fractures are logged in the borehole between 108 m and 118 m (geological log in (Appendix 1). One of these fractures may be producing this radar reflection.

After the initial 2D interpretation presented in Figure 23, the radargram for borehole 4 was imported into the 3D visualisation software package Fresco to have a look at borehole radar data in 3D space.

Slim-line borehole radars are cylindrically omni-directional (Simmat *et al.*, 2002). This directional ambiguity leads to uncertainty in the interpretation of the reef elevation from borehole radar data. According to Du Pisani and Vogt (2004), the borehole radar receiver only receives reflections from sections of the target surface that are oriented perpendicular to the antennas. When borehole radar is applied from a

borehole drilled parallel to the reef horizon, it maps a single illumination line along the reef surface (Du Pisani and Vogt, 2004). One way to resolve the directional ambiguity is through the use of *a priori* information. The regional dip and strike of the ore body are known, and can be used as a first approximation of the position of the reflector. The drill core of the radar borehole is used to orient the borehole within the local stratigraphy; hence it can be determined whether reflections originate above or below the borehole. Furthermore, any other *a priori* geological information is used to improve the interpretation and resolve directional ambiguity. Geological intersections from other boreholes within the borehole radar survey area, as well as reef pegs from mining in the immediate vicinity, are used to get a better picture of the reef surface.

The radargram for borehole 4 was imported into Fresco together with the borehole's trajectory survey. In this way the curvature of the borehole is taken into consideration, and the interpreter is forced to consider the geometry of the borehole in relation to possible reflectors. In Fresco a candidate ore body can be manipulated, and its radar response can be modelled in real time. The model can then be manipulated until its response agrees with the measured response. The forward modelling approach has three advantages:

- It avoids the need for migration of the radar data. When borehole radar data is migrated, it must take into account the curvature of the borehole, which requires an assumption about the direction to various targets.
- Borehole data remains inherently ambiguous in azimuth. The 3D forward modelling environment forces the interpreter to constantly confront the ambiguity, ensuring that the output is a product of the interpreter's understanding of the problem and not simply automatically generated.
- The position of the illumination line on the target is produced directly in 3D space. This is the required product from a borehole radar survey, and is difficult to produce using other techniques.

As seen in Figure 24, candidate surfaces were constructed for the Bastard and Merensky reefs above and below borehole 4. In the three-dimensional modelling for all four boreholes, the Bastard Reef surface is red and the Merensky Reef surface is

blue. Both candidate surfaces were manipulated until forward modelled responses matched the radar reflectors seen on the radargrams. As topography was added to the Merensky Reef surface, an illumination line was produced on this surface, which simulated the radar ray paths emanating from the borehole radar instrument. In Fresco, topography can only be added in either the dip or strike direction of the candidate surface.

Figure 24 shows how topography was added in the strike direction of the Merensky Reef. Another model was constructed, adding topography in the dip direction. The illumination line coordinates from both strike and dip models were exported in XYZ-format and used in the next phase of modelling (presented in section 5.3.6) to construct a three-dimensional surface using the radar results from all four boreholes.

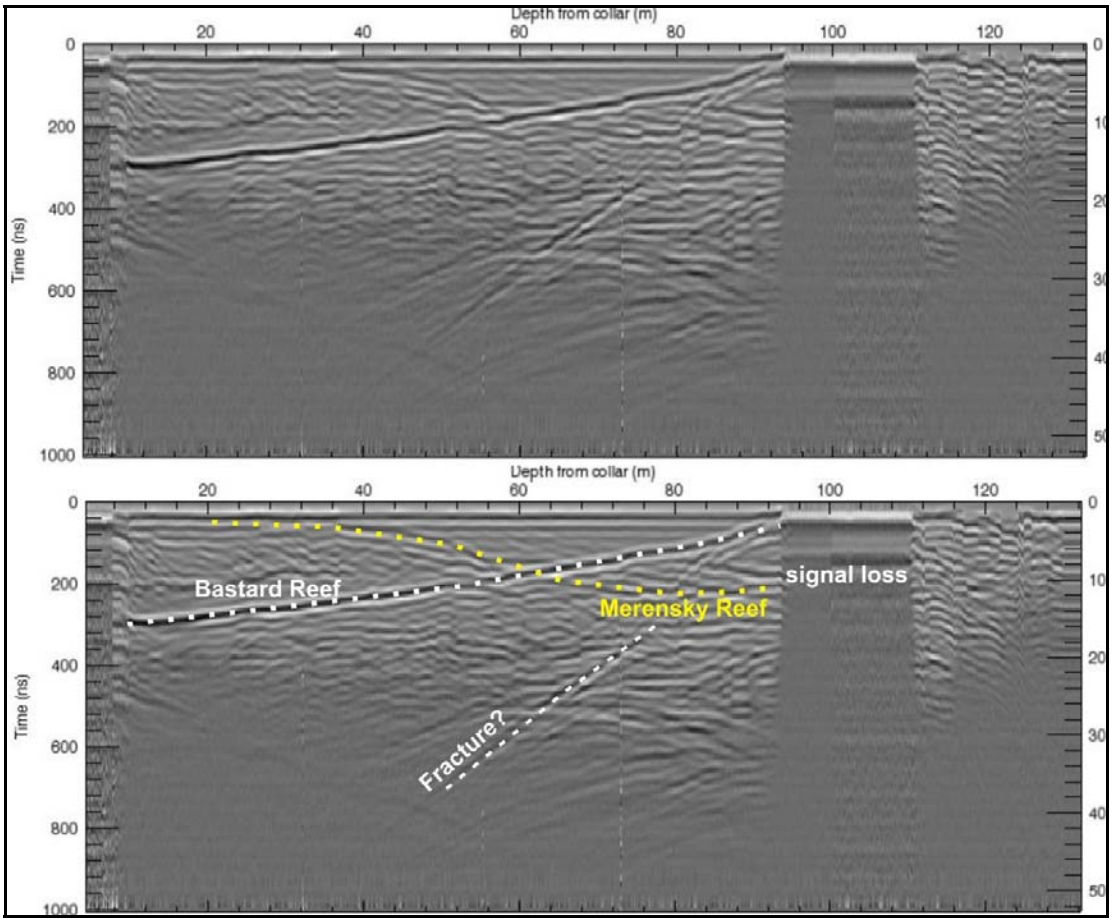

Figure 23: The radargram for borehole 4 without (top) and with interpretation (bottom). The Merensky Reef reflector is indicated by a yellow dotted line and the Bastard Reef reflector is indicated by a white dotted line.

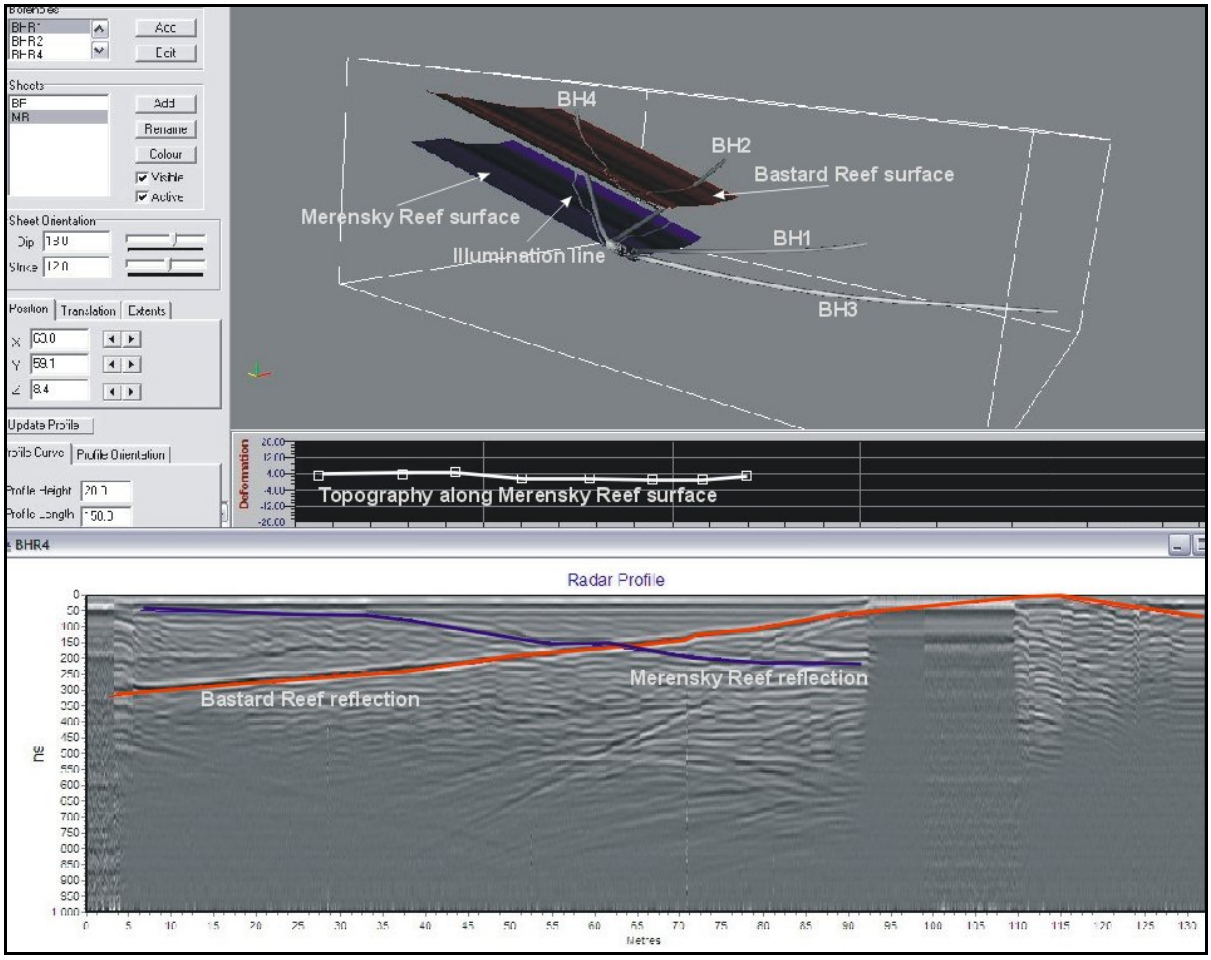

Figure 24: Three-dimensional visualisation for the borehole radar data acquired in borehole 4. The Merensky Reef surface is indicated in blue, while the Bastard Reef surface is shown in red. The radar illumination line is tracked along the Merensky Reef surface.

5.3.3 Borehole 2

The directional survey and geological log for borehole 2 are provided in Appendix 1. The radargram for borehole 2 is shown in Figure 25 with and without interpretation. Borehole radar data were collected for 132 m along borehole 2. The position of the Bastard Reef reflector (indicated in white) could be fixed due to an intersection point in the borehole at approximately 72 m. The interpreted Merensky Reef reflector (indicated by the yellow dotted line) could be imaged clearly for the first 62 m along the borehole, after which its position became unclear. Using three-dimensional visualisation (Figure 26) and adding topography to the Merensky Reef surface in the strike direction, it could be seen that subtle changes in the reef topography led to no reflection line being present between 65 m and approximately 94 m. The Merensky Reef is imaged again between 94 m and 105 m.

Since borehole 2 was oriented along the strike of the ore body, only one three-dimensional visualisation was conducted, i.e. the Merensky Reef surface was only manipulated along the strike direction. Manipulating the topography in the dip direction would not have made a significant difference to the reflection line. The illumination line coordinates for the model constructed in the strike orientation were exported in XYZ-format.

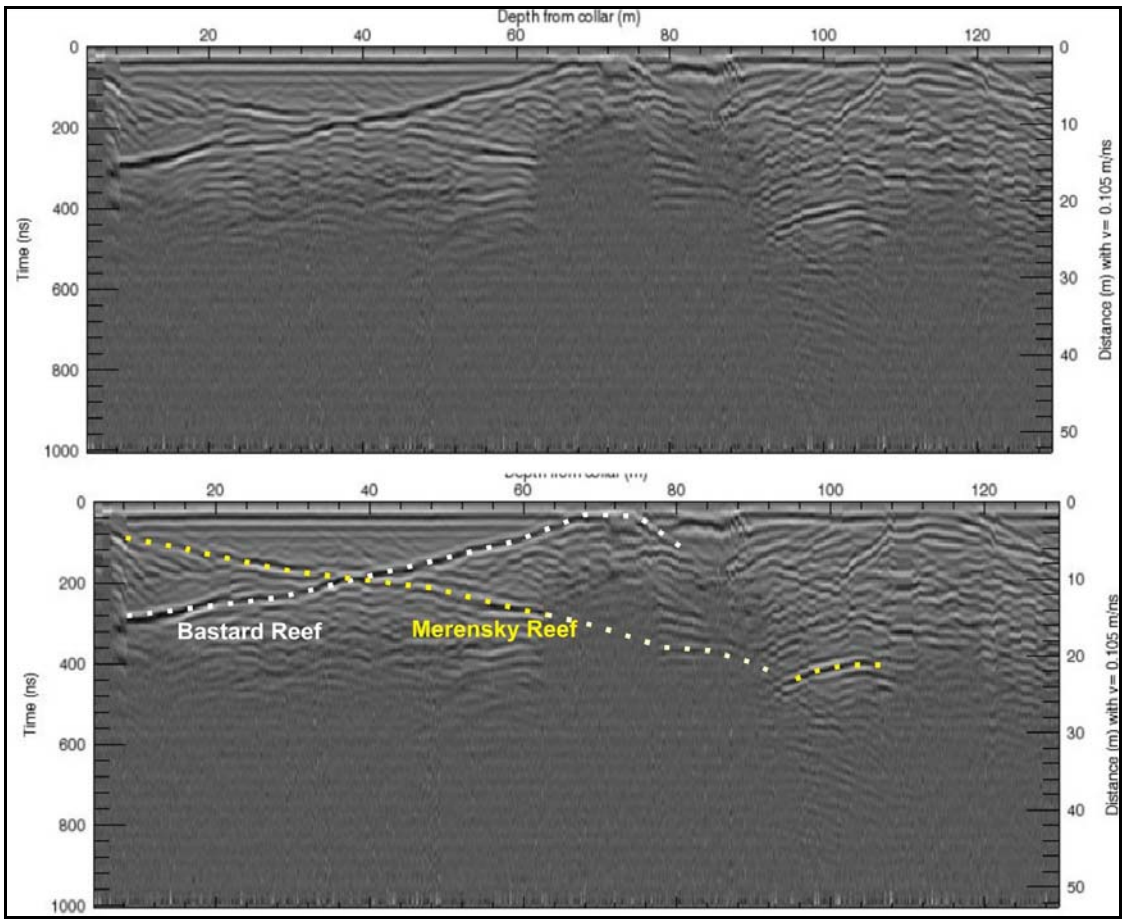

Figure 25: Radargram for borehole 2 without (top) and with interpretation (bottom). The Merensky Reef reflector is indicated by the yellow dotted line, while the Bastard Reef reflector is shown by a white dotted line.

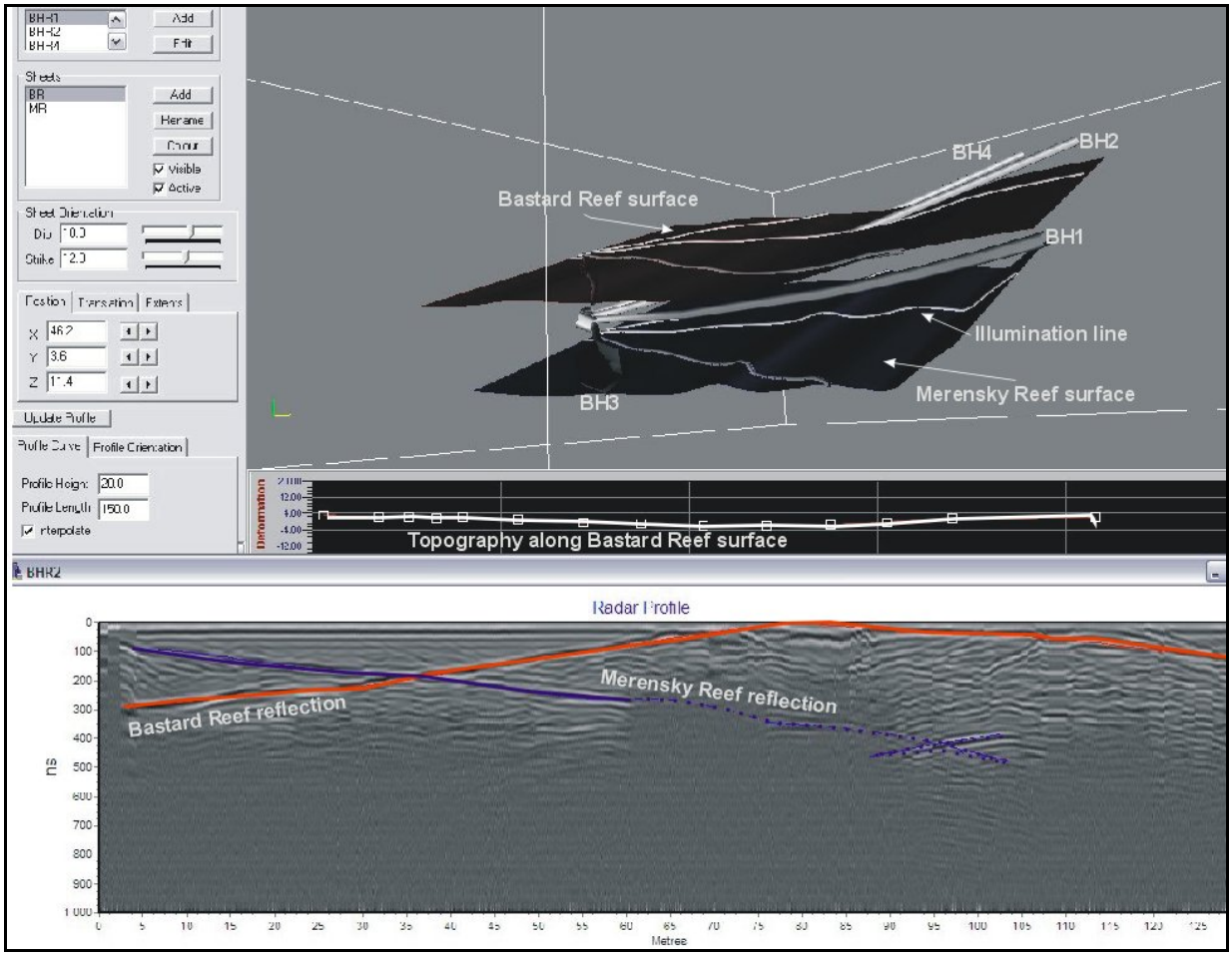

Figure 26:Three-dimensional visualisation in Fresco for the borehole radar data acquired in borehole 2. The Merensky Reef surface is shown in blue and the Bastard Reef surface is shown in red.

5.3.4 Borehole 1

Borehole radar data were collected for 147 m along borehole 1. The directional survey and geological log for borehole 2 are provided in Appendix 1. Both the Bastard and Merensky reefs were imaged clearly for virtually the entire length of the borehole. The Bastard Reef reflector is shown as a white dotted line on Figure 27, while the Merensky Reef reflector is shown as a yellow dotted line. Prominent hyperbolic reflectors seen further away from the borehole may be due to the side-swipe off sharp contacts, possibly due to a pothole structure in the vicinity of borehole 3. These hyperbolic reflectors are not expected to represent reflectors such as the UG2 Reef below the P2 marker, due to the P2's ability to absorb radar waves.

In Figure 28, the surfaces constructed in Fresco for the Bastard and Merensky reefs are shown. Figure 28 shows the three-dimensional visualisation in which topography was added in the strike direction along the Merensky Reef surface. Another model was constructed adding topography in the dip direction. The illumination line coordinates produced along the Merensky Reef surface were exported in XYZ-format for both models.

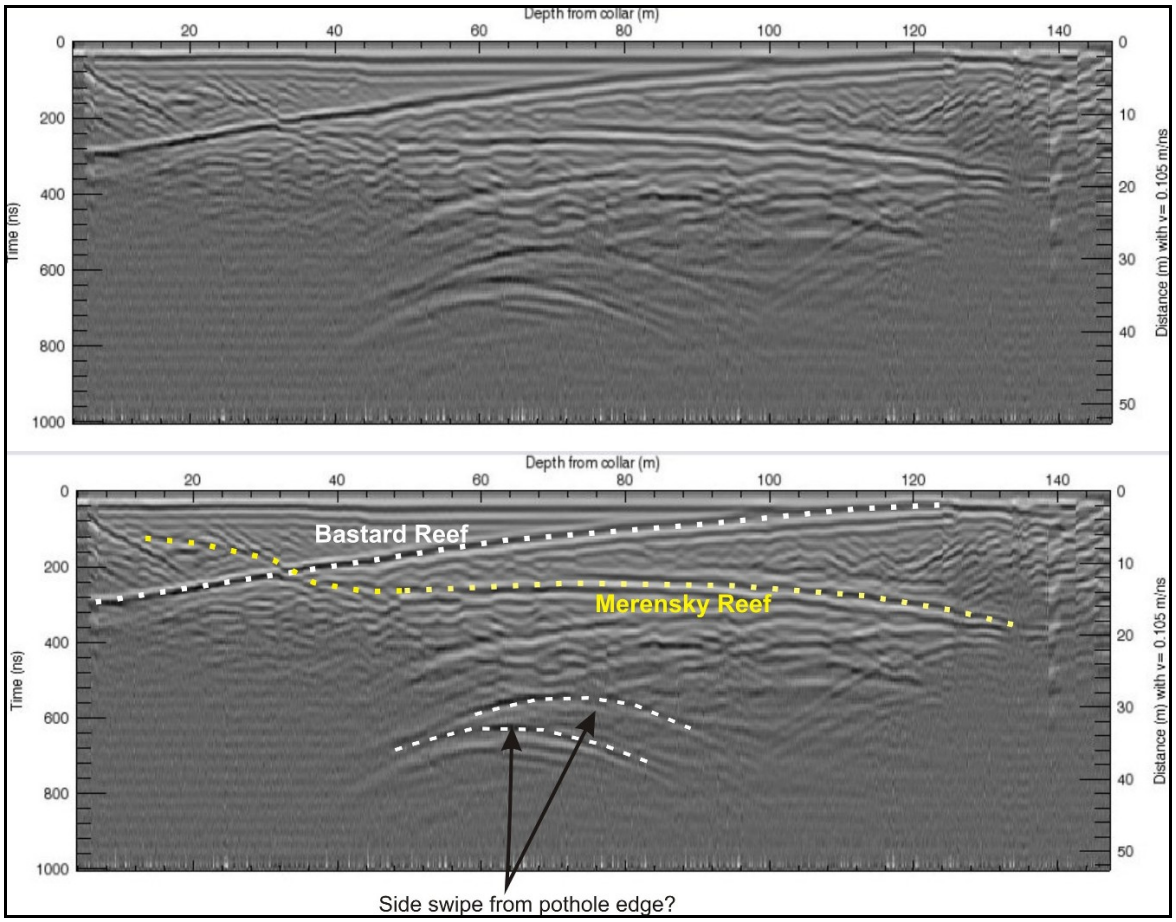

Figure 27: Radargram for borehole 1 without (top) and with interpretation (bottom). The Merensky Reef reflector is shown as a yellow dotted line and the Bastard Reef reflector is shown as a white dotted line.

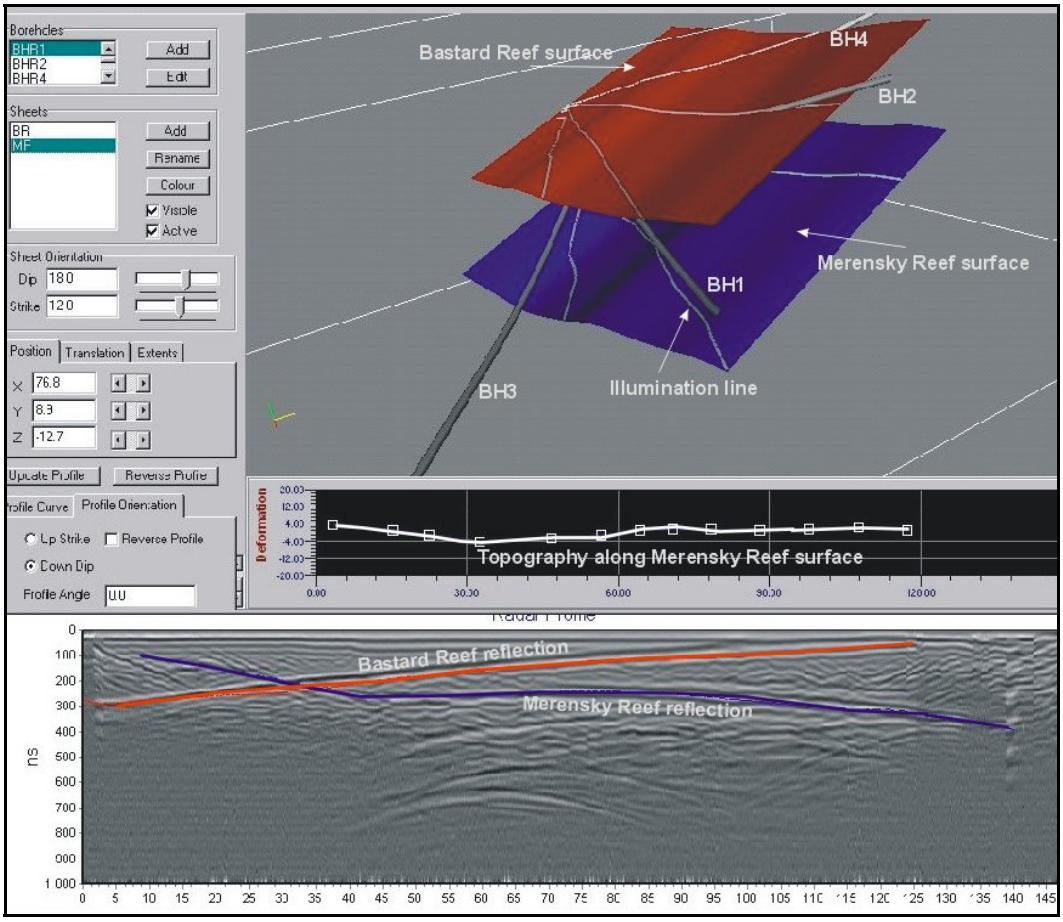

Figure 28: Three-dimensional visualisation for borehole radar data acquired in borehole 1. The Merensky Reef surface is shown in red and the Bastard Reef surface is shown in blue.

5.3.5 Borehole 3

Borehole radar data were collected for 200 m along borehole 3 (Figure 29). The directional survey and geological log for borehole 3 are provided in Appendix 1.

The Bastard Reef reflector (shown in white) can clearly be seen between 0 m and 116 m, after which it intersects the borehole. The Merensky Reef reflector is not very clear on the radargram for borehole 3, but there are sections of a reflector between 0 m and 136 m that correspond to where the Merensky Reef reflector is expected as a result of the three-dimensional visualisation done in the previous three boreholes. The inferred position of the Merensky Reef reflector is shown as a yellow dotted line in Figure 29. Another steeply dipping reflector (represented by the dashed white line in Figure 29), can be seen between 0 m and 80 m on the radargram. This reflector may be due to a dyke in the vicinity of the boreholes.

The Merensky Reef surface produced in Fresco is shown in blue in Figure 30. The visualisation where topography was manipulated in the dip direction is shown here. The illumination line coordinates produced by visualisation in the dip and strike directions were exported in XYZ-format and used for further modelling.

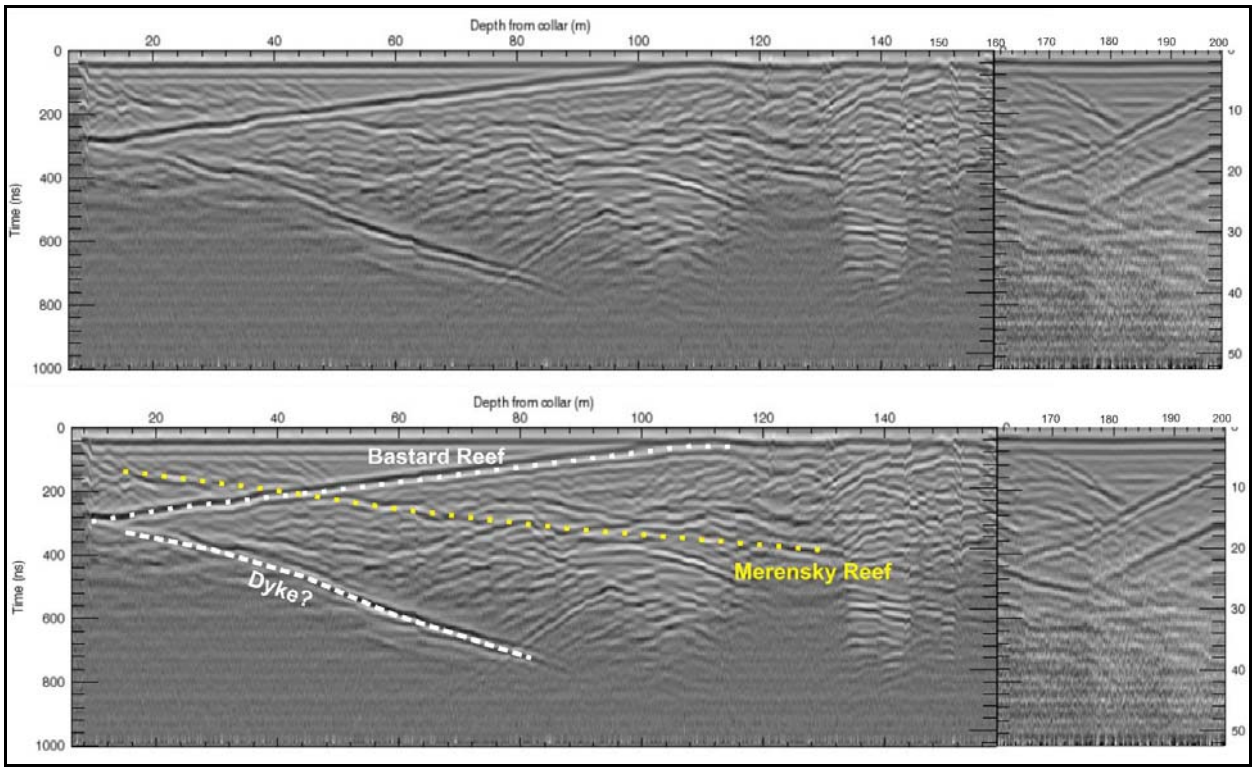

Figure 29: Radargram for borehole 3 without (top) and with interpretation (bottom). The interpreted Merensky Reef reflector is shown as a yellow dotted line and the Bastard Reef reflector is shown as a white dotted line.

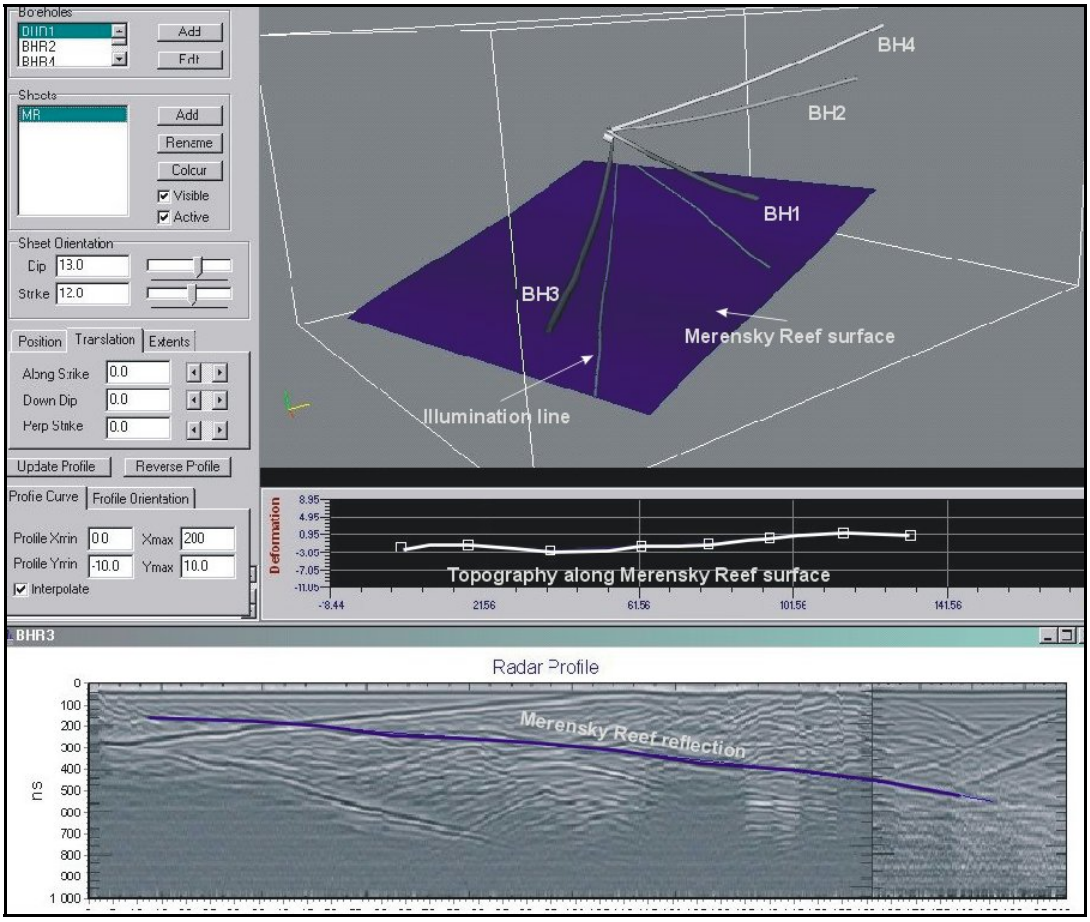

Figure 30: Three-dimensional visualisation for borehole radar data acquired in borehole 3. The Merensky Reef reflector is shown as a blue surface.

5.3.6 Contouring of geological and borehole radar illumination line coordinates

Two contour maps were produced to show the increase in data density if borehole radar is applied. In Figure 31, the contours that were produced by gridding the Merensky Reef intersection coordinates in the geological boreholes in the vicinity of the borehole radar boreholes is presented. Figure 32 shows the contours produced by gridding the illumination line coordinates produced for the Merensky Reef by conducting borehole radar in the four boreholes. It can be observed that more information is available for interrogation after borehole radar was applied. There is much more geological detail to be seen for the Merensky Reef in the area where borehole radar was conducted.

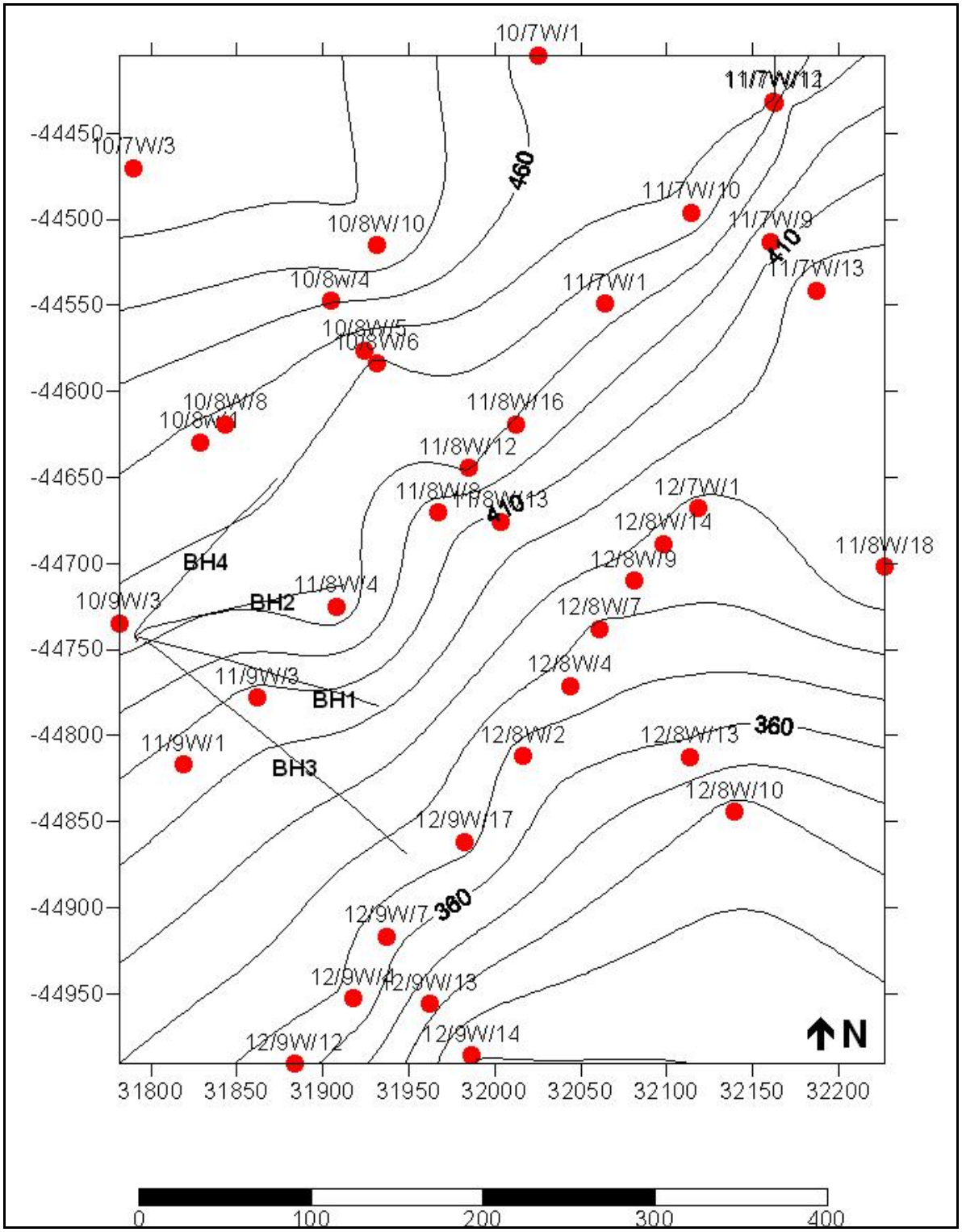

Figure 31: Contour map produced by gridding the Merensky Reef elevation as logged from geological boreholes in the vicinity of the borehole radar survey

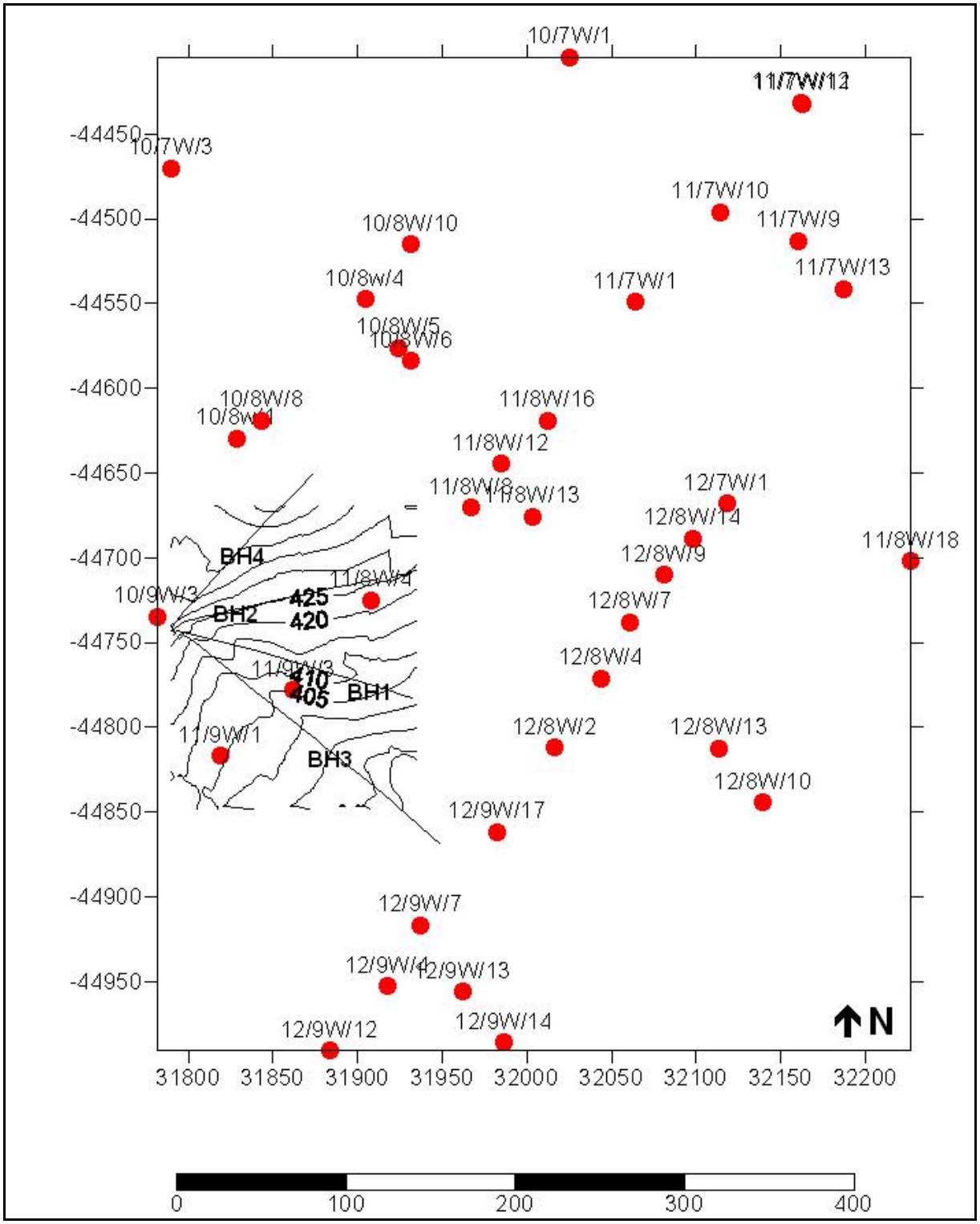

Figure 32: Contour map produced by gridding the illumination line coordinates produced by conducting borehole radar in boreholes 1 to 4

5.3.7 Three-dimensional surface (all boreholes)

The illumination lines produced by all the three-dimensional visualisations done for boreholes 1 to 4 were used, together with some Merensky Reef intersections from geological boreholes in the borehole radar block, to produce a three-dimensional surface. All the illumination line coordinates used for this study are presented in Appendix B.

In Figure 33A, the surface constructed by using only the Merensky Reef intersection from geological boreholes is shown in grey (Surface A). The positions of the geological boreholes are indicated as red dots.

The surface produced by gridding the XYZ-coordinates of all the illumination lines is shown in blue (Surface B). In Figure 33A, it can be observed that Surface B slumps below Surface A, indicating that the borehole radar results show that there is a pothole structure in the west of the mining block that would not have been detected if only the reef intersections from the geological boreholes had been used. Only the portion of the slumped Surface B that differs significantly (more that 1 m) is defined as the pothole in Figure 34.

This pothole (annotated in Figure 34) has an elliptical shape that is approximately 50 m across and slumps approximately 5 m, which would have significant implications for the mining of this block. The financial implication of mining into this pothole is discussed in the cost-benefit analysis conducted in Section 6.

Furthermore, the upward slope of the illumination line for borehole 4 indicates that the reef may be rolling upwards in the north of the block defined by borehole radar. This information may also be useful when this block is eventually mined, both financially and from a safety point of view.

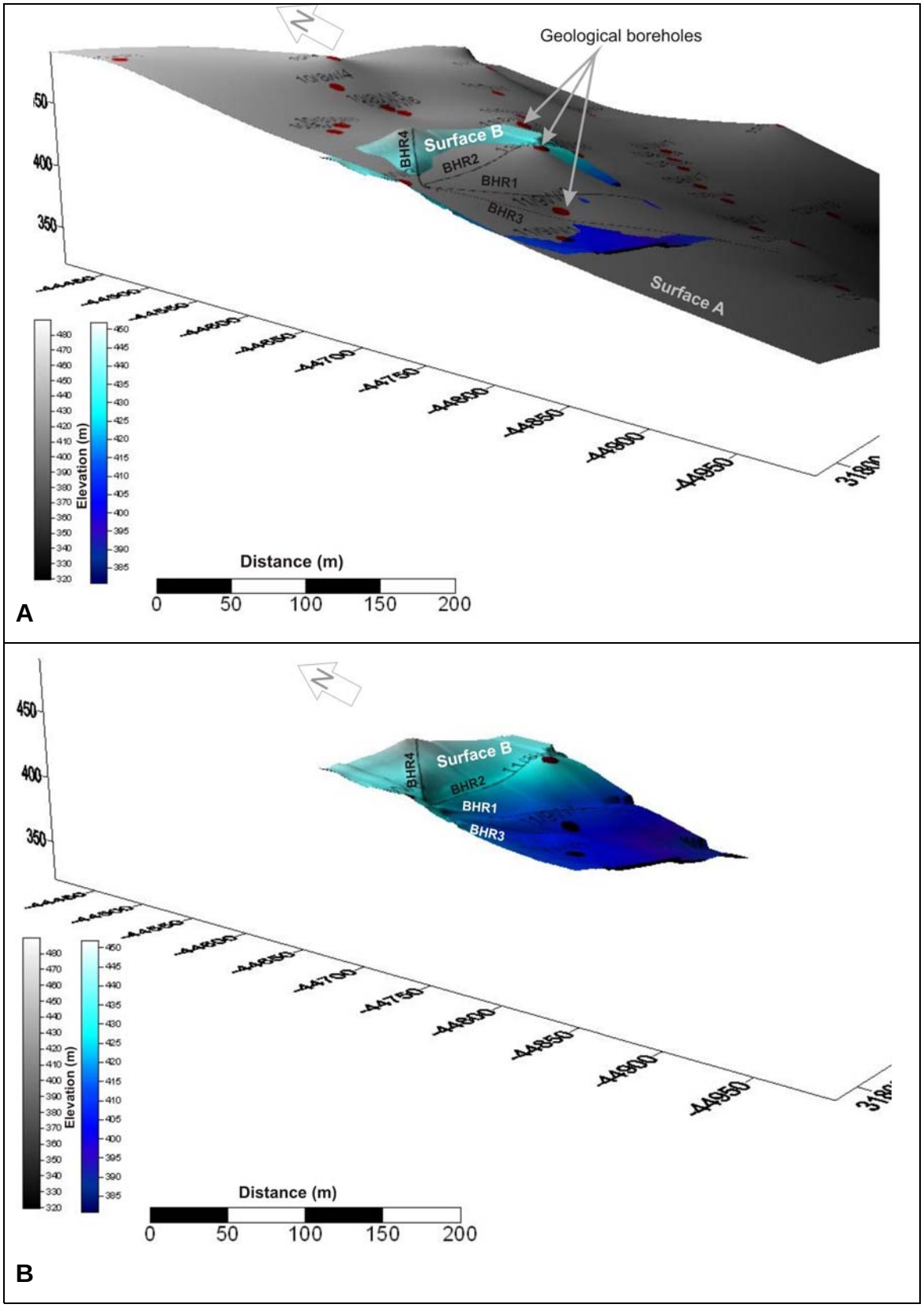

Figure 33: Three-dimensional surfaces constructed for the reef block imaged by borehole radar: A) the grey surface constructed from geological borehole information only, and B) the blue surface constructed by using the borehole radar illumination lines

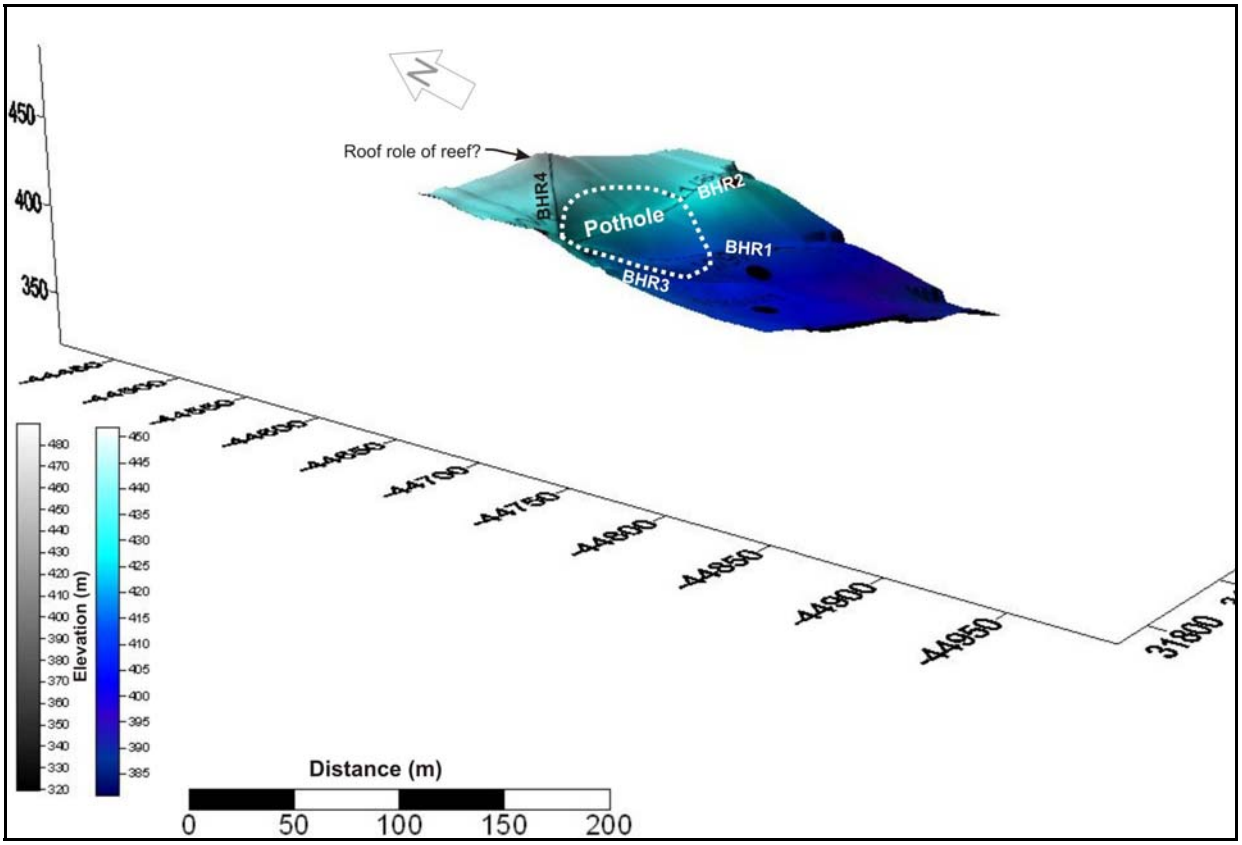

Figure 34: The surface produced by gridding the XYZ-coordinates from the borehole radar modelling, with the positions of the imaged pothole indicated

6 COST-BENEFIT ANALYSIS

6.1 Introduction

Advance knowledge of the reef topography ahead of mining should lead to increased profitability to the mine as a result of reducing the geological risk associated with features such as potholes, faulting, dykes and reef replacement due to iron-rich ultramafic pegmatites (IRUPs). Safety issues associated with the aforementioned geological features can also be negated if the features are known before they are encountered.

Currently, information about the reef is obtained through surface and cover drilling and mapping the reef surface while developing raises and stopes. Both drilling and excavating tunnels are expensive practices. Any way to reduce unnecessary drilling and/or development would imply a cost saving to the mine. The cost-benefit analysis described in this section aims to prove that the use of borehole radar can minimise wasted development and improve efficiencies throughout the mining cycle.

While exploiting an ore body there are various phases through which the mining cycle progresses, namely:

- Ore body definition.
- Mine design.
- Development.
- Extraction.
- Processing.

The effect of applying borehole radar is described in the following sub-sections as it relates to each of the abovementioned mining stages. Where possible, an attempt is made to quantify the cost benefit that borehole radar provides.

6.2 Assumptions

6.2.1 Definition of borehole radar coverage and delineation

The aerial coverage provided by the borehole radar surveys, through the extrapolation of the illumination lines produced by the borehole radar surveys, is shown in Figure 35A. The area covered by borehole radar is calculated to be: 15,231 m².

In Figure 35B, the area covered by the pothole delineated by the borehole radar surveys is schematically illustrated. The area of the pothole was defined in the software package Surfer and measured to be 3,927 m².

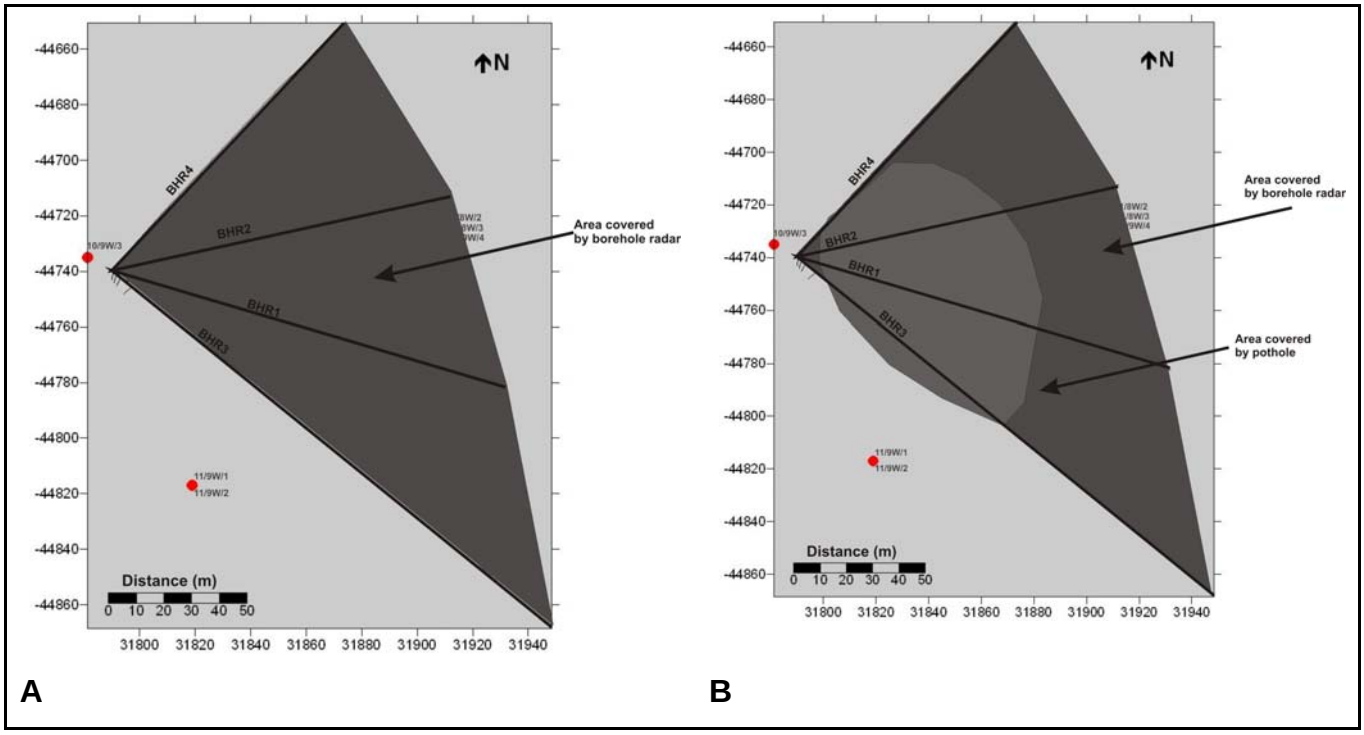

Figure 35: Schematic representation of A) the area covered by borehole radar, and B) the area covered by the pothole defined by borehole radar

6.2.2 Values used in cost-benefit analysis

6.2.2.1 Platinum Price

The daily London platinum prices for 2006 are shown in Figure 36.

The average platinum price for 2006, as defined in Platinum 2007, is used: US$1,141.84

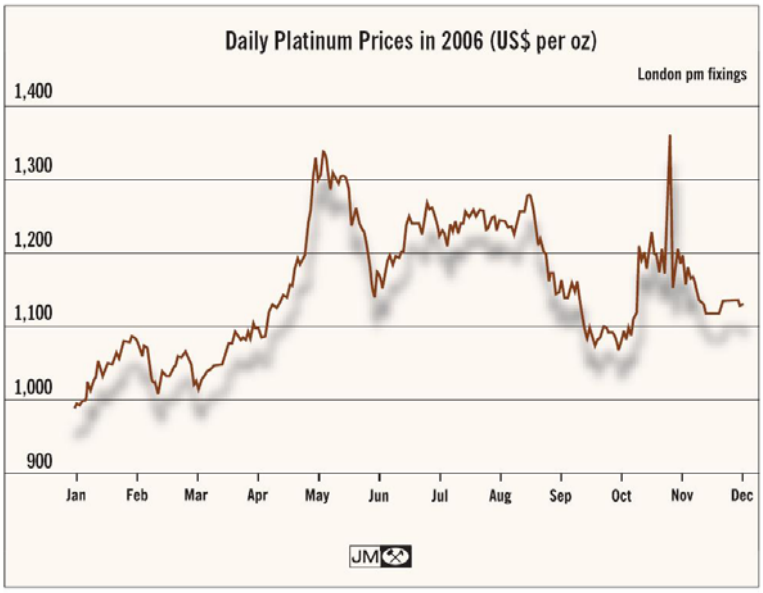

Figure 36: Daily platinum prices in 2006, given in US$, after Platinum 2007

6.2.2.2 Platinum grade

As stated earlier in this treatise, a fixed platinum grade is used for all the financial calculations in this treatise. The platinum grade used for the Merensky Reef at Amandelbult is 6.26 g/t. (Anglo Platinum Annual Report 2006).

For this treatise only the platinum values are used for calculation. The other PGE-metals are not considered.

6.2.2.3 Rand/dollar exchange rate

The average monthly rand/US dollar currency rates for 2006 as provided by www.gocurrency.com are shown in Figure 37.

The exchange rate used in this treatise is the annual average: 6.73.

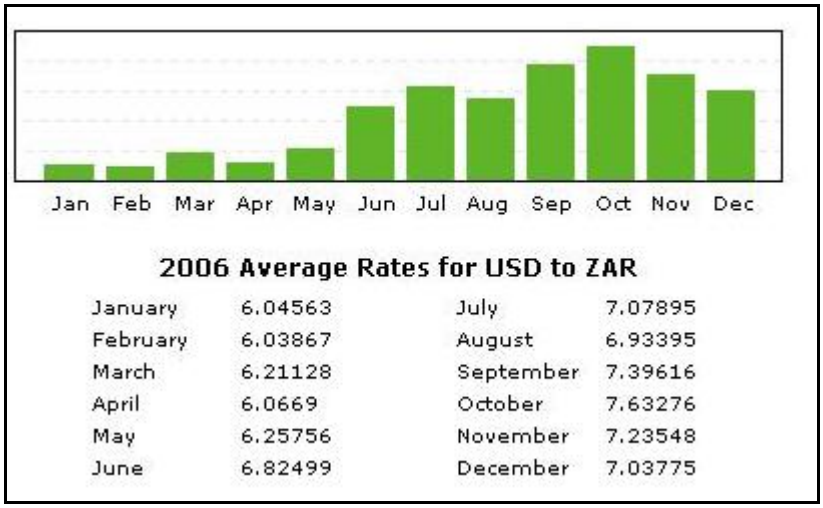

Figure 37: Average 2006 rand/US dollar exchange rate (www.gocurrency.com)

6.2.2.4 Reef thickness

A constant reef thickness of 1 m is used for all the financial calculations in this treatise.

6.2.2.5 Density

A density value of 3.4 t/m³ is used in this treatise.

6.3 Ore body definition

The relationship between mineral resources and mineral reserves as outlined in the SAMREC code (2000) is shown in Figure 38. As confidence in the geoscientific knowledge increases, mineral resources are upgraded from "inferred" to "indicated" and finally to "measured". When further modifying factors relating to the mining, metallurgical processing, economic characteristics, marketing potential, legal implications, environmental impact and governmental factors concerning the ore body are taken into consideration, mineral resources become mineral reserves, which can either be "probable" or "proved".

Borehole radar is a geoscientific method that can be used to increase the level of geoscientific knowledge and therefore improve the confidence in the geological

model. Borehole radar can be used in the process of converting resources to reserves or it can upgrade the status of either of these two classifications.

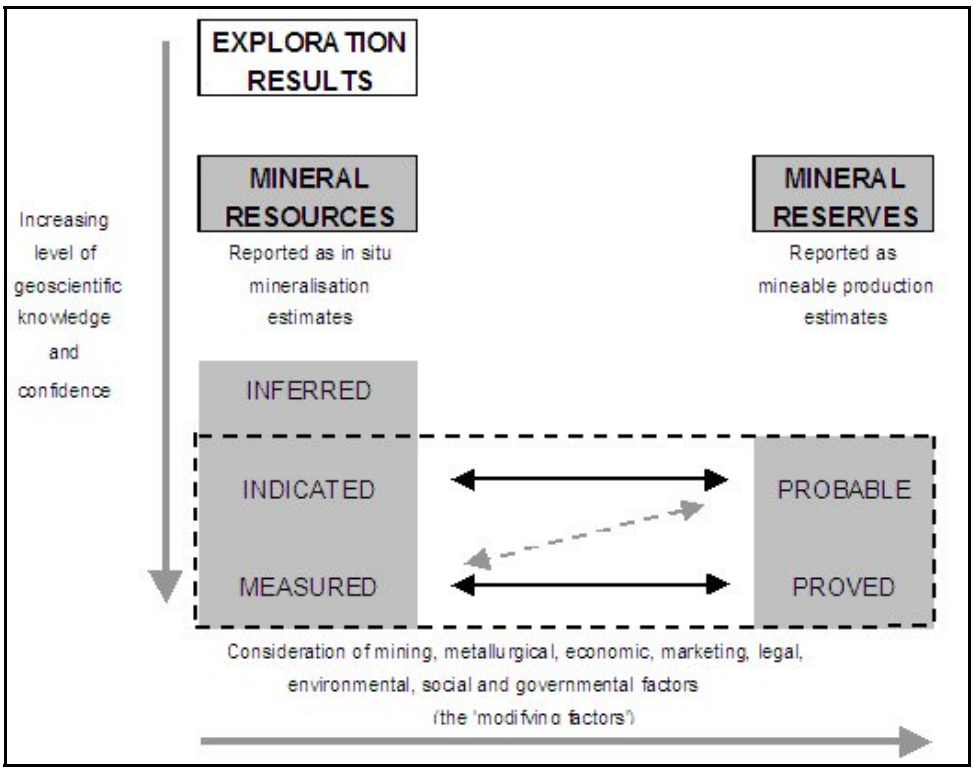

Figure 38: Mineral reserves and resources according to the SAMREC code (2000)

6.3.1 Geological drilling

The case study in Section 5 of this treatise describes how borehole radar was used to image the Merensky Reef within a mining block at Amandelbult Section. Prior to conducting borehole radar, 10 vertical geological boreholes were drilled within the block covered by the borehole radar survey. The positions of these boreholes are given in Figure 39. Due to the complexity of the reef topography in this part of the mine, a number of holes were drilled from similar positions in order to get clarity on how the reef topography was changing. In Figure 39, it can be observed how geological boreholes 11/8W1, 11/8W2, 11/8W3, 11/8W4 and 11/8W5 were drilled within 5 m of each other in order to determine the position of the Merensky Reef. The boreholes located along the straight line running from south-west to north-east were drilled upwards from development on the next lower level (11-Level).

As seen in Table 3, the total amount of geological drilling, prior to borehole radar, up to the bottom Merensky Reef contact adds up to 457 m. At an average cost of R300/m, the total cost of drilling geological boreholes to determine the position of the bottom Merensky Reef contact was R137,000.

In this study, the cost to assay the geological borehole core is not considered. This study focuses on defining the position of the Merensky Reef with the defined block, and not the grade.

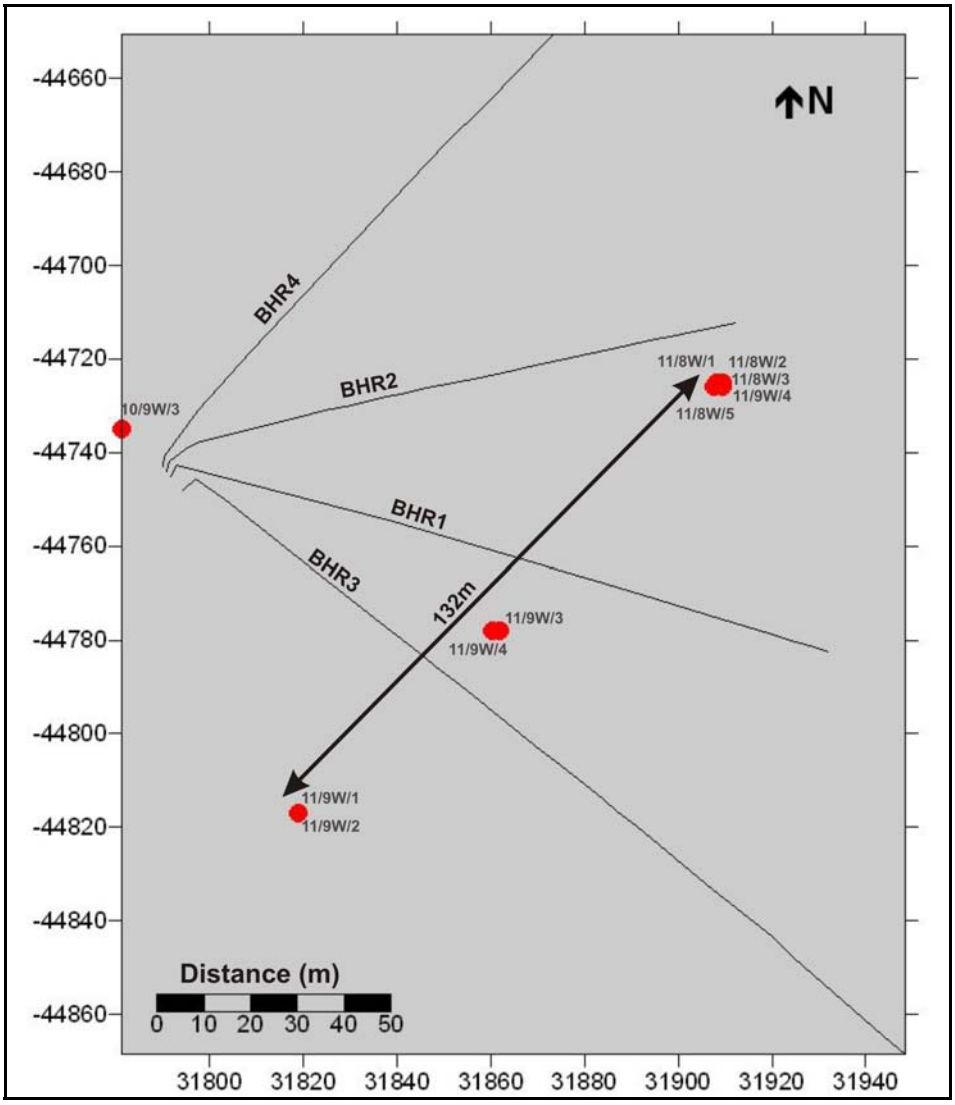

Figure 39: A map showing the area covered by the four borehole radar boreholes, indicating the positions of geological boreholes drilled prior to the borehole radar survey

Table 3: Geological boreholes in the area covered by the borehole radar surveys. The distance from the borehole collar to the bottom Merensky Reef contact is shown in the last column.

Borehole No:	X Collar	Y Collar	Z (Mer)	Merensky Bottom
10/9W/3	-44735.0000	31781.4000	436.0700	2.32
11/8W/1	-44725.5000	31908.0000	413.4400	36.44
11/8W/2	-44726.0000	31909.5000	473.0700	96.07
11/8W/3	-44726.0000	31907.5000	462.0700	85.07
11/8W/4	-44725.0000	31908.0000	436.3100	59.31
11/8W/5	-44725.0000	31909.5000	420.6400	43.64
11/9W/1	-44817.0000	31819.0000	405.1000	29.10
11/9W/2	-44816.5000	31818.5000	412.1200	36.12
11/9W/3	-44778.0000	31862.0000	405.9700	29.47
11/9W/4	-44778.0000	31860.4000	415.7900	39.29
			Total	456.83

Effectively, due to boreholes being drilled from similar positions, only three geological borehole positions along a straight line (approximately 132 m in length) were drilled to intersect the bottom contact of the Merensky Reef. From these boreholes an estimate of the Merensky Reef position could be made at three points along this line.

6.3.2 Borehole radar along a single line

If one borehole was drilled parallel to the Merensky Reef contact along this 132 m-long line, the cost of a borehole radar survey in that hole would be:

Drilling of hole (R300/m): R39,600

Directional survey: R3,000

Borehole radar survey: R44,000

Total: R86,600.

The borehole radar survey will give a continuous line of Merensky Reef coordinates below this theoretical borehole.

6.3.3 Geological intersect drilling vs. borehole radar

Cost of drilling geological boreholes: R137,000

Cost of one borehole radar survey in hypothetical borehole: R86,600

For 1.6 times less the cost of drilling clusters of geological boreholes at three points along an imaginary line, a borehole radar survey conducted from a borehole along this theoretical line will yield continuous reef elevation positions all along the line as opposed to reef intersections at three points. It is clear that the level of geological confidence acquired from reef elevation coordinates along a continuous line is much higher than only having the reef intersection at three points. Conducting borehole radar in a 132 m borehole will yield at the very least 44 illumination line coordinates, if the sampling interval of the trajectory survey is 3 m. In Table 4, the cost per reef elevation point is compared when geological drilling is conducted vs. applying borehole radar. It can be seen that the cost per point is 23 times smaller when using borehole radar to determine the reef elevation.

Table 4: Cost per reef elevation point for geological drilling, compared with conducting a borehole radar survey

	Points defined	Cost	Cost/point
Geological drilling	3	R137,000	R45,667
Borehole radar	44	R86,600	R1,968

This comparison did not take into account that the up-holes drilled from the lower level could not pinpoint the position of the reef.

As the geological confidence is increased, the mineral resource can be converted from “inferred” to “indicated”, which is associated with a reduction in risk when mining the ore body.

6.3.4 Borehole radar over the entire block

Four borehole radar surveys were conducted to define the mining block. The total lengths of borehole radar data collected are given in Table 5.

Table 5: Survey lengths for all four radar boreholes

Borehole	Length (m)
BHR1	147
BHR2	132
BHR3	200
BHR4	132
Total	**611**

The total cost of drilling 611 m for the borehole radar holes at a cost of R300/m is R183,300.

The total cost of applying borehole radar at commercial rates (November 2005) when all four surveys are completed during one week, i.e. mobilisation to Amandelbult, approximately 430 km from Johannesburg takes place only once: R185,000 (including VAT).

Furthermore, directional surveys at an estimated cost of R3,000 per survey are required in order to interpret the borehole radar data.

The total cost of borehole radar:

Drilling:	R183,300
Borehole radar:	R185,000
Directional surveys:	R12,000
Total cost:	**R380,300**

From Section 6.1.1, the cost of drilling geological boreholes within the survey area: R137,000.

Although applying borehole radar in the area was approximately 2.8 times more expensive than all the geological drilling done in the same area, the coverage gained by the borehole radar survey is approximately 15,231 m², as opposed to only three points/intersections spaced approximately 60 m apart along a 132 m straight line.

If the area imaged from the four borehole radar holes represents the area of Merensky Reef for that block, the value of that reef section can be calculated as follows:

Area of Merensky Reef	15,231	m^2	Defined in Section 6.2.1
Average thickness of reef	1	m	
Volume of reef	15,231	m^3	
SG	3.4	t/m^3	
Tonnes of reef	51,785.4	t	
Average grade/tonne (Pt)	6.26	g/t	Anglo Platinum Annual Report (2006)
Grams of Pt in situ	324,176.604	g	
Grams in a troy ounce	31.1		
Ounces of Pt in situ	10,423.68502	$	
Average Pt price (2006)	1,141.84	$	Platinum 2007
Value of Pt in situ	11,902,180.5	$	
Average R/$ exchange (2006)	6.73		www.gocurrency.com
Rand value of Pt in situ	80,101,674.76	R	

If we take the rand value of the platinum in the Merensky Reef (R80,101,674.76) and compare it with the price of applying borehole radar for that mining block (R380,300), we can see that for 0.47% of the value of the in situ reef, the geological confidence in the mining block can be significantly increased.

Expressed differently: if the cost of borehole radar is calculated per tonne of Merensky Reef, it can be shown that to delineate 51,785 t of reef with borehole radar will cost R380,300, i.e. R7.34 per tonne. Compared with an average production cost of R380/t (De Jager, *pers comm*) for producing one tonne of platinum at Amandelbult Section, borehole radar makes out 1.9% of the total production cost.

The cost of applying borehole radar in relation to the in situ value of the platinum as well as in relation to the total production cost for the defined area is represented with pie charts in Figure 40.

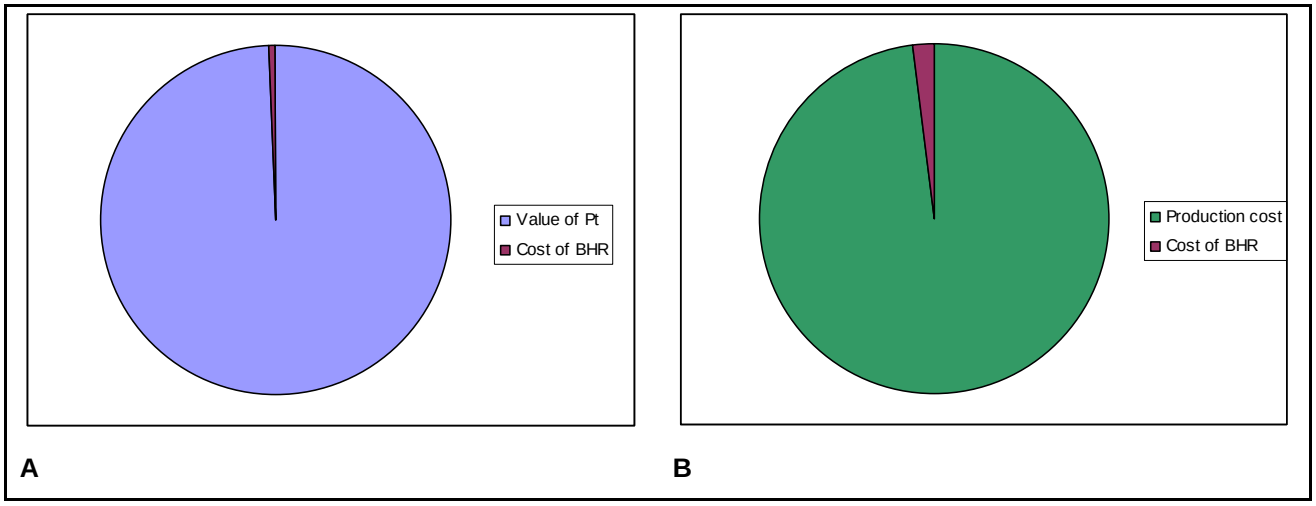

Figure 40: Cost of borehole radar compared with A) the value of the in situ platinum in block delineated by borehole radar and B) the production cost per tonne of platinum

6.3.5 Geostatistical increase in confidence

It was attempted to define the increase in confidence levels for the elevation of the Merensky Reef in the mining block by conducting geostatistical calculations for two scenarios within the Amandelbult mining block.

These scenarios were:

- Using only the available geological drill holes within the block.
- Using the illumination line coordinates from the borehole radar surveys conducted within the block.

6.3.5.1 Scenario 1

Confidence in the reef elevation within the mining block using only the initial geological boreholes

In Scenario 1, 10 geological drill holes were available for geostatistical analysis. The parameter analysed was the elevation (z) of the Merensky Reef measured in metres.

The position of these geological drill holes are shown in Figure 17.

Using the software program Geoeas, standard statistical parameters were calculated:

n:	10 (number of points)
Mean ($\bar{g}$):	428 m
Median:	418.5 m

Standard deviation (s): 23.56 m

Since the mean and median were similar, a normal distribution was assumed for further calculations. Since there were fewer than 10 data points, the following equation was used to calculate confidence levels:

$$\mu - 1.833\frac{s}{\sqrt{n}} < \bar{g} < \mu + 1.833\frac{s}{\sqrt{n}} \quad (2)\ \text{(Clarke, 2000)}$$

In this treatise, the 90% confidence level is used for consistency.

Using equation (2), it can be deducted that the analyst can be 90% sure that the mean of this dataset is between 414 m and 442 m. The confidence range is 28 m.

This means that the elevation of the Merensky Reef within the area defined by the borehole radar boreholes can be estimated with an error of up to 28 m, if only the elevation information from the 10 geological boreholes is used.

6.3.5.2 Scenario 2

Confidence in the reef elevation using the borehole radar illumination line coordinates

In Scenario 2, all the illumination line coordinates produced for radar boreholes 1 to 4 were used for geostatistical analysis. The modelling both in the dip and strike direction was considered. A total of 716 elevation points were generated in the mining block using illumination line forward modelling.

Using the software program Geoeas, various statistical parameters were calculated:

n: 716 (number of points)

Mean ($\bar{g}$): 416 m

Median: 415 m

Standard deviation (σ): 16.33 m

It stands to reason that the increase in data points will improve the level of confidence at which the mean can be calculated.

Since there were more than 25 data points, the following equation was used to determine the confidence levels:

$$\mu - 1.645\frac{\sigma}{\sqrt{n}} < \bar{g} < \mu + 1.645\frac{\sigma}{\sqrt{n}} \quad (3)\ \text{(Clarke, 2000)}$$

Using equation (3), it follows that the analyst can be 90% sure that the mean of this dataset is between 415 m and 417 m, i.e. the confidence range is 2 m.

This means that the elevation of the Merensky Reef can be estimated at a much higher accuracy than using only the geological drilling within the mining block. The confidence range has improved from 28 m to 2 m, a 14-fold improvement.

Therefore, if borehole radar is used to delineate a mining block, the reef elevation can be determined with much more confidence than relying on geological borehole intersections alone.

6.3.5.3 Discussion

Using basic geostatistical equations, it can be concluded that the application of borehole radar in the mining block has significantly improved the level of confidence in the position of the Merensky Reef.

Stated differently, to achieve the same level of confidence as provided by borehole radar, 716 vertical geological boreholes would have been required.

The average length of the geological boreholes used in the mining block to intersect the Merensky Reef was 46 m (using values in Table 3). If 716 of these boreholes were drilled at a drilling cost of R300/m, the total cost would be 716 x 46 x 300m = R9,880,800.

The same level of confidence was achieved with four borehole radar surveys at a cost of R380,300, i.e. 3.84% of the cost of drilling 716 geological boreholes.

6.4 Mine design

Mine design and mine development are very closely related. In this section it is shown that the area that is to be developed is sampled better if borehole radar is applied prior to development as opposed to only using geological boreholes to fix the position of

the reef. If the position of the ore body ahead of mining can be determined accurately, the mine design can be fixed and mining can continue unhindered, without any surprises.

6.4.1 Area of Merensky Reef sampled with standard geological drilling

At Amandelbult Section, it is currently normal practice to drill three vertical boreholes per planned cross-cut spacing, i.e. approximately three boreholes per 200 m of haulage development (Figure 41).

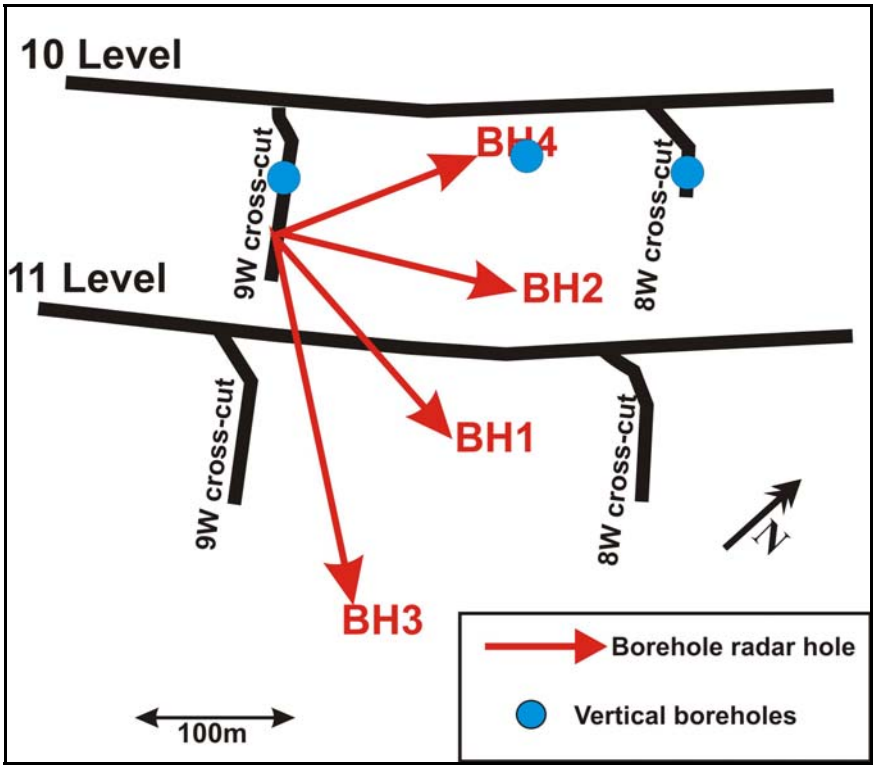

Figure 41: Borehole radar survey layout indicating vertical boreholes meant to "cover" mining block between 9W and 8W crosscut on 10-Level

Approximately 100 m of reef intersection (vertical) drilling is completed in one month to cover the position of cross-cuts and raises. If a drilling cost of R300/m is used, this equates to R30,000 of drilling per month to ensure that development is placed optimally to extract the ore body, and this is assuming that the geology is not complex, i.e. no additional drilling is required to pinpoint the position of the reef.

For R30,000 three pierce points through the Merensky Reef are obtained along a 200 m line defined by the haulage position.

The mine planner can now be confident that the position of the Merensky Reef is fixed where the boreholes pierce the reef. Exploratory underground geological boreholes are drilled with AXT drill bits. These drill bits have a diameter of 48 mm (Heinz, 1994). Since these are vertical up-holes, they intersect the reef plane with a circular shape, i.e. the positions of three circular pieces of reef within the reef plane are known. The area of each piece is:

$A = \pi r^2 = \pi (0.024)^2 = 0.0018 \text{ m}^2$

Area of Merensky Reef sampled: 0.0054 m² (3 x AXT size boreholes)

6.4.2 Area of Merensky Reef sampled using borehole radar

The horizontal resolution of a radar instrument is defined by the size of its first Fresnel zone (Vogt, 2003). The radius of the first Fresnel zone is defined by the distance of the radar antenna from the target horizon as seen in Figure 42.

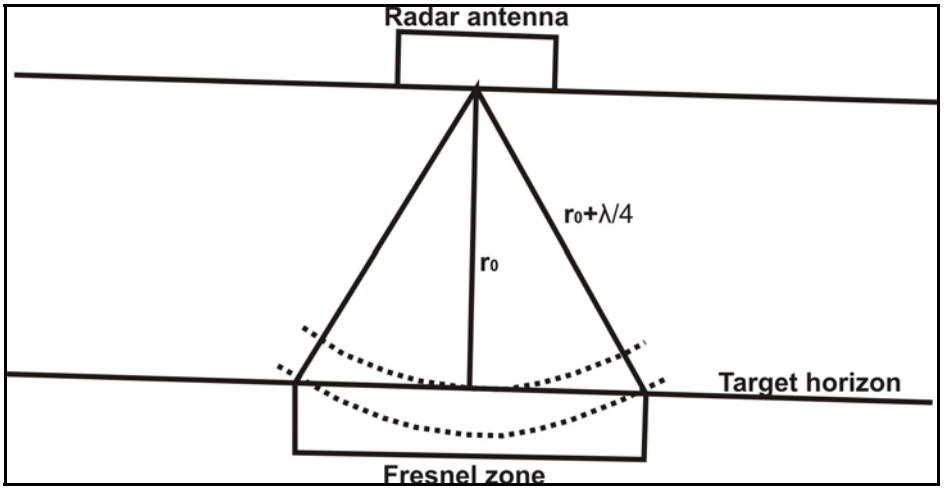

Figure 42: The first Fresnel zone (Vogt 2003)

Radar information about the reflective surface is gathered from an area below the boreholes of the Amandelbult case study as defined by the following equation:

$$R_F = \sqrt{\lambda r_0 + \tfrac{1}{4}\lambda^2} \qquad (4) \qquad \text{(Vogt, 2003)}$$

Equation (4) defines the radius of the first Fresnel zone.

The areas from which radar data are gathered for each of the Amandelbult radar boreholes are shown in Figure 43. This figure shows that borehole radar effectively samples 474 m² + 528 m² + 528 m² + 800 m² = 2,330 m² of the mining block.

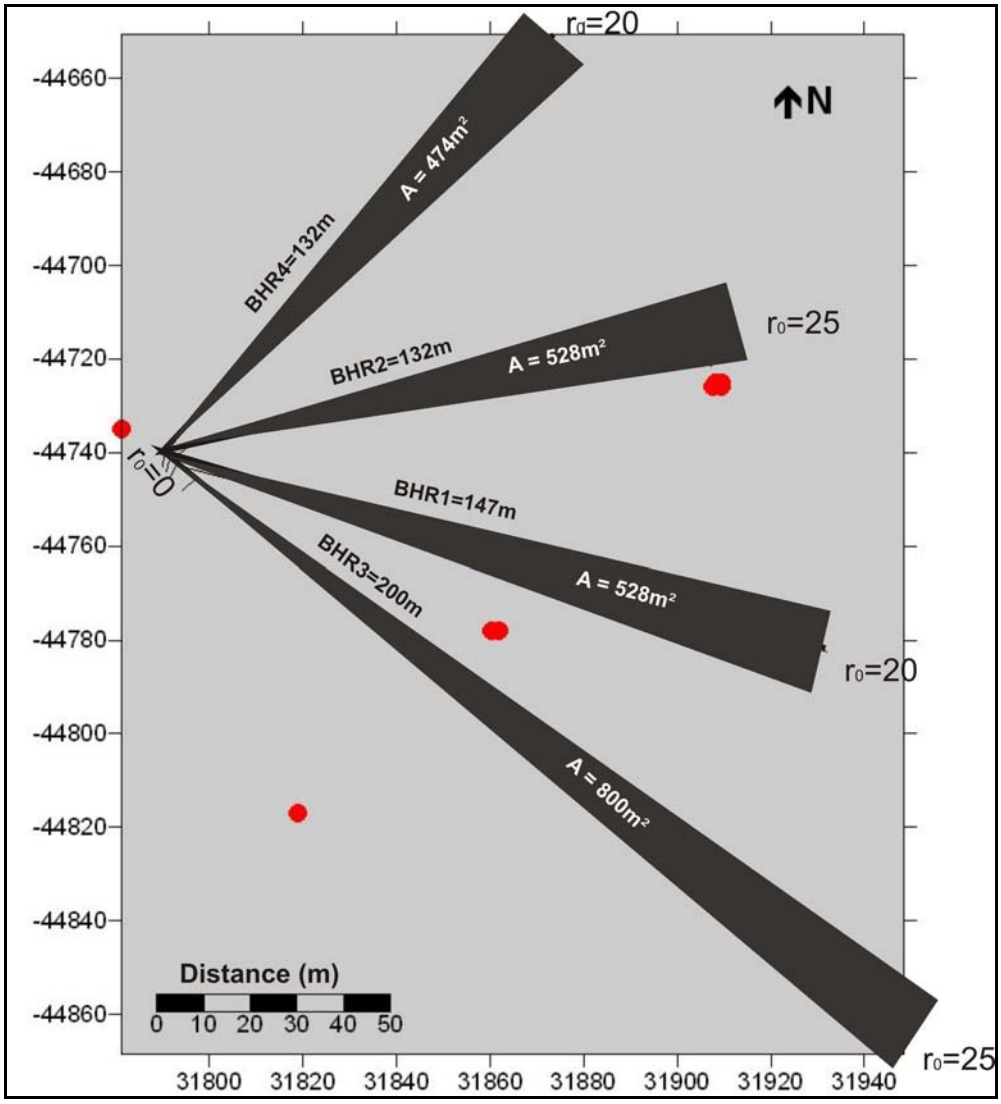

Figure 43: The areas from which borehole radar data is gathered for boreholes 1 to 4

6.4.3 Discussion

When standard geological drilling is done at regular intervals down the haulage to get an idea of the block that is to be mined into, the position of the Merensky Reef is known over an area of 0.0054 m² at a cost of R30,000, i.e. R5,600,000 per m².
Using standard geological drilling, 0.00035% of the 15,231 m² mining block is sampled.

When borehole radar is applied from four boreholes drilled sub-parallel to the target surface, an area of 2,330 m² is sampled at a cost of R380,300, i.e. R163 per m².
Using borehole radar, 15.3% of the 15,231 m² mining block is sampled.

Borehole radar increases the sampling area 431,481 times over standard geological drilling at a significantly reduced cost (Figure 44). It is clear that the application of borehole radar prior to mining significantly increases the knowledge about the ore body prior to mining. A much larger area of the area to be mined is sampled and if the cost of this sampling is compared with standard geological drilling conducted to "cover" the position of the Merensky Reef within the mining block, it can be seen that borehole radar is also significantly cheaper.

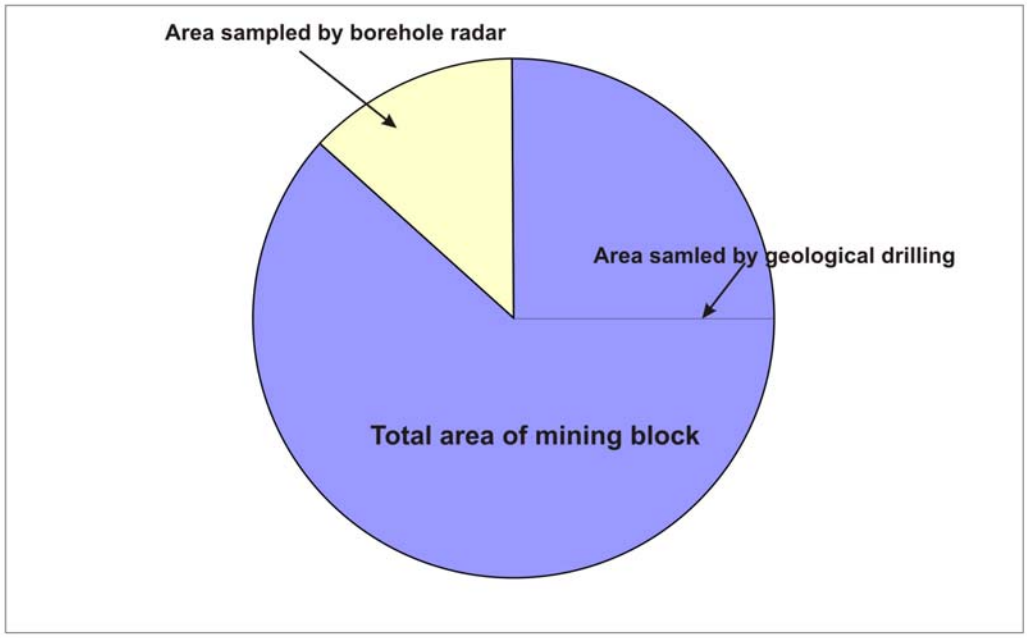

Figure 44: Increase in sampling area if borehole radar is conducted

6.5 Development

The conventional mining layout is used at Amandelbult Section (shown in Figure 15). Development takes place in three ways:

1. Secondary development

   Footwall haulages, developed on strike at a constant distance below the reef plane.

   Cross-cuts, developed horizontally to intersect the reef plane.

2. Primary development

   Raises developed in the reef plane.

3. Ancillary development

   Other development such as travelling ways, ore passes, timber pays, drilling cubbies et cetera.

In Section 4.3.2 (Figure 16), the conventional mining progression within a mining block is described. From opposite raise lines, mining proceeds in panels until a natural dip pillar is left for support in the centre of the block.

Once the raises have been developed, the reef between two neighbouring raises is extracted or stoped. Mine development is expressed as a ratio called the m^2/m ratio, where:

The m^2 refers to the area of reef that is available for mining after the necessary development is done, and the m refers to the development required to provide access to the reef.

The m^2/m ratio is affected by various factors, such as the geometry of the reef, the dip and structural complexity of the reef as well as the mining efficiencies achieved when extracting the reef. According to De Jager (*pers comm*), the m^2/m ratio should theoretically be in the vicinity of 50 m²/m, but due to the factors listed above, typical values range between of 20 m²/m and 25 m²/m.

The m^2/m ratio for the mining block imaged by borehole radar is calculated below.

Let's assume the area of reef available for mining is 15,231 m², i.e. we take the same amount of reef available for mining as imaged by borehole radar described in Section 6.2.1 (Figure 35).

If the *m²/m* ratio is taken as 25, then 609 m of development was required to make this reef available.

This case study described in Section 3 shows that borehole radar imaged a pothole in the Merensky Reef. This pothole is an elliptical feature with a long axis of approximately 100 m, a short axis of approximately 50 m and a slump of approximately 5 m. Due to the size of the slump, this elliptical area defined by the pothole is not available for mining. The area of the pothole was calculated in the mapping software as 3,927 m².

The total area available for mining is now 15,231 m² – 3,927 m² = 11,304 m².
If the presence of the pothole was unknown (i.e. borehole radar had not been applied), then the same amount of development would have taken place, i.e. 609 m.
The *m²/m* ratio would then have been 11,304/609 = 18.56 m²/m, i.e. with the same amount of development, 6.4 m² less would have been available for mining.
Converted to monetary values:

If the development cost is taken at R3,500/m (De Jager, *pers comm*):

	A	B
Development cost	609 x R3,500 =R2,131,500	609 x R3500 =R2,131,500
Reef available	15,231 m²	11,304 m²
Reef thickness	1 m²	1 m²
Reef volume	15,231 m³	11,304 m³
SG	3.4 t/m³	3.4 t/m³
Tonnes of reef	51,784.4 t	38,433.6 t
Average grade	6.26 g/t	6.26 g/t
Grams of Pt in situ	324,177 g	240,594 g
Ounces of Pt in situ	10,423 oz	7,736 oz
Average platinum price	$1141.84/oz	$1141.84/oz
$ value of Pt in situ	$11,902,181	$8,833,448
R/$ exchange (Apr 2006)	6.73	6.73
R value of Pt in situ	R80,101,675	R59,449,106

In Case A, R2,688,000 was spent on development for in situ ore worth R80,101,675, while in Case B the same amount was spent on development for in situ ore worth R20,652,569 less.

As described above, 609 m of development is required to make a potential 15,231 m² of reef available for mining. The percentage of reef affected by pothole A is 25.78%.

Development cost per metre: R3,500

Development metres at risk due to 25.78% geological loss: 157.02 m

Cost of development at risk: **R549,563**

This result relates back to the scenario described in Section 6.4, which relates to mine planning. If the position of the pothole had been known the design of the mine could have been adapted in order to minimise the amount of ore lost due to the pothole. According to Van Wyk (*pers comm*), the position of development can be adapted if the positions of disruptions to the reef plane are known. According to Van Wyk (*pers comm*), cross-cuts can be positioned up to 1 km apart if necessary.

6.6 Extraction

6.6.1 Deferred income

As described in Section 4.3.2, a pothole is considered a problem to mining if it fills up more than one-third of a mining panel. The pothole delineated by borehole radar on 10-Level 9W cross-cut, as described in Section 5.3.7, would have posed a problem to mining, since its side view at this section is approximately 100 m long. If it was mined until one-third of a panel was exposed (i.e. 12 m of the face), the following calculations can be done:

For 1 m advance at a face length of 12 m (i.e. per blast):

Area of Merensky Reef displaced	12	m²	
Average thickness of reef	1	m	
Volume of reef	12	m³	
SG	3.4	t/m³	
Tonnes of reef	40.8	t	
Average grade/tonne (Pt)	6.26	g/t	Anglo Platinum Annual Report (2006)
Grams of Pt in situ	255.408	g	
Grams in a troy ounce	31.1		
Ounces of Pt in situ	8.21	$	
Average Pt price (2006)	1,141.84	$	Platinum 2007
Value of Pt in situ	9377	$	
Average R/$ exchange (2006)	6.73		www.gocurrency.com
Rand value of Pt in situ	63,109	R	

This means that for each blast that is mined into the pothole, R63,109 of income is deferred until a later date.

6.6.2 Labour efficiency

The ore body is extracted by stoping. Stoping is carried out by mining crews. For this exercise it is assumed that there are 14 people in a mining crew.
Average cost to company per month per mining-crew employee: R8,000
Total monthly cost to company for 14-person mining crew: R112,000

Let's assume this mining crew is advancing along a panel that is 35 m wide as shown in Figure 45.

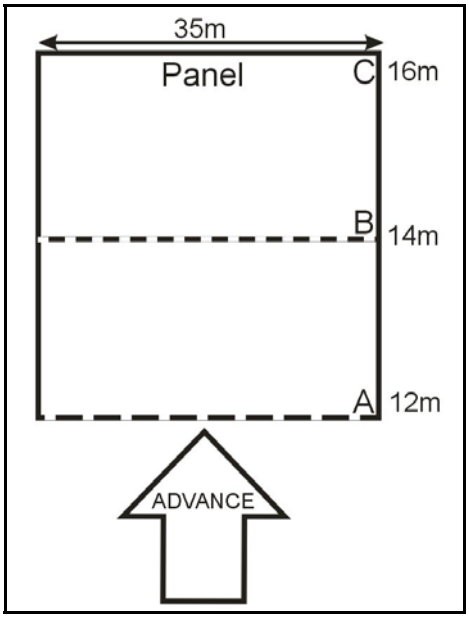

Figure 45: Hypothetical monthly advance of a mining crew along a 35 m long panel

For three cases A, B and C, the situation is as follows:

Per month:	A	B	C
Advance	12 m	14 m	16 m
Area	420 m²	490 m²	560 m²
Employee cost	R112,000	R112,000	R112,000
Employee cost/m²	R267/m²	R229/m²	R200/m²

The calculation above shows that the saving in labour due to efficiency for advancing 14 m instead of 12 m is: R267 – R229 = R38/m².
If this cost is applied to the mining block covered by borehole radar that has a surface area of 15,231 m², the saving is 15,231 m² x R38 = R578,778.

Predicted in situ value of ore in mining block: R80,101,674.76

Although the example given here is hypothetical, it serves to demonstrate that if disruptions in the ore body can be predicted using borehole radar and stope advance can be increased by as little as 2 m the mine can save 0.7% of the value of the in situ ore.

The result is that mining crews can be used more efficiently, and unnecessary development into waste rock can be prevented.

6.7 Processing

The processing of the ore extracted is directly affected by the presence of waste material. The ore is effectively diluted and waste material that displaces ore in the mill will lead to inefficiencies and a loss of revenue.

In this example it is assumed that the pothole material is mined through and reports to ore in the plant, i.e. it is not detected as waste material. According to Marais (*pers comm*), this scenario will most likely be prevented by daily monitoring of the plant head-grade, but another reason why this calculation is of importance is that if the pothole is mined through in the hope that reef will be encountered, the result is "deferred income", i.e. waste is being mined as ore and income that would have been derived from ore is being postponed until a later date.

Tonnes covered by mining block described in Section 6.5:	51,784 t
Tonnes of waste due to pothole A:	13,350 t
Cost per tonne (shaft head + overheads + concentrator):	R380
Mining cost of waste tonnes mined as ore:	**R5,073,000**

The loss of revenue due to mining through the pothole can be calculated as follows:

Tonnes milled from mining block described in Section 6.5:	51,784 t
Planned contained Pt at 6.26g/t:	10,423 ounces
Actual contained Pt (diluted 25.78%):	7,736 ounces
Lost Pt:	2,687 ounces
Lost revenue at $1,141.84/oz and exchange rate of 6.73:	**R20,648,475**

If the loss of revenue for one mining block is R20,648,475, the impact on the entire mine where waste is mined instead of ore due to unpredicted geological losses will be significant.

7 CONCLUSIONS AND RECOMMENDATIONS

7.1 Conclusions

This project aimed to provide clear evidence that incorporating borehole radar in the mining cycle will provide significant cost benefit in the long term.
This study has shown that the application of borehole radar prior to mining:

- Provides more geological information about the reef prior to mining than relying only on geological intersection of the reef.
- Can provide continuous reef coordinates along the illumination line, as opposed to the point intersections provided by geological cover drilling.
- Significantly improves the confidence in the elevation of the Merensky Reef within the mining block.
- Samples a much larger portion of the reef to be extracted than standard geological drilling at a significantly reduced cost.
- Improves mine planning and ensures that mine development is put in the correct place.
- Avoids unnecessary mine development.
- Can ensure that mining teams are deployed more effectively in areas where reef has been defined by borehole radar.
- Can prevent sending waste to the plant instead of ore.
- Can avoid deferring income until a later date.

The findings that were calculated in the previous sections are summarised in Table 6. Results are given for the scenario where only geological drilling would have been used to make mining decisions about the defined mining block, as opposed to the situation after borehole radar was applied. The broad impact of borehole radar at the various mining cycles is shown in Table 7.

Table 6: Conclusions summarised for applying only geological drilling, compared with conducting borehole radar

	Geological drilling (before borehole radar was applied)	**Borehole radar**
Number of reef elevation coordinates	4	716
Cost per reef elevation point	R45,667	R1,968
Extrapolated area covered	4 intersection points within block	15,231 m²
Confidence range (of geostatistical mean)	28 m	2 m
Actual area of reef sampled	0.0054 m²	2,330 m²
% of mining block sampled	0.00035%	15.3%
Cost per m² sampled	R5,600,000	R163
m²/m ratio	18.56	25
Expected value of in situ platinum	R80,101,675	R59,449,106
Cost of development at risk	R549,563	R0
Income deferred	R63,109 per 12 x 1 m advance	R0
Reduction in labour cost per block	R0	R578,778
Cost of processing waste as ore (or deferred income)	R20,648,475	R0

Table 7: The impact of borehole radar at the five stages of mining an ore body

	Mining stage	Impact of borehole radar
1.	Ore body definition	Increased knowledge leads to improved reserve definition and improved confidence
2.	Mine design	Improved mine planning
3.	Development	Improvement in m^2/m ratio
4.	Extraction	Improved planning and improvement of efficiencies
5.	Processing	Dilution lowered and better recoveries

7.2 Recommendations

It is recommended that:

- The borehole radar interpretation made in this treatise be reconciled with the actual situation once the area discussed is mined.
- Further work is done in order to determine how the mine layout can be optimised in order to accommodate operational borehole radar surveys.
- The impact of borehole radar on mine design is investigated further.

Borehole radar should become a routine tool with which to predict disruptions in the reef prior to mining. It is recommended that borehole radar be conducted from regularly spaced boreholes drilled from haulages, prior to developing cross-cuts. The proposed borehole layout is shown in section (Figure 46) and plan (Figure 47).

When disruptions in the reef are detected using borehole radar, the position of development can then be optimised (Figure 48).

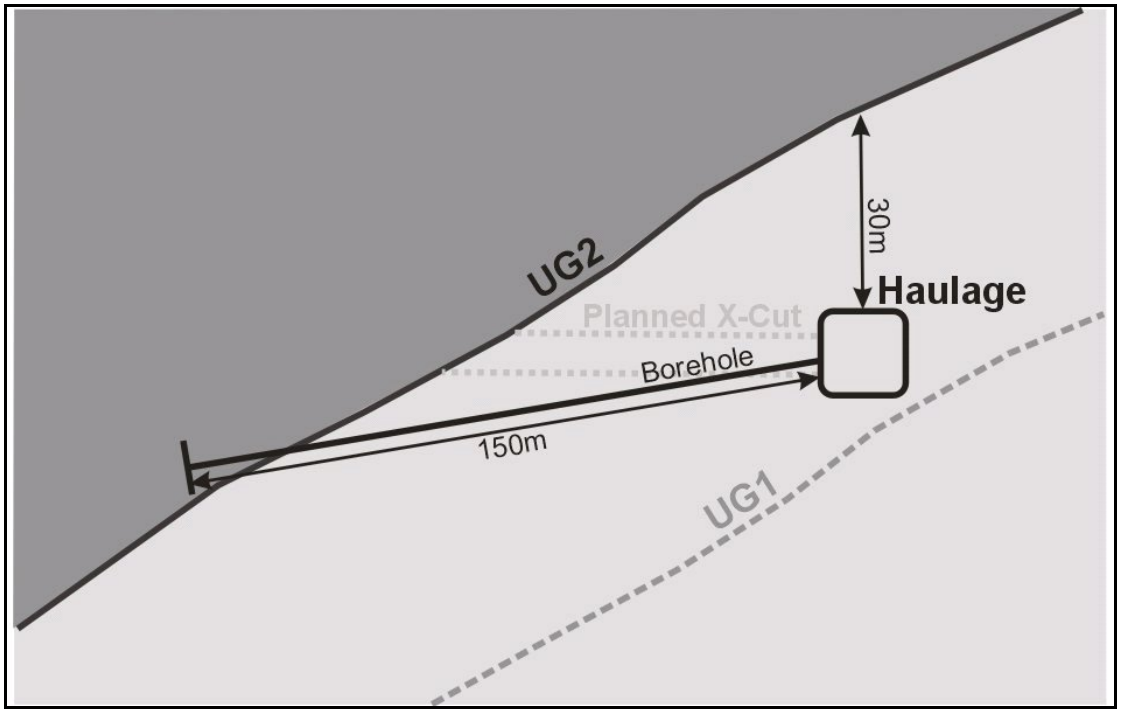

Figure 46: Proposed borehole layout in section for applying borehole radar to detect geological deviations prior to mining

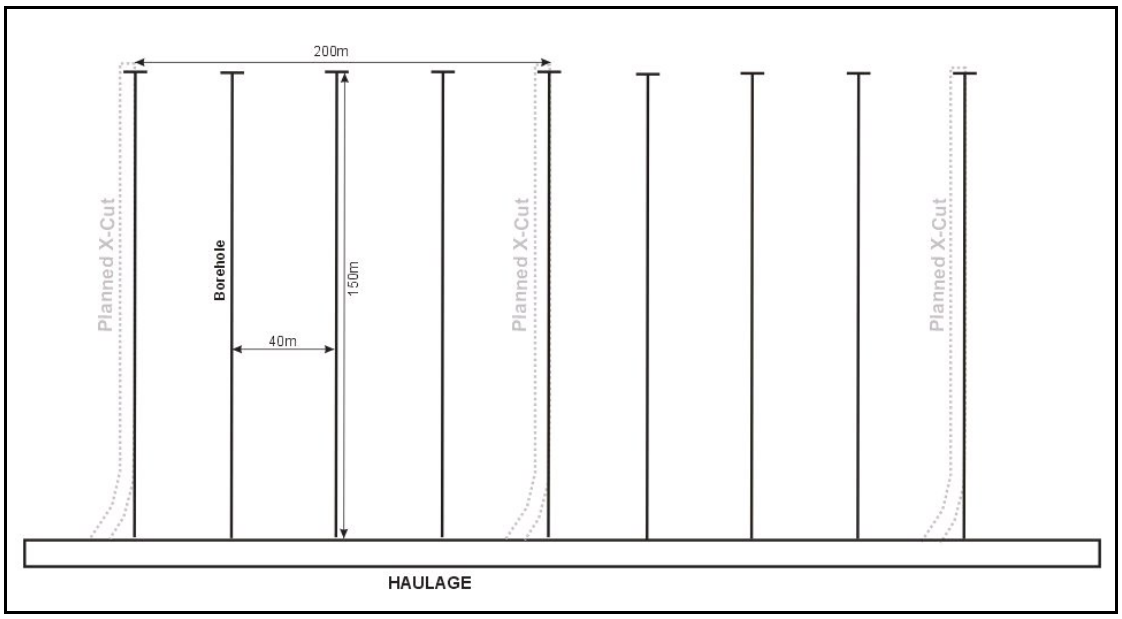

Figure 47: Proposed borehole radar layout in plan for the prediction of geological disruptions prior to mine development

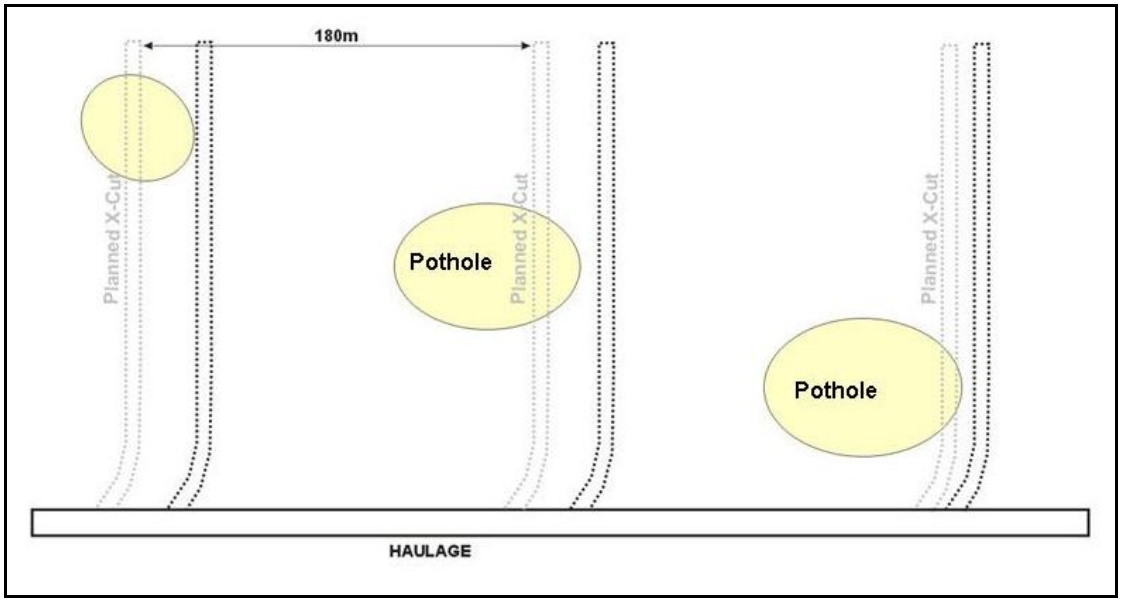

Figure 48: Optimisation of mine development after the application of borehole radar

8 ACKNOWLEDGEMENTS

The Platmine Research Collaborative is thanked for allowing this work to be published.

Declan Vogt at the CSIR, is thanked for many useful discussions and being my borehole radar guru.

Bruce Walters, Quartus Snyman and Wian Marais at Anglo Platinum are thanked for their efforts in securing the case-study site at Amandelbult Section as well as for their inputs in useful discussion relating to the results produced here.

Alan King from Anglo Technical Division is thanked for his valuable input to financial discussions and for motivating me to go the extra mile.

Andy Rompel Stompel is thanked for checking that a geophysicist is getting the geology right.

Carel de Jager from Anglo Platinum is thanked for providing the basis of the financial analysis.

Ferdi Camisani-Calzolari is thanked for teaching me the basics of geostatistics.

Prof. Hennie Theart is thanked for his inputs and suggestions, and for throwing my first draft across the room.

My family is thanked for giving me nonsense whenever I procrastinated.

My friend, “Eagle-eye” Riaan Wolmarans, is thanked for wading through a very technical piece of editing.

My friends are thanked for partying on my behalf while I was chained to my computer.

Last but by no means least, my husband, Albert Swart, is thanked for supporting me in every crazy project that I tackle.

9 REFERENCES

Anglo Platinum. (2006) Annual Report.

Carr, H.W., Groves, D.I. and Cawthorn, R.G. (1994). The importance of synmagmatic deformation of Merensky Reef potholes in the Bushveld Complex, *Economic Geology*, **89**, 1398 – 1410.

Cawthorn, R.G. (1999). The platinum and palladium resources of the Bushveld Complex, *South African Journal of Science,* **95**, 481 – 489.

Chalke, B.L., Chalke, T. and Rompel, A.K.K. (2006) Paardekraal #2 Mine Expansion Project, PDL 159 Geotechnical Interpretation Report. Internal Anglo Technical Division Report Number 15/173/141/2006/158, 51pp.

Clarke, I. and Harper, W.V. (2000) Practical Geostatistics 2000, Ecosse North America Llc, Columbus, Ohio, USA. 342pp.

Daniels, J.D. (2004) Ground Penetrating Radar, 2nd Edition. The Institution of Electrical Engineers, London.

De Jager, C. (2006) Principal Mining Economist, Mining Economics, Anglo Technical Division, *Personal Communication*.

De Vries, P. and Du Pisani, P. (2005) Borehole radar delineation of the UG2 Reef at Modikwa Mine. *9th SAGA Biennial Technical Meeting and Exhibition*. September 2005. Cape Town.

Du Pisani, P. and Vogt, D. (2003) Radar frequency electrical properties of rocks associated with the VCR, UG2 and Merensky ore bodies. *8th SAGA Biennial Technical Meeting and Exhibition*. September 2003. Pilanesberg.

Du Pisani, P. and Vogt, D. (2004) Borehole radar delineation of the Ventersdorp Contact Reef in Three Dimensions. *Exploration Geophysics*. **35**, 319 – 323.

Du Plessis, A. and Kleywegt, R.J. (1987) A dipping sheet model for the mafic lobes of the Bushveld Complex. *South African Journal of Geology*. **90**, 1 – 6.

Eales, H.V., Botha, W.J., Hattingh, P.J., De Klerk, W.J., Maier, W.D. and Odgers, A.T.R. (1993) The mafic rocks of the Bushveld Complex: a review of emplacement and crystallization history, and mineralization, in light of recent data. *Journal of African Earth Science.* **16**, 121 – 142.

Eales, H.V. and Cawthorn, R.G. (1996) The Bushveld Complex. In: Cawthorn, R.G. (Ed.), Layered Intrusions. Elsevier, Amsterdam, 181 – 230.

Farquar, J. (1986) The Western Platinum Mine. In: Anhaeusser, C.R. and Maske, S. (Eds.), Mineral Deposits of Southern Africa. Geological Society of South Africa. Johannesburg, South Africa, **II**, 1135 – 1142.

Heinz, W.F. (1994) Diamond Drilling Handbook 3rd Edition. W.F. Heinz, Halfway House.

Irvine, T.N. (1982) Terminology for layered intrusions. *Journal of Petrology*. **23**, 127 – 162.

Kinloch, E.D. and Peyerl, W. (1990) Platinum-group minerals in various rock types of the Merensky Reef: genetic implications. *Economic Geology*. **85**, 537 – 555.

Kruger, F.J. (1990) The stratigraphy of the Bushveld Complex: a reappraisal and the relocation of the Main Zone boundaries. *South African Journal of Geology*. **94**, 376 – 381.

Leeb Du Toit, A. (1986). The Impala Platinum Mines. In: Anhaeusser, C. R. and Maske, S (Eds.), Mineral Deposits of Southern Africa. Geological Society of South Africa. Johannesburg, South Africa, **II**, 1091 – 1106.

Marais, W. (2007) Senior Geologist, Central Functions, Anglo Platinum Rustenburg Section. *Personal communication.*

Noon, D.A., Stickley, G.F., and Longstaff, D. (1998). A frequency independent characterisation of GPR penetration and resolution performance. *Journal of Applied Geophysics*. **40**, 127 – 137.

Platinum 2007 (2007). Johnson Matthey, Hertfordshyre, England. 56pp.

SAMREC Code. (2000) South African code for reporting of mineral resources and mineral reserves (the SAMREC code) – Prepared by the South African mineral resource committee (SAMREC) under the auspices of the SAIMM. Effective March 2000, SAIMM, Johannesburg, South Africa, 39pp.

Schürmann, L.W. (1991) The geochemistry and petrology of the upper critical zone of the Boshoek section of the western Bushveld Complex. *Bulletin of the Geological Survey of South Africa*. **113**, 88pp.

Simmat, C. M., Osman, N., Hargreaves., Mason, I. M., (2002) Borehole radar imaging from deviating boreholes: *Ninth International Conference on Ground Penetrating Radar*, S.K. Koppenjan, H. Lee, (Eds.), Proceedings of SPIE. **4758**, 404 – 409.

Turner, G., Mason, I., Hargreaves J., and Wellington, A. (2000) Borehole radar surveying for orebody delineation: *Eighth International Conference on Ground Penetrating Radar*, D.A. Noon., G.F. Stickley, D. Longstaff, (Eds.), Proceedings of SPIE. **4084**, 282 – 287.

Turner, G. and Siggins, A.F. (1994) Constant Q attenuation of subsurface radar pulses. *Geophysics*. **59**. 1192 – 1200.

Unknown. (1986) A Guide to the Geology of Amandelbult, based on Anhaeusser and Maske, 1986.

Van Wyk, A. (2006) Production Manager, Amandelbult 1-Shaft. *Personal communication*.

Viljoen, M.J. (1994) A review of regional variations in facies and grade distribution of the Merensky Reef, Western Bushveld Complex, with some mining implications. *Proceedings of the 15th CMMI Congress*. South African Institute of Mining and Metallurgy, 183 – 194.

Viljoen, M.J. (1999) The nature and origin of the Merensky Reef of the Western Bushveld Complex based on geological facies and geophysical data. *South African Journal of Geology*. **102**. 221 – 239.

Viljoen, M.J. and Hieber, R.W. (1986) The Rustenburg Section of Rustenburg Platinum Mines Limited, with reference to the Merensky Reef. In: Anhaeusser, C.R. and Maske, S. (Eds), Mineral Deposits of Southern Africa. Geological Society of South Africa Johannesburg, South Africa, **II**. 1107 – 1134.

Viljoen, M.J. and Schürmann, L.W. (1998) Platinum Group Metals. In: Wilson, M.G.C. and Annhaeusser, C.R. (Eds.), The Mineral Resources of South Africa. Council for Geoscience, South Africa, Pretoria, 532 – 568.

Viljoen, M.J., De Klerk, W.J., Coetzer., Hatch, N.P., Kinloch, E.D. and Peyerl, W. (1986a) The Union Section of Rustenburg Platinum Mines Limited, with reference to the Merensky Reef. In: Anhaeusser, C.R. and Maske, S. (Eds.), Mineral Deposits of Southern Africa. Geological Society of South Africa, Johannesburg, South Africa, **II**. 1061 – 1190.

Viljoen, M.J., Theron, J., Underwood, B., Walters, B.M., Weaver, J. and Peyerl, W. (1986b) The Amandelbult Section of Rustenburg Platinum Mines Limited, with reference to the Merensky Reef. In. Anhaeusser, C.R. and Maske, S. (Eds), Mineral Deposits of Southern Africa. Geological Society of South Africa Johannesburg, South Africa, **II**. 1041 – 1060.

Vogt, D. (2000) The modelling and design of Radio Tomography antennas: D.Phil. Thesis, University of York.

Vogt, D. (2002) A Slimline Borehole Radar for In-Mine Use. *9th International Conference on Ground Penetrating Radar*, Proceedings of SPIE, **5758**, 31 – 36.

Vogt, D. (2003) An introduction to Ground Penetrating Radar. Course notes for geophysicists. Wits University. CSIR Miningtek. Johannesburg.

Vogt, D., Van Schoor, M. and Du Pisani, P. (2005) The application of radar techniques for in-mine feature mapping in the Bushveld Complex of South Africa. *The Journal of the South African Institute of Mining and Metallurgy*. **105**. 391 – 399.

Vogt, D. (2006) A borehole radar system for South African gold and platinum mines. *South African Journal of Geology*. **109**. 521 – 528.

Vogt, D. (2007) Competency Area Manager, Mining, Department of Natural Resources and the Environment, CSIR, *Personal communication*.

Wagner, P.A. (1929) The Platinum Deposits and Mines of South Africa. Oliver and Boyd, Edinburgh, Scotland, 326pp.

www.gocurrency.com, [Web page]: accessed 17 September 2007.

www.platmine.co.za, [Web page]: accessed 9 July 2006.

www.platinummetalsreview.com, [Web page]: accessed 12 July 2007.

APPENDIX A BOREHOLE INFORMATION

Rock and stratigraphy codes

Code	Explanation
BR	Bastard Reef
COL	Collar
DYK	Dyke
EOH	End of hole
FERPL	Iron replacement
FRAC	Fracture
FRZONE	Fracture zone
FWM	Footwall marker
LN	Leuco-norite
MESN	Meso-norite
MN	Mela-norite
POIKFPYX	Poikilitic Feldspathic Pyroxenite
POIKPYX	Poikilitic Pyroxenite
SHR	Shear

Borehole information for borehole 1

BHID	FROM	TO	X	Y	Z	ROCK
10/9W/BHR1 D0	0	0	31791.8	-44745.2	432.665	COL
10/9W/BHR1 D0	0	1.43	31792.02	-44744.4	432.543	POIKFPYX
10/9W/BHR1 D0	1.43	1.44	31792.3	-44743.8	432.4282	SF
10/9W/BHR1 D0	1.44	1.68	31792.35	-44743.6	432.4091	POIKFPYX
10/9W/BHR1 D0	1.68	2.06	31792.5	-44743.4	432.3627	MN
10/9W/BHR1 D0	2.06	2.07	31792.59	-44743.3	432.3341	SF
10/9W/BHR1 D0	2.07	3.91	31793.12	-44742.7	432.2047	MN
10/9W/BHR1 D0	3.91	98.7	31839.2	-44754.7	428.3869	MESN
10/9W/BHR1 D0	98.7	98.91	31884.71	-44768.2	426.4627	LN
10/9W/BHR1 D0	98.91	102.79	31886.67	-44768.7	426.4267	POIKAN
10/9W/BHR1 D0	102.79	103.3	31888.78	-44769.4	426.3924	LN
10/9W/BHR1 D0	103.3	104.92	31889.8	-44769.7	426.3781	POIKAN
10/9W/BHR1 D0	104.92	105.6	31890.9	-44770	426.3646	LN
10/9W/BHR1 D0	105.6	114.8	31895.64	-44771.4	426.3275	POIKAN
10/9W/BHR1 D0	114.8	115.2	31900.23	-44772.8	426.3198	LN
10/9W/BHR1 D0	115.2	117.2	31901.38	-44773.1	426.3226	POIKAN
10/9W/BHR1 D0	117.2	118.08	31902.76	-44773.6	426.3287	LN
10/9W/BHR1 D0	118.08	123.08	31905.57	-44774.4	426.3506	MESN
10/9W/BHR1 D0	123.08	126.04	31909.38	-44775.6	426.4032	POIKAN
10/9W/BHR1 D0	126.04	126.1	31910.82	-44776	426.4304	SHR
10/9W/BHR1 D0	126.1	126.83	31911.2	-44776.1	426.4381	POIKAN
10/9W/BHR1 D0	126.83	135.89	31915.88	-44777.6	426.5486	POIKFPYX
10/9W/BHR1 D0	135.89	135.9	31920.21	-44778.9	426.6759	SF
10/9W/BHR1 D0	135.9	135.93	31920.23	-44778.9	426.6766	POIKFPYX
10/9W/BHR1 D0	135.93	135.95	31920.26	-44778.9	426.6773	SF
10/9W/BHR1 D0	135.95	136.01	31920.29	-44778.9	426.6786	DYK
10/9W/BHR1 D0	136.01	136.12	31920.38	-44778.9	426.6812	POIKFPYX
10/9W/BHR1 D0	136.12	136.55	31920.63	-44779	426.6896	DYK
10/9W/BHR1 D0	136.55	137.49	31921.29	-44779.2	426.7112	POIKFPYX
10/9W/BHR1 D0	137.49	137.54	31921.76	-44779.4	426.7272	DYK
10/9W/BHR1 D0	137.54	138.1	31922.05	-44779.5	426.7372	POIKFPYX
10/9W/BHR1 D0	138.1	138.4	31922.46	-44779.6	426.7515	SF
10/9W/BHR1 D0	138.4	138.84	31922.82	-44779.7	426.7641	POIKFPYX
10/9W/BHR1 D0	138.84	138.85	31923.03	-44779.8	426.7718	SF
10/9W/BHR1 D0	138.85	141.16	31924.14	-44780.1	426.8131	POIKFPYX
10/9W/BHR1 D0	141.16	141.17	31925.25	-44780.4	426.8568	SF
10/9W/BHR1 D0	141.17	143.01	31926.13	-44780.7	426.8933	POIKFPYX
10/9W/BHR1 D0	143.01	145.06	31927.99	-44781.3	426.975	POIKAN
10/9W/BHR1 D0	145.06	145.09	31928.99	-44781.6	427.0214	DYK
10/9W/BHR1 D0	145.09	145.51	31929.2	-44781.6	427.0316	POIKAN
10/9W/BHR1 D0	145.51	149.09	31931.12	-44782.2	427.1269	MN

Borehole information for borehole 2

BHID	FROM	TO	X	Y	Z	ROCK
10/9W/BHR2 D0	0	0	31791	-44744	433.14	COL
10/9W/BHR2 D0	0	0.44	31791.02	-44743.8	433.1676	MN
10/9W/BHR2 D0	0.44	1.06	31791.1	-44743.2	433.2339	FRAC
10/9W/BHR2 D0	1.06	3.03	31791.45	-44742	433.3961	MN
10/9W/BHR2 D0	3.03	3.21	31791.92	-44741.1	433.5328	MESN
10/9W/BHR2 D0	3.21	3.22	31791.97	-44741	433.5452	FRAC
10/9W/BHR2 D0	3.22	4.44	31792.32	-44740.6	433.6259	MESN
10/9W/BHR2 D0	4.44	4.7	31792.82	-44740.1	433.7263	FRAC
10/9W/BHR2 D0	4.7	6.71	31793.77	-44739.4	433.889	MESN
10/9W/BHR2 D0	6.71	7.14	31794.9	-44738.9	434.0543	FRAC
10/9W/BHR2 D0	7.14	8.17	31795.57	-44738.6	434.1497	LN
10/9W/BHR2 D0	8.17	8.26	31796.09	-44738.4	434.223	FRAC
10/9W/BHR2 D0	8.26	9.79	31796.84	-44738.2	434.3289	LN
10/9W/BHR2 D0	9.79	9.84	31797.58	-44737.9	434.4321	FRAC
10/9W/BHR2 D0	9.84	9.94	31797.65	-44737.9	434.4419	LN
10/9W/BHR2 D0	9.94	9.98	31797.71	-44737.9	434.4511	FRAC
10/9W/BHR2 D0	9.98	10.59	31798.02	-44737.8	434.4936	LN
10/9W/BHR2 D0	10.59	11.63	31798.8	-44737.5	434.6015	MESN
10/9W/BHR2 D0	11.63	11.93	31799.44	-44737.3	434.6891	OLVN
10/9W/BHR2 D0	11.93	14.51	31800.82	-44737	434.8776	MESN
10/9W/BHR2 D0	14.51	14.57	31802.09	-44736.6	435.0514	FRAC
10/9W/BHR2 D0	14.57	14.92	31802.28	-44736.6	435.0784	MESN
10/9W/BHR2 D0	14.92	15.01	31802.49	-44736.5	435.1075	FRAC
10/9W/BHR2 D0	15.01	15.46	31802.75	-44736.5	435.1432	MESN
10/9W/BHR2 D0	15.46	16.8	31803.61	-44736.2	435.262	MN
10/9W/BHR2 D0	16.8	17.59	31804.63	-44736	435.4038	MESN
10/9W/BHR2 D0	17.59	17.76	31805.09	-44735.9	435.468	FRAC
10/9W/BHR2 D0	17.76	23.29	31807.83	-44735.2	435.8526	MESN
10/9W/BHR2 D0	23.29	23.35	31810.51	-44734.5	436.2365	FRAC
10/9W/BHR2 D0	23.35	24.8	31811.24	-44734.3	436.3414	MESN
10/9W/BHR2 D0	24.8	25	31812.03	-44734.1	436.4567	LN
10/9W/BHR2 D0	25	25.05	31812.15	-44734.1	436.4742	FRAC
10/9W/BHR2 D0	25.05	27.71	31813.46	-44733.8	436.6655	LN
10/9W/BHR2 D0	27.71	37.84	31819.6	-44732.3	437.5977	MESN
10/9W/BHR2 D0	37.84	37.93	31824.52	-44731.1	438.3833	FRAC
10/9W/BHR2 D0	37.93	49.89	31830.31	-44729.8	439.3584	MESN
10/9W/BHR2 D0	49.89	49.98	31836.1	-44728.5	440.3924	FRAC
10/9W/BHR2 D0	49.98	50.81	31836.55	-44728.4	440.4734	MESN
10/9W/BHR2 D0	50.81	50.83	31836.96	-44728.3	440.5484	FRAC
10/9W/BHR2 D0	50.83	50.89	31836.99	-44728.3	440.5555	LN
10/9W/BHR2 D0	50.89	53.08	31838.07	-44728	440.7553	MESN
10/9W/BHR2 D0	53.08	53.13	31839.15	-44727.8	440.9556	FRAC
10/9W/BHR2 D0	53.13	53.26	31839.24	-44727.8	440.9717	MESN
10/9W/BHR2 D0	53.26	54.07	31839.69	-44727.7	441.0563	LN
10/9W/BHR2 D0	54.07	55.56	31840.79	-44727.5	441.2643	MESN
10/9W/BHR2 D0	55.56	60.67	31843.96	-44726.8	441.8716	LN
10/9W/BHR2 D0	60.67	60.7	31846.43	-44726.2	442.3554	FRAC
10/9W/BHR2 D0	60.7	60.93	31846.56	-44726.2	442.3802	MESN
10/9W/BHR2 D0	60.93	60.98	31846.69	-44726.2	442.4068	FRAC
10/9W/BHR2 D0	60.98	61.64	31847.03	-44726.1	442.4745	MESN
10/9W/BHR2 D0	61.64	61.67	31847.37	-44726	442.5405	FRAC
10/9W/BHR2 D0	61.67	61.77	31847.43	-44726	442.5529	MESN
10/9W/BHR2 D0	61.77	61.82	31847.5	-44726	442.5673	FRAC
10/9W/BHR2 D0	61.82	61.89	31847.56	-44726	442.5788	MESN
10/9W/BHR2 D0	61.89	61.91	31847.6	-44726	442.5874	FRAC
10/9W/BHR2 D0	61.91	64.83	31849.01	-44725.7	442.8709	MESN
10/9W/BHR2 D0	64.83	64.86	31850.43	-44725.4	443.1585	FRAC
10/9W/BHR2 D0	64.86	65.18	31850.6	-44725.4	443.1928	MESN
10/9W/BHR2 D0	65.18	65.21	31850.77	-44725.3	443.2272	FRAC
10/9W/BHR2 D0	65.21	66.22	31851.27	-44725.2	443.3296	MESN
10/9W/BHR2 D0	66.22	71.88	31854.47	-44724.6	443.9966	POIKAN
10/9W/BHR2 D0	71.88	72.71	31857.59	-44724	444.6639	MESN
10/9W/BHR2 D0	72.71	76.41	31859.76	-44723.6	445.1404	POIKAN
10/9W/BHR2 D0	76.41	76.76	31861.7	-44723.2	445.5738	POIKPYX
10/9W/BHR2 D0	76.76	83.53	31865.08	-44722.4	446.352	POIKPYX
10/9W/BHR2 D0	83.53	83.66	31868.37	-44721.7	447.1235	FRAC
10/9W/BHR2 D0	83.66	104.18	31878.17	-44719.5	449.5288	POIKPYX
10/9W/BHR2 D0	104.18	104.28	31887.95	-44717.4	451.9963	FRAC
10/9W/BHR2 D0	104.28	104.62	31888.16	-44717.3	452.049	POIKAN
10/9W/BHR2 D0	104.62	104.7	31888.36	-44717.3	452.0995	FRAC
10/9W/BHR2 D0	104.7	106.17	31889.09	-44717.1	452.2856	POIKAN
10/9W/BHR2 D0	106.17	110.27	31891.74	-44716.6	452.9576	FRAC
10/9W/BHR2 D0	110.27	110.64	31893.86	-44716.1	453.4983	POIKPYX

Borehole information for borehole 3

BHID	FROM	TO	X	Y	Z	ROCK
10/9W/BHR3 D0	0	0	31794.4	-44748	432.013	COL
10/9W/BHR3 D0	0	1.5	31794.69	-44747.2	431.7234	MN
10/9W/BHR3 D0	1.5	7.95	31797.11	-44745.7	430.3627	MESN
10/9W/BHR3 D0	7.95	16.69	31803.24	-44749.9	428.6192	LN
10/9W/BHR3 D0	16.69	41.75	31816.25	-44760.2	425.3955	MESN
10/9W/BHR3 D0	41.75	49.1	31828.74	-44770.1	422.5459	LN
10/9W/BHR3 D0	49.1	58.43	31835.19	-44775.2	421.1751	MESN
10/9W/BHR3 D0	58.43	70.48	31843.49	-44781.8	419.5261	LN
10/9W/BHR3 D0	70.48	73.56	31849.36	-44786.4	418.4584	MESN
10/9W/BHR3 D0	73.56	76.33	31851.63	-44788.2	418.0689	LN
10/9W/BHR3 D0	76.33	78.53	31853.56	-44789.8	417.7497	MESN
10/9W/BHR3 D0	78.53	86.51	31857.52	-44792.9	417.1351	LN
10/9W/BHR3 D0	86.51	97.48	31864.89	-44798.8	416.1231	LN
10/9W/BHR3 D0	97.48	101.65	31870.77	-44803.5	415.4192	POIKAN
10/9W/BHR3 D0	101.65	102.14	31872.58	-44804.9	415.2199	MESN
10/9W/BHR3 D0	102.14	102.41	31872.88	-44805.2	415.1882	LN
10/9W/BHR3 D0	102.41	111.18	31876.39	-44808	414.8332	POIKAN
10/9W/BHR3 D0	111.18	111.57	31879.96	-44810.8	414.5125	MESN
10/9W/BHR3 D0	111.57	114.55	31881.27	-44811.9	414.4024	POIKAN
10/9W/BHR3 D0	114.55	116.08	31883.02	-44813.3	414.2617	LN
10/9W/BHR3 D0	116.08	116.51	31883.78	-44813.9	414.2032	POIKAN
10/9W/BHR3 D0	116.51	116.67	31884.01	-44814.1	414.1859	MESN
10/9W/BHR3 D0	116.67	119.15	31885.04	-44814.9	414.1105	LN
10/9W/BHR3 D0	119.15	119.39	31886.09	-44815.8	414.036	FRAC
10/9W/BHR3 D0	119.39	119.65	31886.29	-44815.9	414.0226	LN
10/9W/BHR3 D0	119.65	119.85	31886.46	-44816.1	414.0105	DYK
10/9W/BHR3 D0	119.85	121.36	31887.13	-44816.6	413.9659	LN
10/9W/BHR3 D0	121.36	125.48	31889.31	-44818.4	413.8268	POIKAN
10/9W/BHR3 D0	125.48	125.6	31890.95	-44819.7	413.7297	FRAC
10/9W/BHR3 D0	125.6	127.03	31891.55	-44820.2	413.6957	POIKPYX
10/9W/BHR3 D0	127.03	127.1	31892.13	-44820.7	413.6627	DYK
10/9W/BHR3 D0	127.1	127.25	31892.21	-44820.8	413.6578	POIKPYX
10/9W/BHR3 D0	127.25	127.37	31892.31	-44820.9	413.6518	DYK
10/9W/BHR3 D0	127.37	162.8	31906.04	-44832.1	412.859	POIKPYX
10/9W/BHR3 D0	162.8	163.44	31920.01	-44843.5	411.9177	POIKPYX
10/9W/BHR3 D0	163.44	174.71	31924.35	-44847.6	411.5753	POIKPYX
10/9W/BHR3 D0	174.71	175.93	31928.95	-44851.8	411.2388	MN
10/9W/BHR3 D0	175.93	176.39	31929.58	-44852.3	411.1966	MESN
10/9W/BHR3 D0	176.39	176.46	31929.78	-44852.5	411.1834	LN
10/9W/BHR3 D0	176.46	213.26	31943.73	-44864.5	410.5221	POIKAN

Borehole information for borehole 4

BHID	FROM	TO	X	Y	Z	ROCK
10/9W/BHR4 D0	0	0	31790.2	-44743	433.554	COL
10/9W/BHR4 D0	0	4.4	31790.45	-44740.9	434.1758	POIKPYX
10/9W/BHR4 D0	4.4	25.56	31797.6	-44731	437.4726	MESN
10/9W/BHR4 D0	25.56	39.28	31808.91	-44718.6	442.0609	MN
10/9W/BHR4 D0	39.28	83.52	31827.71	-44698.1	450.3586	MESN
10/9W/BHR4 D0	83.52	85.33	31842.6	-44682.2	457.7849	LN
10/9W/BHR4 D0	85.33	96.46	31846.75	-44677.8	460.0024	MESN
10/9W/BHR4 D0	96.46	97.17	31850.56	-44673.7	462.0715	POIKPYX
10/9W/BHR4 D0	97.17	97.4	31850.86	-44673.4	462.2373	MESN
10/9W/BHR4 D0	97.17	97.4	31850.86	-44673.4	462.2373	MESN
10/9W/BHR4 D0	97.4	97.87	31851.09	-44673.2	462.3609	FERPL
10/9W/BHR4 D0	97.87	103.34	31853.06	-44671.2	463.4136	POIKPYX
10/9W/BHR4 D0	103.34	106.56	31856	-44668.4	464.9654	FERPL
10/9W/BHR4 D0	106.56	108.14	31857.6	-44666.9	465.8271	POIKPYX
10/9W/BHR4 D0	108.14	108.34	31858.19	-44666.3	466.1474	FRAC
10/9W/BHR4 D0	108.34	109.7	31858.7	-44665.8	466.4285	POIKPYX
10/9W/BHR4 D0	109.7	109.83	31859.19	-44665.3	466.6972	FRAC
10/9W/BHR4 D0	109.83	109.87	31859.25	-44665.2	466.7279	POIKPYX
10/9W/BHR4 D0	109.87	110.01	31859.31	-44665.2	466.7604	FRAC
10/9W/BHR4 D0	110.01	129.71	31865.74	-44658.5	470.3781	POIKPYX
10/9W/BHR4 D0	129.71	129.82	31872.19	-44652	474.0662	DYK
10/9W/BHR4 D0	129.82	139.75	31875.43	-44648.6	475.9535	POIKPYX

APPENDIX B BOREHOLE RADAR ILLUMINATION LINE COORDINATES

Borehole 1: Borehole radar illumination line coordinates – dip direction

X	Y	Z	X	Y	Z
31791	-44739.5	426.972	31843.2	-44756.3	413.384
31839.1	-44754	413.39	31842.1	-44755.7	413.354
31839	-44753.6	413.412	31841.1	-44755	413.348
31838.2	-44753	413.471	31840.1	-44754.3	413.365
31837.2	-44752.3	413.559	31839.1	-44753.6	413.406
31836.3	-44751.7	413.671	31894.5	-44766.3	410.894
31835.5	-44751	413.807	31892.9	-44766.1	411.08
31834.6	-44750.4	413.966	31889.8	-44765.4	411.489
31833.8	-44749.7	414.149	31886.7	-44764.9	411.854
31833	-44749.1	414.356	31908	-44769	408.922
31832.2	-44748.5	414.586	31907.2	-44768.9	409.005
31831.4	-44747.9	414.84	31903.4	-44768.2	409.59
31830.6	-44747.3	415.118	31899.7	-44767.4	410.131
31830.1	-44746.6	415.42	31896.3	-44766.7	410.628
31829.7	-44745.9	415.763	31918.6	-44771.2	407.194
31828.9	-44745.3	416.168	31915.4	-44770.6	407.702
31827.8	-44744.7	416.633	31911.2	-44769.8	408.376
31826.5	-44744.1	417.16	31919.8	-44771.5	406.985
31824.9	-44743.5	417.747			
31823	-44742.9	418.395			
31820.9	-44742.4	419.105			
31818.5	-44741.9	419.875			
31815.8	-44741.4	420.706			
31812.9	-44740.9	421.598			
31809.8	-44740.4	422.551			
31806.4	-44740	423.565			
31802.7	-44739.5	424.639			
31798.9	-44739.1	425.775			
31885.8	-44764.6	411.976			
31883.8	-44764.4	412.174			
31881	-44763.9	412.45			
31878.3	-44763.5	412.682			
31875.6	-44763.2	412.871			
31872.9	-44762.9	413.014			
31870.7	-44762.7	413.114			
31868.9	-44762.3	413.188			
31867.2	-44762	413.254			
31865.4	-44761.6	413.312			
31863.6	-44761.2	413.362			
31861.8	-44760.8	413.404			
31860	-44760.4	413.437			
31858.2	-44760	413.463			
31856.3	-44759.6	413.481			
31854.4	-44759.2	413.491			
31852.5	-44758.7	413.493			
31850.6	-44758.3	413.488			
31848.7	-44757.8	413.474			
31846.7	-44757.4	413.452			
31844.7	-44756.9	413.422			

Borehole 1: Borehole radar illumination line coordinates – strike direction

X	Y	Z	X	Y	Z	X	Y	Z
31799.2	-44743.2	425.805	31856.9	-44754.4	414.819	31900.8	-44767.3	409.863
31801.4	-44743.7	425.008	31857.7	-44754.6	414.915	31901.9	-44767.6	409.807
31803.5	-44744.1	424.265	31858.6	-44754.9	414.969	31902.9	-44767.8	409.757
31805.4	-44744.5	423.576	31859.4	-44755.2	414.982	31904	-44768.1	409.708
31807.1	-44744.9	422.941	31860.2	-44755.6	414.983	31905.2	-44768.6	409.54
31808.7	-44745.2	422.359	31861	-44756	414.97	31906.5	-44769.3	409.292
31810.1	-44745.6	421.831	31861.8	-44756.4	414.945	31907.8	-44769.9	409.008
31811.3	-44745.8	421.354	31862.6	-44756.7	414.905	31909.3	-44770.5	408.688
31812.4	-44746.1	420.928	31863.4	-44757.1	414.852	31910.8	-44771.1	408.327
31813.2	-44746.4	420.55	31864.2	-44757.4	414.786	31912.5	-44771.7	407.922
31814	-44746.6	420.203	31864.9	-44757.8	414.705	31914.2	-44772.3	407.473
31814.8	-44746.8	419.86	31865.6	-44758.1	414.61	31916	-44772.9	406.978
31815.7	-44746.9	419.504	31866.4	-44758.4	414.515	31916.4	-44773.1	406.831
31816.5	-44747.1	419.133	31867.1	-44758.7	414.43	31917.9	-44773.5	406.438
31817.4	-44747.3	418.747	31867.8	-44758.9	414.34	31919.8	-44774.1	405.875
31818.3	-44747.5	418.347	31868.6	-44759.2	414.244			
31819.3	-44747.7	417.932	31869.3	-44759.5	414.142			
31820.2	-44747.9	417.503	31870.1	-44759.7	414.034			
31821.3	-44748.2	417.059	31870.9	-44760	413.92			
31822.3	-44748.4	416.6	31871.7	-44760.2	413.8			
31823.3	-44748.6	416.164	31872.5	-44760.5	413.674			
31824.4	-44748.4	415.856	31873.3	-44760.7	413.541			
31825.5	-44748.3	415.592	31874.1	-44761	413.402			
31826.6	-44748.3	415.362	31874.9	-44761.3	413.255			
31827.8	-44748.2	415.165	31875.8	-44761.5	413.101			
31829	-44748.2	415.002	31876.7	-44761.8	412.939			
31830.3	-44748.3	414.872	31877.6	-44762.1	412.77			
31831.6	-44748.4	414.775	31878.5	-44762.3	412.593			
31832.9	-44748.5	414.71	31879.4	-44762.6	412.407			
31834.3	-44748.6	414.677	31880.4	-44762.9	412.215			
31835.8	-44748.9	414.668	31881.4	-44763.2	412.014			
31837.2	-44749.2	414.621	31882.4	-44763.5	411.805			
31838.7	-44749.6	414.572	31883.4	-44763.7	411.597			
31840	-44749.9	414.53	31884.4	-44763.9	411.426			
31841.4	-44750.3	414.485	31885.1	-44764	411.319			
31842.7	-44750.7	414.447	31885.4	-44764.1	411.269			
31843.9	-44751	414.417	31886.4	-44764.3	411.123			
31845.1	-44751.3	414.395	31887.4	-44764.5	410.987			
31846.3	-44751.6	414.379	31888.5	-44764.6	410.861			
31847.4	-44751.9	414.371	31889.5	-44764.8	410.744			
31848.5	-44752.2	414.371	31890.5	-44765	410.638			
31849.5	-44752.5	414.383	31891.5	-44765.2	410.54			
31850.5	-44752.8	414.406	31892.5	-44765.4	410.453			
31851.5	-44753	414.437	31893.6	-44765.6	410.373			
31852.5	-44753.2	414.478	31894.6	-44765.8	410.289			
31853.4	-44753.5	414.528	31895.6	-44766.1	410.209			
31854.3	-44753.7	414.587	31896.7	-44766.3	410.129			
31855.2	-44753.9	414.655	31897.7	-44766.6	410.055			
31856.1	-44754.1	414.732	31898.8	-44766.8	409.986			

Borehole 2: Borehole radar illumination line coordinates – strike direction

X	Y	Z	X	Y	Z	X	Y	Z
31793.1	-44738.4	429.094	31825.6	-44727.2	427.845	31865.9	-44715.5	426.811
31794.2	-44737.4	429.105	31826.4	-44727	427.838	31866.8	-44715.2	426.823
31794.4	-44737.2	429.106	31827.3	-44726.7	427.822	31867.3	-44715.1	426.822
31795.3	-44736.8	429.01	31828.2	-44726.4	427.796	31867.2	-44715.1	426.829
31796.4	-44736.3	428.896	31828.8	-44726.3	427.774	31868.5	-44714.8	426.871
31796.7	-44736.2	428.857	31829.1	-44726.2	427.76	31870	-44714.4	426.949
31797.4	-44735.9	428.777	31830	-44725.9	427.715	31871.6	-44714	427.06
31798.4	-44735.6	428.659	31831	-44725.6	427.659	31873.3	-44713.5	427.207
31799.4	-44735.2	428.553	31832	-44725.2	427.593	31875.2	-44713.1	427.387
31800.3	-44734.9	428.457	31833	-44724.9	427.524	31877.2	-44712.6	427.602
31801.1	-44734.6	428.373	31834	-44724.6	427.457	31878.9	-44712.1	427.804
31801.4	-44734.5	428.342	31834.5	-44724.5	427.425	31879.3	-44712	427.851
31801.9	-44734.3	428.296	31835	-44724.3	427.393	31881.5	-44711.5	428.133
31802.6	-44734.1	428.23	31836	-44724	427.333	31883.8	-44710.9	428.449
31803.3	-44733.8	428.174	31837	-44723.7	427.277	31886.3	-44710.3	428.798
31804	-44733.6	428.129	31837.9	-44723.5	427.225	31888.9	-44709.6	429.181
31804.6	-44733.4	428.089	31838.8	-44723.2	427.178	31889.5	-44709.5	429.278
31805.3	-44733.2	428.05	31839.7	-44722.9	427.133	31891.6	-44709	429.594
31805.9	-44733	428.011	31840.6	-44722.7	427.094			
31806.6	-44732.8	427.972	31841.5	-44722.4	427.058			
31807.2	-44732.6	427.932	31842.4	-44722.2	427.026			
31807.9	-44732.4	427.892	31843.2	-44721.9	426.999			
31808.6	-44732.2	427.852	31844.1	-44721.7	426.975			
31809.3	-44731.9	427.813	31844.7	-44721.5	426.959			
31810	-44731.7	427.774	31844.9	-44721.4	426.954			
31810.7	-44731.5	427.735	31845.7	-44721.2	426.933			
31810.8	-44731.4	427.727	31846.5	-44721	426.913			
31811.4	-44731.3	427.695	31847.3	-44720.8	426.895			
31812.1	-44731	427.656	31848.1	-44720.5	426.878			
31812.9	-44730.8	427.617	31848.9	-44720.3	426.863			
31813.6	-44730.6	427.583	31849.7	-44720.1	426.847			
31814.3	-44730.4	427.557	31850.5	-44719.9	426.833			
31815	-44730.2	427.537	31851.2	-44719.7	426.82			
31815.7	-44730	427.524	31852	-44719.5	426.808			
31816.4	-44729.8	427.519	31852.7	-44719.3	426.798			
31817.1	-44729.6	427.52	31853.5	-44719.1	426.789			
31817.8	-44729.4	427.529	31854.2	-44718.9	426.781			
31818.5	-44729.2	427.545	31855	-44718.7	426.774			
31819.1	-44729	427.564	31855.8	-44718.4	426.768			
31819.2	-44729	427.568	31856	-44718.4	426.767			
31819.9	-44728.8	427.597	31856.7	-44718.2	426.767			
31820.5	-44728.7	427.634	31857.5	-44717.9	426.767			
31821.2	-44728.5	427.678	31858.5	-44717.7	426.769			
31821.9	-44728.3	427.726	31859.4	-44717.4	426.771			
31822.5	-44728.1	427.77	31860.4	-44717.1	426.774			
31823.3	-44727.9	427.804	31861.4	-44716.8	426.778			
31823.9	-44727.7	427.824	31862.5	-44716.5	426.783			
31824	-44727.7	427.828	31863.4	-44716.3	426.787			
31824.8	-44727.5	427.841	31863.6	-44716.2	426.789			

Borehole 3: Borehole radar illumination line coordinates – dip direction

X	Y	Z	X	Y	Z	X	Y	Z
31802.7	-44747.4	419.844	31858.2	-44790.1	402.535	31916.9	-44834.7	387.42
31815.6	-44757.3	416.084	31857.1	-44789.4	402.811	31915.7	-44833.9	387.765
31814.4	-44756.4	416.469	31869.8	-44798.9	399.401	31914.4	-44833	388.095
31813	-44755.3	416.883	31869.6	-44798.8	399.445	31913.2	-44832.2	388.411
31811.6	-44754.2	417.301	31868.8	-44798.2	399.687	31912.1	-44831.4	388.713
31810.1	-44753.1	417.723	31867.9	-44797.5	399.931	31910.9	-44830.7	389
31808.7	-44752	418.149	31866.9	-44796.8	400.179	31909.8	-44830	389.273
31807.2	-44750.9	418.579	31866	-44796.1	400.429	31908.8	-44829.2	389.531
31805.6	-44749.7	419.012	31865.1	-44795.4	400.682	31907.7	-44828.6	389.775
31804.1	-44748.5	419.449	31864.1	-44794.7	400.939	31906.8	-44827.9	390.005
31827.9	-44766.3	412.164	31871.6	-44800.3	398.914	31905.9	-44827.2	390.23
31826.8	-44765.6	412.536	31871.4	-44800.1	398.97	31905	-44826.5	390.451
31825.7	-44764.7	412.912	31870.5	-44799.5	399.206	31922.6	-44839.1	385.65
31824.5	-44763.9	413.292	31875.4	-44803.2	397.851	31921.8	-44838.5	385.895
31823.3	-44763	413.676	31874.7	-44802.7	398.054	31920.6	-44837.5	386.298
31822.1	-44762.2	414.063	31873.9	-44802	398.279	31919.4	-44836.6	386.686
31820.9	-44761.2	414.455	31873.1	-44801.4	398.506	31927	-44842.7	384.15
31819.6	-44760.3	414.85	31872.2	-44800.8	398.737	31925.7	-44841.6	384.6
31818.4	-44759.4	415.249	31879	-44806.1	396.854	31924.4	-44840.6	385.046
31817.1	-44758.4	415.652	31878.5	-44805.8	396.973	31923.1	-44839.5	385.478
31815.7	-44757.4	416.058	31877.8	-44805.1	397.183	31934.7	-44848.4	381.62
31834.3	-44771.1	409.857	31877	-44804.5	397.397	31933.1	-44847.2	382.153
31833.9	-44770.8	410.007	31876.2	-44803.9	397.613	31931.5	-44846	382.671
31833	-44770.1	410.358	31883	-44809.4	395.768	31930	-44844.9	383.175
31832.1	-44769.3	410.712	31882.3	-44808.8	395.962	31928.5	-44843.8	383.665
31831.1	-44768.6	411.07	31881.5	-44808.2	396.158			
31830.1	-44767.9	411.431	31880.8	-44807.6	396.358			
31829	-44767.1	411.795	31880	-44807	396.56			
31842.6	-44777.8	407	31879.3	-44806.4	396.765			
31841.7	-44777	407.313	31886.1	-44812	394.951			
31840.7	-44776.2	407.639	31885.9	-44811.8	395.021			
31839.7	-44775.4	407.967	31885.2	-44811.2	395.204			
31838.7	-44774.6	408.299	31884.5	-44810.6	395.389			
31837.8	-44773.9	408.634	31883.7	-44810	395.577			
31836.8	-44773.1	408.973	31890	-44815.2	394.018			
31835.8	-44772.3	409.314	31889.4	-44814.7	394.151			
31834.9	-44771.6	409.659	31888.7	-44814.1	394.32			
31848.5	-44782.6	405.174	31888	-44813.6	394.491			
31847.7	-44781.9	405.427	31887.3	-44813	394.665			
31846.7	-44781.1	405.734	31886.6	-44812.4	394.842			
31845.7	-44780.2	406.043	31904.8	-44826.4	390.49			
31844.7	-44779.4	406.356	31904.1	-44825.9	390.671			
31843.7	-44778.6	406.672	31903.2	-44825.2	390.887			
31852.8	-44786	403.971	31902.3	-44824.5	391.101			
31851.8	-44785.3	404.234	31901.5	-44823.9	391.312			
31850.8	-44784.4	404.528	31900.6	-44823.2	391.52			
31849.7	-44783.6	404.824	31899.8	-44822.6	391.726			
31848.7	-44782.7	405.124	31898.9	-44822	391.929			
31856.7	-44789	402.929	31898.1	-44821.3	392.129			
31856.1	-44788.6	403.09	31897.3	-44820.7	392.326			
31855	-44787.8	403.372	31896.5	-44820.1	392.521			
31854	-44786.9	403.656	31895.6	-44819.5	392.713			
31852.9	-44786.1	403.944	31894.8	-44818.9	392.902			
31864	-44794.6	400.975	31894	-44818.2	393.089			
31863.2	-44793.9	401.197	31893.2	-44817.6	393.273			
31862.2	-44793.2	401.459	31892.5	-44817.1	393.454			
31861.2	-44792.5	401.724	31891.7	-44816.5	393.632			
31860.2	-44791.7	401.991	31890.9	-44815.9	393.808			
31859.2	-44790.9	402.262	31890.1	-44815.3	393.981			

Borehole 3: Borehole radar illumination line coordinates – strike direction

X	Y	Z	X	Y	Z	X	Y	Z
31800.1	-44746.3	421.041	31853	-44785.3	403.385	31891.2	-44813.9	393.73
31801.7	-44747.3	420.477	31853.9	-44786	403.13	31892.2	-44814.7	393.442
31802	-44747.5	420.393	31854.9	-44786.6	402.88	31893.2	-44815.5	393.15
31803.3	-44748.5	419.869	31855.8	-44787.3	402.634	31894.2	-44816.3	392.852
31804.9	-44749.7	419.264	31856.7	-44787.9	402.392	31895.3	-44817.2	392.534
31806.5	-44750.9	418.67	31857	-44788.1	402.322	31896.5	-44818.1	392.195
31808.1	-44752.1	418.087	31857.6	-44788.5	402.153	31897.8	-44819.1	391.835
31809.6	-44753.2	417.516	31858.6	-44789.2	401.918	31899.1	-44820.1	391.453
31811.2	-44754.4	416.956	31859.5	-44789.8	401.686	31900.5	-44821.2	391.048
31812.7	-44755.5	416.409	31860.4	-44790.5	401.457	31902	-44822.3	390.622
31814.1	-44756.6	415.872	31861.3	-44791.1	401.231	31903.5	-44823.5	390.174
31815	-44757.2	415.581	31862.2	-44791.7	401.009	31905.1	-44824.7	389.731
31815.6	-44757.7	415.348	31863.1	-44792.4	400.79	31905.2	-44824.7	389.704
31817	-44758.8	414.835	31864.1	-44793	400.575	31906.9	-44826	389.215
31818.5	-44759.9	414.334	31864.9	-44793.6	400.391	31908.7	-44827.4	388.703
31819.9	-44760.9	413.844	31865	-44793.6	400.362	31910.6	-44828.8	388.17
31821.2	-44761.9	413.366	31865.9	-44794.3	400.154	31912.5	-44830.2	387.614
31822.6	-44762.9	412.899	31866.8	-44794.9	399.949	31914.5	-44831.8	387.037
31823.9	-44763.9	412.445	31867.7	-44795.5	399.747	31916.6	-44833.3	386.437
31825.2	-44764.9	412.002	31868.6	-44796.2	399.548	31918.8	-44835	385.815
31826.5	-44765.9	411.57	31869.5	-44796.8	399.353	31918.9	-44835.1	385.785
31827.6	-44766.6	411.225	31870.4	-44797.4	399.16	31921.1	-44837	385.071
31827.8	-44766.8	411.151	31871.2	-44797.9	399.006	31923.2	-44838.8	384.398
31829.1	-44767.7	410.746	31871.3	-44798.1	398.971	31923.5	-44839.1	384.299
31830.3	-44768.6	410.349	31872.3	-44798.7	398.787	31925.9	-44841.1	383.519
31831.5	-44769.5	409.951	31873.1	-44799.3	398.604	31927.7	-44842.6	382.957
31832.8	-44770.4	409.557	31874.1	-44800.1	398.36	31928.5	-44843.2	382.73
31834	-44771.3	409.171	31875	-44800.9	398.127	31931.1	-44845.3	381.955
31834.2	-44771.5	409.114	31876	-44801.6	397.891			
31835.1	-44772.2	408.793	31876.7	-44802.2	397.703			
31836.3	-44773.1	408.422	31876.9	-44802.4	397.653			
31837.5	-44773.9	408.058	31877.9	-44803.1	397.413			
31838.6	-44774.8	407.701	31878.8	-44803.9	397.17			
31839.7	-44775.6	407.349	31879.8	-44804.7	396.924			
31840.8	-44776.4	407.004	31880.1	-44804.9	396.833			
31841.9	-44777.2	406.666	31880.7	-44805.4	396.675			
31842.5	-44777.7	406.488	31881.7	-44806.2	396.424			
31843	-44778	406.335	31882.6	-44807	396.169			
31844.1	-44778.8	406.01	31883.6	-44807.7	395.912			
31845.1	-44779.6	405.691	31883.9	-44808	395.81			
31846.2	-44780.3	405.379	31884.5	-44808.5	395.651			
31847.2	-44781.1	405.074	31885.5	-44809.3	395.386			
31848.2	-44781.8	404.776	31886.4	-44810	395.118			
31848.5	-44782	404.69	31886.8	-44810.4	394.995			
31849.2	-44782.5	404.484	31887.4	-44810.8	394.846			
31850.2	-44783.3	404.199	31888.3	-44811.6	394.572			
31851.1	-44784	403.921	31889.3	-44812.4	394.295			
31852.1	-44784.6	403.649	31890.3	-44813.2	394.015			
31852.8	-44785.2	403.443	31890.4	-44813.3	393.966			

Borehole 4: Borehole radar illumination line coordinates – dip direction

X	Y	Z	X	Y	Z
31790.1	-44741.9	430.542	31832.6	-44690.7	440.797
31790.3	-44740.5	430.825	31833.2	-44689.4	441.008
31790.3	-44740.2	430.898	31833.7	-44688.2	441.257
31791	-44739.1	431.088	31834.1	-44687.1	441.542
31792	-44737.8	431.331	31834.4	-44686.1	441.864
31792.9	-44736.5	431.555	31834.5	-44685.1	442.223
31793.8	-44735.3	431.76	31834.6	-44684.2	442.619
31794.5	-44734.2	431.944	31834.6	-44683.4	443.051
31795.3	-44733.1	432.109	31834.6	-44682.6	443.521
31795.9	-44732.2	432.278	31834.9	-44681.8	444.065
31796.3	-44731.3	432.489	31835.6	-44680.7	444.704
31796.7	-44730.4	432.744	31836.6	-44679.5	445.438
31797.2	-44729.5	433.042	31837.8	-44678.1	446.268
31797.2	-44729.2	433.149	31839.1	-44676.7	447.194
31797.8	-44728.5	433.383	31840.6	-44675.1	448.214
31798.5	-44727.6	433.768	31841	-44674.6	448.516
31799.2	-44726.6	434.196	31842.3	-44673.4	449.33
31800	-44725.6	434.668	31844.1	-44671.5	450.541
31800.8	-44724.6	435.183	31845.2	-44670.4	451.277
31801.7	-44723.6	435.722	31846.1	-44669.5	451.848
31802.8	-44722.5	436.232			
31803.9	-44721.5	436.712			
31805	-44720.5	437.16			
31806.1	-44719.4	437.577			
31807.1	-44718.4	437.962			
31808.2	-44717.4	438.316			
31808.6	-44717.1	438.417			
31809.2	-44716.4	438.638			
31810.2	-44715.4	438.929			
31811.2	-44714.4	439.189			
31812.3	-44713.4	439.416			
31813.4	-44712.3	439.61			
31814.6	-44711.2	439.772			
31815.8	-44710.1	439.901			
31817.1	-44708.9	439.998			
31818.4	-44707.7	440.062			
31819.7	-44706.5	440.094			
31821.2	-44705.3	440.092			
31822.6	-44704	440.063			
31823.6	-44702.7	440.046			
31824.6	-44701.5	440.048			
31825.5	-44700.2	440.07			
31826.5	-44699	440.112			
31827.5	-44697.6	440.174			
31827.6	-44697.4	440.19			
31828.6	-44696.3	440.256			
31829.6	-44694.9	440.358			
31830.7	-44693.5	440.48			
31831.8	-44692	440.622			

Borehole 4: Borehole radar illumination line coordinates – strike direction

X	Y	Z	X	Y	Z
31789.5	-44740.1	431.174	31818.2	-44704.1	440.146
31790	-44739.3	431.236	31819.3	-44702.6	440.2
31790.9	-44737.9	431.35	31820.4	-44701.1	440.226
31791.8	-44736.6	431.472	31821.5	-44699.8	440.239
31792.6	-44735.4	431.604	31822.6	-44698.5	440.27
31793.5	-44734.3	431.745	31823.7	-44697.3	440.32
31794.2	-44733.3	431.894	31824.8	-44696.1	440.389
31795	-44732.4	432.052	31825.6	-44695.3	440.444
31795.6	-44731.6	432.219	31825.8	-44695	440.48
31796.3	-44731	432.393	31826.9	-44693.9	440.593
31796.9	-44730.4	432.575	31827.9	-44692.9	440.725
31797.5	-44730	432.763	31829	-44691.9	440.878
31798.1	-44729.6	432.958	31830	-44691	441.053
31798.5	-44729.4	433.15	31831	-44690.1	441.248
31799	-44728.9	433.454	31832	-44689.3	441.466
31799.5	-44728.3	433.744	31833	-44688.5	441.709
31799.9	-44727.8	434.025	31834.1	-44687.7	442.006
31800.4	-44727.2	434.298	31835.3	-44686.7	442.397
31800.8	-44726.7	434.561	31836.6	-44685.6	442.884
31801.3	-44726.1	434.817	31838	-44684.4	443.463
31801.7	-44725.6	435.063	31839.4	-44683.1	444.133
31802.2	-44725.1	435.302	31841	-44681.6	444.893
31802.6	-44724.5	435.532	31842.6	-44680	445.741
31803.1	-44724	435.753	31844.4	-44678.4	446.677
31803.5	-44723.4	435.967	31844.7	-44678.1	446.826
31804	-44722.8	436.173	31846.2	-44676.5	447.7
31804.4	-44722.3	436.367	31848.1	-44674.6	448.81
31804.9	-44721.8	436.554	31849	-44673.8	449.344
31805.4	-44721.3	436.741	31850.1	-44672.6	450.004
31805.8	-44720.8	436.928	31852.2	-44670.5	451.282
31806.3	-44720.3	437.115			
31806.8	-44719.8	437.302			
31807.2	-44719.2	437.489			
31807.7	-44718.7	437.675			
31808.2	-44718.2	437.862			
31808.6	-44717.7	438.049			
31809	-44717.3	438.21			
31809.5	-44716.7	438.422			
31810	-44716.1	438.615			
31810.5	-44715.4	438.84			
31811	-44714.6	439.048			
31811.6	-44713.7	439.234			
31812.3	-44712.8	439.402			
31813	-44711.8	439.552			
31813.7	-44710.7	439.686			
31814.5	-44709.5	439.805			
31815.4	-44708.3	439.91			
31816.3	-44707	440.001			
31817.2	-44705.6	440.08			